NEtwork of **R**esearch **I**nfrastructures for **E**uropean **S**eismology

Earthquake **L**oss **E**stimation **R**outine

ELER© v3.0

Technical Manual and Users Guide

Prepared by
Bogazici University, Department of Earthquake Engineering
Istanbul, July 2010

Contributors

This documentation is prepared by the following researchers from Bogazici University in alphabetical order:

Mine B. Demircioglu, Mustafa Erdik (NERIES JRA3 Coordinator), Ufuk Hancilar, Ebru Harmandar, Yaver Kamer, Karin Sesetyan, Cuneyt Tuzun, Cem Yenidogan and A.Can Zulfikar

Acknowledgements

In connection with the preparation of this manual the following individuals and institutions from NERIES Project - JRA3 Workgroup have contributed. This contribution is gratefully acknowledged.

Remy Bossu, European-Mediterranean Seismological Centre, EMSC, Arpajon, France
Xavier Goula, Janira Irizarry, Antoni Roca, Institut Geologic de Catalunya, Barcelona, Spain
Julian J. Bommer, Peter J.Stafford, Fleur O. Strasser, Imperial College, London, UK
Zehra Cagnan, Middle-East Technical University, Northern Cyprus
Eser Durukal Kandilli Observatory and Earthquake Research Institute, Istanbul, Turkey
Hilmar Bungum, Dominik H. Lang, Conrad D. Lindholm, NORSAR, Kjeller, Norway

Furthermore we are also thankful for the support and cooperation of following individuals:
David Wald, US Geological Survey, USGS, Denver, Colorado, USA
Alberto Michelini, Istituto Nazionale di Geofisica e Vulcanologia, INGV, Italy

FOREWORD

Under the JRA-3 component of the EU FP-6 NERIES Project, a methodology and software (ELER - **E**arthquake **L**oss **E**stimation **R**outine) for the rapid estimation of earthquake shaking and losses in the Euro-Mediterranean region has been developed. ELER V1.0 has been released in April 2009 and distributed among NERIES partners for testing and evaluation purposes. ELER V2.0 included modifications mainly based on feedbacks from users. The present version of the software, ELER V3.0, includes additional features on both ground motion and damage assessment components, developed during the period July 2009 – July 2010.

In contrast with the documentation provided for previous versions, the present version of ELER is presented with only one manual comprising both the Technical Manual and the Users Guide. The developer team of ELER is looking forward to receiving comments and suggestions from all users for the improvement and enhancement of the methodology, the coded software and the related documentation. Please address all correspondence to eler.support@boun.edu.tr.

Disclaimer

This software is provided "as is" without warranty of any kind, either expressed or implied, including, but not limited to, the implied warranties of merchantability and fitness for a particular purpose. The entire risk as to the quality and performance of the software is with you. Should the software prove to be defective, you assume the cost of all necessary servicing, repair or correction. In no event will the author or any other party who may have distributed the software, be liable to you for damages, including any general, special, incidental or consequential damages arising out of the use or inability to use the software (including but not limited to loss of data or data being rendered inaccurate or losses sustained by you or third parties or a failure of the software to operate with any other programs), even if such holder or other party has been advised of the possibility of such damages.

TABLE OF CONTENTS

INTRODUCTION

Under the JRA-3 component of the EU FP-6 NERIES Project, a methodology and software (ELER - **E**arthquake **L**oss **E**stimation **R**outine) for the rapid estimation of earthquake shaking and losses in the Euro-Mediterranean region has been developed. This multi-level methodology developed together with researchers from Imperial College, NORSAR, and EMSC is capable of incorporating regional variability and sources of uncertainty stemming from ground motion predictions, fault finiteness, site modifications, inventory of physical and social elements subjected to earthquake hazard and the associated vulnerability relationships. Although primarily intended for post-earthquake rapid loss estimation, the routine is also equally capable of developing scenario earthquake based loss assessments.

The methodology encompasses the following general steps:

1. For a given earthquake magnitude and epicenter information, estimation of the spatial distribution of selected ground motion parameters through region specific ground motion prediction equations and using shear wave velocity distributions or other site descriptors.

2. If available, incorporation of strong ground motion data for the improvement and bias adjustment of theoretical estimations.

3. Estimation of the building damage and human casualty at different levels of sophistication that commensurate with the availability of inventory of human built environment.

4. Estimation of direct economic losses stemming from building damages.

5. Estimation of damages for urban pipeline systems

The analysis procedure is given in Figure 1.

Both Level 0 (similar to PAGER system of USGS) and Level 1 analysis of the ELER software are based on obtaining intensity distributions analytically and estimating total number of casualties either using regionally adjusted intensity-casualty or magnitude-casualty correlations (Level 0) of using regional building inventory data bases (Level 1). Level 0 analysis is similar to the PAGER of USGS. For given basic source parameters the intensity distributions can be computed using: Regional ground motion prediction equations and Intensity correlations with PGV and PGA. Options are also available for more sophisticated treatment of site response through externally entered data and improvement of the shake map through incorporation of accelerometric data with bias adjustments made at the bedrock or directly at the surface.

Level 2 analysis of the ELER software is similar to HAZUS and SELENA and it is essentially intended for earthquake loss assessment (building damage and consequential human casualties) in urban areas. It employs a variety of well tested analytical techniques that include: Capacity Spectrum Method, Modified Acceleration-Displacement Response Spectrum Method, Reduction Factor Method and Coefficient Method. For building classification, the European building taxonomy developed within the EU-FP5 RISK-UE project as well as the model building types of HAZUS-MH (FEMA, 2003) are used.

In version 3.0 of ELER, Level 1 and Level 2 analyses also include calculation of direct monetary losses as a result of building damage. This tool allows for repair-cost estimations and specific investigations associated with earthquake insurance applications (PML and AAL estimations).

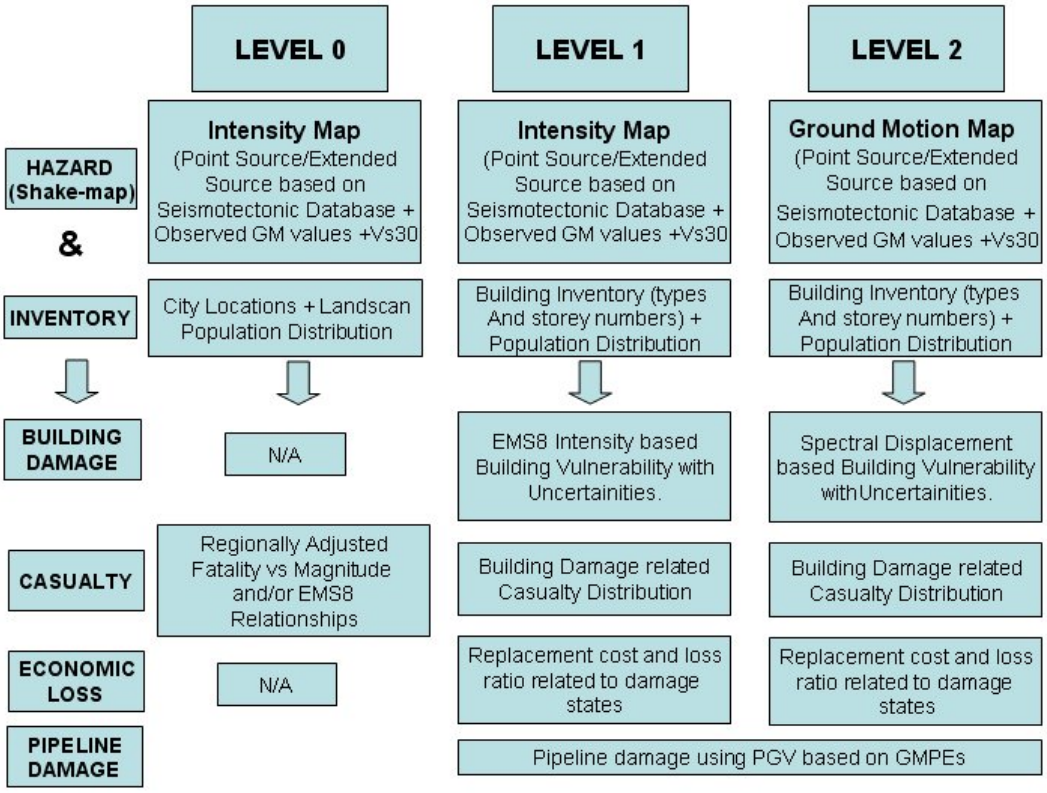

Figure 1. Flow chart for multi-level analysis methodology of ELER

HAZUS-MH (FEMA, 2003) methodology is used for the estimation of grid based urban pipeline damages.

The urban earthquake shaking and loss information is intended for dissemination in a timely manner to related agencies for the planning and coordination of the post-earthquake emergency response. However ELER software can also be used for scenario earthquake loss estimation, related Monte-Carlo type simulations and earthquake insurance applications.

MATLAB programming environment is used for programming, as well as for the display of results. However the data can be exported to popular GIS programs for further elaboration and plotting. MATLAB is a cross-platform programming language and, as such, ELER can run on the following operating systems without any code modification: Windows (x64), Linux (x86-64), Mac OS X and Solaris 64. ELER can be used both from a GUI and command line. The GUI enables even the inexperienced user to obtain results easily. The command line interface can be used for automated, scheduled or event triggered runs.

This manual intends to give the user the required information for the installation of and running ELER (the Users Guide in Section B) as well as the background information on the methodology and techniques involved (the Technical Manual in Section C). The newly added features of v3.0 are covered in Section A, as well as in the corresponding sections of the Users Guide and the Technical Manual. The development of ELER is funded by the EU- FP6 NERIES project. Our thanks are due to Project Coordinator: Domenico Giardini, Project Manager: Torild van Eck and JRA Activity Coordinator: Stefan Wiemer for facilitating our research and development work.

A. WHAT IS NEW IN V3.0?

A.1. Hazard Module

A.1.1. Modified Kriging Method

A new method for the calculation of a ground motion distribution has been developed in ELER v3.0. The Modified Kriging method is a new numerical technique based on Kriging method (Krige, 1966) and has been developed with the aim of interpolation of ground motion parameters using information obtained from geo-statistical analysis. This method can be effectively applied in regions with dense station coverage.

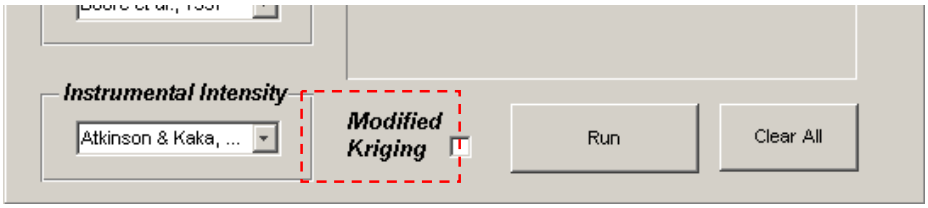

Figure 2. Modified Kriging checkbox

In case actual station (observed) data are supplied for ground motion estimation, ELER presents the user the option to implement the Modified Kriging method in regions which satisfy a certain coverage condition (Figure 2). The ground motion distribution in the remaining regions is calculated using the default Hazard module methodology. The outputs for a sample M4.9 event in South California have been given in Figure 3 and Figure 4.

Figure 3. Without Modified Kriging

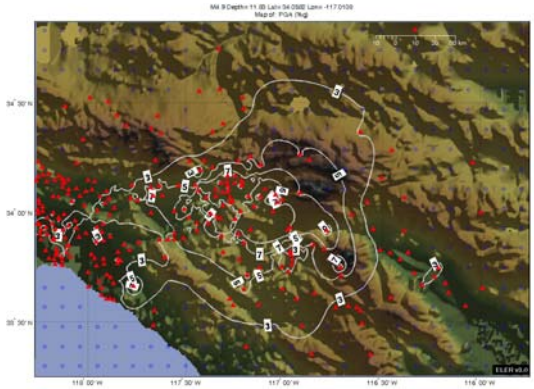

Figure 4. With Modified Kriging

When applicable, ELER v3.0 outputs detailed graphs of the Modified Kriging method in order to give the user a better understanding of the new technique. Figure 5 shows the region which satisfies the coverage conditions, the stations in the whole map extent and the output of the Modified Kriging process.

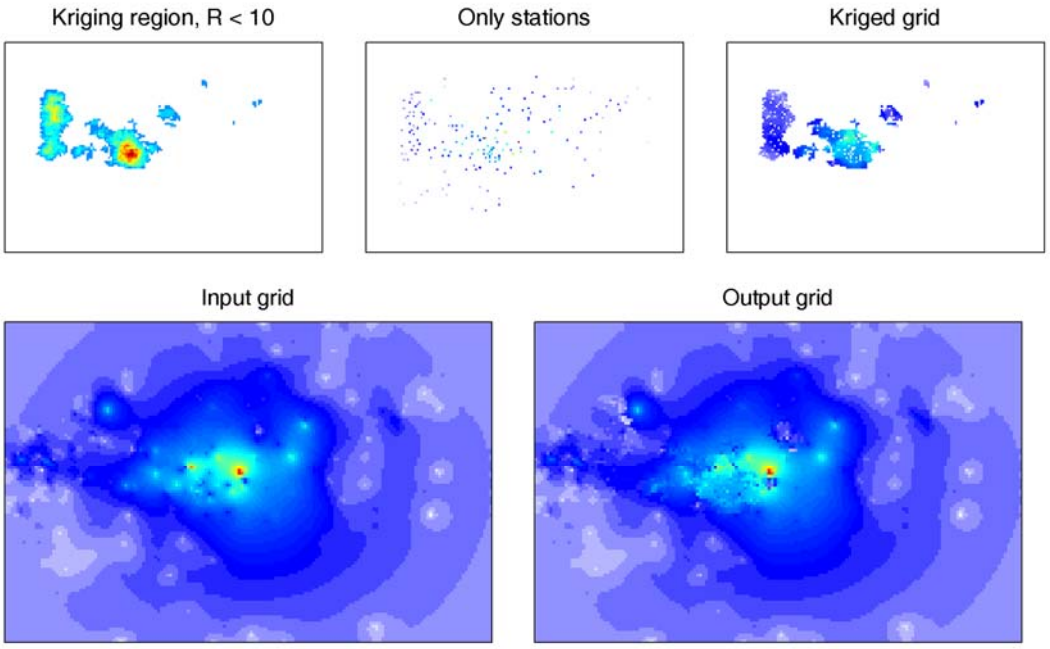

Figure 5. Details of the Modified Kriging Implementation

A.1.2. User Defined GMPEs

One of the new features of ELER v3.0 Hazard Module is the introduction of user defined ground motion prediction equations (GMPEs) as well as two new equations (Abrahamson and Silva, 1997 and Campbell and Bozorgnia, 2003). With this feature the user is enabled to input his/her custom GMPEs in a simple text file format. Similarly the user can define instrumental intensity prediction equations (IIPEs). The user defined GMPEs can be functions of the event and local parameters given in Table 1. These parameters are assigned by ELER prior to the evaluation.

Table 1: Event and local parameters of custom GMPEs

Event parameters*:* Constant for every estimation node	***Local parameters*****:** Varying according to the location of estimation nodes
mag: magnitude of the event *depth*: focal depth of the event	*Rjb*: Joyner-Boore distance (distance to the vertical projection of the source) *Vs*: Average shear wave velocity for the top 30 m (determined from the site condition map used)

Hazard Module's user defined GMPE input screen is given in Figure 6, while Figure 7 shows an example GMPE text file.

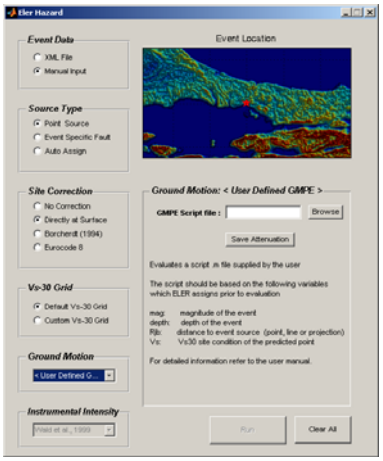

Figure 6. User defined GMPE GUI Screen

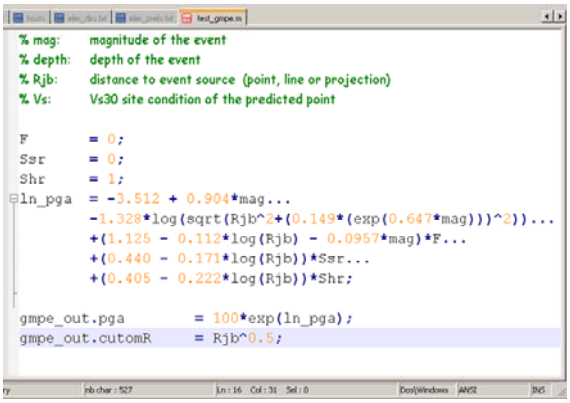

Figure 7. A simple user defined GMPE

The output structure of user defined GMPEs are not restricted and this gives the user ability and flexibility to obtain numerous maps. For example the user can define a custom output parameter as $\sqrt{Rjb}$ and plot its distribution as shown in Figure 8.

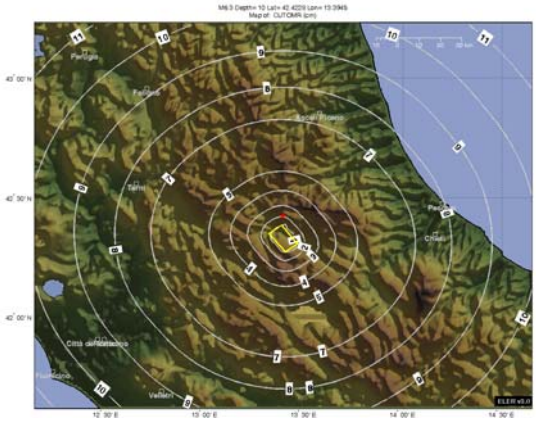

Figure 8. Custom map of $\sqrt{Rjb}$

A.1.3. Global elevation data Gtopo30

The Gtopo30 (30 arc second resolution) elevation data files for the whole world have been included in the data folder of ELER v3. This enables the user to plot the distribution of ground motions on tohic maps for any given region. The *gtopo30* folder includes the compressed gtopo30 files with their snapshot GIF images. The Euro-Mediterranean tiles (E020N40, E020N90, E040N40, E040N90) and the east coast region of North America (W020N40, W020N90) are already extracted. The user can extract the corresponding files to extent the coverage to his/her region of interest.

A.2. Level 0 Module

A.2.1. Detailed notifications for SB2002 approach

Additional notifications regarding the casualty estimation incorporating the Samardjieva and Badal (2002) method have been included in ELER v3. These notifications are based on the following prerequisites:

1. Contour VI exists
2. Contour VI encloses a land (populated) area

A.3. Level 1 Module

A.3.1. User defined Beta distribution parameter t

ELER v3 allows the user to define the Beta distribution parameter *t* via the *VQ* table. In addition to the vulnerability and ductility parameters *V* and *Q*, the user can also input different *t* parameters for each building type, allowing for a more detailed building characterization. Figure 9 shows the effect of *t* parameter on the shape of the distribution function and the discrete damage classes while all other parameters (vulnerability, ductility and intensity) are kept constant.

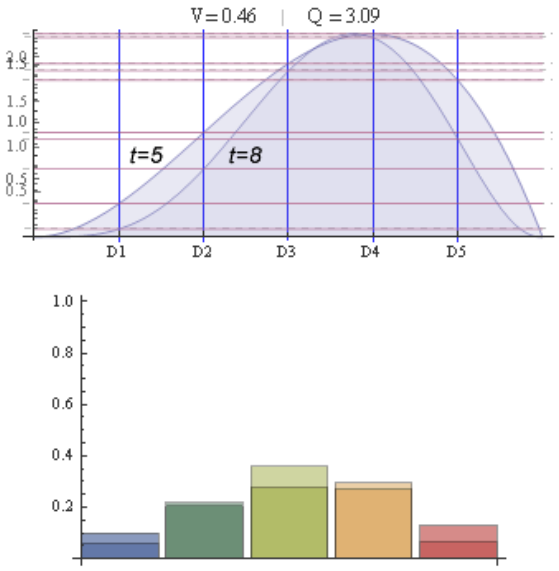

Figure 9. Effect of *t* parameter

A.3.2. Economic Loss

Economic losses can be estimated by the user defined loss ratio and building replacement cost variables. In Level 1 the user assigns a cost to each building in the *VQ* table. As shown in Figure 10 in ELER v3 the table consists of vulnerability, ductility, t parameter and replacement cost for each building. The loss ratio for each damage class is specified in the

Level 1 Module GUI as given in Figure 11. The loss estimation is obtained by multiplying a building's replacement cost with the loss ratio corresponding to its damage state.

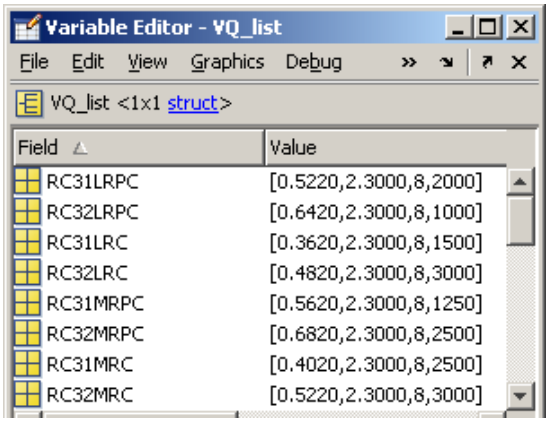

Figure 10. *VQ* Table

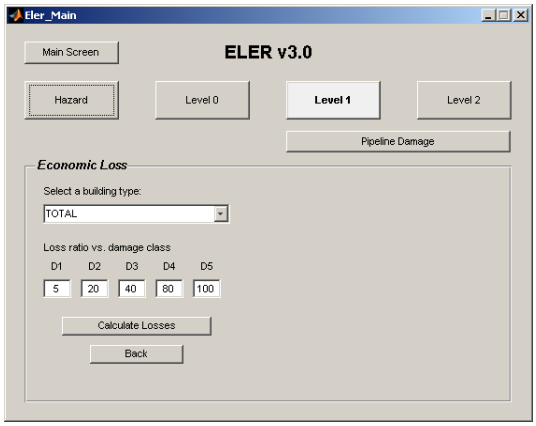

Figure 11. Loss ratios

A.4. Level 2 Module

A.4.1. Economic Loss

Economic losses are calculated as in Level 1, this time instead of 5 damage classes the user has to specify the loss ratio for 4 damage classes (Slight, Moderate, Extensive, Complete). The building replacement values are specified during the building database generation procedure using either the Xls2BDB or the Building DB-C tools.

A.4.2. Xls2BDB

The Xls2BDB tool converts a normal Excel document to a Level 2 Building Database file. This allows the user to integrate large databases into Level 2 loss estimation easily. Xls2BDB will automatically determine which spectral displacement based method can be utilized according to the parameters supplied within the Excel document. The template Excel sheet format is given in Figure 12.

	A	B	C	D	E	F	G	H	I	J	K	L	M
1		Fragility Curves								Capacity Curve			
2		Slight		Moderate		Extensive		Complete		Yield		Ultimate	
3	Building Name	Median	Beta	Median	Beta	Median	Beta	Median	Beta	Displacement	Acceleration	Displacement	Acceleration
4	B111	0.018	0.95	0.036	0.91	0.09	0.85	0.18	0.97	0.007753097	1.913	0.015506194	1.913
5	B211	0.0394	0.7	0.09	0.74	0.18	0.86	0.3375	0.98	0.024108109	1.692	0.048216218	1.692
6	B221	0.018	0.95	0.036	0.91	0.09	0.85	0.18	0.97	0.007753097	1.913	0.015506194	1.913
7	B212	0.0394	0.7	0.09	0.74	0.18	0.86	0.3375	0.98	0.024108109	1.692	0.048216218	1.692

	N	O	P	Q	R	S	T	U	V
			Economic Loss	Structural Behaviour				Building Charactreristics	
	Elastic			Degradation Factor					
	Displacement	Damping	Building Cost	Short	Moderate	Long	Ductility Value	C0 coefficient	Period
	0.006590132	5	1000	0.8	0.4	0.2	2	1.1	0.211
	0.020491893	5	1500	0.9	0.6	0.3	3	1.3	0.355
	0.006590132	5	1000	0.8	0.4	0.2	2	1.1	0.211
	0.020491893	5	1500	0.9	0.6	0.3	3	1.3	0.355

Figure 12. Xls2BDB example Excel document

The building inventory created from the provided .xls is saved inside the Level 2 building inventory folder with the proper filename format, thus the user can select the new inventory directly from the Level 2 GUI's Classification drop down menu.

A.4.3. Performance improvement in calculations

Due to their nonlinear approach, the functions used in Level 2 analysis tend to consume more time compared to Hazard and Level 1 modules. In ELER v3 the functions causing bottleneck have been pinned down by calculating the number of calls to each specific function together with the execution times. Performance optimizations in those specific functions have improved the overall calculation times by %100-%150 for some methods.

A.5. Pipeline Damage Module

ELER v3.0 enables the user to calculate pipeline damage based on peak ground velocity (PGV) distributions. If the PGV distribution is calculated in the Hazard module the user is given the option to proceed to lifeline damage estimations directly.

As shown in Figure 13 the PGV distribution grid should be supplied together with the pipeline database and a BD (brittle-ductile) table.

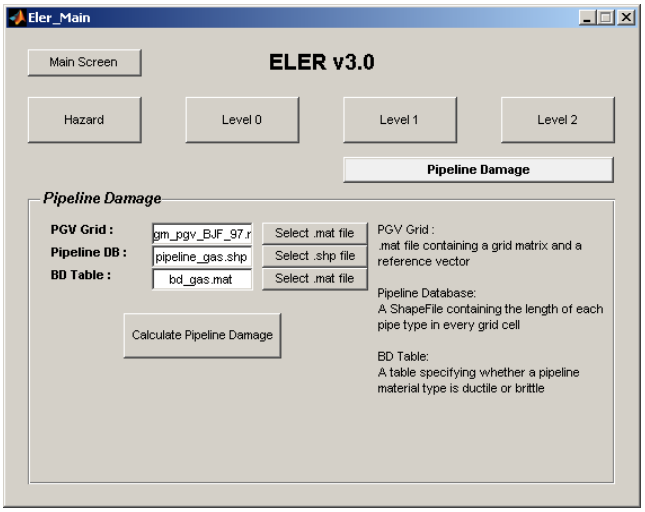

Figure 13. Level 1 Pipeline Damage Module GUI

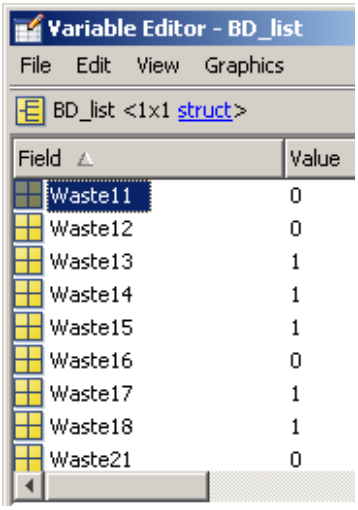

Figure 14. Brittle-Ductile Table

A.5.1. Additional option in the Xls2Mat tool

With the introduction of the Pipeline Damage module, the Xls2Mat tool can now also be used to create BD tables specifying whether a pipeline material is ductile or brittle. The user can specify the table he/she wants to create via the radio buttons on the Xls2Mat GUI as given in Figure 49.

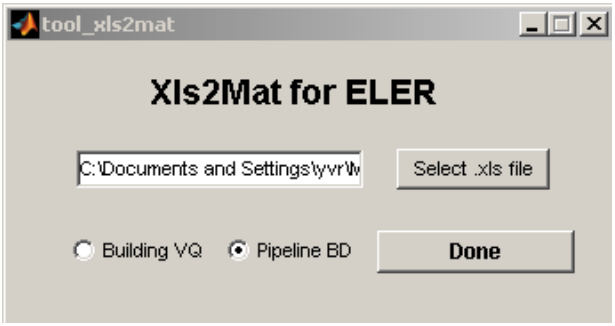

Figure 15. Xls2Mat GUI

B. USERS GUIDE

B.1. INTRODUCTION

ELER has been coded in MATLAB programming environment. All the analyses are performed by utilizing the computational and statistical toolboxes of MATLAB and the Mapping Toolbox is used for the display of the results. However data can be exported to popular GIS programs for further elaboration and plotting. The software can be used both from a GUI (Graphical User Interface) and command line. The GUI enables even the inexperienced user to obtain results easily (Figure 16). The command line interface can be used for automated, scheduled or event triggered runs.

ELER consists of four modules, for earthquake hazard and loss assessments, namely:

1. HAZARD
2. LEVEL 0
3. LEVEL 1
4. LEVEL 2

This Users Guide aims helping the user with the installation of and running ELER, encompassing chapters on *Hazard Module, Level 0 Module, Level 1 Module, Level 2 Module, Tools for External Data Integration and User Preferences*. The user might refer to the Technical Manual for further information about the theoretical background of the methodologies adopted in ELER.

In a simplified form, ELER methodology employs following steps:

1. In Hazard module, for a given earthquake magnitude and epicenter information, spatially distributed intensity and ground motion parameters PGA, PGV, Sa, Sd were estimated through region specific ground motion prediction equations and gridded shear wave velocity information.

2. In Level 0 module, the casualty estimation is done utilizing regionally adjusted intensity-casualty or magnitude-casualty correlations based on the Landscan population distribution inventory.

3. Level 1 module calculates number of damaged buildings and associated casualty. The intensity based empirical vulnerability relationship is employed to find number of damaged buildings. The casualty estimation is done through number of damaged buildings.

4. Level 2 module also calculates number of damaged buildings and associated casualty. The spectral acceleration-displacement-based vulnerability assessment methodology is utilized for the building damage estimation. The casualty estimation is done through number of damaged buildings using HAZUS99 (FEMA, 1999) and HAZUS-MH (FEMA, 2003) methodologies.

For detailed information on each step please refer to relevant section in this guide.

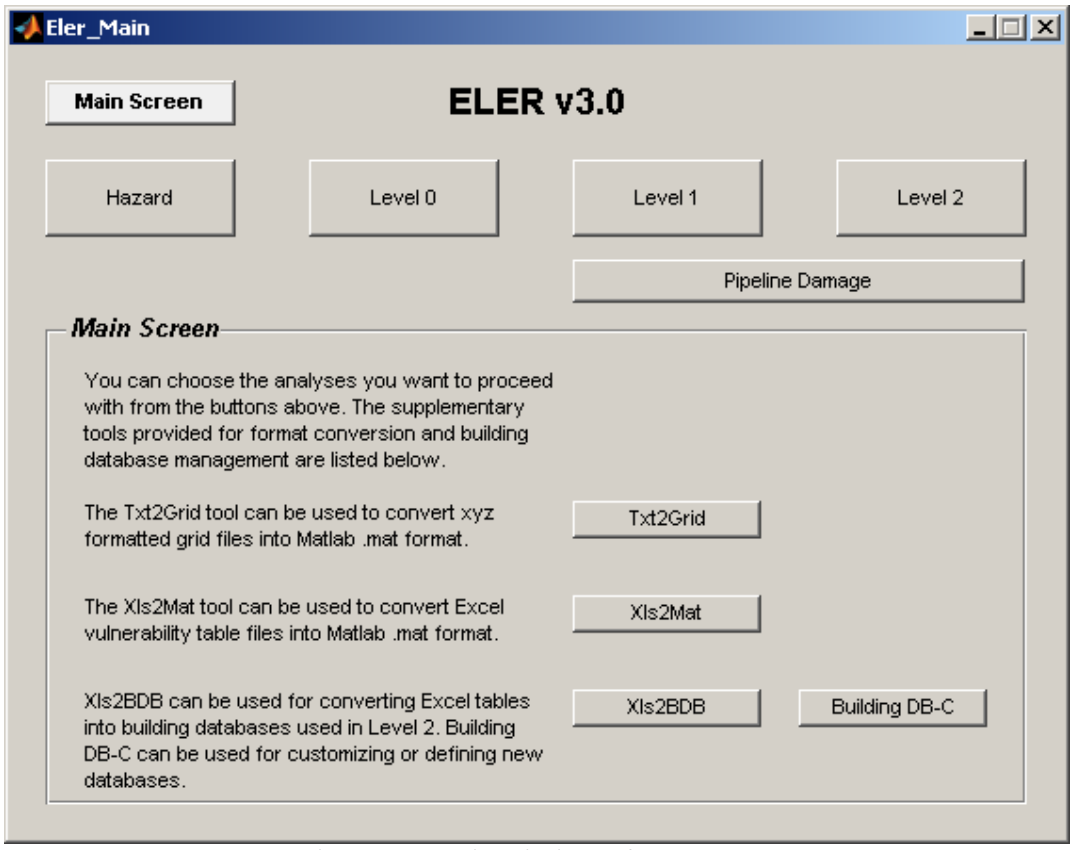

Figure 16. Main window of ELER GUI

B.1.1. Installation

The programming language of ELER is MATLAB® (R2008b). MATLAB is a cross-platform programming language and, as such, ELER can run on the following operating systems without any code modification: Windows (x64), Linux (x86-64), Mac OS X and Solaris 64.

For the installation of ELER, the MATLAB Component Runtime (MCR) 7.9 is required. The MATLAB Component Runtime is a free redistributable that allows you to run programs written in a specific version of MATLAB without installing the MATLAB version itself. There is no harm in having MATLAB and the MCR installed simultaneously, or in having multiple versions of each one installed. The installation procedure is as follows:

1) Create an installation directory: **C:\ELER_V3**. Verify that you have a free space of 8 GB on the **C:** drive. If you are installing ELER on a custom location do not forget to modify the ***eler_dirs.txt*** file in step 6 so that it will point to the correct directory locations. There is no need to modify this file if your installation directory is **C:\ELER_V3**

2) Navigate to the folder **ELER_V3_install** in the ELER DVD. Double click on the ***ELER_DATA.exe*** file and extract it into your installation directory (**C:\ELER_V3**).

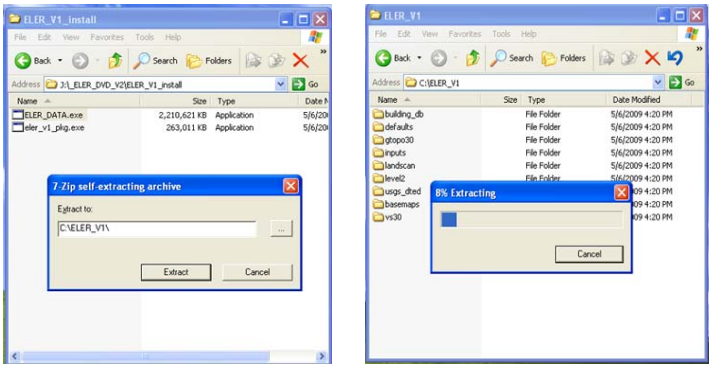

3) Copy the file ***eler_v3_pkg.exe*** to your installation directory (**C:\ELER_V3**).

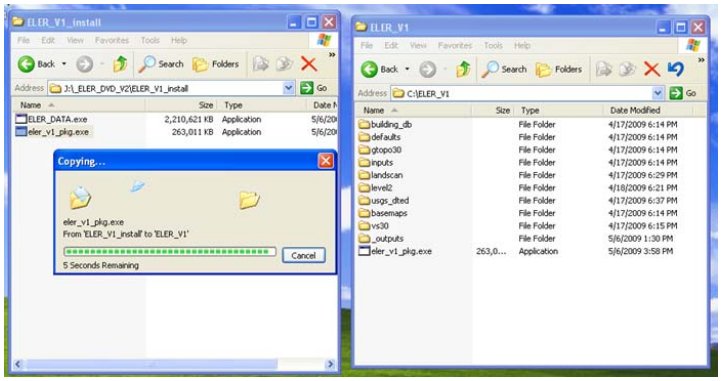

4) Then double click on ***eler_v3_pkg.exe***. The required files will be extracted.

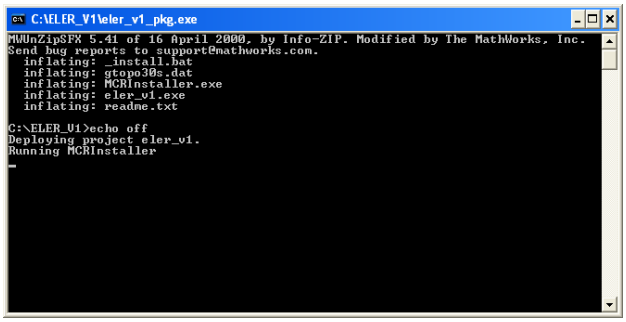

5) The installation of the MATLAB Runtime Components 7.9 will be initialized. Choose your preferences and proceed with the MCR installation.

6) After the MCR installation is completed your installation is complete. If you have changed the installation directories in the previous steps be sure to modify the ***eler_dirs.txt*** file accordingly. The first 6 fields of this text file are crucial for ELER and must point to the data folders extracted from the ELER DVD. The *hazard_outputs* field

should point to a valid, write enabled directory in your computer. The remaining input fields are set to point to the default inputs and example datasets.

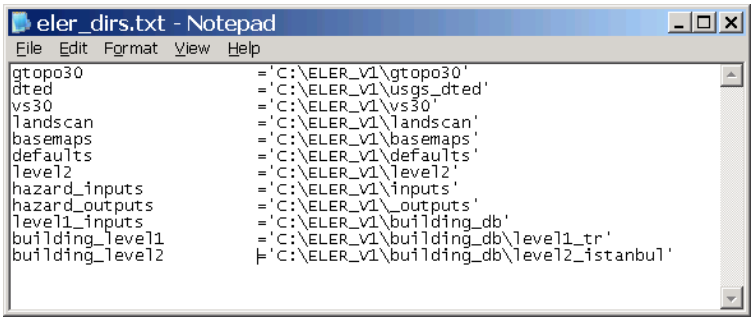

7) You can start ELER by double clicking on the ***eler_v3.exe*** file inside the ***C:\ELER_V3*** directory. It is recommended that you run ELER from the Command Prompt. This will enable you to see any error message during the process. Please note that in some systems you may encounter an error message indicating that "*mclmcrrt79.dll can not be found",* in such cases restarting your system will update your system path variables and the newly installed file will be found on your next run.

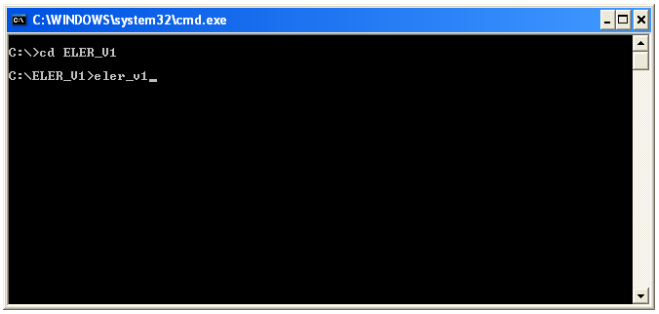

B.2. HAZARD MODULE

The Hazard Module can be run independently or in connection with the loss assessment modules. On the other hand the required ground motion parameters for each level of loss assessment can be calculated using the Hazard Module or provided externally.

The computation of ground motion parameters in the Hazard module is based on, but not limited to the ShakeMap methodology developed by Wald et al (1999a, 2003, 2005, 2006b). This Section B will cover the implementation of the ShakeMap algorithm and the new features developed in the ELER Software.

The user is capable of specifying all parameters, options and modes of the ground computation through the graphical user interface of the Hazard module. Firstly this input specification stage will be explained and then the implementation of the methodology will be presented.

B.2.1. Input Specification

The input specification of the Hazard Module is done by "Hazard" button in main GUI window. The flowchart and a snapshot of the Hazard GUI are given in Figure 17 and Figure 18.

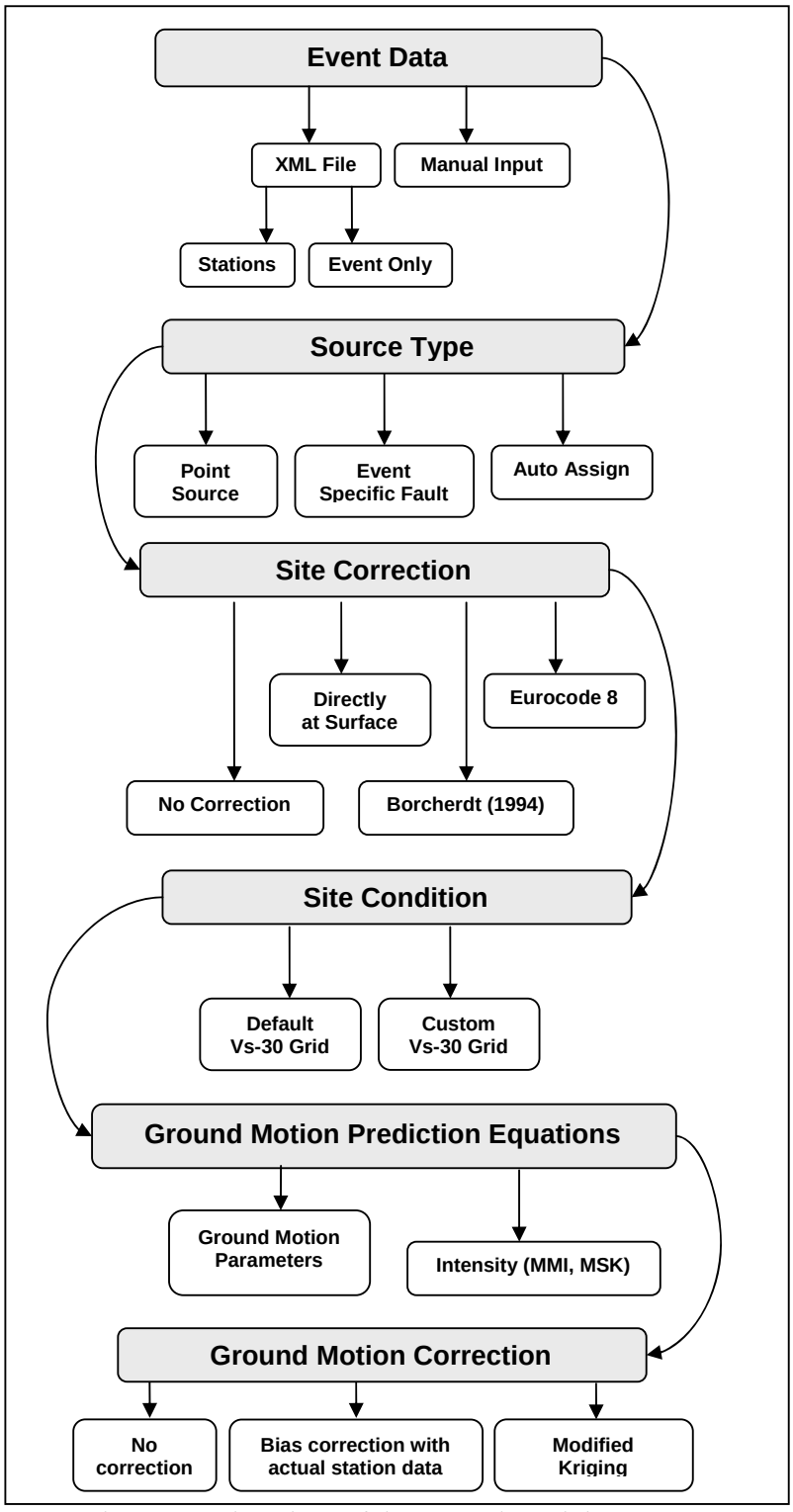

Figure 17. Flowchart of the Hazard Module GUI

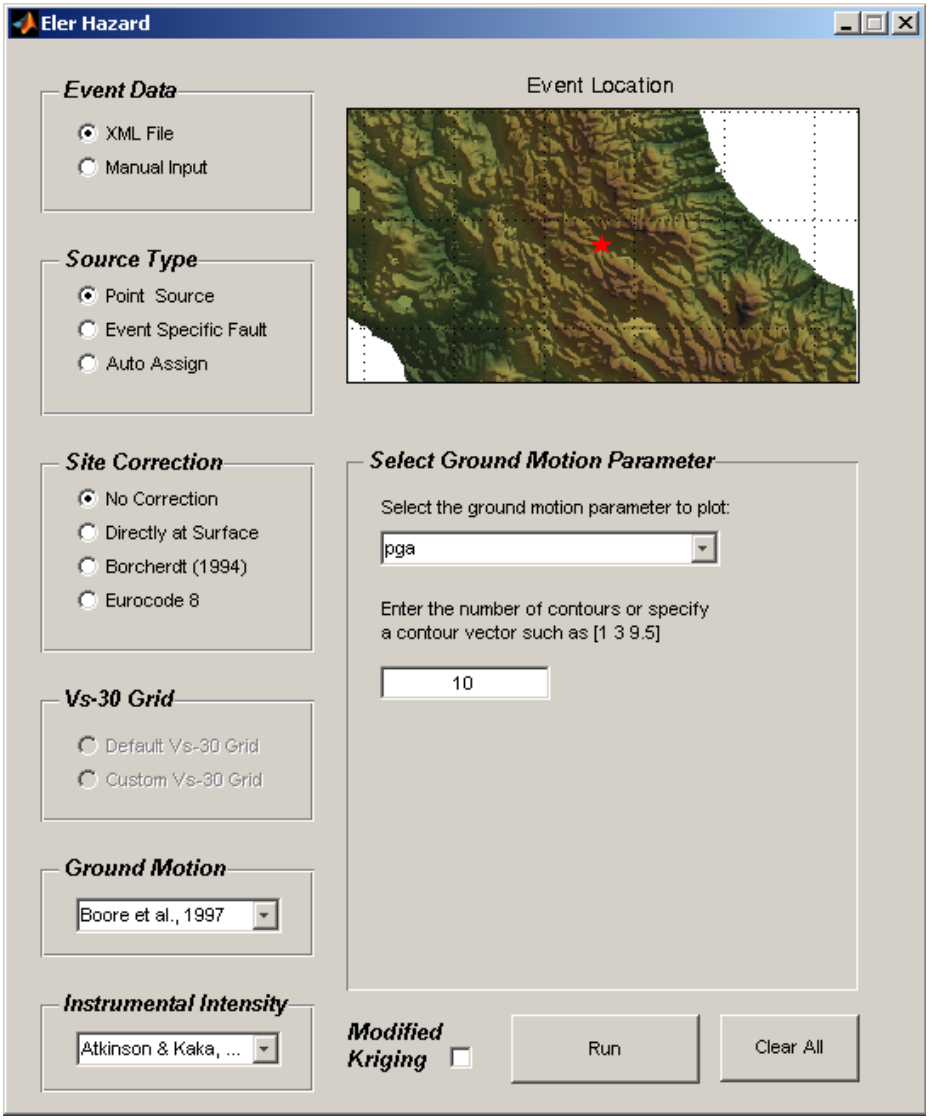

Figure 18. Hazard Module GUI

Event Data

The user has two options to enter the event data. The first option is to use an XML file containing the event parameters and station information, if available. The second option is to enter event data manually from the Hazard GUI.

XML Files

Similar to ShakeMap, ELER can be run using station list and event XML files as inputs. The original ShakeMap format is adopted for this purpose. An example event XML file is given below:

```
   <shakemap-data>
   <earthquake id="9583002_se" lat="38.11" lon="23.60" mag="6"
year="1992" month="3" day="13" hour="00" minute="00"
```

```
second="00" timezone="GMT" depth="10" locstring="Greece"
created="982348863"/>
   </shakemap-data>
```

If the XML file contains only event data, ELER uses only the location of the hypocenter and the magnitude of the event in the ground motion calculation.

An example station list XML file is given below:

```
   <shakemap-data>
   <earthquake id="51148805" lat="35.9533" lon="-120.5020"
mag="5.00" year="2004" month="09" day="29" hour="17"
minute="10" second="04" timezone="GMT" depth="11.47"
locstring="9 km NW of  Parkfield, CA" created="1122491643" />
   <stationlist created="1122491643">
   <station code="BDM" name="Black Diamond Mines Park"
insttype="" lat="37.953972" lon="-121.865540" dist="253.07"
source="Berkeley Digital Seismic Network" commtype="DIG"
loc="">
   <comp name="HLZ">
   <acc value="0.0094" flag="0" />
   <vel value="0.0202" flag="0" />
   </comp>
   <comp name="HLE">
   <acc value="0.0136" flag="0" />
   <vel value="0.0344" flag="0" />
   </comp>
   <comp name="HLN">
   <acc value="0.0092" flag="0" />
   <vel value="0.0177" flag="0" />
   </comp>
   </station>
   <station code="BKS" name="Byerly Seismographic Vault
   …
```

If the XML file is a station list file containing both event and station data (such as the one above) ELER takes into account both event data and the amplitudes of the horizontal components of the recorded event at the listed stations. This will be explained in detail in Section B.2.1

For more detailed explanation of the XML file format the user can refer to the ShakeMap Manual Section 3.6.

Manual Input

If the user selects the *Manual Input* option a panel with multiple input fields is activated. After entering the desired event specific values and clicking the *Save Event Data* button a map showing the epicenter of the event is generated (see Figure 19)

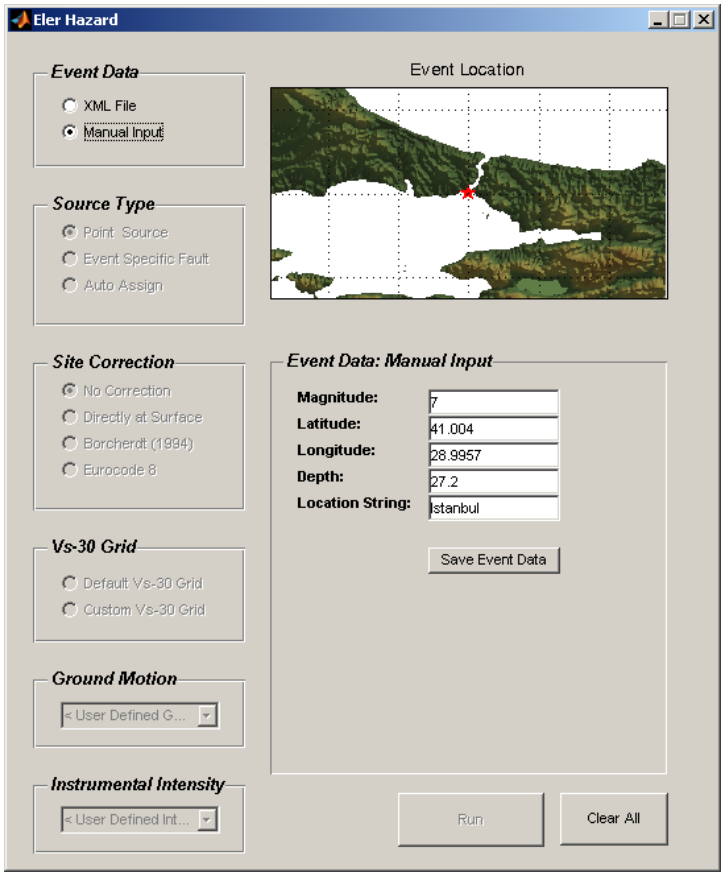

Figure 19. Manual input screen

Source Type

The *Source Type* panel defines the source mechanism associated with the event. For small magnitude events the source can be given as a point, for large magnitude events the user can specify the source type as a finite fault.

Point Source

In this mode a point source will be defined by the epicentral coordinates and the depth of the event. The ground motion distribution will be calculated for this point source.

Event Specific Fault

To define the source as a finite fault, the user should select a text file containing the coordinates of the ruptured fault. Examples of single and multi-segment fault files are given in Table 2.

Table 2. Single and Multi-segment Faults

```
>
 40.852921 28.218996
 40.900656 28.855777
 40.742723 29.229201
 40.741384 29.581306
>
```

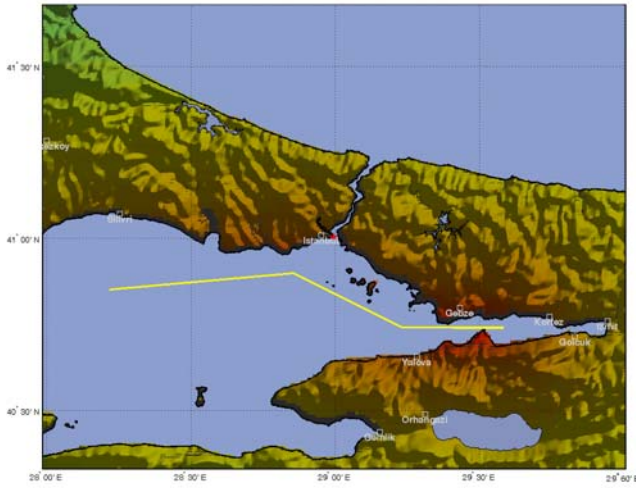

Single Segment Fault File

```
>
 40.714594 29.380615
 40.695632 30.671500
>
 40.689311 30.727665
 40.803988 31.028354
>
```

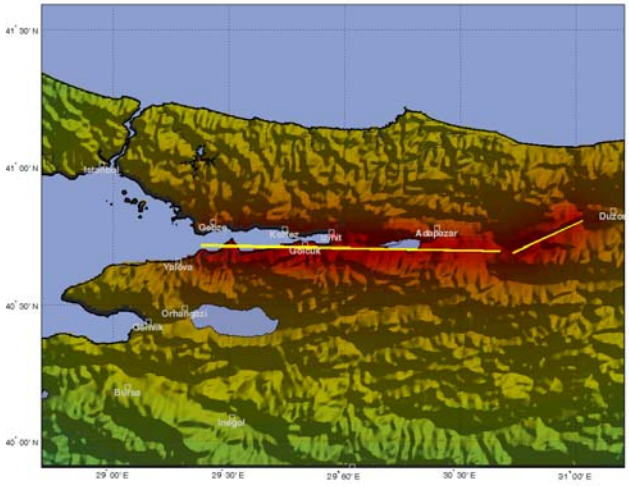

Multi-Segment Fault File

As given in Table 2 faults are defined by their vertices. For single segmented faults the source file should consist of the coordinates of each vertex as a pair of latitude and longitude separated by a space. The list of coordinates should begin and end with the '>' character.

For multi-segment faults each segment's vertices should be listed and enclosed by the '>' characters separately. The example multi-segment fault given in Table 2 consists of two segments each defined by two vertices.

Closed fault geometries are considered as fault projection planes.

Automatic Assignment of a Fault

One of the new features developed in ELER is the automatic assignment of a fault to an event. This procedure will be explained in detail in 0. In this mode the user is required to select a fault database containing the candidate faults. The fault database file has the same structure as a multi-segment fault file given in the previous section. Since in this mode each segment

represents a single candidate fault, the assignment always produces a single segment rupture. An example of a fault database file is given in

Table 3.

Table 3. Fault Database File

```
>
 40.142002 27.393937
 40.069300 27.295475
>
 40.064286 27.170756
 39.996599 26.993523
>
 40.852921 28.218996
 40.900656 28.855777
 40.742723 29.229201
 40.741384 29.581306
>
 39.758438 26.813008
 39.715820 26.721110
>
...
```

Fault Database File

Site Correction

The *Site Correction* panel determines how the effect of the local site conditions will be incorporated into the calculations of ground motion parameters. The modes presented in this section will be explained in detail in Section B.2.1.

No Site Correction

In this mode all ground motion estimations are calculated at the engineering bedrock. Site condition is not taken into account, thus the site condition selection panel remains disabled. Since site correction requires additional computing *No Correction* mode is considerably faster than the other site correction modes.

Borcherdt (1994)

In this method, also used in ShakeMap, all ground motion parameters are calculated at the engineering bedrock. The obtained grid based ground motion is then corrected with the site amplification factors (F_a and F_v) given in Borcherdt (1994) according to the selected Vs30 map. Since this procedure involves element-wise operations on large grids, it is considerably slower.

Eurocode 8

This mode differs from *Borcherdt (1994)* in the calculation of the site amplification factors. In *Eurocode 8* mode only the peak ground acceleration values are modified according to the site condition. Thus in this mode ELER produces only the site corrected PGA distribution. The same element-wise site correction procedure used in *Borcherdt (1994)* mode is utilized.

Calculation at Surface

In this newly developed approach rather than calculating bedrock values and then amplifying these with respect to site conditions, ELER uses ground motion prediction equations taking Vs30 (Boore et al., 1997, Campbell and Bozorgnia, 2008, Boore and Atkinson, 2008, Chiou and Youngs, 2008) as an input parameter to calculate the ground motion values directly at the surface.

Site Condition

In order to calculate the effect of the geologic conditions ELER needs the site condition map of the region. Site condition is represented by a parameter: the upper 30-m average shear wave-velocity (Vs30). The user has the following two options in choosing the site condition.

Default Site Condition Map

ELER comes with a default site condition map covering the entire Euro-Mediterranean region. The default site condition map has been compiled from the USGS Global Vs30 Map Server.

Custom Site Condition Map

Custom site condition maps should be in form of Vs30 grids. In MATLAB grids are defined by a matrix containing the values of each cell and a reference vector which is used to map each cell to its corresponding geographical location. An example of a grid matrix, its reference vector and the resulting map is given in Table 4. The first element of the reference vector defines the number of cells per degree while the second and third elements specify the latitude and longitude of the upper left corner of the grid.

Table 4. Grids in MATLAB

Grid Matrix + Reference Vector

```
grid_matrix =

   406   406   406   406   406 ..
   406   406   406   406   406 ..
   406   406   406   406   406 ..
   406   406   333   406   333 ..
   406   333   333   406   333 ..
   406   333   333   406   406 ..
   406   406   406   333   406 ..
   406   406   406   406   406 ..
   406   406   406   406   333 ..
   406   406   406     1   333 ..
   406   406   406     1     1 ..
   406   406     1     1   406 ..
   406   406   406     1   406 ..

ref_vector =

   80.0000   42.1051   25.6788
```

Map

```
geoshow(grid_matrix,ref_vector,...
'DisplayType','texturemap')
```

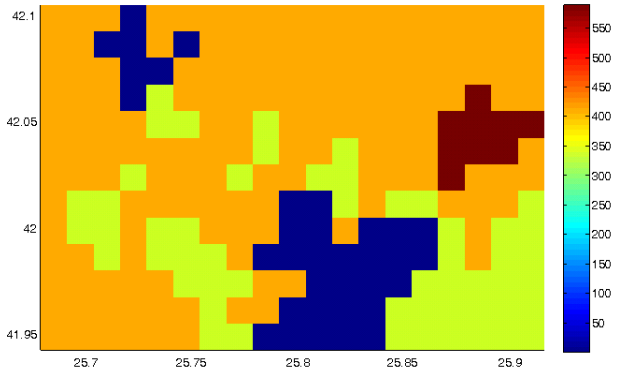

Ground Motion Prediction Equations (GMPEs)

The final stage of the input specification is the selection of ground motion prediction equations. Since different prediction equations are derived from different event catalogues the

user should select a suitable equation taking into account the regional characteristics, magnitude and ground motion parameter of interest. Detailed information about GMPEs coded in ELER can be found in Section C.2.1.

Ground Motion Estimation

The selected ground motion prediction equation is used to estimate measurable ground motion parameters such as PGA and spectral accelerations. Each prediction equation has its unique set of input parameters resulting from the regression analysis. The common parameters such as event magnitude, distance to source and site condition are set automatically. The remaining parameters such as fault type, hanging wall effect etc. should be specified by the user.

Instrumental Intensity Estimation

The selected method is used to obtain the estimated intensity distribution.

Custom Ground Motion Prediction Equations

ELER Hazard Module also enables the user to define custom ground motion prediction equations (GMPEs). With this feature the user is able to input his/her custom GMPEs in a simple text file format. A user defined equation can also be used for the estimation of intensity values. The screen for custom GMPE selection is shown in Figure 20.

The user defined GMPEs can be functions of event and local parameters. In order to predict a ground motion at a given site the Hazard Module will invoke the user specified equation. The event and the local variables are assigned by ELER prior to the evaluation. Table describes these variables which can be used in the user defined custom GMPEs.

Table 5 Event and local parameters of custom GMPEs

Event parameters*:* Constant for every estimation node	***Local parameters*****:** Varying according to the location of estimation nodes
mag: magnitude of the event *depth*: focal depth of the event	*Rjb*: Joyner-Boore distance (distance to the vertical projection of the source) *Vs*: Average shear wave velocity for the top 30 m (determined from the site condition map used)

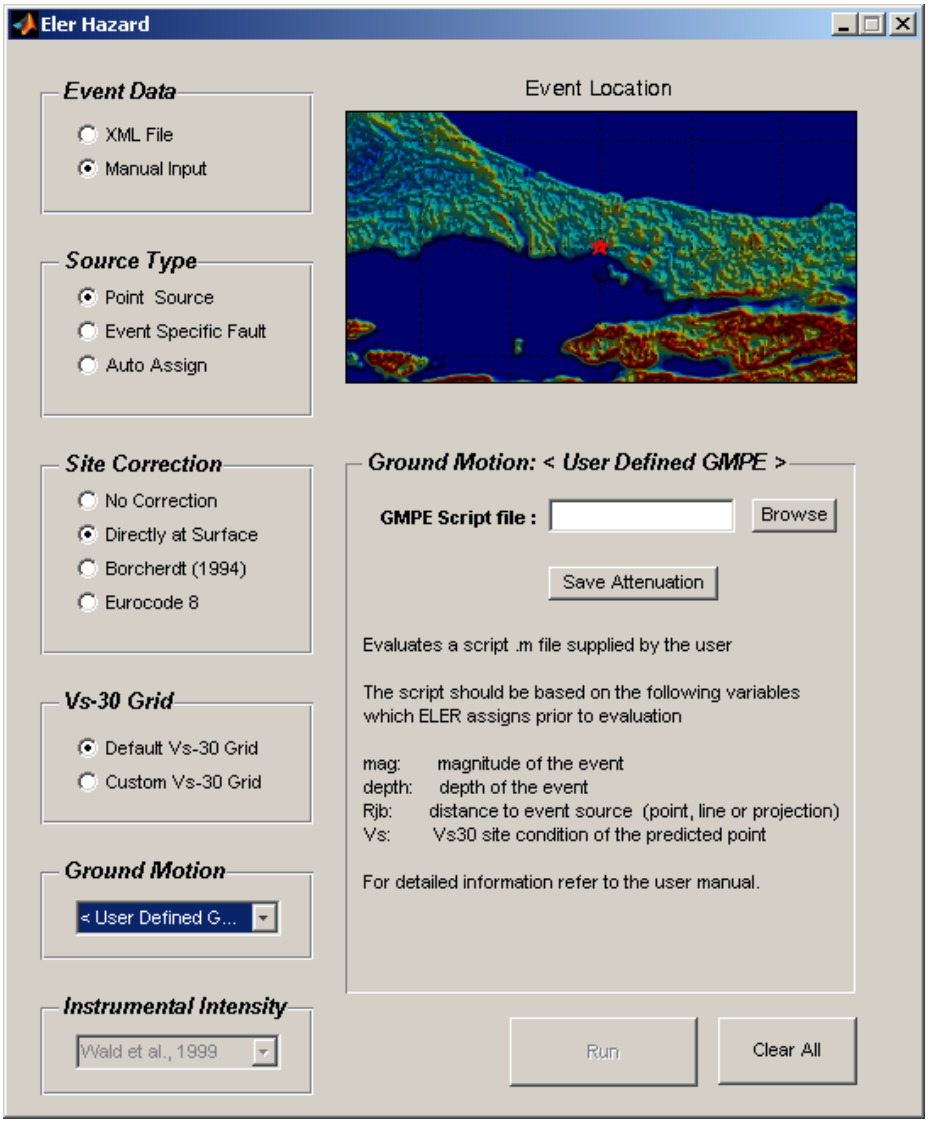

Figure 20. Custom GMPE input screen

The outputs of the user defined GMPEs should be assigned to a structure named *gmpe_out*. An example text file of user defined GMPE is given below. In this PHA equation of Campbell and Bozorgnia (1994) the pre-assigned variables *mag*, *Rjb* and are used. If a site correction option has been selected the GMPE is required to contain the variable *Vs*, to be able to take into account the site conditions. The GMPE will output the parameters *customR* and *pga* as they are assigned to the gmpe_out structure. Notice the user defined variables *F, Ssr* and *Shr* which are defined in the GMPE itself and then used to calculate the parameter *ln_pga*. For this equation *F* takes on values of 0 for strike-slip and normal faulting, and 1 for reverse and thrust faulting; *Shr* = 1 for hard rock sites, *Ssr* = 1 for soft rock sites and *Ssr* = *Shr*=0 for alluvium sites. Note that these parameters are hard coded inside the GMPE text file, thus for different faulting and site conditions the text file has to be modified manually.

```
F       = 0;
Ssr     = 0;
Shr     = 1;
ln_pga  = -3.512 + 0.904*mag...
```

```
        -1.328*log(sqrt(Rjb^2+(0.149*(exp(0.647*mag)))^2))...
        +(1.125 - 0.112*log(Rjb) - 0.0957*mag)*F...
        +(0.440 - 0.171*log(Rjb))*Ssr...
        +(0.405 - 0.222*log(Rjb))*Shr;

gmpe_out.pga         = 100*exp(ln_pga);
gmpe_out.cutomR      = Rjb^0.5;
```

Similarly the user can define instrumental intensity prediction equations (IIPEs). The IIPEs use the parameters previously calculated with the GMPEs. Thus the variables in these equations are referred from a structure named *motion* (i.e *motion.pga, motion.pgv*). The outputs of the user defined IIPEs should be assigned to a structure named *intens_out*. An example user defined IIPE equation is given below.

```
intens_out = 5*(motion.psa02/(motion.pga+motion.pgv));
```

All parameters calculated by the GMPE can be used in the intensity estimation. For custom GMPEs these are the parameters assigned in the *gmpe_out* structure, whereas for the GMPEs included in ELER the calculated parameters are displayed as *Outputs* during the GMPE selection screen.

B.2.2. Algorithm

The main purpose of the ELER Hazard module is to compute ground motion parameters and intensity distribution based on the earthquake magnitude, epicenter location input and if available actual station records of the event. To achieve this, the concept of phantom stations is introduced (Wald et al 1999a, 2003, 2005, 2006b). When actual stations have little or no coverage for a region, an estimation is made as if there were an actual station. The results of these estimations are assigned to a point which is called a phantom station. The output of the Hazard module is basically a combination of ground motions taken from actual and obtained for phantom stations. Thus it would be suitable to break up the Hazard module into two cases: '*no actual stations*' and '*with actual stations*'. The procedure for each case with respect to the selected site correction mode is given in Table 6 and

Table 7.

Table 6. No actual stations

No Actual Stations (Only Phantoms)	
A. No Site Correction	Set Vs30=760 and calculate ground motions at phantom stations at engineering bedrock
B. Borcherdt / EuroCode 8	• Set Vs30=760 and calculate phantom stations at engineering bedrock • Correct the interpolated fine grid element-wise according to the Vs30 grid used: a.)Borcherdt coefficients (Fa, Fv) b.)EuroCode 8 Soil amplification factors for PGA only)

C. Directly at Surface	Get Vs30 value form the Vs30 grid. calculate ground motions At each phantom station with its corresponding Vs30 value.

Table 7. With Actual stations

With Actual Stations	
A. No Site Correction	• Set Vs30=760 and calculate ground motions at phantom stations at engineering bedrock • Calculate bias between the phantoms (at engineering bedrock) and actual stations (at surface) • Create ground motion grid from actual and phantom stations.
B. Borcherdt / EuroCode 8	• Set Vs30=760 and calculate phantom stations at engineering bedrock • Transfer the actual stations to engineering bedrock using the Vs30 grid. • Calculate bias between the phantoms (at engineering bedrock) and the transferred actual stations (at engineering bedrock) • Create ground motion grid from the transferred actual stations and phantom stations. • Correct the interpolated fine grid element-wise according to the Vs30 grid using: a.) Borcherdt coefficients (Fa, Fv) b.) EuroCode 8 soil amplification factors (for PGA only)
C. Directly at Surface	• Get Vs30 value form the Vs30 grid. Calculate ground motions at each phantom station with its corresponding Vs30 value. • Calculate bias between the phantoms (at surface) and the transferred actual stations (at surface) • Create ground motion grid from the actual stations and phantom stations

Ground Motion Estimation for a Single Point (Phantom Station)

In Hazard module ELER firstly creates a grid of phantom stations. The ground motion parameters at the phantom stations are calculated using the selected ground motion prediction equation. Parameters of the selected prediction equation such as distance to source and site condition change according to the phantom station location while others parameters as event magnitude, event depth remain constant.

The selected source type defines the calculation of the distances used in the ground motion estimation algorithm. For point sources; point to point, for a single segment faults; point to line and for multi-segment faults the minimum of each point to line distances is assigned as distance to source. An example for these three different cases is given in Figure 21.

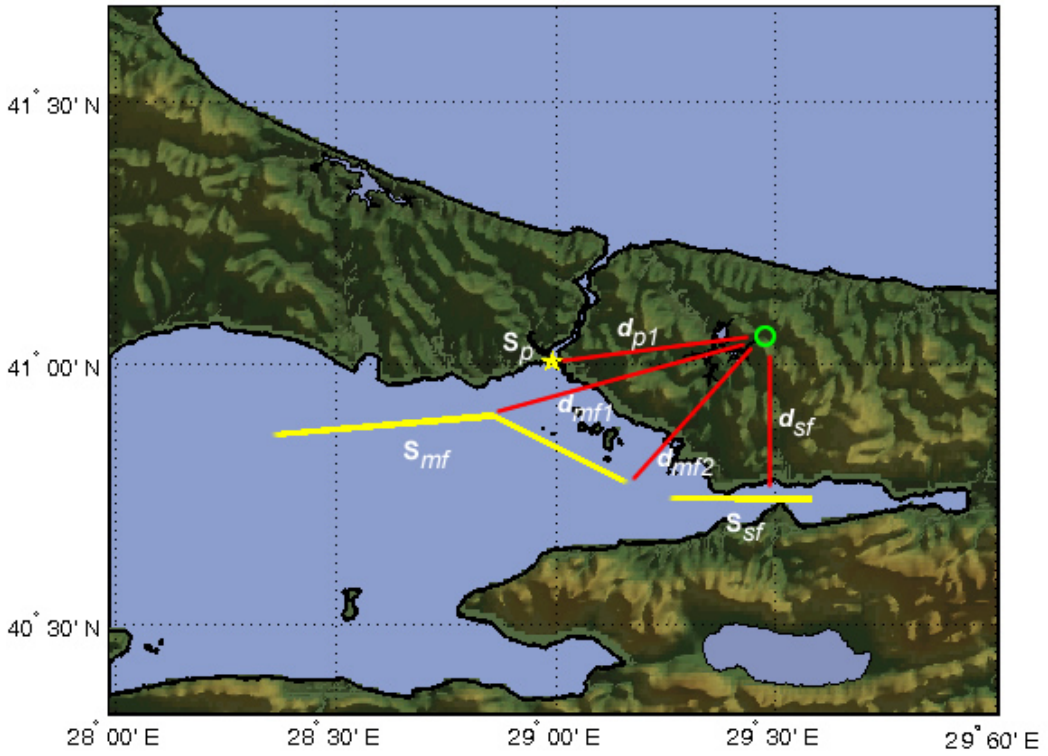

Point Source (S_P)	Single Segment Fault (S_{SF})	Multi-segment Fault (S_{MF})
d_{p1}	d_{sf1}	$\min(d_{mf1}, d_{mf2}) = d_{mf2}$

Figure 21. Distance to Source

For each phantom station, ELER computes the ground motion with the selected ground motion prediction equation. An example for the Boore & Atkinson (2008) ground motion prediction equation is given in Table 8. The input parameter *mag* (event magnitude) and the attenuation specific inputs *Fault_Type* (1 denotes unspecified fault), *std* (standard deviation multiplier) and *intens* (intensity prediction equation) remain constant for all phantom stations, while *Rjb* (distance to source) and *Vs* (Vs30 defining site condition) are dependant to the location of each phantom station.

Table 8. A ground motion prediction equation

Input Parameters	Output Parameters

`mag = 6`
`Rjb = 10`
`Vs = 680`
`Fault_Type = 1;`
`std = 0;`
`intens = 'Reg_Intens_wald(motion.pga,motion.pgv)';`
 	
`Ground Motion Prediction Equation (GMPE):`
	`pga: 13.1644`
	`pgv: 7.6074`
	`psa02: 30.4551`
	`psa03: 24.0913`
	`psa10: 6.9799`
	`psa30: 1.4004`
	`intens: 5.7147`

`Atten BA 2007 arr(mag,Rjb,Vs,Fault Type,std,intens)`	

The Boore & Atkinson (2008) ground motion prediction equation Table 8 takes Vs30 as input parameter, thus it is possible to calculate the ground motion directly at the surface. However when the site correction mode is set to Borcherdt (1994) ELER uses a different approach for estimating the surface ground motion values. Firstly ELER makes the estimations on engineering bedrock level (Vs30 is set to 760 m/s for ground motion prediction equations which take Vs30 as an input) then the obtained ground motion values are corrected with the short and long period site amplification factors (F_a and F_v) given in Borcherdt (1994). Please refer to Section C.2.3 for details.

In Eurocode 8 site correction mode only the PGA estimation is taken into account. The estimations are made for bedrock level as in Borcherdt (1994) mode. Then according to Eurocode 8 a soil type is assigned to the Vs30 value of each station, a site amplification factor is selected from Table 17 through Table 19, given in Section C.2.3 of the Technical Manual depending on the magnitude of the event. The PGA estimated at engineering bedrock is then multiplied with this factor and the site corrected value is obtained.

Combining Actual and Phantom Stations

When there are no actual station recordings the grid based ground motion distribution is obtained by interpolating the phantom station to a denser grid. By default phantom stations are placed at an interval of 11.11 km then these are interpolated to a denser grid with intervals of 1.5 km. These values can be changed from the *eler_pref.txt* file according to user needs.

If the site correction mode is selected as Borcherdt (1994), each of these dense points is site corrected according to the site amplification factors (F_a and F_v). Whereas if the site correction mode is chosen as *Directly at Surface*, the site correction is done implicitly since the attenuation is a function of the Vs30 parameter. Thus in this mode it is not needed to correct the interpolated grid. Figure 22 shows the results of these two modes. The jerky contours in Borcherdt (1994) mode are result of the dense site correction.

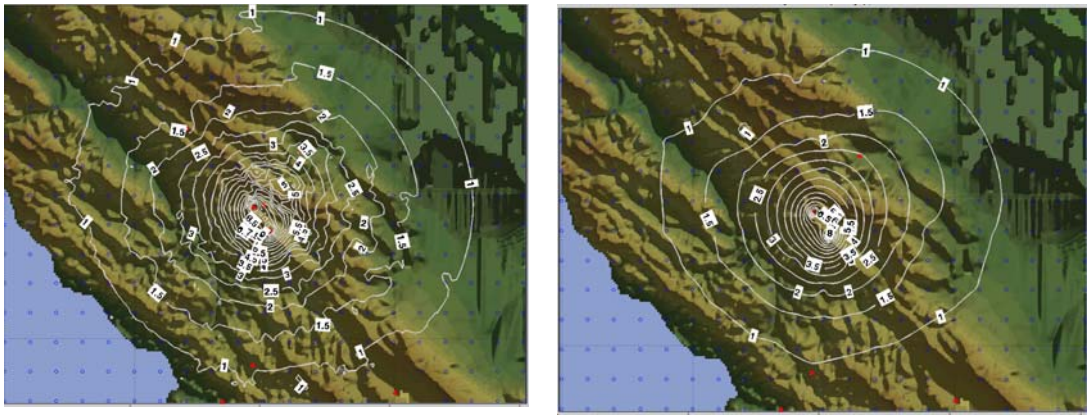

Borcherdt (1994) Directly at Surface

Figure 22. Comparison of site correction modes

If there are actual station recordings for an event, these are given precedence. In order to achieve this firstly all phantom stations in the vicinity of actual stations are discarded. This vicinity is defined by a radius *pthresh* (10 km). Also if there are no actual stations in the vicinity of the epicenter, defined by a radius of *cthresh* (15 km), the epicenter itself is added as a new phantom station. This procedure is illustrated in Figure 23 where two actual stations cancel a total of eight phantom stations and the epicenter is added as a new phantom station since there are no actual stations nearby.

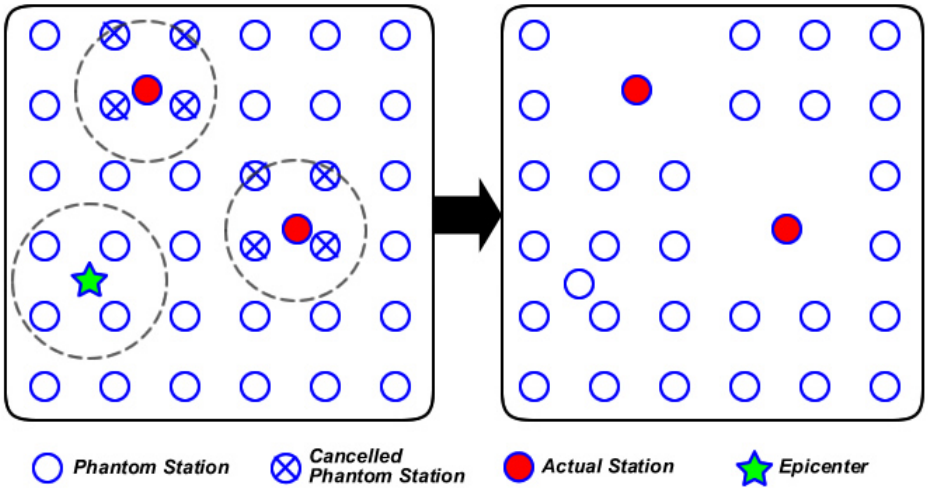

Figure 23. Combining Actual and Phantom Stations

In order to optimize the predictions at the phantom stations with respect to actual stations, bias factors are computed for each ground motion parameter. These bias factors minimize the difference between actual station values and the predictions at those sites. In Borcherdt (1994) site correction mode this comparison is made at engineering bedrock. In order to achieve this actual station values are transferred to bedrock. In *Directly at Surface* mode actual station values are compared with the estimated values at the surface.

An example of the bias correction procedure is given in Figure 24. In this particular case eight actual stations are presented. The actual values of PGA are compared with the predicted values using a ground motion prediction equation. The bias factor is calculated in order to minimize the absolute deviation. The sum of the absolute error has been lowered from 10.9064 to 6.7294 with the calculated bias factor of 1.38.

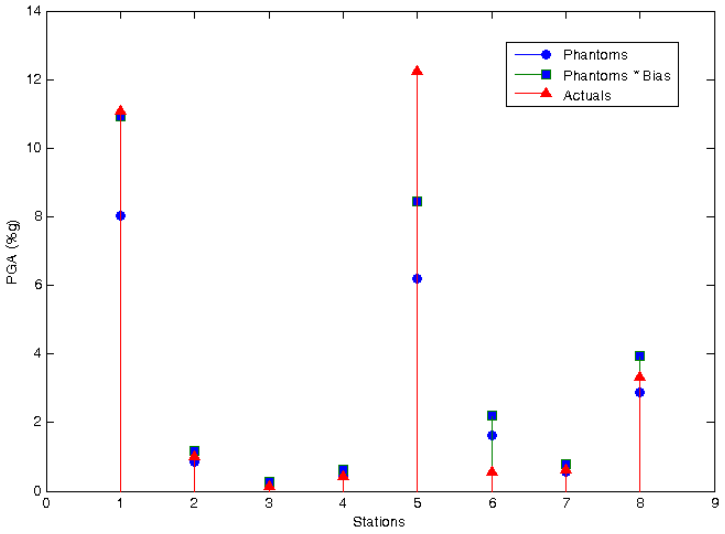

Figure 24. Bias correction

Modified Kriging Method

In regions with dense station coverage instead of using interpolation, ELER will implement the modified kriging method in order to assign ground motion values to regions in the vicinity of the stations. The method is independent of region, event, and past or future data and relies on station data obtained from a certain earthquake to estimate regional distribution of ground motion parameters for the same event. When actual station (observed) data are used for ground motion estimation, ELER implements the modified kriging method in regions which satisfy a certain coverage condition. The ground motion distribution in the remaining regions is calculated using the default Hazard module methodology.

For events with actual station recordings (i.e events with a *stationlist* element in their XML file) when the modified kriging checkbox is ticked (see Figure 2) ELER will firstly determine if the method is applicable by checking the coverage condition. A given point will satisfy the coverage condition if it is within the range of a minimum number of stations. The range and the minimum number of stations can be defined by the user via the *mdk_radius* and *mdk_minsta* parameters in the *eler_prefs.txt* file. Figure 26(a) shows the region which satisfies the coverage condition of being 10 km in the range of at least 5 stations, the distribution of stations is given in Figure 26(b). The coloring of the kriging region depicts the number of stations covering a single point, thus the warmer colors in the center where the stations are denser.

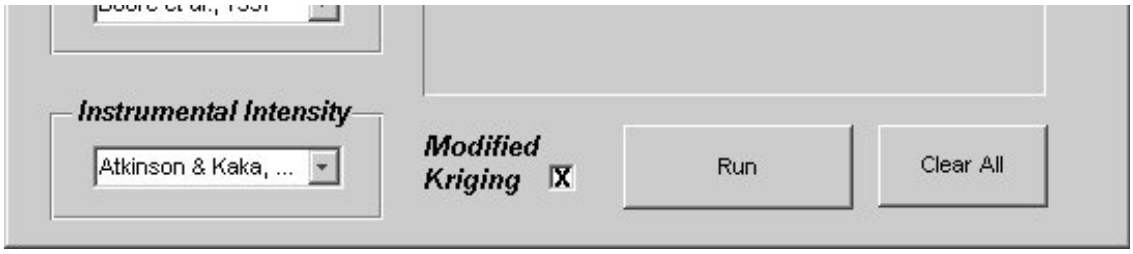

Figure 25. Modified Kriging checkbox

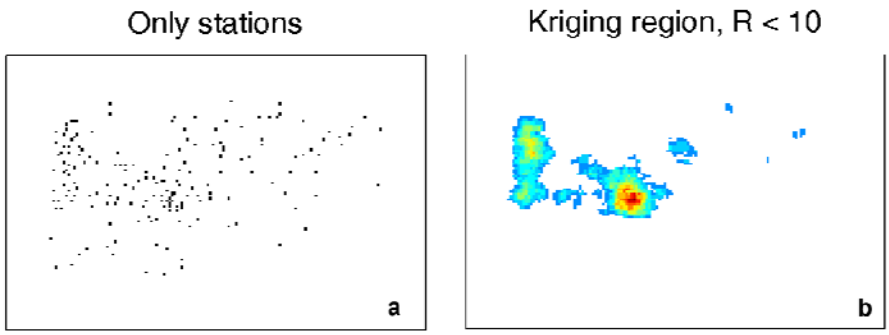

Figure 26. Kriging region for *mdk_radius* =10 and *mdk_minsta* = 5

Following the determination of the kriging region, for each point of the interpolation grid in that region ELER estimates the ground motion using data from all the stations within its range. The resulting kriged grid is embedded into the already calculated ground motion distribution grid. In this way the points which do not satisfy the coverage conditions remain unaltered by the modified kriging method.

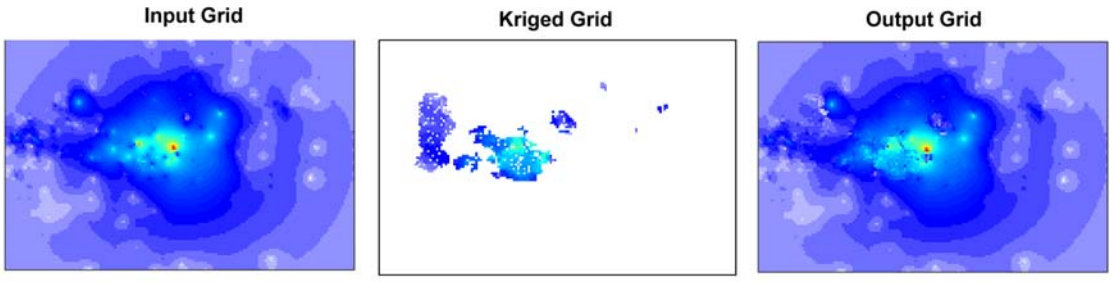

Figure 27. Modified kriging input and output grids.

Figure 26 and Figure 27 graphs are saved in the hazard module output directory if modified kriging method is invoked. Detailed information about the estimation of ground motion values with the modified kriging method is given in the Technical Manual.

Automatic Fault Assignment

Automatic fault assignment procedure reads all candidate faults in the region from the fault database selected by the user. The fault with the minimum epicentral distance is selected automatically to be ruptured. The rupture length is calculated with Wells & Coppersmith's (1994) equation according to the event magnitude and fault type. The selected fault's nearest point to the epicenter is taken as the center of the rupture. From this point on there are a total of three possible cases. These cases are presented for a selected fault with a length of 38.5 km in Figure 28 as an example.

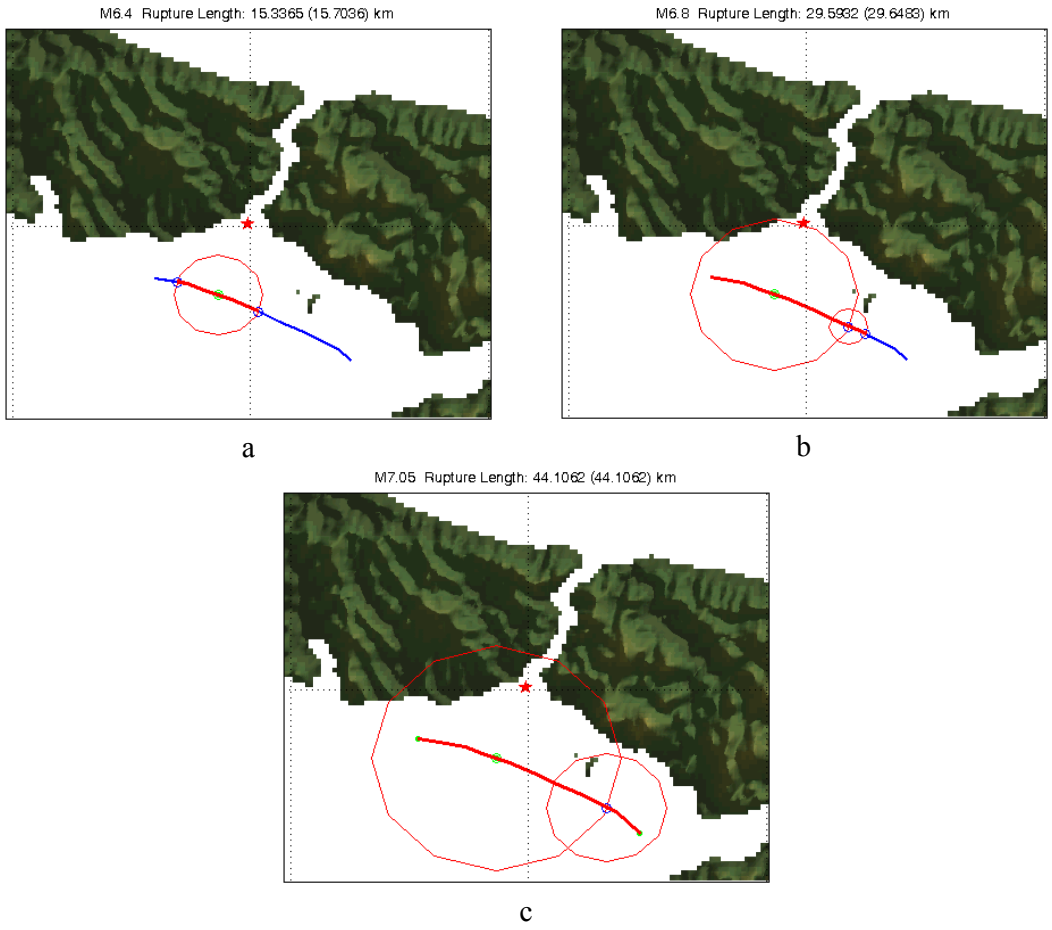

Figure 28. Calculation of fault rupture

Firstly ELER tries to extend the rupture in both directions. A circle with the radius of the calculated rupture length and a center point located at the nearest point to the epicenter (shown as a green dot) is plotted. If the limits of the selected fault are not exceeded the fault rupture geometry is defined by the intersection of the selected fault and the circle (see Figure 28.a).

If the rupture length is not greater than the selected fault length but the rupture exceeds the limits of the fault in one direction, ELER calculates the exceedance and plots an additional circle with a radius of this exceedance. The fault rupture geometry is defined by the intersection of the selected fault and these two circles (see Figure 28.b).

When the rupture length exceeds the fault length, ELER extends the fault equally from both ends in order to match the calculated fault rupture length (see Figure 28.c).

Proceeding to other levels

The user will be allowed to proceed directly to the building/pipeline damage or casualty assessment module according to the ground motion parameter selected for output. Table 9 presents these modules with the ground motion parameters required for directly proceeding from the Hazard module.

Table 9. Proceeding from Hazard to Damage and Loss

Ground Motion Parameters	***Loss Assessment Module***
Instrumental Intensity	Level 0 or Level 1
Peak Ground Acceleration	Level 2 (EC8)
Peak Ground Velocity	Pipeline Damage
Peak Spectral Acceleration (at 0.2s and 1.0s)	Level 2 (IBC2006)

B.2.3. Outputs

In addition to the ground motion distribution figures generated by MATLAB, these maps are also optionally saved in Google Earth KML file format. The default ShakeMap intensity colormap is used for intensity. For all other ground motions plots the HSV colormap is used. Figure 29 and Figure 30 show these different KML outputs and their colormaps (see Section B.8).

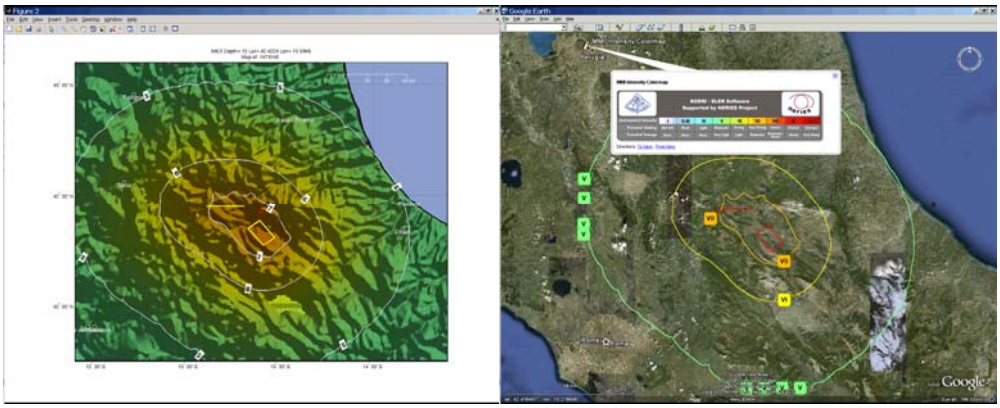

Figure 29. Intensity figure and KML output

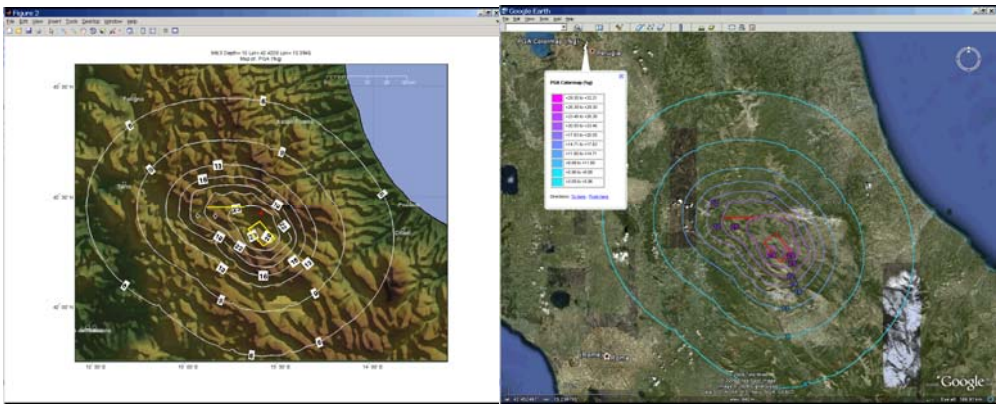

Figure 30. PGA figure and KML output

The estimated ground motion distribution grids are also saved as XYZ text files (Figure 31). The coordinates and the estimated ground motion value of each interpolation node are written

into a XYZ text file as [latitude – longitude – ground motion value]. For denser interpolation grids the resulting text file will be larger and the required computation time will also increase.

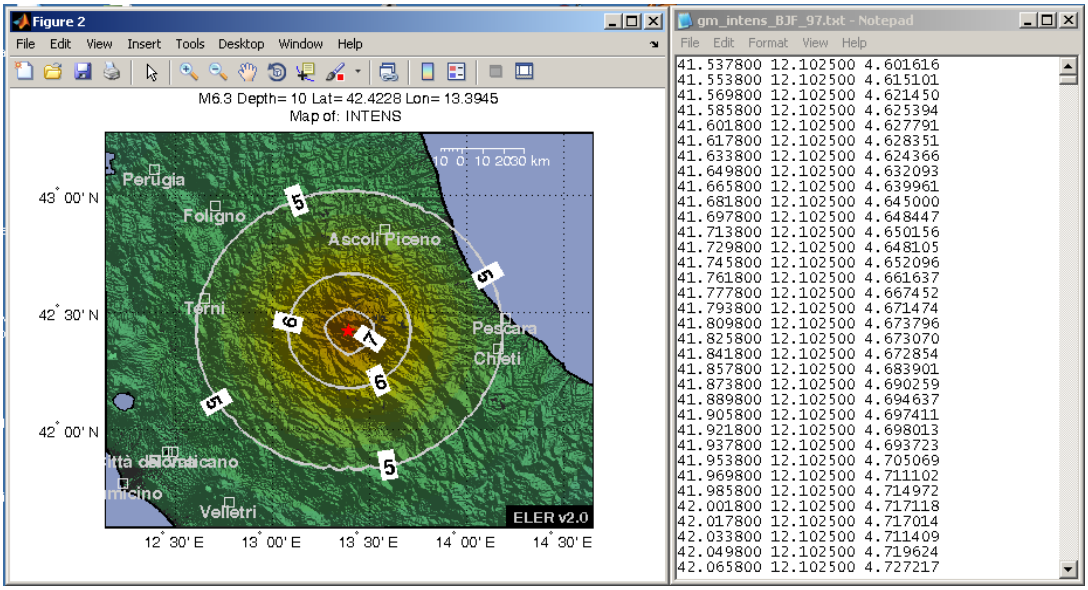

Figure 31. Ground motion XYZ text output

B.3. LEVEL 0 MODULE

For a given region Level 0 Module uses intensity and population distribution to make casualty estimations. A snapshot of the Level 0 Module GUI is given in Figure 32.

B.3.1. Input Specification

If the user proceeds to Level 0 directly from the Hazard Module then all fields are automatically set. If the user starts the analysis from Level 0, the following inputs should be specified.

Intensity Grid

Intensity grid should be a MATLAB (.mat) file containing a grid matrix and a reference vector. The intensity grid is defined similarly to the custom site condition map given in Section B.2.1

Source

If the event source is a point, this field should contain a vector specifying the epicenter coordinates in the form of *[latitude longitude]*. If the event source is a finite fault, this field should contain the name of a *filename.mat* containing the fault geometry. The *filename.mat* file should include a structure containing the latitudes and longitudes of the fault vertices. An example is given below:

```
fault(1).lat =[40.7146 40.6956]
```

```
fault(1).lon =[29.3806 30.6715]
```

Magnitude

Level 0 casualty estimation routines except RGELFE (1992) take the magnitude of the event as parameter (Section C.4.1). Thus the user should provide the event magnitude via this field.

B.3.2. Algorithm

Samerdjieva & Badal (2002)

In this approach ELER incorporates the following procedure:

Firstly a single density value is calculated by dividing the total population residing inside the intensity VI+ contour by the encircled area. A casualty estimation is computed with Samerdjieva & Badal (2002) approach using the calculated density and the event magnitude.

The estimated casualty is distributed over the intensity contours according to each contour's distance to the source mechanism. Detailed information is given in Section C.4.1 of the Technical Manual.

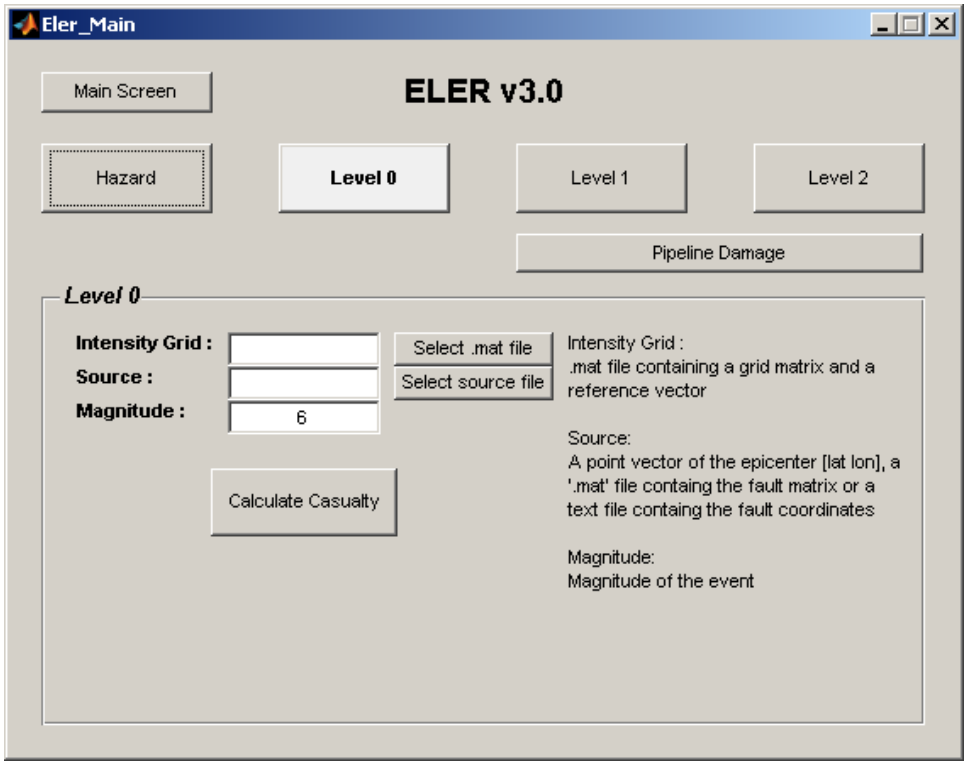

Figure 32. Level 0 Module GUI

RGELFE (1992)

This procedure involves the calculation of the total population residing in the intensity zones VI, VII, VIII and IX. The casualty is calculated by multiplying each intensity zone's population with its corresponding casualty rate given in Section C.4.1 of the Technical Manual.

Vacareanu et al. (2004)

This approach uses only the event magnitude to calculate an estimated casualty. The lower and upper boundaries of confidence are calculated together with the median values. Detailed information is given in Section C.4.1 of the Technical Manual.

B.4. LEVEL 1 MODULE

The Level 1 loss estimation engine is based on macroseismic damage estimation tools and aims at the assessment of both the building damage and the casualties. The intensity based empirical vulnerability relationships of Giovinazzi and Logomarsino (2005) and casualty vulnerability models based on various approaches are utilized.

B.4.1. Input Specification

The input specification of the Level 1 Building Damage Module is done via the Level 1 GUI window. A snapshot of the Level 1 GUI is given in Figure 33.

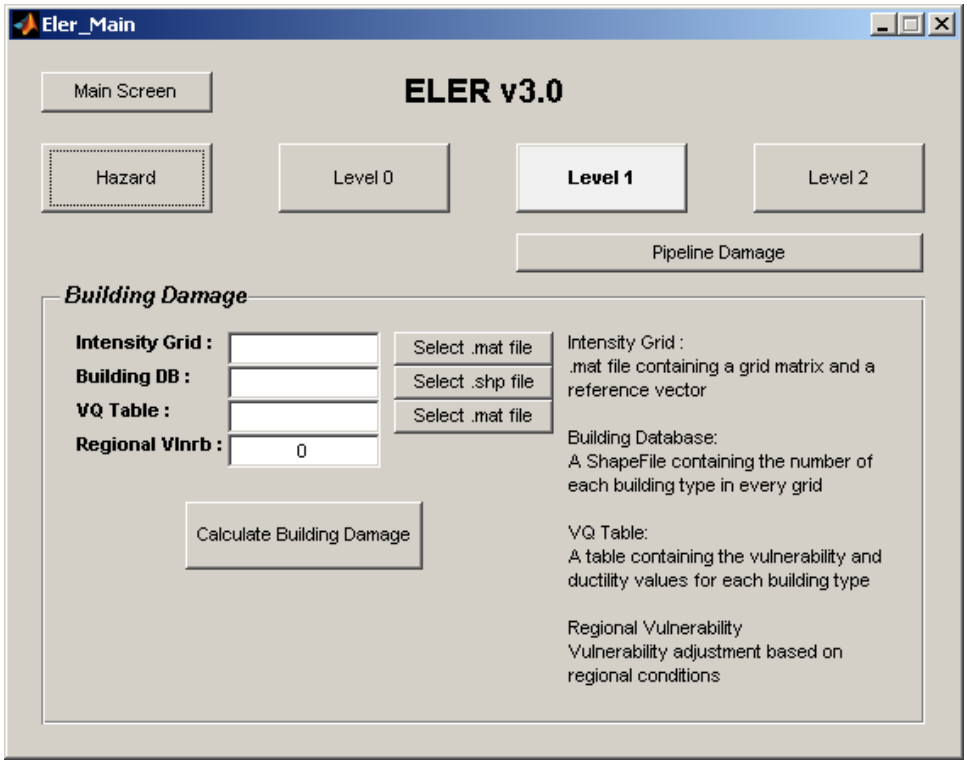

Figure 33. Level 1 Building Damage Module GUI

Intensity Grid

Intensity grid should be specified similarly to Level 0 (see Section B.3.1).

Building Database

The building database file is basically a Shapefile (.shp) containing the building distribution for each cell. Additionally this file may contain the population of each cell for the computation of casualties. If there is no *POPULATION* field in the building database, casualty estimations are calculated with the approximation of the regional population (obtained from the Land Scan population distribution). The structure of building database shapefile is given in Table 10.

Table 10. Structure of building database shapefile

Shape File Field Name	*Description*	
Geometry	Defines the type of the Shapefile. Possible values are 'Point', 'Multipoint', and 'PolyLine'. Only 'Polygon' is relevant for ELER damage analysis.	Standard
Bounding Box	Defines the lower right and upper left corners of the cell.	
X (Lat)	Defines the polygon's vertices' latitudes	
Y (Lon)	Defines the polygon's vertices' longitudes	
M1_L	The number of each building type should be given in its corresponding field.	User Defined
RC3_DCL_II_H		
….		
POPULATION	If this field exists casualty will be calculated according to each cells population, otherwise regional population approximations will be used	
TOTAL_BLD	Total number of buildings in each cell.	

Vulnerability-Ductility Table

The vulnerability-ductility table should be a MATLAB (.mat) file containing a table defining each building types vulnerability, ductility, t parameter and replacement cost. An example table for Italian buildings is given in Figure 34. ELER searches the building database for each building type defined in the vulnerability-ductility table and if found proceeds with the damage calculation.

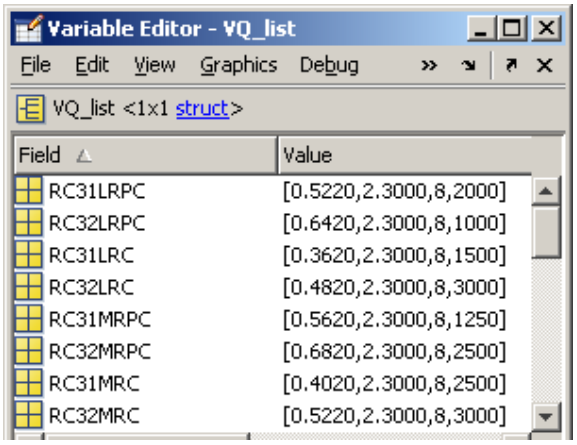

Figure 34. Vulnerability-Ductility Table

Regional Vulnerability

This parameter is used in the region dependant adjustment of the building vulnerabilities. Detailed information is given in Section C.4.2 of the Technical Manual.

B.4.2. Algorithm

Building Damage Estimation

The approach used in Level 1 damage estimation is to obtain a normally distributed cumulative damage probability for each building type. The damage probability distribution is a function of each building's vulnerability and ductility parameters (Lagomarsino and Giovinazzi, 2006). As mentioned above, these parameters are given for each building type in the *VQ Table*. The cumulative damage probability is discretized to obtain the five damage states given in Table 11.

Table 11. Level 1 Damage States

D1	Slight Damage
D2	Moderate Damage
D3	Substantial to Heavy Damage
D4	Very Heavy Damage
D5	Destruction

Casualty Estimation

Coburn & Spence 1992

The number of buildings and population in each cell are the main parameters to estimate casualties. To obtain casualty estimations from the number of buildings in different damage states, an average number of population per building should be known. To estimate this, the user should define an average number of dwelling units per building type, which is usually a function of the number of floors. Using the user-defined average number of dwellings per

building type and the grid based population data (POPULATION field) entered by the user, or the default Landscan population data of the region, the program computes an average number of population per dwelling unit, which in turn can be used to check if the estimated number of dwellings per building type were correct. For each of the two cases, the population is distributed to each building type according to the *Dwelling per building vector*. This vector specifies the number of dwellings in each rise class. For instance, the vector [3 12 18] specifies that there are 3 dwellings in low rise, 12 in mid rise and 18 dwellings in high rise buildings.

In order to take this dwelling information into account, the user should specify the buildings' rise classification. Also since different casualty rates are used for masonry and reinforced concrete buildings, these should also be specified. The specification of rise and building class is done by selecting the radio buttons on the appropriate column. *L, M*, and *H* are the rise columns, while *RC* and *MS* represent the structural type (masonry or reinforced concrete).

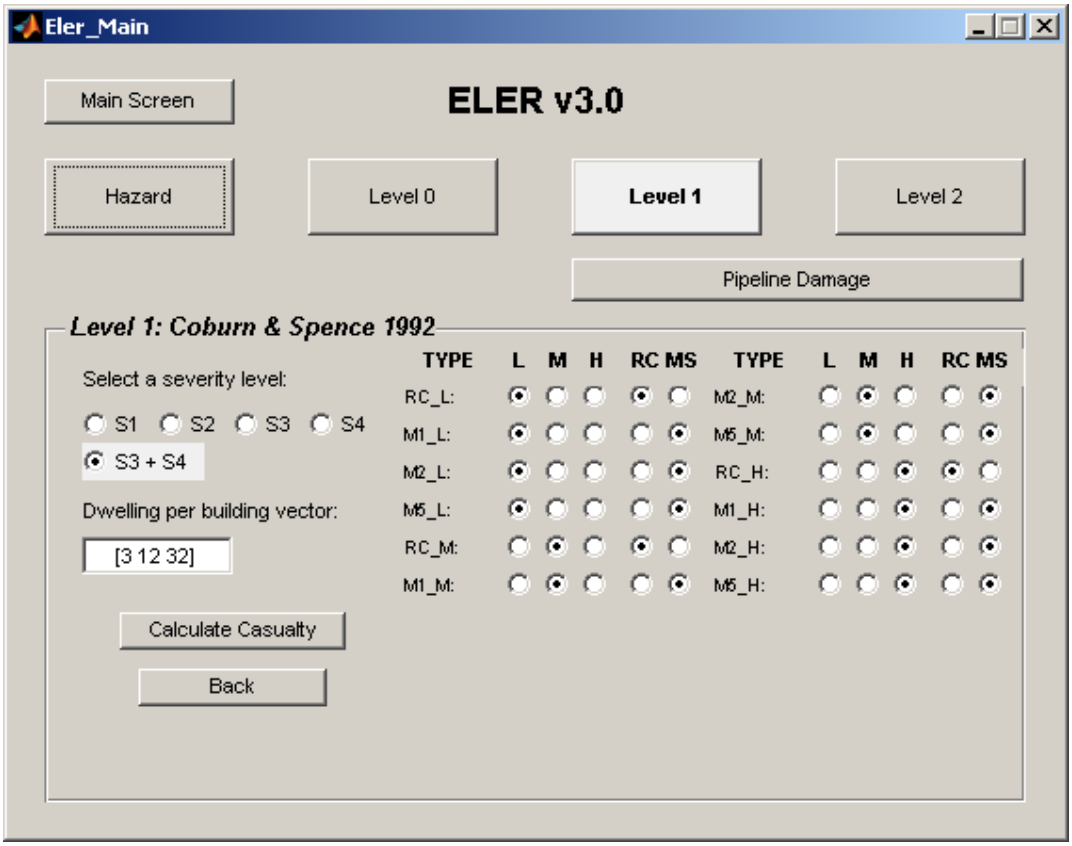

Figure 35. Casualty Estimation (Coburn & Spence 1992)

Risk-UE

The computation procedure in this approach is similar to Coburn & Spence 1992. To use this method, the user has to specify the *Dwelling per building vector* and the building rise classification.

KOERI, 2002

This approach is based only on building damage results, the population data is not taken into consideration. For the assessment of human casualties from damage data computed from intensity based vulnerabilities number of fatalities is taken equal to the number of buildings in D4 and D5 damage states. The number of hospitalized injuries is found by multiplying the death figure by 4 based on ATC-13 recommendations.

Economic Loss Estimation

The economic loss is calculated by multiplying a building's replacement cost with the loss ratio corresponding to its damage state. Buildings' replacement costs are specified in the vulnerability-ductility table prior to analysis. The user can choose to visualize the economic loss distribution for all buildings or a specific building type only. The graphical user interface of the economic loss module is given in Figure 36.

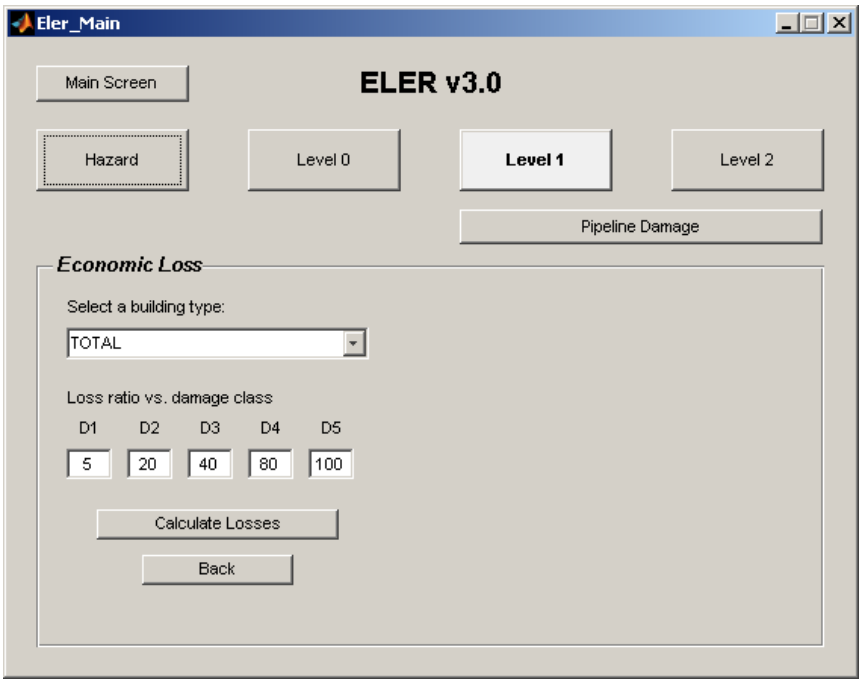

Figure 36. Economic Loss GUI

B.4.3. Outputs

In addition to the building/pipeline damage and casualty distribution figures generated by MATLAB, these maps are also optionally saved in shape file format (see Section B.8). These files can be manipulated with GIS editors for custom visualization and further analysis. Figure 37 shows a shapefile output of ELER together with its attribute table.

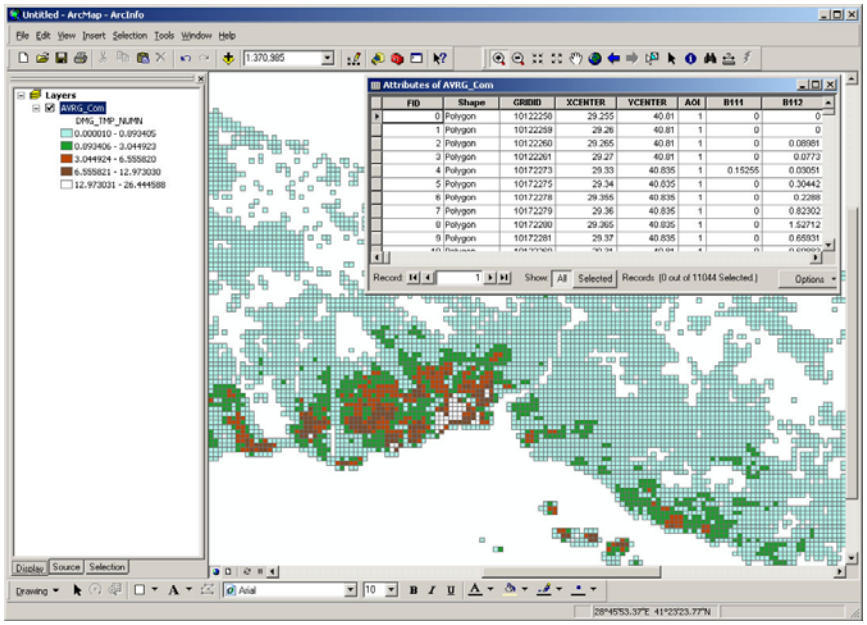

Figure 37. Shapefile output

B.5. LEVEL 2 MODULE

The spectral capacity-based vulnerability assessment methodology is utilized for the building damage estimation by Level 2 Module. The main ingredients of the capacity spectrum method can be summarized as follow:

- Seismic demand representation : Demand Spectrum
- Structural system representation : Building Capacity Spectrum
- Structural response assessment : Performance Point
- Representation of the damage probability : Fragility Curves

The user must specify the seismic demand and building capacity spectra for the calculation of the performance point. The damage probabilities at each damage state are calculated by use of fragility curves. Casualties are estimated based on the number of buildings in different damage states and the casualty rates for each building type and damage level.

B.5.1. Input Specification

The input specification of the Level 2 Module is done by “Level 2” button in main GUI window. A snapshot of the Level 2 GUI is shown in Figure 38.

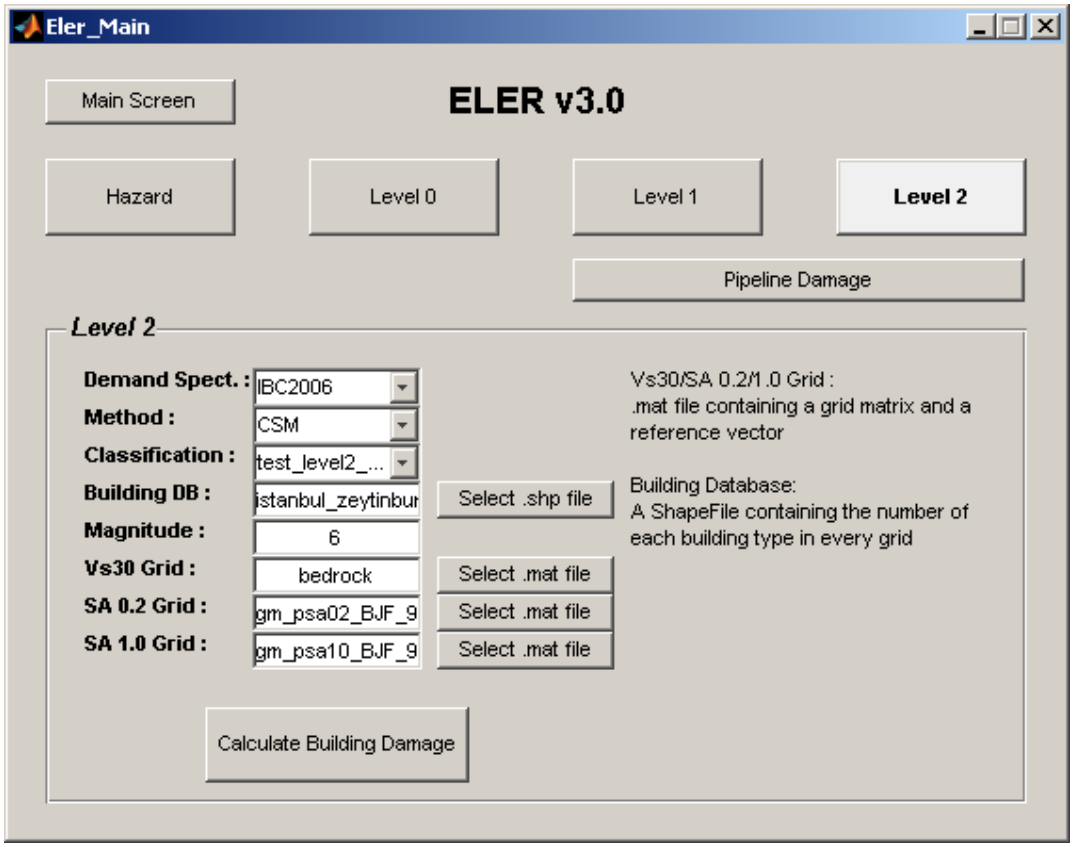

Figure 38. Level 2 GUI

Demand Spectrum

There are two options for the representation the seismic demand. The construction of the 5%-damped elastic response spectra is based on:

1. Euro Code 8 Spectrum
2. IBC 2006 Spectrum

The user must select one of the design spectra from pull-down menu of demand spectrum as provided in Figure 39.

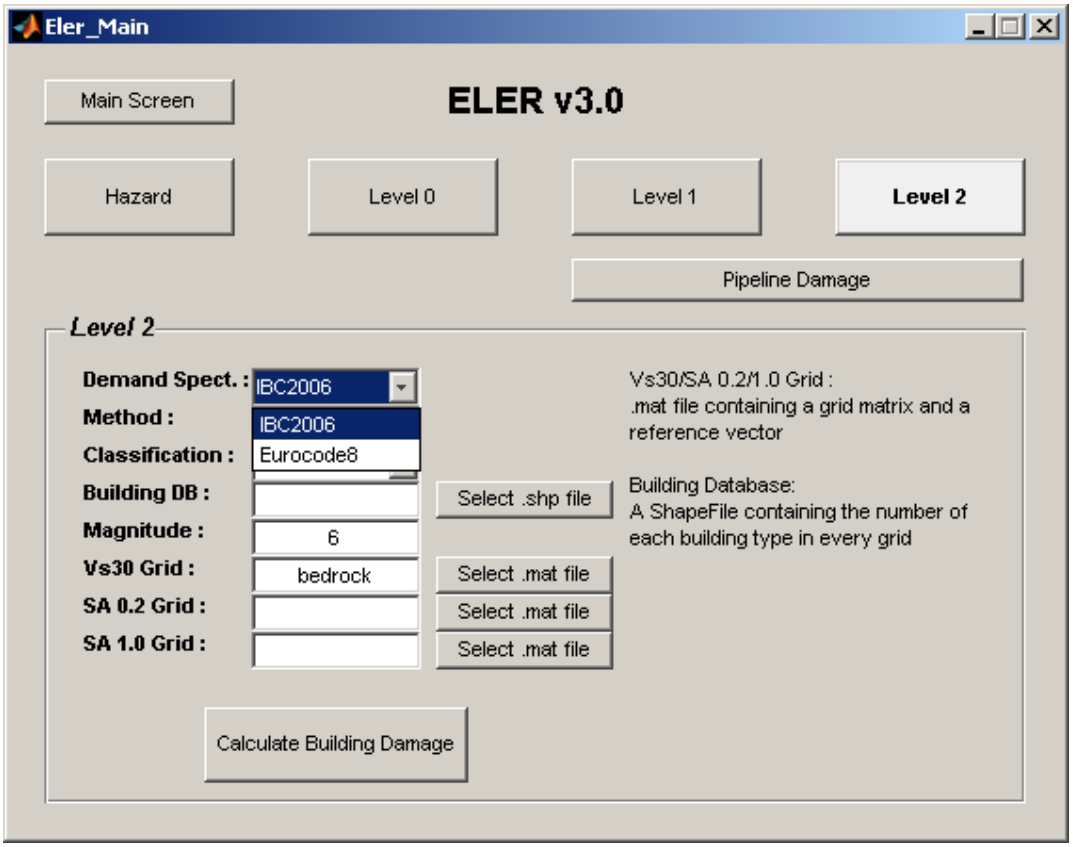

Figure 39. Selection of demand spectrum

Magnitude

Magnitude should be specified by the user for the selection of the corresponding Eurocode-8 spectrum. If the user proceeds to Level 2 directly from the Hazard Module this field is automatically assigned.

SA 0.2 / SA 1.0 Grid

Spectral acceleration values at 0.2 and 1 sec periods are required to construct the IBC-2006 demand spectrum for each geographical unit. Two MATLAB (.mat) files containing a grid matrix and a reference vector of 0.2 and 1.0 sec spectral accelerations have to be supplied by the user. These two spectral acceleration files can be obtained from the previous calculations in Hazard Module or it can be created by the user in an appropriate format for Level 2. The unit of the values should be in %g. The structure of such a grid file is given in detail in Section B.2.1.

PGA Grid

If the Eurocode-8 Spectrum is selected, horizontal PGA values are required to construct the spectrum. A MATLAB (.mat) file containing a grid matrix and a reference vector of PGA values has to be supplied by the user. This PGA file can be obtained from the previous calculations in Hazard Module or it can be created by the user in an appropriate format for Level 2. The unit of the values should be in %g.

Vs30 Grid

To construct the demand spectrum the program needs a Vs30 distribution grid. If the user proceeds to Level 2 directly from the Hazard Module this field is automatically assigned. Otherwise the user should select a custom Vs30 map of the study region as defined in Section 0. The unit of the Vs30 values should be in m/s.

Building Database

The building database file has the same structure as in Level 1 (Section B.4.1).

Building Classification

The building inventory data consist of grid (geo-cell) based urban building and demographic inventories. For building grouping the European building taxonomy developed within the EU-FP5 RISK-UE project (Lagomarsino and Giovinazzi, 2006) and model building types of HAZUS-MH (FEMA, 2003) are used. The software database includes the building capacity and the analytical fragility parameters for both the European and HAZUS building taxonomies (Figure 40). The user is also capable of defining a custom building classification by *Building Database Creator- BDC* in order to use with any selected method of the Level 2 analysis (Section B.7.3).

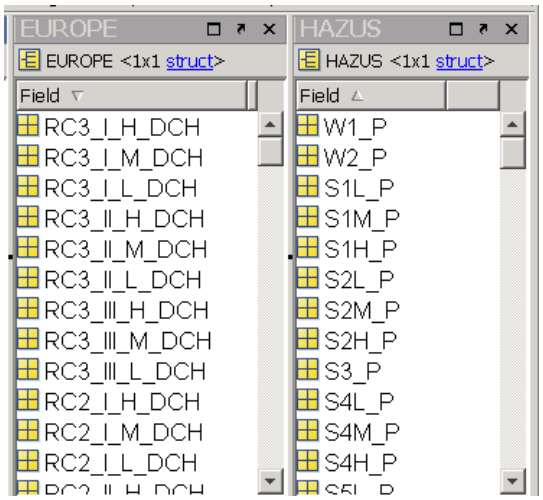

Figure 40. Default building taxonomy databases for Level 2 Module

Analysis Methods

The analysis methods given in Table 12 can be chosen for the calculation of the performance point.

Table 12. Level 2 Analysis Methods

CSM	Capacity Spectrum Method-Procedure A (ATC-40)
MADRS-1	Modified Acceleration-Displacement Response Spectrum Bilinear Hysteretic Model (FEMA-440)
MADRS-2	Modified Acceleration-Displacement Response Spectrum Stiffness Degrading Model (FEMA-440)
MADRS-3	Modified Acceleration-Displacement Response Spectrum Strength Degrading Model (FEMA-440)
MADRS-4	Modified Acceleration-Displacement Response Spectrum Approximate Equations Model (FEMA-440)
RFM	Reduction Factor Method
CM	Coefficient Method

B.5.2. Algorithm

Building Damage Calculation

The flow chart of building damage assessment in Level 2 is given in Figure 41. After estimating the performance point by one of the methods of Level 2 Module the damage probability is obtained through the use of fragility curves. Fragility curves calculate the probability of being equal or exceeding a damage state assuming log-normal distribution of damage. To estimate the performance of a group of buildings of a particular class under given ground shaking, the spectral response of the building at the performance point for the standard building of that class, as defined above, is used in conjunction with a set of fragility curves for that class, which estimate the probability of any particular building exceeding each of the damage states after shaking at any given spectral response level (Figure 42 and Figure 43). The damage states are represented in Table 13.

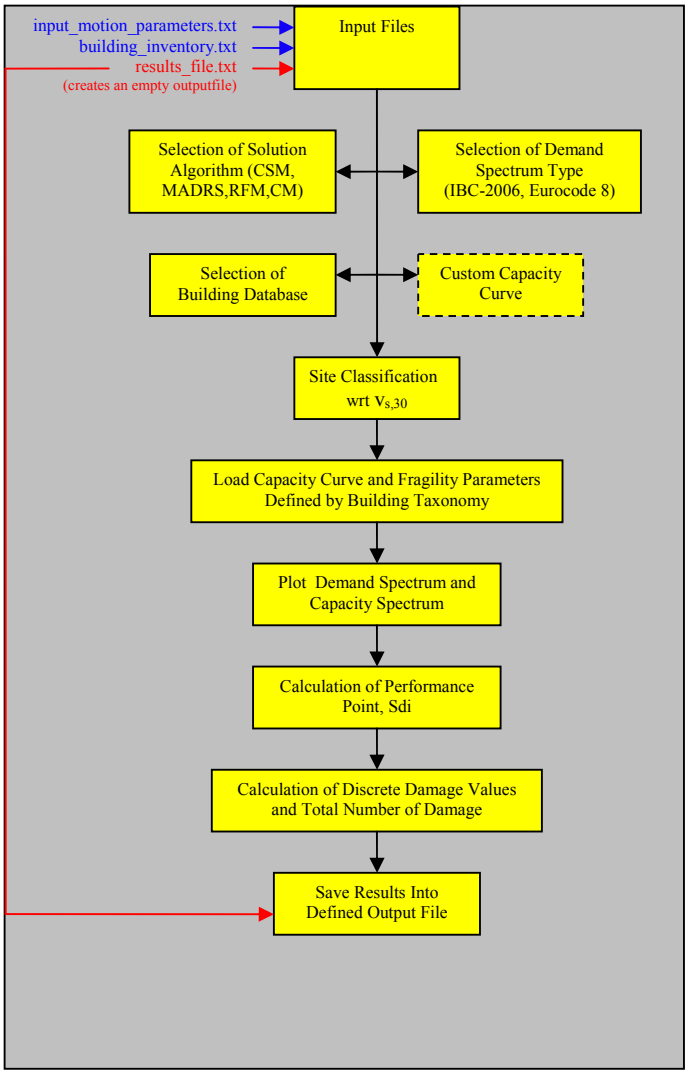

Figure 41. Flow chart of the Level 2 module

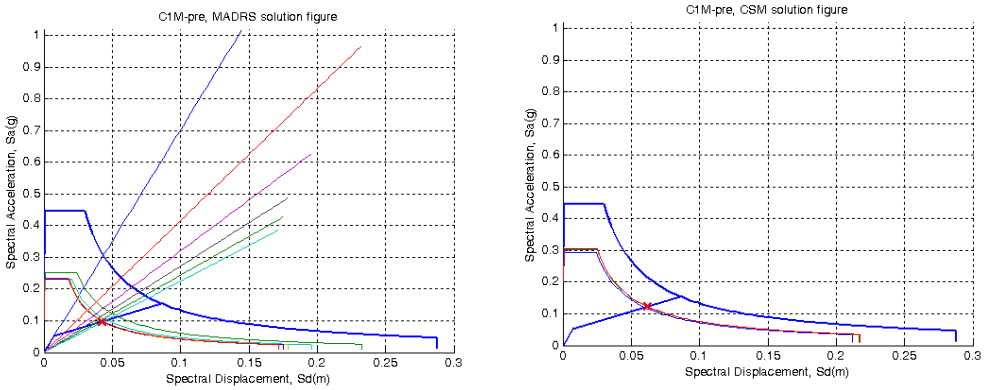

Figure 42. Graphical representation of the performance point estimation by CSM and MADRS method

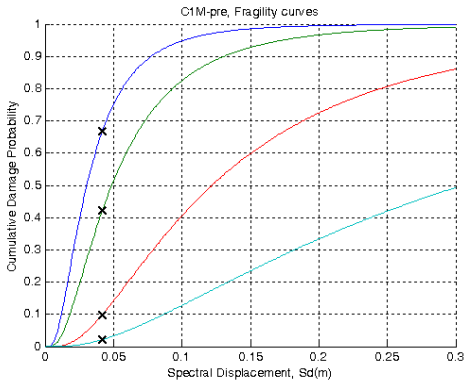

Figure 43. Intersecting the performance point with the fragility curves representing the cumulative damage probabilities at four damage states (dark blue: slight damage, green: moderate damage, red: extensive damage and light blue: complete damage)

Table 13. Level 2 Damage States

No	No Damage
Sli	Slight Damage
Mod	Moderate Damage
Ext	Extensive Damage
Com	Complete

Casualty Estimation

Casualty estimation in Level 2 is similar to that of Level 1. Following the definition of a grid based building inventory and a grid based population distribution by the user, the software computes the number of dwelling units (using user defined estimated number of dwellings per building type) and an average population per dwelling unit for each cell. Then, casualties for any given building type, building damage level and injury severity level can be calculated by the following equation:

K_{ij} = *Population per Building * Number of Damaged Building in damage state j* Casualty Rate for severity level i and damage state j* [1]

At present three casualty models are included in ELER. These are HAZUS99 (FEMA, 1999), HAZUS-MH (FEMA, 2003) and the KOERI (2002) casualty models. The predefined *Casualty Rate Tables* are *HAZUS-MH*, *HAZUS-99* and *KOERI (2002)*. Detailed information on casualty rates is given in Section C.4.3 of the Technical Manual. The same approaches used in Level 1 are incorporated to estimate population per building (see Section B.4.2)

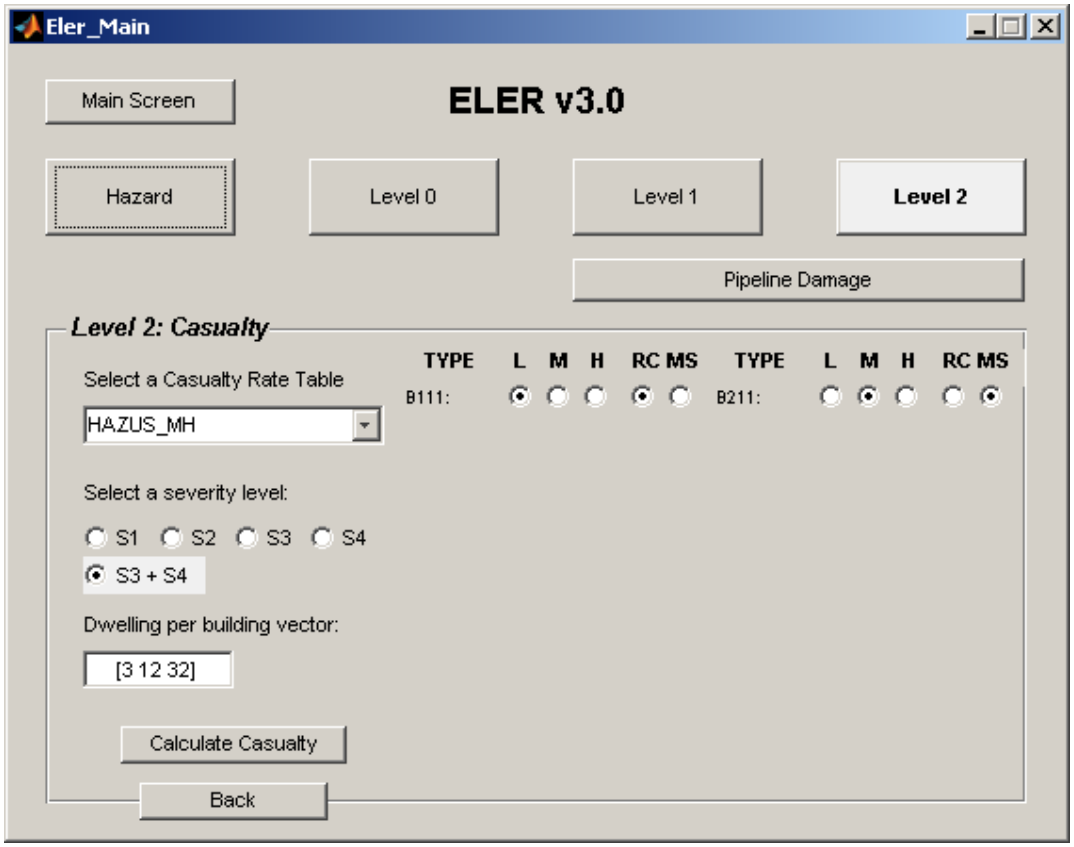

Figure 44. Level 2 Casualty Estimation

B.5.3. Economic Loss Estimation

Economic losses are calculated as in Level 1 (see B.4.2), this time instead of 5 damage classes the user has to specify the loss ratio for 4 damage classes. The building replacement values are specified during the building database generation procedure using either the Xls2BDB or the Building DB-C tools.

B.5.4. Outputs

As in Level 1, in addition to the building damage and casualty distribution figures generated by MATLAB, these maps are also optionally saved in shape file format (see Section B.8). These files can be manipulated with GIS editors for custom visualization and further analysis.

B.6. PIPELINE DAMAGE MODULE

B.6.1. Input Specification

Pipeline damage module is based on peak ground velocity values obtained from the Hazard module. The pipe material type (ductile or brittle) is also taken into account.

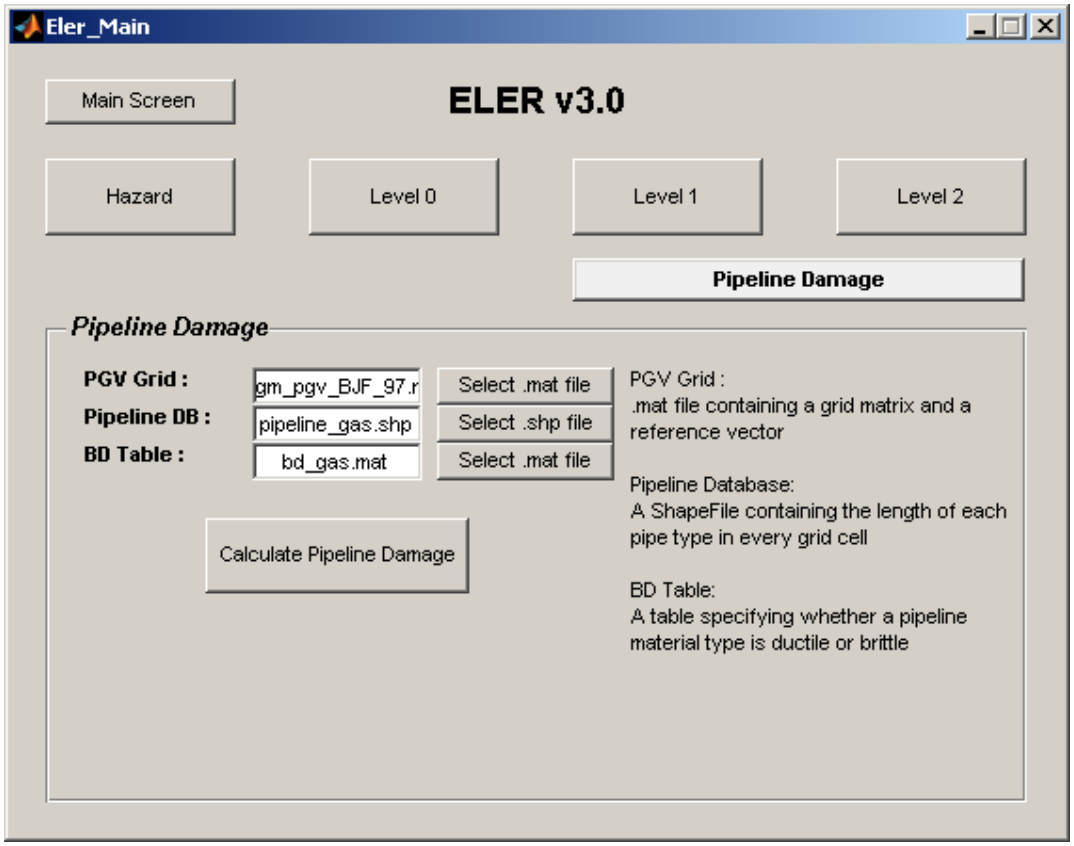

Figure 45. Level 1 Pipeline Damage Module GUI

PGV Grid

Peak ground velocity grid should be specified similarly to Level 0 (see Section B.3.1).

Pipeline Database

The pipeline database file is basically a Shapefile (.shp) containing the pipeline length distribution for each cell. Similar to the structure given in Table 10 the file should contain the length of each pipe type for each cell. A specific field named "*TOTAL_PIPE*" should contain the total length of pipelines for the whole cell. The potable water pipeline inventory for Istanbul's district Zeytinburnu (*pipeline_zeytinburnu.shp*) is included in the data folder of the program as a sample input.

BD Table

The BD Table is a Matlab table specifying if a pipeline type is ductile (1) or brittle (0). An example table is given in Figure 34. ELER searches the pipeline database for each pipeline type defined in the brittle-ductile table and if found proceeds with the damage calculation.

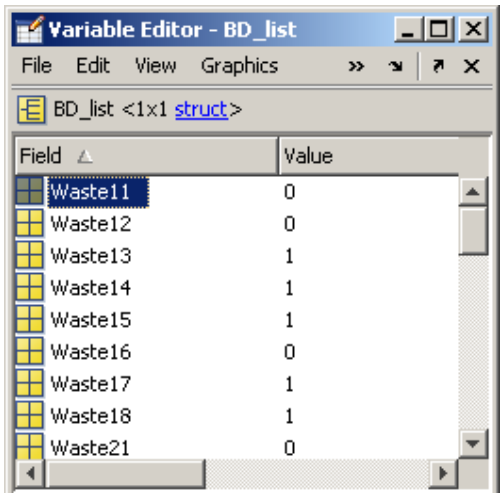

Figure 46. Brittle-Ductile Table

B.6.2. Algorithm

The pipeline damage is calculated according to the approach used in HAZUS-MH (FEMA, 2003) considering the pipeline material type. Higher vulnerability is assigned to brittle pipelines with respect to ductile ones. The output is given as the total number of repairs in each cell. The repairs are divided into two categories, leaks and breaks. An example output is given in Figure 47.

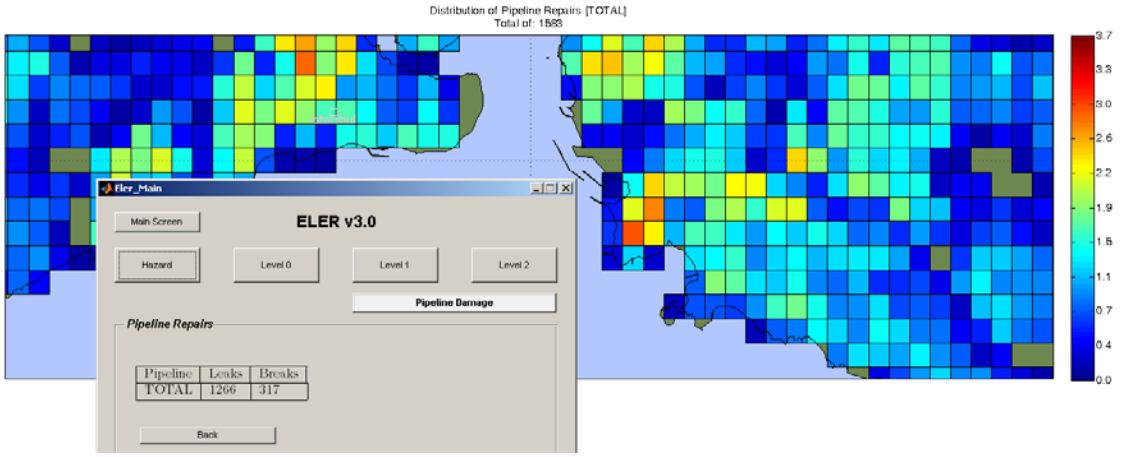

Figure 47. Pipeline damage estimation output

B.7. TOOLS FOR EXTERNAL DATA INTEGRATION

The following tools have been developed in v2.0 for external data integration:

- *Text2Grid:* Tool for integration of external ground motions or site conditions
- *Xls2Mat:* Tool for creation of building specification databases for Level 1

- *BDC*: Tool for user-defined building database creation and modification for Level 2

B.7.1. Text2Grid

This tool can be used to convert text files containing grid data in xyz format into MATLAB matrices to be used in ELER.

Figure 48 shows the Text2Grid tool, the input text file and the figure obtained from the converted MATLAB matrix. The *Header lines* parameter defines the number of lines to be ignored when processing the text file. The *Grid interval* parameter specifies the density at which the points in the text file are located. These points do not need to be sorted in any particular order, but the x y z columns should be separated by a whitespace or a tab. The resulting MATLAB matrix file is saved automatically with the same name as the input file, with a .mat extension.

The Text2Grid tool can be used for creating ground motion grids to be used in Levels 0, 1 and 2 or for creating custom site condition maps for use in the Hazard module.

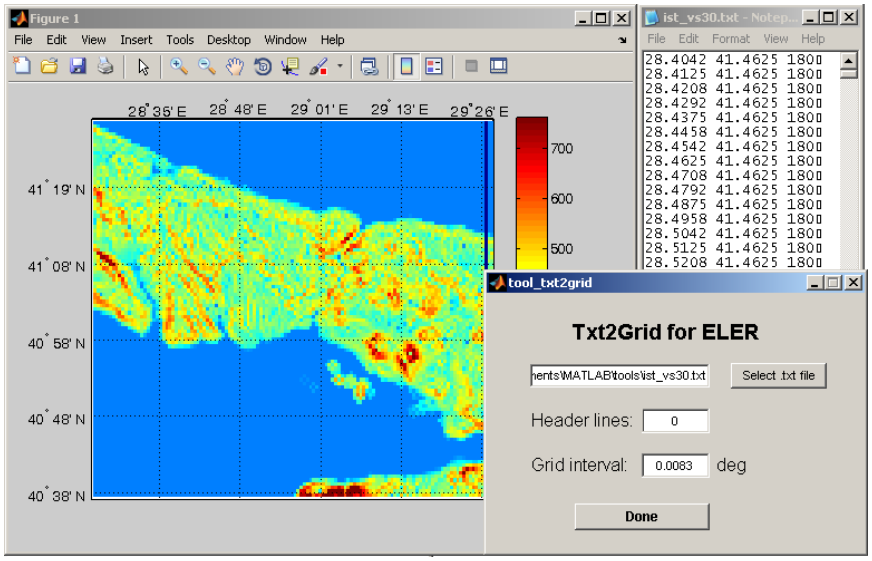

Figure 48. Text2Grid GUI, input and output

B.7.2. Xls2Mat

This tool can be used to convert Excel files containing vulnerability, ductility, t parameter and replacement cost values of building types into MATLAB structure arrays. The resulting MATLAB matrix file is saved automatically with the same name as the input file, with a .mat extension. This .mat file can be used in Level 1 as a vulnerability-ductility table. ELER will check the building database only for the building types specified in this file.

With the introduction of the Pipeline Damage module, the Xls2Mat tool can also be used to create BD tables specifying whether a pipeline material is ductile or brittle. As in the Level 1 analysis only the pipeline types defined in this table will be taken into account during the

damage estimation procedure. The user can specify the table that he/she wants to create via the radio buttons on the Xls2Mat GUI as given in Figure 49.

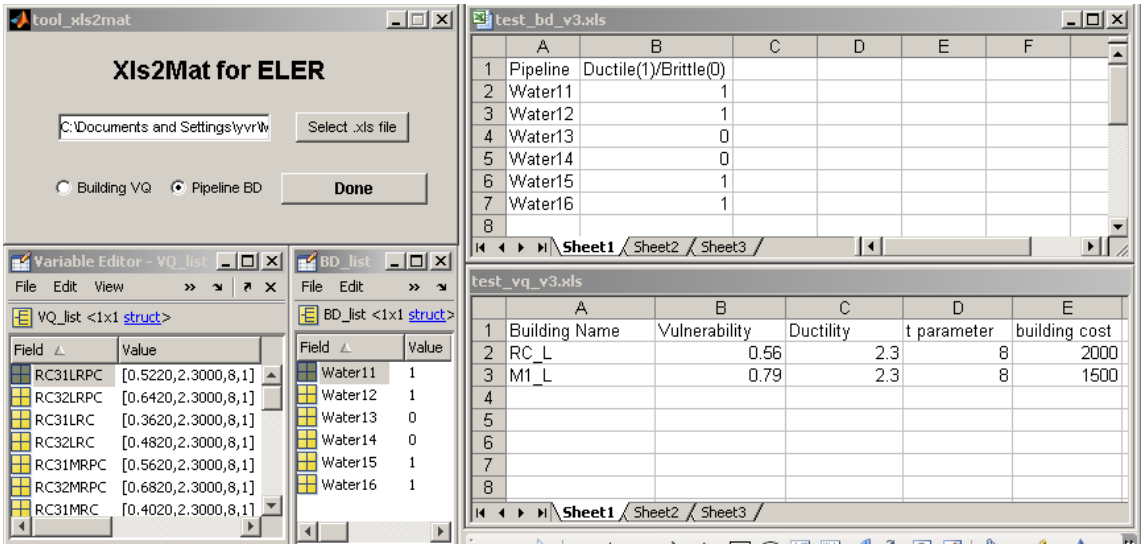

Figure 49. Xls2Mat GUI, input and output

B.7.3. Xls2BDB

The Xls2BDB tool converts a normal Excel document to a Level 2 Building Database file. This will allow the user to integrate large databases into Level 2 loss estimation easily. Xls2BDB will automatically determine which spectral displacement based method can be utilized according to the parameters supplied within the Excel document. The template Excel sheet format is given in Figure 50.

	A	B	C	D	E	F	G	H	I	J	K	L	M
1		Fragility Curves								Capacity Curve			
2		Slight		Moderate		Extensive		Complete		Yield		Ultimate	
3	Building Name	Median	Beta	Median	Beta	Median	Beta	Median	Beta	Displacement	Acceleration	Displacement	Acceleration
4	B111	0.018	0.95	0.036	0.91	0.09	0.85	0.18	0.97	0.007753097	1.913	0.015506194	1.913
5	B211	0.0394	0.7	0.09	0.74	0.18	0.86	0.3375	0.98	0.024108109	1.692	0.048216218	1.692
6	B221	0.018	0.95	0.036	0.91	0.09	0.85	0.18	0.97	0.007753097	1.913	0.015506194	1.913
7	B212	0.0394	0.7	0.09	0.74	0.18	0.86	0.3375	0.98	0.024108109	1.692	0.048216218	1.692

N	O	P	Q	R	S	T	U	V
		Economic Loss	Structural Behaviour				Building Charactreristics	
Elastic			Degradation Factor					
Displacement	Damping	Building Cost	Short	Moderate	Long	Ductility Value	C0 coefficient	Period
0.006590132	5	1000	0.8	0.4	0.2	2	1.1	0.211
0.020491893	5	1500	0.9	0.6	0.3	3	1.3	0.355
0.006590132	5	1000	0.8	0.4	0.2	2	1.1	0.211
0.020491893	5	1500	0.9	0.6	0.3	3	1.3	0.355

Figure 50. Xls2BDB example Excel document

The building inventory created from the provided .xls is saved inside the Level 2 building inventory folder with the proper filename format, thus the user can select the new inventory directly from the Level 2 GUI's Classification drop down menu.

B.7.4. BDC-Building Database Creator

Building Database Creator-BDC allows the user to input custom building capacity and fragility parameters for Level 2 analysis and to create a user-defined building inventory database independent from default building taxonomies of ELER, i.e. European and HAZUS building taxonomies. The user is capable of externally providing input parameters for the calculation of performance point by the available analysis methods of Level 2 Module.

Basic Steps of Building Database Formation

The BDC is composed of four components:

i. Definition of Building Taxonomy
ii. Definition of Fragility Curve Parameters
iii. Definitions Analytical Methodology Parameters
iv. Definition of Building Capacity Parameters

Figure 51 illustrates the main menu of the BDC where the number of building types and the corresponding design levels are entered as well as the working units are assigned.

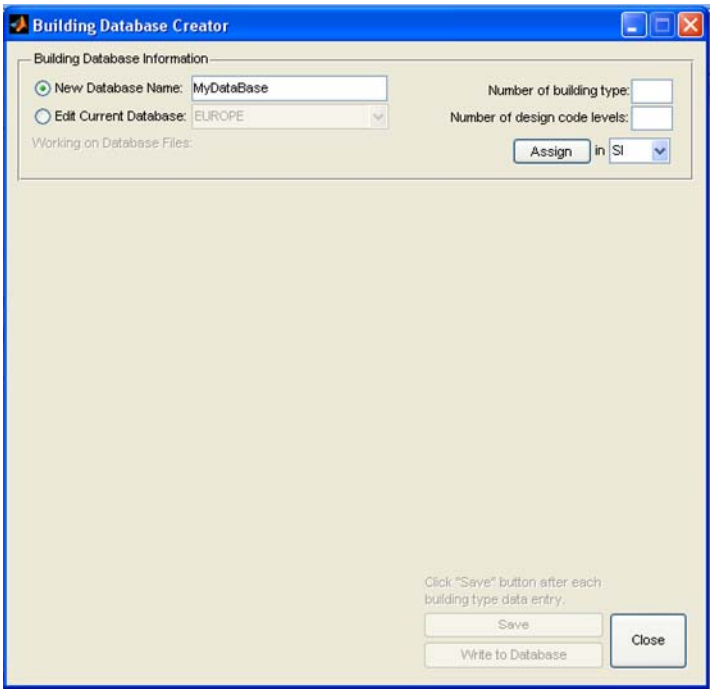

Figure 51. Main menu of Building Database Creator

All the parameters defined for a specific building inventory can be saved at each step and can be written to a “new” database. Additionally an existing database can be modified and another “new” database can be created.

The units of the input parameter can either be in SI or US version. Conversion from one unit system to another is possible at any level of parameter entry. Finally the database is

transformed in one unit system which is defined in the main menu of the graphical user interface.
The basic steps of building database formation using the graphical user interface are summarized below.

Definition of Building Types in the Building Inventory

Building type definition is done based on the number of building types and design Code levels. A "Building Name" tag is assigned to each building typology (Figure 52).

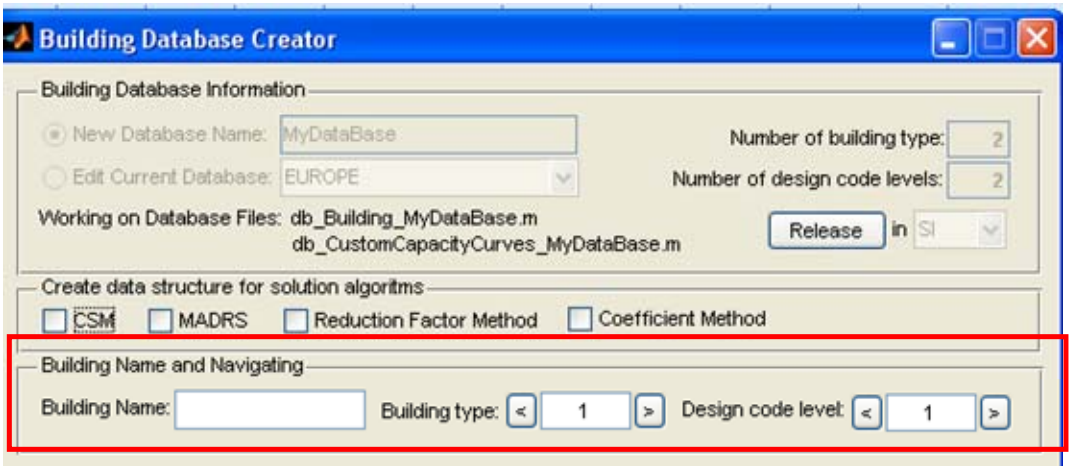

Figure 52. Definition of building name for each building type and Code level

Definition of Analytical Methodology

The methodology for analytical vulnerability analysis is selected from the menu given below. The user can select any of the analysis methods defined in the software such as "*Capacity Spectrum Method (CSM)*", "*Modified Acceleration Displacement Response Spectrum Method (MADRS)*", "*Coefficient Method (CM)*"and "*Reduction Factor Method (RFM)*". Each method has its own parameter to be defined whose details are given below.

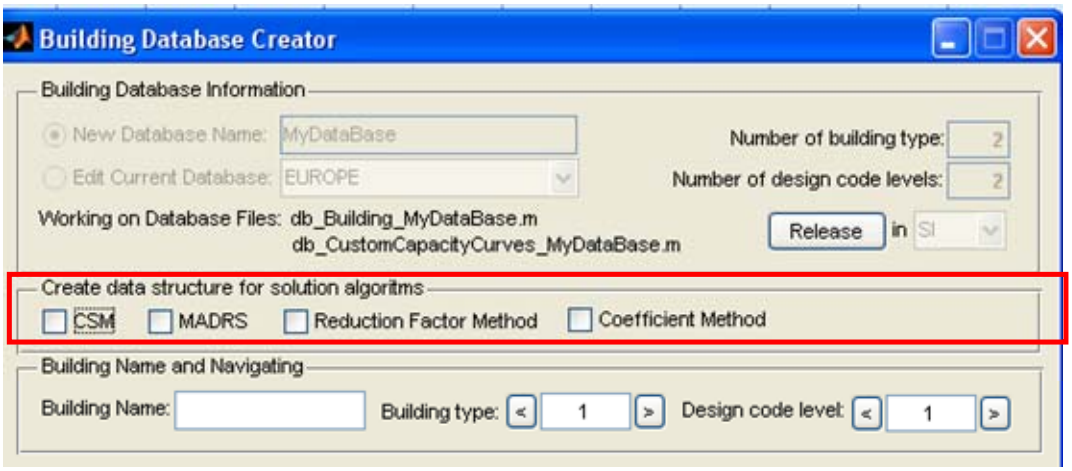

Figure 53. Selection of methodology to be used in vulnerability assessment

Definition of Fragility Parameters for Each Damage State

The building specific fragility curves are introduced by the median value of the damage state threshold spectral displacements and the log-normal standard deviations for each damage state, i.e. Slight, Moderate, Extensive and Complete. It should be noted that the data entry could be done in both unit system.

By the selection of each methodology a new window appears in order to define the spectral displacement based fragility curve parameters for each damage level (Slight / Moderate / Extensive / Complete).

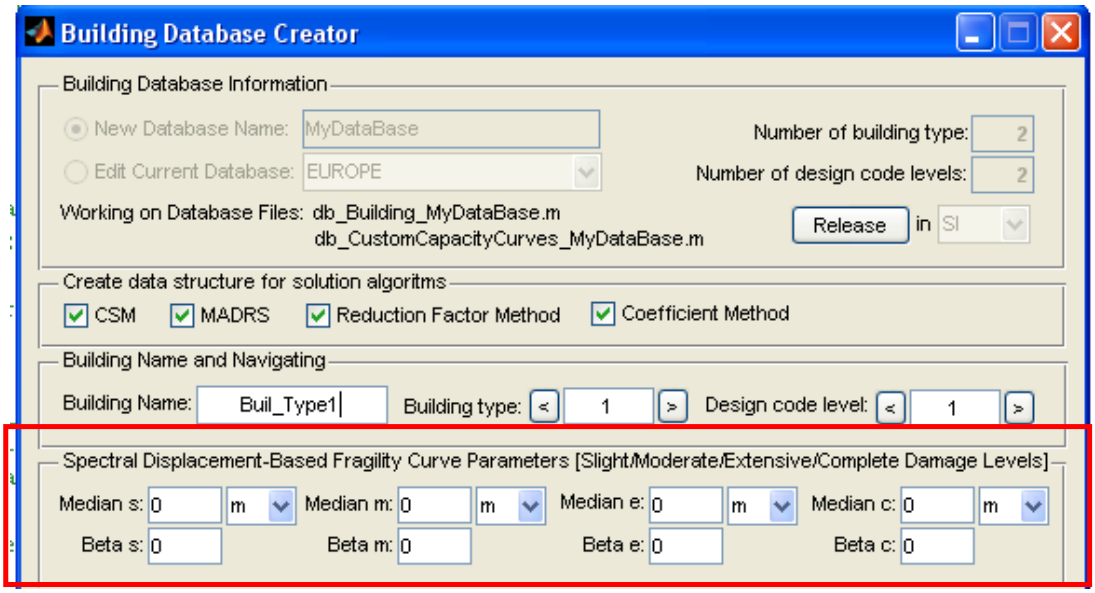

Figure 54. Definition of spectral displacement based fragility curve parameters for each damage state

Definition of Building Capacity Parameters

The parameter used to define the capacity of each building type in building inventory is given in this section. The user has two options to introduce the building capacity spectrum:

- Bilinear Curve
- Real Curve from push-over analysis

In order to define the capacity of each building type two points should be defined as yield and ultimate points. The acceleration and displacement values for both yield and ultimate level should be defined. Additionally once the user has all the values of the capacity curve, it can be defined through a text file. The user has also the option to provide the yield and ultimate points with the real curve.

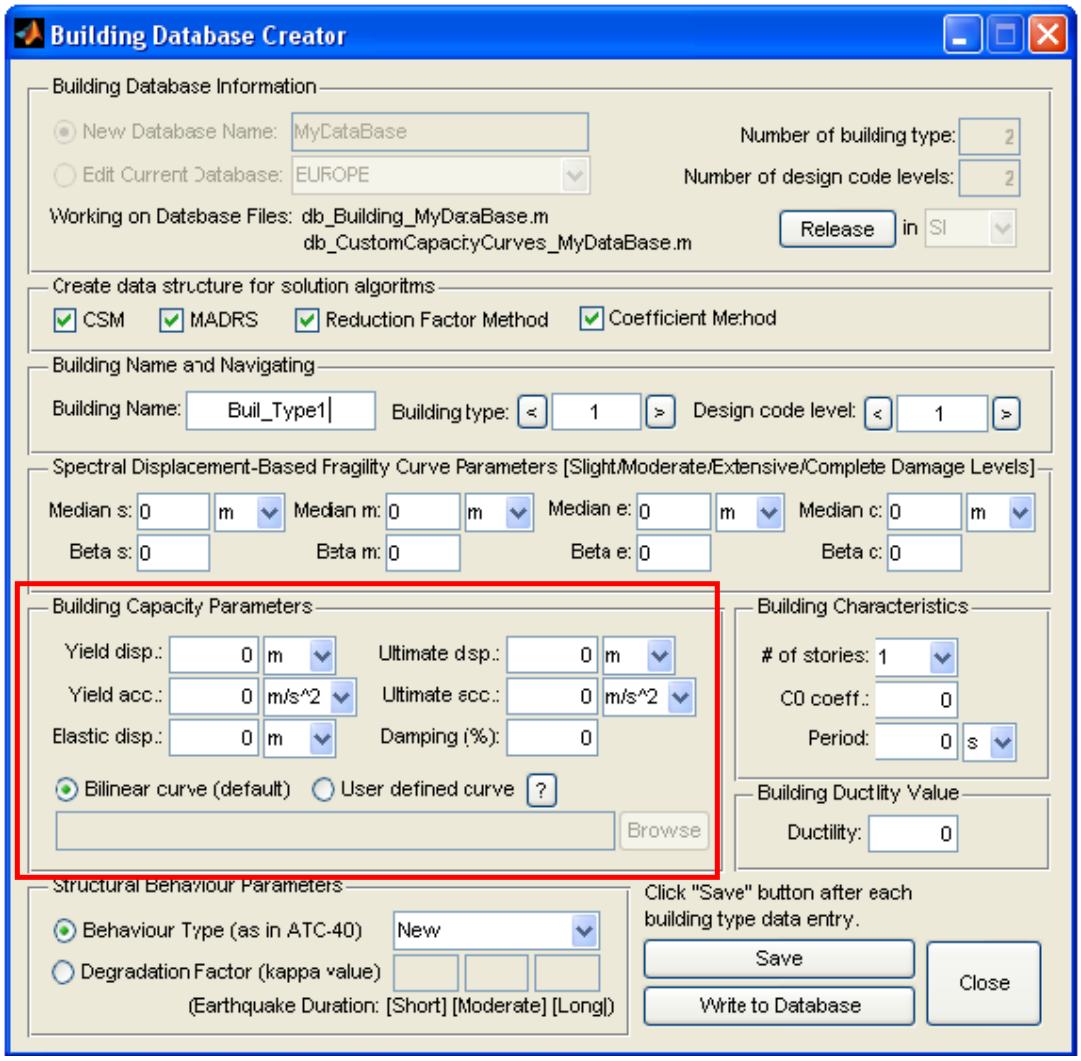

Figure 55. Definition of building capacity parameters

Definition of Additional Parameters

Other parameters to be used for analytical vulnerability analysis for the relevant methodologies are defined under "*Structural Behavior Parameters*" in terms of "*Behavior Type*" (new, average or poor) as defined in ATC-40 and "*Degradation Factor*" for *short*, *moderate* and *long* duration earthquake.

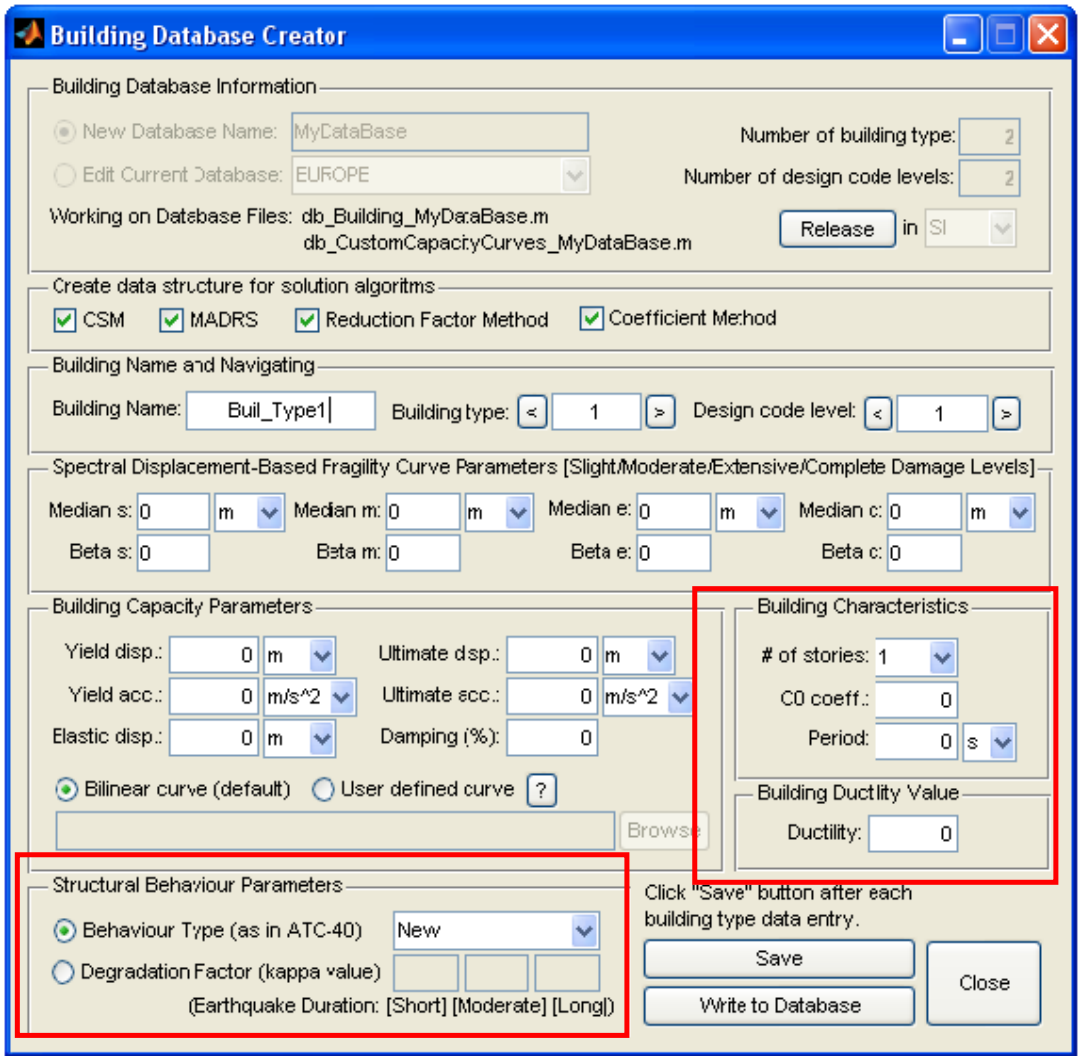

Figure 56. Definition of building characteristics and structural behavior parameters

Formation and Modification of Building Database

The defined parameters in the previous sections can be saved to a file. It should be noted that after completing the data entry for each building type the defined data should be saved by using "*Save*" button. After completing the definition of all parameters for all building types in the building inventory the new database file can be created by using "*New Database Name*" field by using "*Release"* button. The name of the new database file should be in the form of "*db_Building_XXX.m*". Similarly building capacity data is created at the same time. The name of the custom capacity curve file will be in the form of "*db_CustomCapacityCurve_XXX.m*". Once a database is created modification is possible by using "*Edit Current Database*" option. After making the necessary modifications in the existing database it may be saved by using another name or save using the same name.

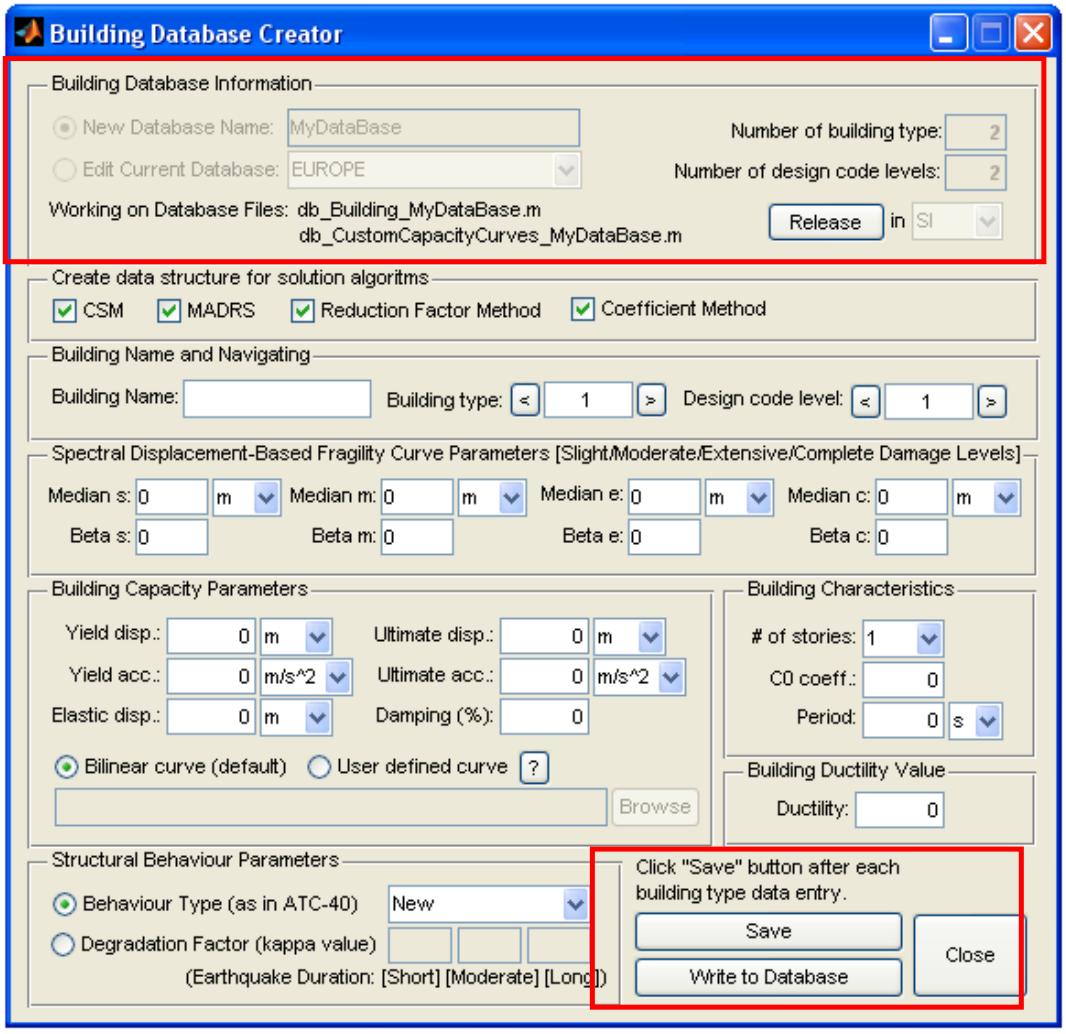

Figure 57. Formation and modification of a building data

B.8. USER PREFERENCES (Options - Preferences File)

With the introduction of an external preferences file (*eler_prefs.txt*) the user is able to adjust several parameters in ELER to better suit his/her needs. An example preferences file is given in Figure 58. Lines preceded by a '*%*' sign are regarded as comments and thus are ignored.

```
1  %map_extent     = [latspan lonspan]
2  %map_extent     = [N S E W]
3  map_extent      = [1.6 2.5]
4  phantom_grid    = 10
5  cthresh         = 15
6  pthresh         = 10
7  interp_grid     = 0.016
8  save_kml    = 1
9  save_shp    = 1
10 mdk_radius = 10
11 mdk_minsta = 5
```

Figure 58. eler_prefs.txt

Detailed explanation of these parameters is given below.

map_extent:

If specified by a two element vector such as [a b], a and b constitute the latitude and longitude span of the map area respectively. The center point of the map is taken as the epicenter of the event (Figure 59).

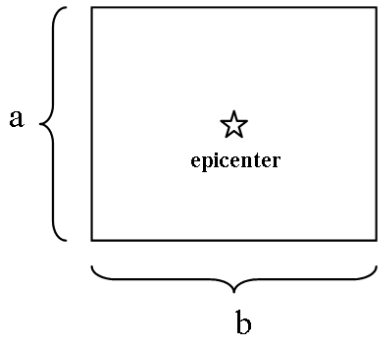

Figure 59. Map extent

If specified by a four-element vector, these elements will determine the boundary of the mapping area. The order is given as north, south (latitudes), east and west (longitudes). All values are in decimal degrees.

All ground motion, building damage and casualty estimations will be computed for the specified map extent.

phantom_grid:

Phantom station grid spacing should be given in kilometers. The calculation time is determined mainly by this parameter. Small values will increase the total number of phantom stations to be estimated and this will affect the elapsed time. For small areas however this value can be decreased accordingly to obtain a suitable resolution.

pthresh & cthresh:

ELER discards all phantom stations in the vicinity of actual stations. This vicinity is defined by a radius *pthresh (km)*. If there are no actual stations in the vicinity of the epicenter, defined by a radius of *cthresh (km)*, the epicenter itself is added as a new phantom station. For detailed information refer to ELER Users Guide Section B.2.1. Combining Actual and Phantom Stations.

interp_grid:

Specifies the interpolation density between phantom stations. This parameter, given in decimal degrees, defines the resolution of the output grid. It affects the computation time and should be used in accordance with the *phantom_grid* parameter.

save_kml:

Specifies if ELER should create a Google Earth KML file output for the ground motion distribution calculated in the Hazard module. A value of 1 enables this option whereas 0 disables it.

save_shp:

Specifies if ELER should create a Shape file output for building damage and casualty distribution calculated in Level 1 and 2 modules. A value of 1 enables this option whereas 0 disables it.

mdk_radius:

Defines the first coverage condition for the modified kriging method. Given in kilometers *mdk_radius* specifies a point's minimum distance to a station. Points which are out of this range are excluded from the kriging process.

mdk_minsta:

Defines the second coverage condition for the modified kriging method. Specifies the minimum number of stations which should be in the vicinity of a point. If a point is covered (not in the range of *mdk_radius*) by fewer stations it is excluded from the kriging process.

C. TECHNICAL MANUAL

C.1. INTRODUCTION

The ELER software has two main modules which are the Earthquake Hazard Assessment module and the Earthquake Loss Assessment module.

Earthquake Hazard Assessment includes estimation of ground motion and intensity distributions using ground motion prediction equations, correlation between intensity and ground motion parameters and soil condition information.

Earthquake Loss Assessment module uses ground motion and intensity information from Earthquake Hazard Assessment module, demography and building inventory. This module includes three levels (Level0, Level1 and Level2) of analysis for estimation of building damages, economic losses and casualties. Level0 analysis estimates casualties based on magnitude and intensity information. Level1 analysis estimates building damages, casualties and economic losses based on intensity information, Level2 analysis estimates building damages, casualties and economic losses based on ground motion and spectral parameters.

This Technical Manual intends to give the background information on the methodology and techniques involved in ELER, encompassing chapters on EARTHQUAKE HAZARD ASSESSMENT, ELEMENTS at RISK, EARTHQUAKE LOSS ASSESSMENT (Levels 0, 1 and 2) and VERIFICATION & VALIDATION (V&V) STUDIES. The user might refer to the Users Guide for the installation of and to run ELER.

C.1.1. Assessment of Ground Motion

Assessment of ground motion is based on event parameters defined by the user. The minimum data required for the analysis are the magnitude and the epicentral location of the event. Additional data that can be defined by the user are the rupture parameters or a fault database and accelerometric data.

Seismic Hazard

Seismic hazard is deterministically computed based on empirical ground motion and/or macroseismic intensity prediction models.

Site Response

Site response is incorporated with the help of either the default or the user defined Vs30 data, by the use of amplification coefficients or by computing ground motions directly at surface depending on the selected ground motion prediction model.

C.1.2. Assessment of Building Damage, Casualties, Economic Loss and Pipeline Damage

Building damage assessment and casualty estimation methodologies that are identified for utilization in ELER can be studied under the different levels of analysis. For Level 1 and

Level 2 the economic losses are calculated via the damaged building results and the replacement costs of each building. Pipeline damage estimation is performed in a separate module.

Level 0 Methodology

For this level of analysis the default inventory consists of population density (LandScan Population Distribution Data, 30 Sec-arc), city names, locations and populations. This level of analysis does not normally include any building damage assessment. Casualty estimations are based on the empirical magnitude – casualty relationship developed by Samardjieva and Badal (2002).

Level 1 Methodology

The building inventory and population data for the Level 1 analysis consists of grid (geo-cell) based building and population distribution. The building inventory should be classified in terms of Risk UE building Taxonomy. Data from Turkey is provided to set an example for other regions and countries to develop/incorporate their own inventory data. The intensity based empirical vulnerability relationships developed by Lagomarsino and Giovinazzi (2006) are used for the building damage assessment.

In addition to the default data provided for Level 0 analysis, an approximated grid based distribution of the number of buildings and associated structural types are also be provided as the default inventory of Level 1 for 27 countries in Europe.

Level 2 Methodology

Analytical fragility relationships and spectral acceleration-displacement-based vulnerability assessment methodologies are utilized for the building damage estimation in Level 2 analysis. The following methods can be employed:

- Capacity Spectrum Method (CSM-ATC 40)
- Modified Acceleration-Displacement Response Spectrum Method (MADRS-FEMA 440)
- Reduction Factor Method (Fajfar, 2000)
- Coefficient Method (ASCE 41-06)

Casualties are estimated based on the HAZUS methodology relating casualties in different severity levels with number of buildings in different damage states.

Pipeline Damage Methodology

HAZUS-MH (FEMA, 2003) methodology which is based on peak ground velocity distribution is used for pipeline damage assessment. The pipeline inventory is a grid based distribution of pipe length for each cell. The damage results are given in the form of repair numbers per kilometer, due to leaks and breaks.

C.1.3. Input Requirements, Analysis and Outputs for Level 0

1. HAZARD

a. The software produces ShakeMap (MSK'98 Intensity) based on point and extended sources. (Sample extended source data are provided only for Turkey). Information on how to complement the extended source data for other countries/regions is given in the Users Guide.
b. Provision for inclusion of user specified hazard and/or site classification data is also available.

2. INVENTORY
   a. City Locations for the Euro-Med Region,
   b. Grid based population distribution data (LandScan Population Distribution Data for the Euro-Med Region).

3. CASUALTY
   a. Casualties are calculated with the help of regionally adjusted fatality vs. MSK'98 intensity relationships.
   b. The number of injured people who need hospitalization are calculated based on number of fatalities.

4. ANALYSIS OUTPUT
   a. Isoseismic maps,
   b. Maps displaying grid –based estimations of casualties.

C.1.4. Input Requirements, Analysis and Outputs for Level 1

1. HAZARD
   a. Instrumental intensity distribution is used for building damage estimations

2. INVENTORY
   a. Grid based building inventory, building cost and demographic data.
   b. Default data for Number of Buildings (population related) and building types (region specific) for countries are provided for 27 EU countries.
   c. Building distribution for Marmara region, Turkey based on Risk UE building taxonomy is provided as sample data.
   d. Information on how to complement inventory data for other countries/regions is given in the Users Guide.

3. BUILDING DAMAGE
   a. Building damage distribution is calculated using intensity based structural vulnerabilities

4. CASUALTY
   a. Casualty and hospitalized injury distributions are calculated based on building damages.

5. ECONOMIC LOSS
   a. The distribution of direct economic losses is calculated based on building damages.

6. ANALYSIS OUTPUT
   a. Isoseismic maps,

b. Grid based distribution of buildings in different damage states
c. Grid based distribution of fatalities and severe injuries
d. Grid based distribution of economic losses

C.1.5. Input, Analysis and Output Requirements for Level 2

1. HAZARD
   a. Distributions of spectral acceleration at 0.2s and 1s are used for IBC 2006 spectrum.
   b. Distribution of peak ground acceleration is used for Euro Code 8 spectrum.

2. INVENTORY
   a. Grid based building inventory, building cost and demographic data
   b. Sample data is provided for the Zeytinburnu district of Istanbul.
   c. Inventory (Building and/or Population) data for other cities can be imported using system compatible data formats.

3. BUILDING DAMAGE
   a. Building damage distribution is obtained using spectral displacement based building vulnerabilities.
   b. Parametric vulnerability relationships are provided with suggested parameters and with provision for the use of alternate parameters.

4. CASUALTY
   a. Casualty distributions are calculated based on building damage.

5. ECONOMIC LOSS
   a. The distribution of direct economic losses is calculated based on building damages.

6. ANALYSIS OUTPUT
   a. Isoseismic and other ground motion distribution maps.
   b. Grid based distribution of buildings in different damage states
   c. Grid based distribution of fatalities and injuries
   d. Grid based distribution of economic losses

C.1.6. Input, Analysis and Output Requirements for Pipeline Damage

1. HAZARD
   a. Distribution of peak ground velocity is used for HAZUS-MH (FEMA, 2003) methodology.

2. INVENTORY
   a. Grid based pipeline length inventory.
   b. Sample dataset is provided for the Zeytinburnu district of Istanbul.
   c. Inventory data for other cities can be imported using system compatible data formats.

3. PIPELINE DAMAGE

a. Pipeline damage distribution is calculated using the HAZUS-MH (FEMA, 2003) methodology based on peak ground velocity.
b. Pipeline material types (ductile, brittle) can be specified externally.

4. ANALYSIS OUTPUT
   a. Grid based distribution of pipeline repair numbers (breaks and leaks).

C.2. EARTHQUAKE HAZARD ASSESSMENT

The ELER software Earthquake Hazard Assessment (EHA) module provides ground shaking intensity maps and maps with parameters of PGA, PGV, S_a and S_d at 0.2, 1.0 and 3.0s. These maps form the base for damage and casualty-loss calculations in Level 0, Level 1 and Level 2 modules. As in USGS ShakeMap, the ELER EHA module uses earthquake epicenter, magnitude and, if available, fault information as input and with the help of empirical ground motion prediction equations (GMPEs), which will be mentioned in detail in Section-C.2.1. The ground shaking maps are produced on bedrock (Section-C.2.2) and on ground surface levels (Section-C.2.3). If available, ground motion recordings are taken into account for a more accurate estimation (Section-C.2.4).

The following step by step procedure is used in the estimation of ground motions:

1. Depending on the earthquake epicenter location, the extent of the Shake-Map area is drawn.
2. The phantom stations with a uniform spaced grid within the Shake-Map extent are created.
3. Using the ground motion prediction equations (Section C.2.1), the ground motion parameters for each phantom station on the bedrock level (Section-C.2.2) are calculated. Interpolation between phantom stations is achieved with nodes in user defined spacing. In the case of Next Generation Attenuation (NGA) relations, the ground motion parameters can be directly estimated on the ground surface (Section- C.2.3).
4. If there are ground motion recordings available at the site, the obtained parameters are transferred from surface to the bedrock level, and a bias correction is applied to the estimated ground motion parameters on bedrock level (Section-C.2.3). In the case of GMPEs with site correction as a function of Vs30 (e.g. Boore et al., 1997 and NGA relations), the bias correction can be applied on the ground surface directly (Section-C.2.4).
5. The estimated ground motion parameters on bedrock level are transferred to the surface level by taking into account local site conditions with default gridded Vs30 values (Allen and Wald, 2007) for Euro-Med region or any other site information if available (Section-C.2.3).

C.2.1. Source Characteristics and GMPEs

The ELER EHA module allows the user to input the earthquake parameters manually or with an XML file for the estimation of rapid ground shaking maps. The earthquake epicenter coordinates and magnitude information is necessary for all point source and extended source earthquakes and if available fault coordinate information is required for the extended source

earthquakes. A sample manual input and XML input file to produce shake maps will be given in Users Guide.

The EHA module has three options to define the earthquake source which are: user defined point source, user defined extended source and auto assigned extended source.

The faulting information is necessary for extended sources. The user defined extended source requires fault coordinates of the surface projection. The auto assigned option is accessible for extended source earthquakes where a fault database is available. In this case, the earthquake's source is automatically assigned to the closest fault segment.

The EHA module is capable of calculating the rupture length with Wells and Coppersmith, 1994 approach automatically for extended source earthquakes. If the calculated fault rupture length is longer than what is given by the user or fault database, then the fault length is extended as it is calculated. The detailed information for fault length calculation and extension is given in Users Guide.

The EHA module allows calculation of ground motion parameters PGA, PGV, S_a and S_d through GMPEs at bedrock and ground surface levels given in Table 14.

In addition to the ground motion parameters PGA, PGV, S_a and S_d, regression relationships between Modified Mercalli Intensity (MMI) and ground motion parameters PGA and PGV developed by Wald et al., (1999a and 1999b) are used to estimate intensity distribution. These relationships were developed based on data from eight significant California earthquakes with magnitudes ranging between 5.8 -7.3.

For the Intensity estimation V< I_{mm} <VIII related with PGA,

$$I_{mm}=3.66\log(PGA) - 1.66 \qquad \sigma=1.08 \qquad [2]$$

For the Intensity estimation V< I_{mm} <IX related with PGV

$$I_{mm}=3.47\log(PGV) + 2.35 \qquad \sigma=0.98 \qquad [3]$$

The user can also create and use his/her own ground motion and instrumental intensity prediction equations in the form of a text file. Detailed information on how to create these user defined GMPEs and instrumental intensity prediction equations is given in Section B.2.1of the ELER Users Guide.

Table 14. Ground motion prediction equations coded in ELER

		Parameters used		
Reference Works	Estimated Parameters	Earthquake Rupture related Parameters	Site related Parameters	Propagatio - effect related Parameters
Boore, Joyner, and Fumal, 1997	PGA Sa	Magnitude Fault type (Reverse, Strike Slip or Unknown)	Vs30	JB Distance
Shakemap small regression (Boatwright and others,2003)	PGA PGV Sa	Magnitude Depth)	-	JB Distance
Akkar & Bommer, 2007	PGA PGV Sd	Magnitude Fault type (Normal fault, reverse fault)	soft soil stiff soil	
Campbell & Bozorgnia, 2008	PGA PGV PGD Sa	Magnitude Fault type Rupture top depth Dip	Vs30	Distance to Rupture
			Depth to Vs=2.5 km/s	(distRup-distJB)/distRup
Chiou & Young, 2008	PGA PGV Sa	Magnitude Fault type (Reverse, Normal) Rupture top depth Dip angle	Vs30	Distance to Rupture
				(distRup-distJB)/distRup
			Depth to Vs=1.0 km/s	Hanging Wall
Boore & Atkinson, 2008	PGA PGV Sa	Magnitude Fault type (Thrust /Reverse, Normal, Strike-Slip,Unknown)	Vs30	Joyner-Boore(JB) Distance
✢ Abrahamson & Silva (1997)	PGA Sa	Magnitude Fault type (Reverse, Reverse/Oblique fault ,Otherwise)	Rock or Shallow soil Deep Soil	Distance to Rupture
✢ Campbell & Bozorgnia (2003)	PGA Sa	Magnitude Fault type (Strike-Slip /normal, Reverse, Thrust)	Firm rock Soft rock Very Firm Soil Firm Soil	Distance to Seimogenic Rupture

**GMPEs have been added in the version of ELER v3.*

C.2.2. Ground Motion at Reference Ground

The default mode of the EHA module provides ground motion maps on the bedrock using ground motion prediction equations mentioned in Section C.2.1. The ground motion parameters are estimated for phantom stations which are assumed to be uniformly distributed with grid spacing defined in the file *eler_prefs.txt* (see the Users Guide for further details). Interpolation between phantom stations is achieved by the nodes with spacing also defined in the file *eler_prefs.txt.*

C.2.3. Site Specific Ground Motion

The effects of local site conditions on the estimation of ground motion parameters are taken into consideration in EHA module. The effect of site condition parameter V_s30 on ground motion parameter PGA with increasing distance by using Boore and Atkinson, 2008 ground motion prediction equation is shown in Figure 60. The dashed line represents the values calculated for Vs30 = 760 (engineering bedrock conditions) and the solid line shows the values computed with the Vs30 values (plotted with the blue line).

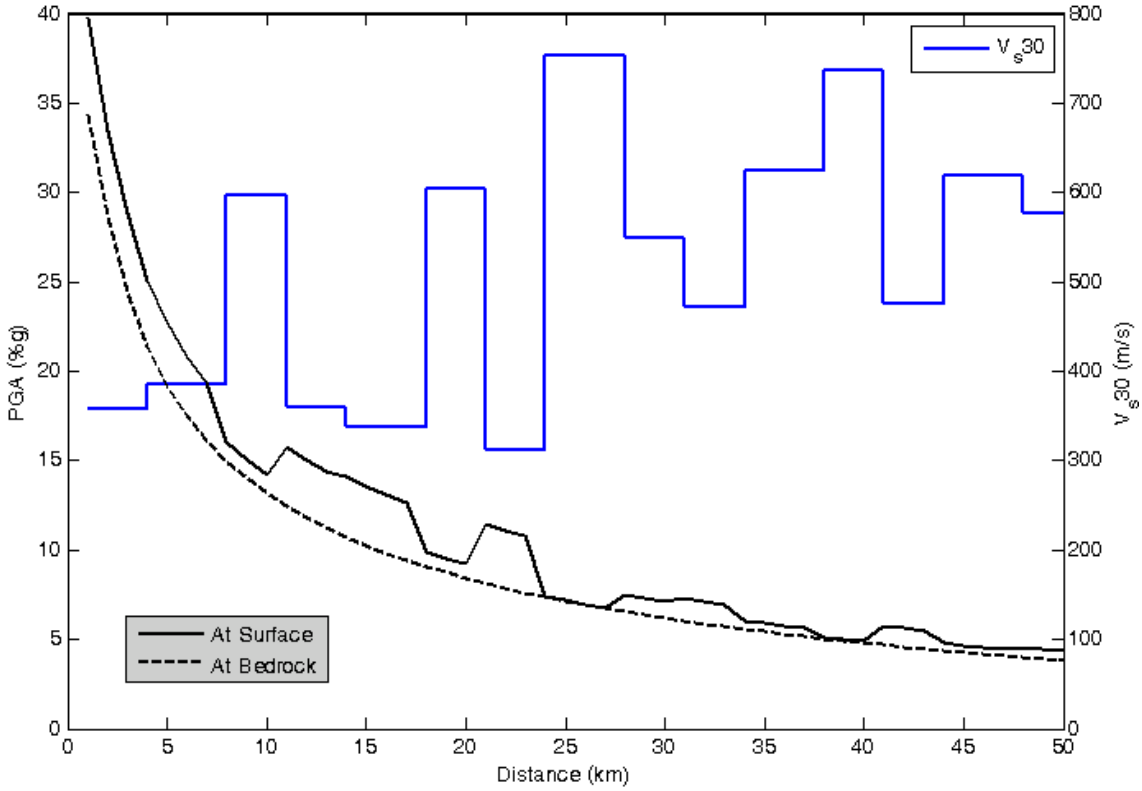

Figure 60. The effect of site condition parameter V_s30 on ground motion parameter PGA with increasing distance by using Boore and Atkinson, 2008 ground motion prediction equation

The following two approaches have been utilized in EHA module to consider the site effects.

Site Modification of Reference Ground Motion

The ground motion parameters estimated on the bedrock level are transferred to the ground surface level using available Vs30 maps. Topographic slope based Vs30 map (Wald and Allen, 2007) for Euro-Med region, and QTM map for Turkey are available in EHA module. NEHRP site classes are assigned to the available Vs30 map, and Borcherdt, 1994 frequency and amplitude dependent amplification factors (Table 15 and Table 16) are used for each grid and the ground motion parameters' maps on surface are obtained.

Table 15. Soil profile type classification for seismic amplification (FEMA, 1994).

Soil profile type classification for seismic amplification (FEMA, 1994).					
Soil Type	General Description	Avg. Shear Wave Velocity (feet/s)	Avg. Shear Wave Velocity (m/s)	Avg. Blow Counts	Avg. Shear Strength (lbs/sq.ft.)
A	Hard Rock	> 5,000	> 1,500		
B	Rock	2,500 - 5,000	760 - 1,500		
C	Hard and/or stiff/very stiff soils; most gravels	1,200 - 2,500	360 - 760	> 50	2,000
D	Sands, silts and/or stiff/very stiff clays, some gravels	600 - 1,200	180 - 360	15 - 50	1,000 - 2,000
E	Small to moderate thickness (10 to 50 feet) soft to medium stiff clay, Plasticity Index > 20, water content > 40 percent	< 600	< 180	< 15	< 1,000
E_2	Large thickness (50 to 120 feet) soft to medium stiff clay Plasticity Index > 20, water content > 40 percent	< 600	< 180	< 15	< 1000
F_1	Soils vulnerable to potential failure or collapse under seismic loading such as liquefiable soils, quick and highly sensitive clays, collapsible weakly cemented soils.	By definition the F classification requires that a site dependent evaluation of the engineering parameters be conducted, as they do not fall into any of the other soil classifications.			
F_2	Peats and/or highly organic clays greater than 10 feet thick				
F_3	Very high plasticity clays greater than 25 feet thick with Plasticity Index > 75				
F_4	Very thick soft/medium stiff clays greater than 120 feet thick				

Table 16. Site Amplification Factors (ShakeMap Manual 2006, Borcherdt 1994)

Class	**Vel**	**Short-Period (PGA)**				**Mid-Period (PGV)**			
			150	**250**	**350**		**150**	**250**	**350**
B	**686**	1.00	1.00	1.00	1.00	1.00	1.00	1.00	1.00
BC	**724**	0.98	0.99	0.99	1.00	0.97	0.97	0.97	0.98
C	**464**	1.15	1.10	1.04	0.98	1.29	1.26	1.23	1.19
CD	**372**	1.24	1.17	1.06	0.97	1.49	1.44	1.38	1.32
D	**301**	1.33	1.23	1.09	0.96	1.71	1.64	1.55	1.45
DE	**298**	1.34	1.23	1.09	0.96	1.72	1.65	1.56	1.46
E	**163**	1.65	1.43	1.15	0.93	2.55	2.37	2.14	1.91

In addition to Borcherdt's site amplification factors and differently from the USGS ShakeMap, ELER EHA module provides site correction according to Eurocode 8. This site correction mode is used for the Level2 analysis of ELER. Only the PGA estimation is taken into account in this mode. The estimations are made for bedrock level. Then according to the Eurocode 8, a soil type is assigned for each phantom station depending on the Vs30 value as shown in Table 17. The site amplification factors for Type 1 and Type 2 elastic response spectra are shown in Table 18 and Table 19. The site corrected PGA distribution on ground level is obtained by using these site amplification factors.

Table 17. Eurocode 8 Site Classification

Ground type	Description of stratigraphic profile	Parameters		
		$v_{s,30}$ (m/s)	N_{SPT} (blows/30cm)	c_u (kPa)
A	Rock or other rock-like geological formation, including at most 5 m of weaker material at the surface.	> 800	–	–
B	Deposits of very dense sand, gravel, or very stiff clay, at least several tens of metres in thickness, characterised by a gradual increase of mechanical properties with depth.	360 – 800	> 50	> 250
C	Deep deposits of dense or medium-dense sand, gravel or stiff clay with thickness from several tens to many hundreds of metres.	180 – 360	15 - 50	70 - 250
D	Deposits of loose-to-medium cohesionless soil (with or without some soft cohesive layers), or of predominantly soft-to-firm cohesive soil.	< 180	< 15	< 70
E	A soil profile consisting of a surface alluvium layer with v_s values of type C or D and thickness varying between about 5 m and 20 m, underlain by stiffer material with v_s > 800 m/s.			
S_1	Deposits consisting, or containing a layer at least 10 m thick, of soft clays/silts with a high plasticity index (PI > 40) and high water content	< 100 (indicative)	–	10 - 20
S_2	Deposits of liquefiable soils, of sensitive clays, or any other soil profile not included in types A – E or S_1			

Table 18. Eurocode 8 site amplification factors for Type 1 elastic response spectra

Ground type	S	T_B (s)	T_C (s)	T_D (s)
A	1,0	0,15	0,4	2,0
B	1,2	0,15	0,5	2,0
C	1,15	0,20	0,6	2,0
D	1,35	0,20	0,8	2,0
E	1,4	0,15	0,5	2,0

Table 19. Eurocode 8 site amplification factors for Type 2 elastic response spectra

Ground type	S	T_B (s)	T_C (s)	T_D (s)
A	1,0	0,05	0,25	1,2
B	1,35	0,05	0,25	1,2
C	1,5	0,10	0,25	1,2
D	1,8	0,10	0,30	1,2
E	1,6	0,05	0,25	1,2

Direct Computation at Surface

The Next Generation Attenuation (NGA) relations and Boore et al., 1997 GMPE allow the computation of ground motion parameters at the ground surface by taking into account the local site effects with Vs30 parameter. These models are used in EHA module to estimate ground motion parameters directly at the ground surface.

C.2.4. Incorporation of Empirical Data

In EHA module, the ground motion parameters are estimated basically for the phantom stations through the ground motion prediction equations. However, if there are ground motion recording stations in and around of the event region their recordings are used for bias correction to better estimate the predicted ground motion values for the phantom stations. A recording station beyond 120km distance is not considered for bias correction factor computation. If there is an actual station located within a distance less than 10km to the phantom station, the actual station ground motion value only is considered and phantom station value is ignored.

The bias correction factor between an actual station and a phantom station is computed by a least square approach or an absolute-deviation approach. As it is indicated in USGS ShakeMap manual the absolute-deviation approach gives better results and it is used as default approach for bias correction factor computation. The maximum and minimum values of the bias correction factor are set to 4.0 and 0.25 respectively.

Bias Correction at Reference Ground

If available, a bias correction factor is computed and applied to the estimated phantom station ground motion values to make them consistent with the recorded ground motion parameters. The bias correction is applied at the bedrock level in order to eliminate local site effects on the recorded ground motion values. This is achieved by transferring the recorded ground motion values from surface to bedrock level by using Borcherdt (1994) amplification factors.

Bias Correction at Surface

As some of the ground motion prediction equations consider local site effects with the Vs30 a parameter in the equations, this allows the estimation of ground motion parameters on ground surface directly as explained in Section C.2.3. If there are ground motion recordings available, that will allow bias correction of the estimated ground motion parameters on surface directly.

Modified Kriging Method

As an alternative to the default ShakeMap methodology, in regions with dense station coverage, instead of using interpolation ELER will optionally implement the modified Kriging method in order to assign ground motion values to regions in the vicinity of the stations.

A rational and rigorous methodology for the interpolation of measured ground motion from discrete array stations has recently been developed (Harmandar, 2009). The spatial distribution of ground motion parameters is analyzed by geo-statistical analysis. The new numerical technique based on Kriging method (Krige, 1966) is developed with the aim of interpolation of ground motion parameters using information obtained from geo-statistical analysis. A dense array is needed to develop, test and apply the method, effectively. The proposed method is independent of region, event, and past or future data. It relies on data obtained from a certain earthquake to estimate regional distribution of ground motion parameters for the same event.

Kriging assigns weights according to a (moderately) data-driven weighting function, rather than an arbitrary function (Isaaks and Srivastava, 1989). In the modified Kriging method, a new formula is introduced for the calculation of the weights to estimate the PGA as:

$$w_i = \sqrt{PGA_i^{obs} \times PGA^{est}} \times d_i \qquad [4]$$

where d_i is the distance between the i^{th} record and station where the PGA is estimated; PGA_i^{obs} is the observed PGA and PGA^{est} is the estimated PGA

The computation of the weights based on Equation 4 in terms of separation distance is graphically demonstrated in Figure 61(b). For the estimation of PGA at a point, minimum four records around this point are considered. The distance between the estimation point and the location of observation is set on a minimum value (e.g. 3 km), if the number of available observations within this radius is four. Otherwise, it can increase. The selection of data is shown in Figure 61(a). Selected data are used to calculate the weights using Equation 4. The weights are grouped with respect to station separation distances with 0.1 km intervals to generate a regression curve fit. Gaussian, rational linear and rational quadratic fit and different exponential formulae are applied to find the best fit with minimum error. The best fit was obtained using the following functional form

$$w_i = a \times d_i^b \qquad [5]$$

where a and b are the variables that differ for each estimated point.

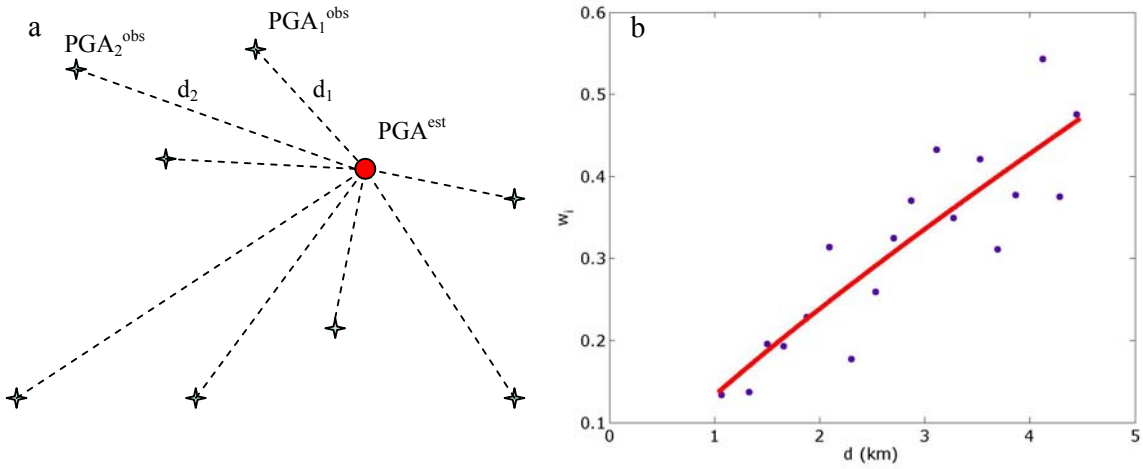

Figure 61. Selection of the observed data to predict PGA at an unknown point (a) and diagram for the calculation of the weights with respect to Equation (4) (b)

Then, a mathematical expression is developed to estimate PGA from observed PGA's, their weights and separation distances as:

$$PGA^{est} = \frac{1}{\sqrt[n]{\prod_{i=1}^{n} PGA_i^{obs}}} \prod_{i=1}^{n} \left(\frac{w_i}{d_i} \right)^{\frac{2}{n}} \quad [6]$$

where PGA^{est} is the estimated PGA, PGA^{obs} is the observed PGA, n is the number of observed PGA's used to find PGA^{est}, w_i is the weight of observed PGA at i^{th} station, calculated by Equation 4, and d_i is the separation distance between the observed and estimated PGA's (Figure 61(a)). The proposed method for the estimation of ground motion parameters is outlined in Figure 62 where the ground motion parameter PGA is used for a better illustration of the methodology. The methodology uses a data-set consisting of any ground motion parameter recorded by an urban dense strong ground motion array during an earthquake.

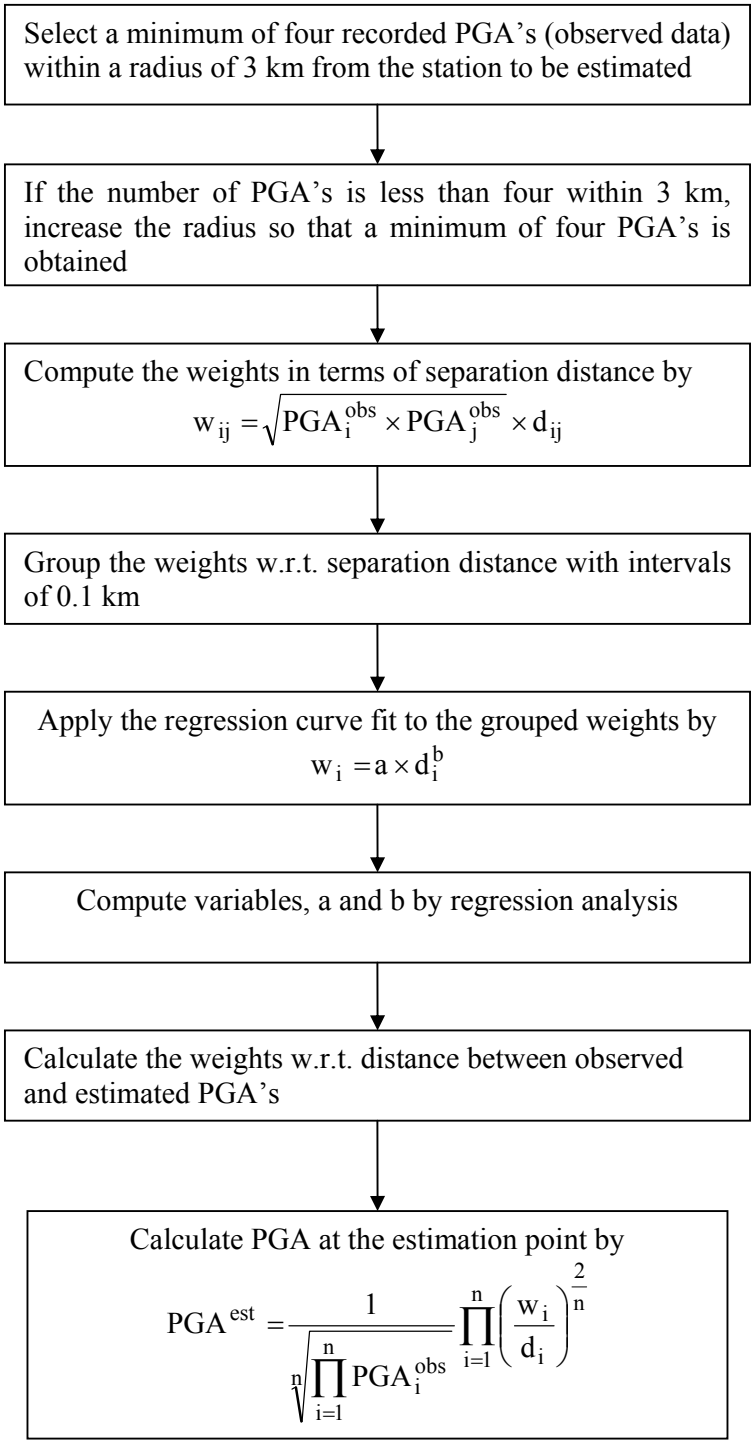

Figure 62. Procedure of the modified Kriging method

C.3. ELEMENTS at RISK

To perform a seismic loss assessment, an inventory of the elements at risk should be defined. ELER estimates the losses for buildings and population. The classification systems used to define the inventories, the necessary inputs for each level of analysis and the default databases of the software are described in the following sections.

C.3.1. Buildings

The definition of a classification system for the characterization of the exposed building stock and the description of its damage is an essential step in a risk analysis in order to ensure a uniform interpretation of data and results. For a general building stock the following parameters affect the damage and loss characteristics: structural (system, height, and building practices), nonstructural elements and occupancy (such as residential, commercial, and governmental).

The building classification systems used in vulnerability and loss assessments should not be country-, even region-specific to have uniform applicability in all major urban centers. The inter-regional difference in building architecture and construction practices should be reflected in building classifications for the development of inventories and vulnerability information.

The compilation of a suitable inventory of building stock is a major task and a key point in a loss estimation study. The quality of the available inventory both in terms of structural and occupational parameters and its geographical distribution will determine the methodology that will be used in the analysis as well as the quality of the resulting estimations.

Taxonomy

HAZUS99, EMS-98, and RISK-UE building taxonomies are the main classification systems envisaged in the development of ELER. In fact, ELER is structured in such a way that a building inventory can be classified in terms of any classification system as long as the empirical and/or mechanical vulnerabilities and performance curves associated with each building type is defined by the user.

In HAZUS99 the general building inventory includes residential, commercial, industrial, agricultural, religious, governmental, and educational buildings. In EMS'1998 a building inventory classification system is utilized to group buildings with similar damage/loss characteristics into a set of building classes to commensurate with the vulnerability relationship classes. A comparison of EMS-98 and HAZUS99 building classifications is provided in Table 20.

Considering the building materials, for masonry constructions EMS-98 classification considers six classes, very varied in material, techniques of installation and construction particulars. For reinforced concrete constructions, EMS-98 differentiates the constructions in relation to the seismo-resistant system (frame or shear wall) and to the level of anti-seismic design adopted to build them. For constructions in steel and in wood only one category is considered. Finally, EMS-98 does not make reference to prefabricated constructions. With regard to design level, EMS-98 uses three different Earthquake Resistance Design (ERD)

levels for Reinforced Concrete taxonomies (Table 22). ERD levels refer to a different amount of the design lateral load usually prescribed by the codes of different European regions, depending on the seismicity.

HAZUS99 (FEMA, 1999) envisages a classification by the height of the structure as portrayed in Table 21 (three classes are distinguished depending on the number of floor), in addition to a further classification of each structural system by the design level (four code levels: High-Code, Moderate-Code, Low-Code, Pre-Code) as in Table 22. An exception is made for Steel Frame with Unreinforced Masonry Infill Walls and Concrete Frame with Unreinforced Masonry Infill Walls for which Moderate Code is not considered and for Unreinforced Masonry Bearing Walls for which High Code is not present.

For earthquake loss estimation purposes for the city of Istanbul (Erdik et al., 2003) the building inventory of the city was divided into 24 groups according to the construction type (Reinforced concrete frame, Masonry, Reinforced concrete shears wall and Precast), number of floors (Low-rise, Mid-rise and High-rise) and construction date (Pre-1979 and Post-1980).

A comprehensive building type classification for Europe, that incorporated the characteristic features of the European building taxonomy, was developed in the European Commission funded RISK-UE project (RISK-UE, 2001-2004) entitled “An Advanced Approach to Earthquake Risk Scenarios with Application to Different European Towns”. The building taxonomy developed in RISK-UE is given in Table 23. Table 23 also includes a comparison of the RISK-UE and EMS-98 building classifications.

The European building classification proposed in Giovinazzi (2005) is given in Table 24 through Table 26. The classification includes a basic division in terms of construction type and associated sub-divisions.

Table 20. EMS'98 and HAZUS99 building classifications

EMS 98 Classification	HAZUS99 Classification
Unreinforced Masonry	**Masonry Typologies**
Rubble Stone	Unreinforced Masonry Bearing Walls (URM)
Adobe (earth bricks)	
Simple Stone	
Massive Stone	
U. Masonry (old brick)	
U Masonry – R.C.floors	
Reinforced / confined masonry	**Reinforced / confined masonry**
Reinforced / confined masonry	RM Bearing walls with wood or metal deck diaphragms
	RM Bearing walls with precast concrete diaphragms
Reinforced Concrete	**Reinforced Concrete**
Frame in R.C.	Concrete Moment Frame
Shear Walls	Concrete Shear Walls
	Concrete Frame with U. Masonry Infill Walls
Steel Typologies	**Steel Typologies**
Steel Structures	Steel Moment Frame Low Rise
	Steel Braced Frame
	Steel Light Frame
	Steel Frame with Cast-in-Place Concrete Shear Walls
	Steel Frame with Unreinforced Masonry Infill Walls
Timber Typologies	**Timber Typologies**
Timber structures	Wood, Light Frame
	Wood, Commercial and Industrial
	Pre Cast Typologies
	Precast Concrete Tilt-Up Walls
	Precast Concrete Frames with Concrete Shear Walls
	Mobile Homes

Table 21. HAZUS99 classes of height

	Floor Number
Low –Rise	1-3
Mid – Rise	4-7
High – Rise	8+

*Low Rise=1-2 for URM and W1

Table 22. EMS-98 ERD Level and HAZUS99 code levels

EMS'1998
Without ERD
Moderate ERD
High ERD

HAZUS99
Pre-Code
Low-Code
Medium-Code
High-Code

Table 23. The Risk UE and EMS'98 Building Taxonomies

RISK UE		EMS98	
Taxonomy	Description		
M1	Stone Masonry Bearing Walls made of …		
M 1.1	Rubble stone, fieldstone	M1	RUBBLE STONE
M 1.2	Simple Stone	M3	SIMPLE STONE
M 1.3	Massive Stone	M4	MASSIVE STONE
M2	**Adobe**	M2	ADOBE (EARTH BRICKS)
M3	**Unreinforced Masonry Bearing walls with..**		
M 3.1	Masonry with wooden slabs		
M.3.2	Masonry vaults		
M 3.3	Composite steel and masonry slabs		
M 3.4	Reinforced concrete slabs	M6	U masonry rc floors
M4	Reinforced or confined masonry walls	M7	REINFORCED CONFINED MASONRY
M5	Overall strengthened		
RC 1	Concrete Moment Frame	RC1.1	FRAME IN RC (WITHOUT E.R.D.)
RC 2	Concrete Shear walls	RC2.1	SHEAR WALLS (WITOUT E.R.D.)
RC 3	Concrete Frames with unreinforced masonry infill walls		
RC 3.1	Regulary infilled walls	RC1.2	FRAME IN RC (MODERATE E.R.D.)
RC 3.2	Irregularly infilled walls	RC1.1	FRAME IN RC (WITHOUT E.R.D.)
RC 4	RC Dual systems (RC frame and wall)	RC2.2	SHEAR WALLS (MODERATE E.R.D.)
RC 5	Precast Concrete Tilt-up Walls		
RC 6	Precast C. Frames, C Shear walls		
S1	Steel Moment Frames		
S2	Steel Braced Frames		
S3	Steel Frame+unreinforced. Mas. Infill walls		
S4	Steel frame+cast – in –place shear walls		
S5	Steel and RC composite system		
W	Wood Structures		

Table 24. Proposal for a European Building taxonomy classification

Building Taxonomy	
Unreinforced Masonry	
M1	Rubble stone
M2	Adobe (earth bricks)
M3	Simple stone
M4	Massive stone
M5	U Masonry (old bricks)
M6	U Masonry – R.C. floors
Reinforced/confined masonry	
M7	Reinforced/confined masonry
Reinforced Concrete	
RC1	Frame in r.c. (without ERD)
RC2	Frame in r.c. (moderate ERD)
RC3	Frame in r.c. (high ERD)
Steel Taxonomy	
S	Steel structures
	Timber Taxonomy
W	Timber structures

Table 25. Sub-taxonomies considered for the proposed classification system

Masonry Building Horizontal Structure Taxonomy	
M_w	Wooden slabs
M_v	Masonry vaults
M_sm	Composite steel and masonry slabs
M_ca	Reinforced concrete slabs

Reinforced Concrete Building	
RC1_i	Infill Walls
RC_p	Pilotis

Table 26. Classes of height considered for the proposed classification system

		Floor Number	
		Masonry	Reinforced Concrete
_L	Low - Rise	1÷2	1÷3
_M	Mid - Rise	3÷5	4÷7
_H	Heigh - Rise	≥7	≥8

Inventory

A building inventory is a catalog of the buildings and facilities in each class of the assumed classification system. In ELER structure, the building inventory should be associated with geographical coordinates in order to perform a loss estimation study resulting from the ground motion generated by a specific earthquake, or obtained from a hazard study.

The sophistication and completeness level of the building inventory is also a function of the regional scale and will determine the level of analysis that will be used in loss estimation. Level 1 and Level 2 analyses of ELER will deal with building damage estimations and three levels of building inventory definition are envisaged within these two levels of analysis.

The crudest level of building inventory corresponds to an approximated European database of the number of buildings and their geographic distribution and aims at a rough estimation of building damages in a country scale in Europe. This approximated building database is obtained from Corine Land Cover and Population databases and is provided within ELER as the default data of Level 1 analysis. This countrywide approximated building database is provided in 30 sec and 150 sec arc grids for 27 countries in Europe for which the Corine Land Cover data are available (Table 27 and Figure 63). The methodology used in obtaining the country basis geographic distribution of the number of buildings from Corine Land Cover and Population databases are covered in Appendix A.

Once the 30 sec and 150 sec arc grid distributions of the total number of buildings were obtained, the grid based approximate number of buildings in each building class as defined in the European building classification system were computed using the countrywide overall building class ratios provided in PAGER database.

Table 27. Countries covered in Corine Land Cover database

No.	Country Name	No.	Country Name
1	Austria	15	Latvia
2	Belgium	16	Malta
3	Bulgaria	17	Netherlands
4	Cyprus	18	Poland
5	Czech Republic	19	Portugal
6	Germany	20	Romania
7	Denmark	21	Sweden
8	Estonia	22	Slovenia
9	Finland	23	Slovakia
10	Greece	24	United Kingdom
11	Hungary	25	Spain
12	Ireland	26	France
13	Lithuania	27	Italy
14	Luxemburg		

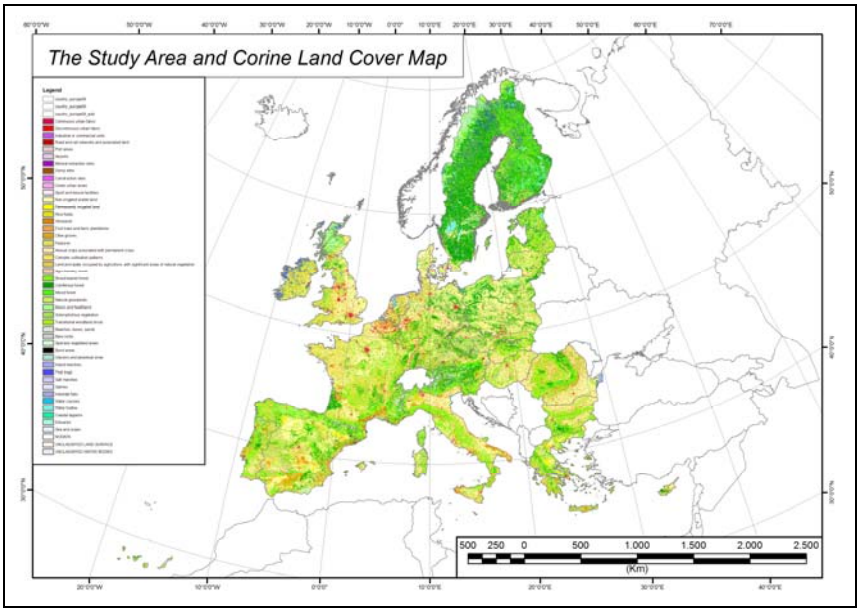

Figure 63. Corine Land Cover coverage area

This approximation approach aims at providing the user the opportunity to run a Level 1 building damage and casualty estimation analysis in county scale using the default data available within the software.

For a more rigorous loss estimation, the user should provide a grid based database of the actual number of buildings corresponding to building taxonomies defined in Section C.3.1 of this report. Two typical datasets are provided within the software. These are the grid based building inventory of Marmara, Turkey region adopted for the macroseismic loss estimation methodology (Level 1) and a more detailed building inventory of the Zeytinburnu district of Istanbul adopted for the mechanical loss estimation methodology (Level 2).

The grid based building inventory of Marmara region is based on the year 2000 building census tracts carried out by Turkish Statistical Institute (TUIK). The data include the construction year, the occupational type, the construction type and the number of floors of each building. The construction type and number of floors are the main parameters affecting the earthquake performance of buildings. Since the seismic design code applicable in Turkey improved particularly after 1975, the buildings were classified as pre-1979 (included) and post-1980 reflecting the state of seismic design applications. The inventory is classified in the following way in accordance with the EMS building classification system.

In terms of the construction type:

1. Reinforce Concrete (RC1- Moderate Code):
2. Unreinforced Masonry (M5)
3. Adobe (M2)
4. Rubble Stone (M1)

In terms of the number of floors:

1. Low Rise (1-3 floors + Unknown data)
2. Mid Rise (4-6 floors)
3. High Rise (7-16 floors)

Although the macroseismic vulnerability relationships predefined in Level 1 do not utilize the age of the building as a parameter the database can further be sub-divided considering the construction date if necessary.

The TUIK data were geocoded at district level. They were transferred to 0.05^o x 0.05^o grids using the LandScan population distribution as a basis. The construction type was selected as the basic parameter to be distributed to geocells. Next, the number of floors and the age of building were added using a logic tree and the district based ratios of these two parameters (Table 28).

Table 28. The logic tree to obtain the numbers for each of building class

Construction Type	The story Number of Buildings	Construction Year
RC1	Low Rise	Pre – 1980
M1- Rubble	Mid Rise	Post - 1980
M2- Adobe	High Rise	
M5 – Unreinforced Masonry		

In addition to the building database of Marmara region, a more detailed inventory is provided for the Zeytinburnu district of Istanbul as an example dataset to be used in Level 2. This inventory was based on the 1/5000 scale building footprint maps of the Istanbul Metropolitan Municipality (IBB) and TUIK year 2000 building census (KOERI, 2002). The building inventory is classified both in terms of the European Building Classification System and also a HAZUS similar system considering the construction type, the height and the construction year of the buildings. The building inventory is provided in 0.005^o x 0.005^o geocell level.

Table 29. Building inventory of Istanbul based on RISK-UE Building taxonomy

		Alternative Building Class Risk UE Building Classification Level1					
KOERI Building Class	Description	Percentage Rate (%) / Building Type					Description
B111	RC Frame, 1-4 stories, pre-1979	50	RC31	50	RC32	LRPC	Low Rise- Pre Code
B112	RC Frame, 1-4 stories, post-1980	50	RC31	50	RC32	LRC	Low Rise - Code
B121	RC Frame, 5-8 stories, pre-1981	50	RC31	50	RC32	MRPC	Mid Rise- Pre Code
B122	RC Frame, 5-8 stories, post-1982	50	RC31	50	RC32	MRC	Mid Rise- Code
B131	RC Frame,>-8 stories, pre-1981	50	RC31	50	RC32	HRPC	High Rise - Pre Code
B132	RC Frame, >8 stores, post-1982	50	RC31	50	RC32	HRC	High Rise - Code
B211	Masonry, 1-4 stories, pre-1979	50	M32	50	M33	LRPC	Low Rise- Pre Code
B212	Masonry, 1-4 stories, post-1979	50	M33	50	M34	LRC	Low Rise - Code
B221	Masonry, 5-8 stories, pre-1979	50	M32	50	M34	MRPC	Mid Rise- Pre Code
B222	Masonry, 5-8 stories, post-1979	50	M33	50	M34	MRC	Mid Rise- Code
B311	Shear wall, 1-4 stories, pre-1979	RC2				LRPC	Low Rise- Pre Code
B312	Shear wall, 1-4 stories, post-1979	RC2				LRC	Low Rise - Code
B322	Shear wall, 5-8 stories, post-1979	RC2				MRC	-
B331	Shear wall, >8 stories, pre-1979	RC2				HRPC	High Rise - Pre Code
B332	Shear wall, >8 stories, post-1979	RC2				HRC	High Rise - Code
B411	Prefabricated, 1-4 stories, pre-1979	50	RC5	50	RC6	LRPC	Low Rise- Pre Code
B412	Prefabricated, 1-4 stories, post-1979	50	RC5	50	RC6	LRC	Low Rise - Code

C.3.2. Demography

Grid based demographic data should be provided for casualty estimations. The required level of sophistication with respect to levels of analysis is similar to the building inventory. 30 arc sec grid based Landscan population data are provided for Level 0 analysis. The same database is also used as default for Levels 1 and 2. Additionally the Corine population data are provided for countries for which approximate building inventories based on Corine Land Cover are given for Level 1 analysis. For both the Level 1 and Level 2 analyses, if the user desires to estimate casualties based on local data, an additional population field, defining the number of people residing in the cell should be provided together with the building inventory data.

C.4. EARTHQUAKE LOSS ASSESSMENT

C.4.1. LEVEL 0

The Level 0 analysis of ELER software consists of non building specified approaches developed human causality estimates for geographical area or for population density correlating with the size of the earthquake (magnitude or intensity). Empirical models rely directly on the fatality rates of exposed population as functions of earthquake intensity, regional vulnerability level, regional growth rate and time of the day. Regional vulnerability levels can be assigned on the basis of the level of economic development, general building types and building occupancy rates with various degrees of refinement and resolution. The number of people exposed to various levels of earthquake ground motion intensities can be assessed through the use of the Gridded global ambient population database prepared by Oak Ridge National Laboratory (http://www.ornl.gov/sci/landscan/landscan2005/index.html). Samardjieva and Badal (2002), RGELFE (1992) and Vacareanu et al.(2004) empirical approaches are used in this level to estimate the human casualty.

Vacareanu et al.(2004) Approach

A proposal made in the framework of Risk-UE Project WP7-Report (Vacareanu et al., 2004) relates the number of deaths to the magnitude of the earthquake. A correlation of human losses with the earthquake magnitude is provided in Figure 64. Representing human losses from several earthquakes occurred in different country as a function of the earthquake magnitude (Figure 64) a correlation has been derived:

$$D=ce^{1.5M} \quad [7]$$

where D is the number of deaths, M is the magnitude of the earthquake and c is a coefficient assuming different values for lower, median and upper bounds (respectively c = 0.002, c = 0.06, c = 0.4). As it can be seen uncertainties in such correlations can reach two orders of magnitude.

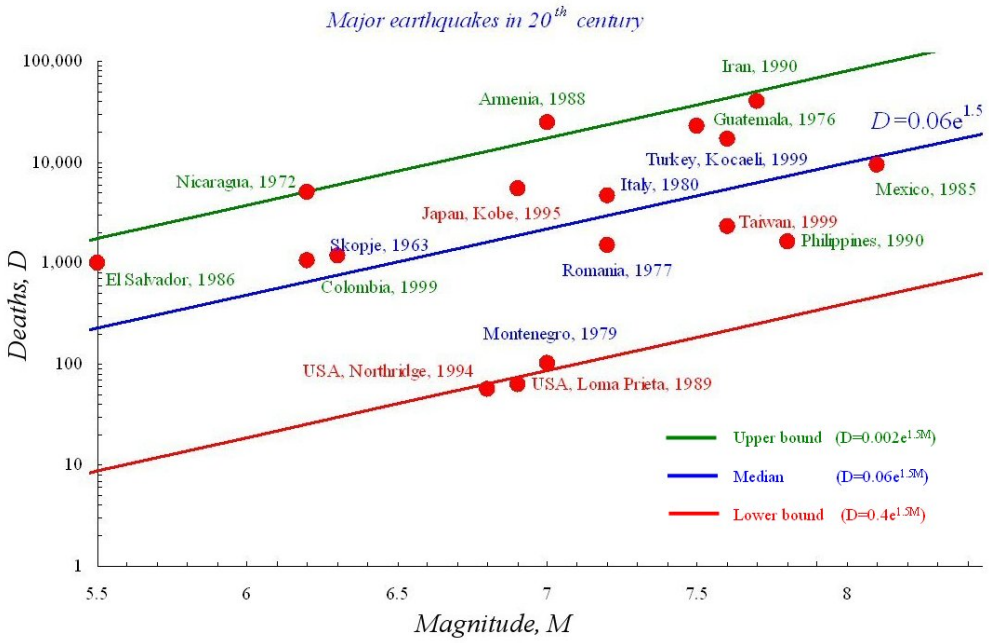

Figure 64. Correlation of deaths with earthquake magnitude (After, Vacareanu et.al., 2004, Seismic Risk Scenarios, Risk-UE Report)

RGELFE (1992) Empirical Approach

Based on empirical data RGELFE (1992) provides for major cities, the following fatality rates for various levels of intensity: 0.0014%, 0.031%, 0.48% and 6.8% for intensity zones VI, VII, VIII and IX respectively. As it can be observed from that study, this kind of crude casualty prediction models exhibit a high level of regional dependency.

Samardjieva and Badal (2002) Empirical Approach

Samardjieva and Badal (2002) conducted a regression analysis between the number of casualties (in log scale) and the earthquake magnitude for different ranges of population density in the affected region using events from 1945 till 2000.

In the approach proposed by Christoskov and Samardjieva (1984) to estimate the possible number of casualties, it was assumed that the total number of human losses, N_k, is mainly a function of the earthquake magnitude, M, and the actual population density, D, in the affected area. Taking into account only earthquakes at normal focal depth (h< 60 km), the number of victims is calculated by;

$$\log N_k(D) = a(D) + b(D)M \qquad [8]$$

where the coefficients a and b are regression parameters depending on the average population density D of the affected area. Samardjieva and Badal (2002) applied a standard least-squares method and grouped the data according to the most frequently met density groups in the world: D <25, D= 25–50, D= 50–100, D = 100–200, and D> 200 people/km^2. The values of

the coefficients *a* and *b* in Equation (8) for the period 1951–1999 and for various population density groups are given in Table 30.

Table 30. Regression Coefficients a and b in Equation (8) for the Periods 1900–1950 and 1951–1999 and Different Population Density Groups

		Regression Coefficient			
		a	b	R	sigma
D<25	1900-1950	-3.41	0.66	0.88	0.341
	1951-1999	-3.11	0.67	0.84	0.343
D=25-50	1900-1950	-3	0.71	0.9	0.295
	1951-1999	-3.32	0.75	0.85	0.342
D=50-100	1900-1950	-2.6	0.75	0.92	0.295
	1951-1999	-3.13	0.84	0.82	0.345
D=100-200	1900-1950	-2.17	0.77	0.92	0.292
	1951-1999	-3.22	0.92	0.7	0.397
D>200	1900-1950	-2.09	0.86	0.83	0.344
	1951-1999	-3.15	0.97	0.75	0.348

Christoskov and Samardjieva (1984) suggested an analogous relationship for the assessment of the number of the injured people N_{inj}. The ratio N_{inj}/N_k was obtained as in the following equation:

$$\log\left(N_{inj}/N_k\right) = -0.99 + 0.21M \qquad [9]$$

The coefficient of correlation was $r = 0.70$.

For reliable results, the implementation of the methods specified above requires the following prerequisites to be satisfied:

1. Contour VI exists.

   This is important since ELER uses contour VI as the boundary of the affected area, calculating the population density inside this region. Events which do not produce intensity values of VI are considered too low for the use of SB2002 methodology. Nevertheless the other Level 0 approaches can be used in such cases. For cases where the intensity distribution is too high (i.e. the contour VI is not observed) the user should consider increasing the map extent.

2. Contour VI encloses a land (populated) area.

   Since the lowest density range in the SB2002 approach is defined as <25 people per km^2 theoretically even densities close to zero will output a number of casualty as function of the event magnitude. It is problematic to implement the Christoskov et al., (1990) distribution model for cases where the estimated casualty is actually larger than the affected population (e.g. water or desert areas).

The following procedure is used to obtain the grid based distribution of the estimated number of casualties in Level 0.

1. Obtain the intensity distribution resulting from the earthquake (ShakeMap).

2. Obtain grid based population distribution and average population density (D_I) for zones of intensity I.

3. Obtain the distribution of the casualties in different intensity zones from the model suggested by Christoskov et al. (1990). This model assumes that the number of casualties decreases proportionally with the square of the epicentral distance, R, similar to the attenuation of the seismic energy, $N \sim 1/R^2$. A factor W_i, depending on the radii R_I of the areas of intensity I was introduced. For example, in the case of observed intensities I = VII, VIII, VIX (MSK), the weighting coefficients W_I are:

$$W_i = 1/\left[R_I^2 \sum_j \left(1/R_j^2\right) \right], j = \text{VII, VIII, IX} \quad [10]$$

Then, the number of people killed within the area of intensity I can be determined by the equation:

$$N_k^I = W_I \cdot N_k(D_I) \quad [11]$$

where the value of $N_k(D_I)$ is estimated from Equation (11) for the average population density D_I in the area intensity I. The total number of human losses is the sum of the values N_k^I.

4. Obtain the grid based casualty distribution from:

$$Deaths\ per\ unit\ area_I = N_k^I \cdot \frac{Population\ per\ unit\ area_I}{Total\ population_I} \quad [12]$$

$$Injuries\ per\ unit\ area_I = N_{inj}^I \cdot \frac{Population\ per\ unit\ area_I}{Total\ population_I} \quad [13]$$

C.4.2. LEVEL 1

The Level 1 loss estimation engine of ELER is based on macroseismic damage estimation tools and aims at the assessment of both the building damage and the casualties. The intensity based empirical vulnerability relationships of Giovinazzi and Logomarsino (2005) and casualty vulnerability models based on the various analytical approaches are utilized.

Building Damage Estimation

The observed damage based vulnerability method referred to as macroseismic method was originally developed by Giovinazzi and Logomarsino (2004) from the definition provided by the European Macroseismic Scale (EMS-98, Grunthal, 1998) making use of classical probability theory and of the fuzzy-set theory. The idea behind this study was: as the aim of a Macroseismic Scale is to obtain a measure of the earthquake severity from the observation of the damage suffered by the buildings, similarly the scale itself can be used as a vulnerability model for forecast purposes to supply the probable damage distribution for a given intensity. The EMS-98 scale provides a damage matrix that contains the probability of the buildings belonging to a certain vulnerability class suffering a certain damage level under a given intensity. However these damage matrices can only provide a vague and incomplete vulnerability model. As the damage probabilities are provided in a fuzzy way through three narrowly overlapping percentage ranges and as the damage matrices are incomplete considering only the most common and easily observable situations. In that study the incompleteness matter was solved by introducing Beta distribution to model damage grade variation. This enabled the development of an analytical expression for the relationship between mean damage grade, μ_D (mean of the discrete beta distribution) – intensity, I and vulnerability index, V (Equation 14), allowing estimation of the building damage distribution once vulnerability index V dominant in the area of interest is known.

$$\mu_D = 2.5\left[1+\tanh\left(\frac{I+6.5V-13.1}{2.3}\right)\right] \quad [14]$$

The vulnerability indices obtained for different building types are summarized in Table 31.

The mean damage grade values (Equation 14) are then connected to the two parameters *r* and *t* (Equations 15 and 16) required to fully describe the continuous beta distribution with a 3rd degree polynomial of the form shown below (Equation 15). The t parameter governs the dispersion of beta distribution, where increasing *t* decreases the scatter. In this study based on empirical data, *t* values were assigned to different building types (Table 32). So the only unknown parameter required to describe the damage distribution is *r*.

$$pdf_\beta(x) = \frac{\Gamma(t)}{\Gamma(r)\Gamma(t-r)}\frac{x^{r-1}(6-x)^{t-r-1}}{6^{t-1}} \quad [15]$$

where Γ is the gamma function.

$$r = t(0.007\mu_D{}^3 - 0.0525\mu_D{}^2 + 0.2875\mu_D) \quad [16]$$

Table 31. Computed vulnerability indices for different building typologies

Building Typologies		Building type	Vulnerability indices				
			V_{min}	V_{-}	V_o	V_+	V_{max}
Masonry	M1	Rubble stone	0.62	0.81	0.873	0.98	1.02
	M2	Adobe	0.62	0.687	0.84	0.98	1.02
	M3	Simple stone	0.46	0.65	0.74	0.83	1.02
	M4	Massive stone	0.3	0.49	0.616	0.793	0.86
	M5	U Masonry (old bricks)	0.46	0.65	0.74	0.83	1.02
	M6	U Masonry – r.c. floors	0.3	0.49	0.616	0.79	0.86
	M7	Reinforced/confined masonry	0.14	0.33	0.451	0.633	0.7
Reinforced Concrete	RC1	Frame in r.c. (without ERD)	0.3	0.49	0.644	0.8	1.02
	RC2	Frame in r.c. (moderate ERD)	0.14	0.33	0.484	0.64	0.86
	RC3	Frame in r.c. (high ERD)	-0.02	0.17	0.324	0.48	0.7
	RC4	Shear walls (without ERD)	0.3	0.367	0.544	0.67	0.86
	RC5	Shear walls (moderate ERD)	0.14	0.21	0.384	0.51	0.7
	RC6	Shear walls (high ERD)	-0.02	0.047	0.224	0.35	0.54
Steel	S	Steel structures	-0.02	0.17	0.324	0.48	0.7
Timber	W	Timber structures	0.14	0.207	0.447	0.64	0.86

Table 32. t values for given different building typologies (Giovinazzi and Lagomarsino, 2004)

t		
Building Typologies	M1, M2, M3	6
	M4, M5, M6, M7, RC4, RC5, RC6	4
	RC1, RC2, RC3, S, W	3

Besides the building type, there are several other factors that affect the overall vulnerability of a structure caused by both the variety of the constructive methods and the structural details and materials used in different regions. Thus, a regional vulnerability variability factor should be defined to obtain a more reliable evaluation. On the basis of the historical data or the experience, the Vr value is allowed to modify the typological vulnerability index. If regional intensity based vulnerability curves or sufficient observed damage data are available, the average curve can be shifted to obtain a better approximation of the regional data (Figure 65, Giovinazzi and Lagomarsino, 2004). ELER software allows the incorporation of a regional vulnerability variability factor if such information is available.

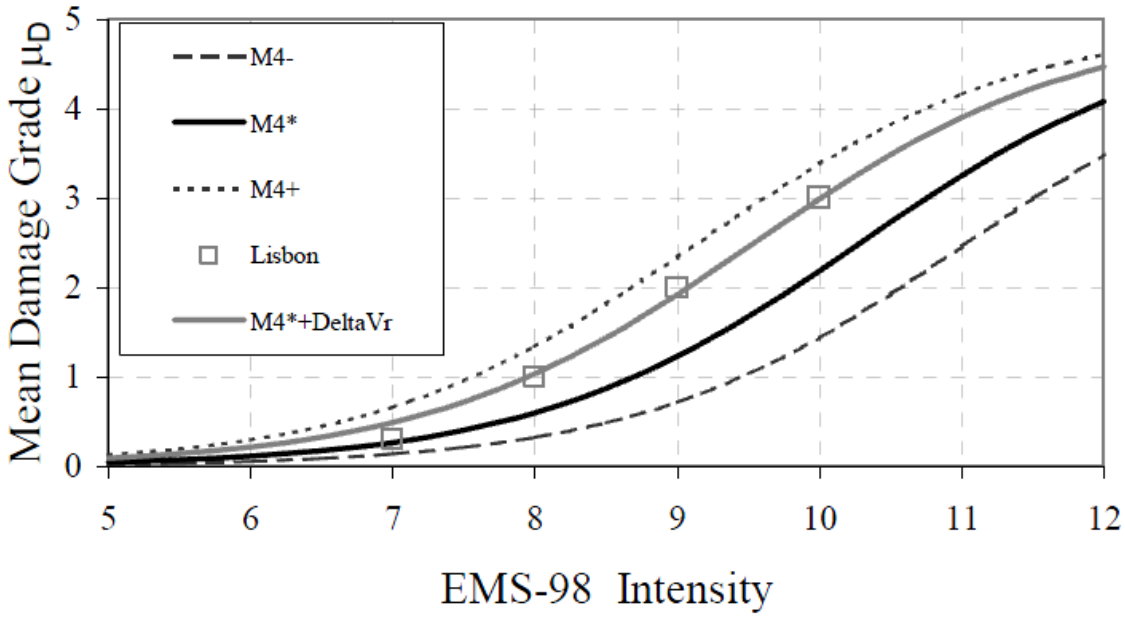

Figure 65. Massive Stone shows a better behavior (Oliveira et al., 1984) than the average for M4 in Lisbon; ΔVr=0.12 is applied.

Casualty Estimation

Analytical human loss models use building damage and consequential physical damage (e.g. post-earthquake fire, explosion, hazmat release) as the starting point for the evaluation of casualties. This casualty assessment approach requires the knowledge of building occupancy data and the probability of several levels of injury and death for different building types with given states of building damage. This however, is not easily attainable due to the limited quality and lack of information on earthquake casualty data. There are three approaches used in this level.

Coburn and Spence (1992) Method

For the estimation of the fatalities due to structural damage (the K_s parameter), which is the controlling factor for most destructive earthquakes, Coburn and Spence (1992, 2002) proposed the equation given below:

$$K_{sb}=TC_b x\ [M_1 x\ M_2 x\ M_3 x\ (M_4+M_5(1-M_4))] \quad [17]$$

where TC_b is the total number of collapsed buildings of type b, M_1 is the factor taking into account regional variation of population per building, M_2 is the factor taking into account variation of occupancy depending on the time (Figure 66), M_3 is the factor taking into account percentage of trapped occupants under collapsed buildings (Table 33), M_4 is the factor taking into account different injury levels of trapped people (Table 34), and M_5 is the factor taking into account change of injury levels of trapped people with time (Table 35). Using Equation 17 and Table 33 through Table 35, the casualty rates applicable immediately after the earthquake for masonry and reinforced concrete buildings corresponding to different severity levels are calculated (Table 36 and Table 37). For severity level S4, final casualty levels

corresponding to level 3 type emergency response described in Table 35 are also given in Table 36 and Table 37.

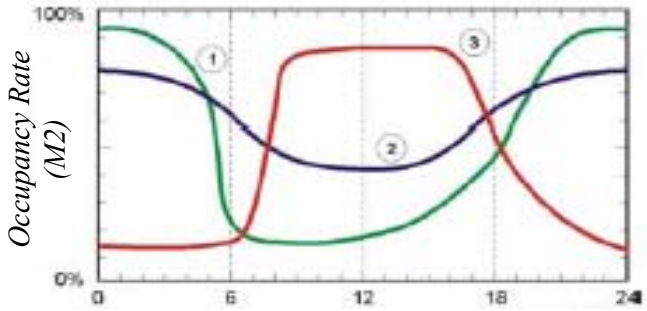

1. Rural agricultural buildings
2. Urban residential buildings
3. Non residential buildings

Figure 66. Variation of occupancy with time

Table 33. Factor M3 for Masonry and RC structures

Collapsed Masonry Buildings (up to 3 storeys)				
MSK Intensity	VII 5%	VIII 30%	IX 60%	X 70%
Collapsed RC Structures (3-5 storeys)				
Near-field, high-frequency ground motion	70%			
Distant, long period ground motion	50%			

Table 34. Factor M4 for Masonry and RC structures

Injury Category	**Masonry**	**RC**
Light Injury (S1)	20%	10%
Injury requiring hospital treatment (S2)	30%	40%
Severe Injury (S3)	30%	10%
Dead or unsaveable (S4)	20%	40%

Table 35. Factor M5 for Masonry and RC structures

Situation	**Masonry**	**RC**
Level 1: Community incapacitated by high casualty rate	95%	-
Level 2: Community capable of organizing rescue activity	60%	90%
Level 3: Community + emergency squads after 12 hours	50%	80%
Level 4: Community + emergency squads+SAR experts after 36 hours	45%	70%

Table 36. Casualty rates for masonry structures

		Injury distribution at collapse				**Post**
	Intensity	S1	S2	S3	S4	**S4**
Masonry Building	VII	0.01	0.015	0.015	0.01	**0.03**
	VIII	0.06	0.09	0.09	0.06	**0.18**
	IX	0.12	0.18	0.18	0.12	**0.36**

	X	0.14	0.21	0.21	0.14	**0.42**

Table 37. Casualty rates for reinforced concrete structures.

	Frequency Content	Injury distribution at collapse				**Post**
		S1	S2	S3	S4	**S4**
Reinforced Concrete Building	Near-field, high frequency ground motion	0.07	0.28	0.07	0.28	**0.62**
	Distant, long period ground motion	0.05	0.2	0.05	0.2	**0.44**

The number of buildings and population in each cell are the main parameters to estimate casualties. To obtain casualty estimations from the number of buildings in different damage states, an average number of population per building should be known. To estimate this, the user should define an average number of dwelling units per building type, which is usually a function of the number of floors. Using the user-defined average number of dwellings per building type and the grid based population data entered by the user, or the default Landscan population data of the region, the program computes an average number of population per dwelling unit, which in turn can be used to check if the estimated number of dwellings per building type were correct. The analysis of population and building census tracks of the city of Istanbul revealed an average of three people per dwelling unit in Istanbul (Table 38) (KOERI, 2002).

Table 38. Population for different building types in Istanbul

Building Type	Number of floors	Number of dwelling units	Population
Low Rise	1 -4	3	9
Mid Rise	5-8	12	36
High Rise	>=9	32	96

KOERI (2002) Method

Casualty rates, especially deaths, depend largely on the probability of the building being in the "complete" damage state. Casualty data in urbanized areas from Turkish earthquakes indicate much higher fatalities in heavily damaged multi-storey R/C buildings. Data from the 1992 Erzincan earthquake indicate 1 death and 3 hospitalized injures per collapsed or heavily damaged R/C building (Erdik 1993) Similar statistics are also valid for the 1999 Kocaeli earthquake. About 20,000 R/C buildings were collapsed or heavily damaged and the total dead count was around 19,000. The death to hospitalized injury ratio in this earthquake was 1:2.5. For the assessment of human casualties from damage data computed from intensity based vulnerabilities we have assumed that the number of deaths will be equal to the number of buildings with damages in D4 and D5 level. The number of hospitalized injuries is found by multiplying the death figure by 4 based on ATC-13 recommendations (Table 39).

Table 39. ATC-13 Casualty rates

Damage State	Range	Minor Injuries	Serios Injuries	Deaths
Slight	0-1	3/100,000	1/250,000	1/1,000,000
Light	1-10	3-10,000	1/25,000	1/100,000
Moderate	10-30	3/1,000	1/2,500	1/10,000
Heavy	30-60	3/100	1/250	1/1,000
Major	30-100	3/10	1/25	1/100
Destroyed	100	2/5	2/5	1/5
		RATE=30A	RATE=4A	RATE=A

* for light steel and wood-frame construction, multiply all numerators by 0.1

Risk-UE Casualty Vulnerability Relationships

The casualty vulnerability relationships used in the Risk-UE project are based on the findings of Bramerini et al. (1995) that studied the statistics on casualties, severely injured and homeless people in Italy. The study of Bramerini et al. (1995) resulted in the following correlations between damage grades and effects of these on population:

Table 40. Correlation between damage grades and their effects on the built environment and population

Effects to people and impact on the built environment		
BUILDINGS	Unusuable	40% of buildings with damage grade 3 and 100% of buildings with damage grades 4 and 5
	Collapsed	Buildings with damage grade 5
PEOPLE	Homeless	100% of the population living in unusable buildings – casualties and severely injured
	Casualties and severely injured	30% of the population living in collapsed buildings

Estimation of Direct Economic Loss

Economic loss is, essentially, the translation of physical damage into total monetary loss using local estimates of repair and reconstruction costs. Studies on economic impacts of earthquakes have been usually examined in two categories: a) loss caused by damage to built environment (direct loss), and b) loss caused by interruption of economic activities (indirect loss).

Through use of statistical regression techniques, data from past earthquakes can be used to develop relationships (Loss Functions) for predicting economic losses. However the existing economic loss data are scarce, biased for heavy damage and could also be proprietary. Loss functions can be estimated by using analytical procedures in connection with a Monte Carlo simulation technique.

The estimates of the direct economic losses due to building damages are relatively easier to be included in rapid loss assessments. These losses are generally quantified as Loss Ratios (LR) - the loss as a percentage of the building replacement value. The economic losses to other elements of the built environment and indirect economic losses, representing the losses due to various forms of post-earthquake socioeconomic disruptions (such as employment and income, insurance and financial aids, construction, production and import-export of goods and services) cannot be rationally included in rapid earthquake loss assessment estimations and are therefore excluded from ELER methodology.

The methodology given HAZUS MH (FEMA, 2003) Technical Manual describes the conversion of damage state information into estimates of monetary losses. This methodology is used to convert the estimated building damages to mean damage states and building repair and replacement costs.

The economic loss module developed in ELER v3.0 relies on user-defined loss ratios for the damage states of the corresponding level of analysis. These are EMS98 D1 to D5 for Level 1. The loss ratio is defined as the ratio between repair and reconstruction costs of a structure. The loss ratios are used to convert the number of damaged buildings in each grid to cell based loss ratio values. ELER computes the monetary value of direct economic losses by multiplying the loss ratios with the total building cost for each building type of the used inventory. This can be expressed with the following simple equation:

$$Loss\left(Btype, D_k\right) = LR\left(D_k\right) \times RC\left(Btype\right) \quad [18]$$

where the loss ratio *LR* is a function of the building's damage states, namely from D_k (k=1-5), and the replacement cost *RC* is defined for each building type (*Btype*) in the building database. The overall economic loss is obtained by grid based aggregation.

KOERI (2002) default values of direct economic loss for structural and nonstructural systems are based on the following assumptions of the loss ratio corresponding to each state of damage:

- D1 damage state would correspond to a loss of 5% of building's replacement cost
- D2 damage state would correspond to a loss of 20% of building's replacement cost
- D3 damage state would correspond to a loss of 50% of building's replacement cost
- D4 damage state would correspond to a loss of 80% of building's replacement cost
- D5 damage state would correspond to a loss of 100% of building's replacement cost

C.4.3. LEVEL 2

Level 2 analysis is essentially intended for earthquake loss assessment (building damage, consequential human casualties and macro economic loss quantifiers) in urban areas. The basic Shake Mapping is similar to the Level 0 and Level 1 analysis. The spectral acceleration-displacement-based vulnerability assessment methodology is utilized for the building damage estimation. The following methods can be chosen for the analysis:

1. Capacity Spectrum Method (CSM)
2. Modified Acceleration-Displacement Response Spectrum (MADRS) Method
3. Reduction Factor Method (RFM)
4. Coefficient Method (CM)

The building and population data for the Level 2 analysis consist of grid (geo-cell) based urban building and demographic inventories. For building grouping the European building taxonomy developed within the EU-FP5 RISK-UE project (Lagomarsino and Giovinazzi, 2006) and model building types of HAZUS-MH (FEMA, 2003) are used. The software database includes the building capacity and the analytical fragility parameters for both of the building taxonomies. The user has also the capability to define custom capacity and fragility curves by Building Database Creator- BDC in order to use with any selected method of the Level 2 analysis. Once having calculated the damaged buildings by one of the above methods, casualties in Level 2 analysis are estimated based on the number of buildings in different damage states and the casualty rates for each building type and damage level. Modifications to the casualty rates can be used if necessary.

In the forthcoming sections, following the brief information about the main items of the spectral capacity-based vulnerability assessment methodology, i.e. representation of the seismic demand, representation of the building capacity and estimation of the performance point, the implementation of the analytical methods and the casualty estimation methodology are explained in detail. The user might refer to the D3 Report of JRA3 Task 2b for further information about the methodology and the methods adopted in Level 2 Analysis.

Spectral Capacity-Based Vulnerability Assessment

The so-called Capacity Spectrum Method (ATC-40, 1996 and HAZUS99) developed for the analytical assessment of the structural vulnerabilities evaluates the seismic performance of structures (represented by equivalent single-degree-of-freedom, SDOF, models) by comparing their structural capacity and the seismic demand curves drawn in spectral acceleration (S_a) versus spectral displacement (S_d) coordinates (hence the terminology: capacity spectrum and demand spectrum). The key to this method is the reduction of 5%-damped elastic response spectra of the ground motion (in S_a-S_d or the so-called ADRS format) to take into account the inelastic behavior of the structure under consideration. The performance of the building structure to earthquake ground shaking is then identified by the so-called “performance point” located at the intersection of the capacity spectrum of the equivalent non-linear single-degree-of-freedom system and the earthquake demand spectrum. After estimation of the performance point the damage is estimated through the use of fragility curves. Fragility curves calculate the probability of being equal or exceeding a damage state assuming log-normal distribution of damage.

The main ingredients of the capacity spectrum method can be summarized as follow:

- Seismic demand representation : Demand Spectrum
- Structural system representation : Building Capacity Spectrum
- Structural response assessment : Performance Point
- Representation of the damage probability : Fragility Curves

A schematic description of the methodology is provided in Figure 67. The inelastic acceleration-displacement spectrum for the ground motion (seismic demand spectrum) superimposed with the capacity of a building (capacity spectrum) and the fragility relationship. The probability distributions, drawn over both the capacity and demand curves, indicate the associated uncertainty and randomness of performance. The intersection of these spectra gives the expected level of performance (performance point). As it can be seen from Figure 67 there is a substantial uncertainty of the location of the performance point and the fragility curves should be able to characterize this probabilistic nature of the problem.

The capacity spectrum method is an approximate heuristic method which essentially assumes that a complex non-linear multi-degree-of-freedom system such as a multi-storey building undergoing severe plastic deformations during an earthquake can be modeled as an equivalent single degree of freedom system with an appropriate level of inelasticity. The advantage of the method is its simplicity that is no time history analyses is needed to be performed.

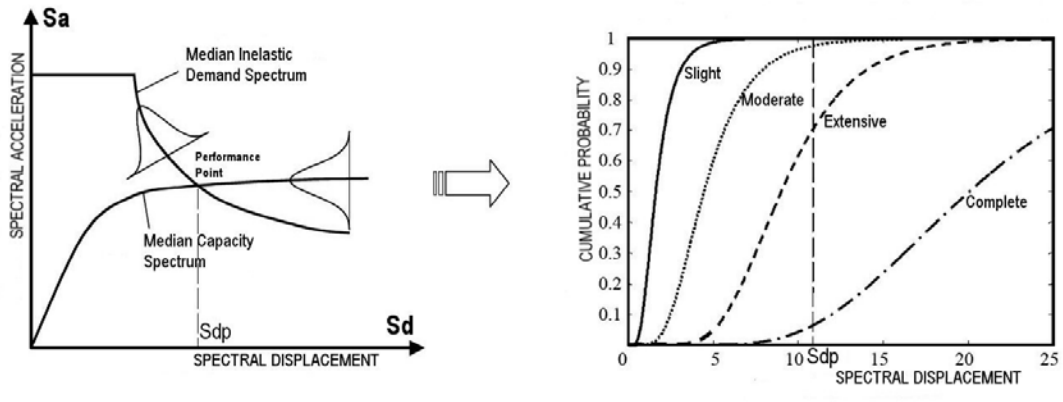

Figure 67. Spectral capacity-based vulnerability and damage assessment methodology

Representation of the Seismic Demand

Seismic demand is represented by 5%-damped elastic response spectrum. ELER provides two options for the construction of the response spectral shape:

3. Euro Code 8 Spectrum
4. IBC 2006 Spectrum

In the development process of CSM and MADRS methods NEHRP design spectrum is conducted to obtain the performance point of the buildings.

Euro Code 8-EC8 (European Committee for Standardization CEN, 2003)

EC8 suggests two types of elastic acceleration response spectra for horizontal components of the ground motion: Type 1 and Type 2. The shape of the elastic response spectrum is taken the same for the two levels of seismic action (Figure 68).

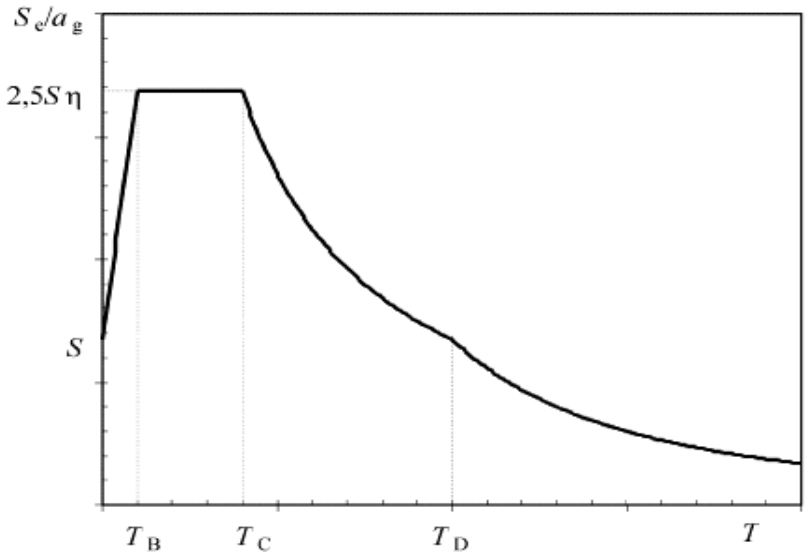

Figure 68. Shape of the horizontal elastic response spectrum by EC8

If the earthquakes that contribute most to the seismic hazard defined for the site for the purpose of probabilistic hazard assessment has a surface-wave magnitude, M_s, not greater than 5.5, it is recommended that the Type 2 spectrum is adopted. Type 1 spectrum is used for the earthquakes with magnitude greater than 5.5.

The horizontal elastic response spectrum is defined by:

a_g : Design ground acceleration on type A ground
T_B, T_C : The periods that limit the constant spectral acceleration region
T_D : The period that define the beginning of the constant displacement range of the spectrum
S : Soil factor
η : Damping correction factor

The values of T_B, T_C, T_D and S for each ground type and type (shape) of spectrum to be used as well as the damping corrections for different levels of damping are given in EC8.

International Building Code-IBC 2006 (International Building Council)

IBC 2006 provides a general horizontal elastic acceleration response spectrum (Figure 69). It is defined by:

S_S, S_1 : Spectral accelerations at short periods and 1-sec period, respectively
S_{DS}, S_{D1} : Short period and 1-sec period design response spectral accelerations adjusted for the specified site class and damping value
T_0, T_S : Corner periods of the constant spectral acceleration region given by $T_0=0.2T_S$ and $T_S= S_{D1}/S_{DS}$
T_L : Long-period transition period. It is a regional-dependent parameter and it is assumed that T_L=5s herein.

The recommended values for the site and damping corrections are given in IBC 2006 and NEHRP 2003 Provisions.

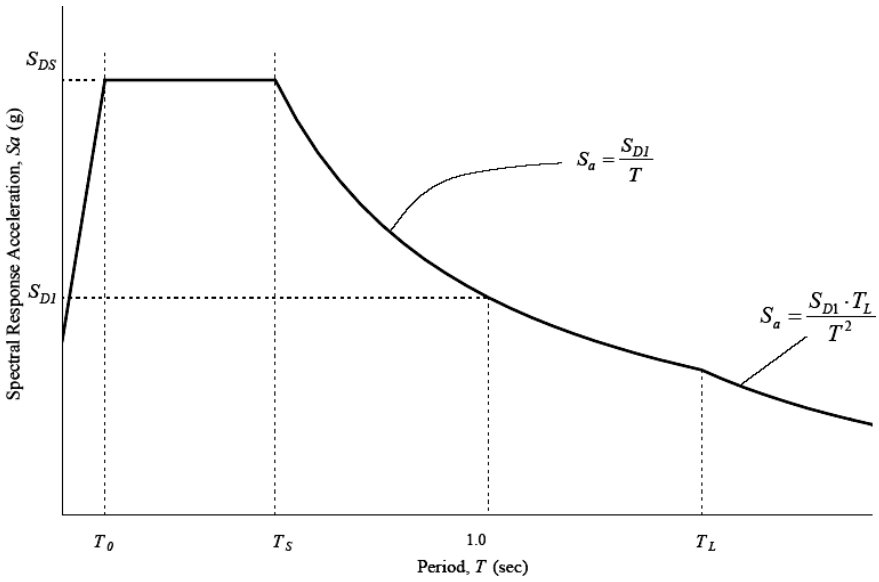

Figure 69. Shape of the horizontal elastic response spectrum by IBC-2006

Representation of the Building Capacity

A building capacity curve is the plot of the building's lateral load resistance as a function of a characteristic lateral displacement and quantifies the inelastic structural capacity of the structure. Capacity spectrum can be approximated from a "pushover" analysis in which monotonically increasing lateral loads are applied to the structure and the characteristic deformations (usually roof level displacement) are plotted against the lateral load. The capacity spectrum based vulnerability analysis requires the pushover curve of the MDOF system, quantified by the base shear (V) and the top floor displacement (D), be converted to the capacity spectrum of the equivalent single-degree-of-freedom (SDOF) system quantified by the spectral acceleration (S_a) and spectral displacement (S_d) for direct comparison with the associated demand spectrum.

For each building type the capacity spectrum has an initial linear section where the slope depends on the typical natural frequency of vibration of the building class, and rises to a plateau level of spectral acceleration at which the maximum attainable resistance to static lateral force has been reached. As an example, a capacity spectrum is shown in Figure 70. As

it can be seen the capacity spectrum is controlled by the points of design, yield and ultimate capacities. These points can be correlated with the damage limit states.

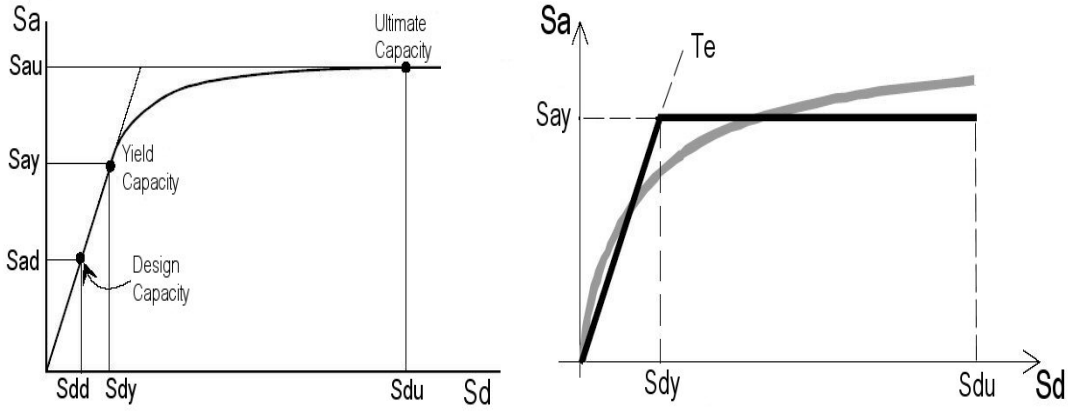

Figure 70. Typical structural capacity spectrum (left) and its simplified form (right)

For the building taxonomies, RISK-UE building typologies and model building types of HAZUS99, the capacity curve parameters as described above are provided in the ELER database.

Demand Spectrum and the Performance Point

For utilization in capacity spectrum-based vulnerability analysis, the elastic 5% damped response spectra (in spectral acceleration versus period format, S_{ae}, T) is converted into the spectral acceleration (S_{ae}) versus spectral displacement (S_{de}), the so-called ADRS format, through the use of the following transformation:

$$S_{de} = \left(\frac{T^2}{4\pi^2} \right) S_{ae} \qquad [19]$$

Figure 71 illustrates the NEHRP – IBC 2006 standardized spectrum shape plotted in ADRS format.

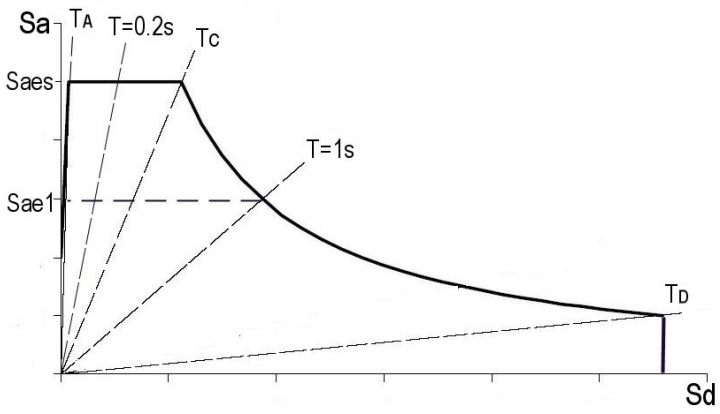

Figure 71. NEHRP Spectrum Plotted in ADRS Format (T_A, T_C and T_D show the characteristic periods. S_{aes} and S_{ae1} respectively indicate the short period and 1s period spectral (elastic) accelerations)

Nonlinear Static Procedures are widely used procedures to estimate the performance point (target displacement). The three of commonly used (code-based) procedures are: the Capacity Spectrum Method specified in ATC-40 (1996), its recently modified and improved version Modified Acceleration-Displacement Response Spectrum Method (FEMA-440) and the Coefficient Method originally incorporated in FEMA-356 (2000).

The Capacity Spectrum Method is a form of equivalent linearization that uses empirically derived relationships for the effective period and damping to estimate the response of an equivalent linear SDOF model. The Modified Acceleration-Displacement Response Spectrum Method basically differs from the Capacity Spectrum Method in the reduction of the elastic demand curve. The basic assumption of the equivalent linearization is that the maximum displacement of a nonlinear SDOF system can be estimated from the maximum displacement of a linear elastic SDOF system that has a period and a damping ratio that are larger than those of the initial values for the nonlinear system. The elastic SDOF system that is used to estimate the maximum inelastic displacement of the nonlinear system is usually referred to as the equivalent or substitute system. Similarly, the period of vibration and damping ratio of the elastic system are commonly referred to as equivalent period and equivalent damping ratio, respectively. The equivalent period is computed from the initial period of vibration of the nonlinear system and from the maximum displacement ductility ratio, μ. On the other hand, the equivalent damping ratio is computed as a function of damping ratio in the nonlinear system and the displacement ductility ratio.

The Coefficient Method is essentially a spectral displacement modification procedure in which several empirically derived factors are used to modify the response of a linearly-elastic equivalent SDOF model of the building structure.

Another nonlinear static procedure is the so-called “N2” method (Fajfar, 2000) in which the inelastic demand spectra is obtained from standardized (code-based) elastic design spectra using ductility factor based reduction factors. The “N2” method (herein called the Reduction Factor Method) has been implemented in the so-called “Mechanical-Based Method” of vulnerability analysis (Lagomarsino and Giovinazzi, 2006) in the RISK-UE (2001-2004) project.

All four of these methodologies require development of a pushover curve (capacity spectrum for the equivalent SDOF system) to provide the relationship between the base shear and lateral displacement of a control node (usually located at roof level). They differ mainly in the computation of the demand spectrum and the performance point. For the *Level 2 Loss Assessment*, computation of the demand spectrum and estimation of the performance point by each method is explained in the forthcoming sections. Following the computation of the performance point, calculation of the damage probabilities by use of fragility curves and the estimation of causalities are described.

Capacity Spectrum Method (CSM)

The Capacity Spectrum Method (CSM) utilizes the equivalent linearization for the estimation of the performance point which is the intersection of the building capacity spectrum with the demand response spectrum reduced for nonlinear effects. The performance point represents the condition for which the seismic capacity of the structure is equal to the seismic demand imposed on the structure by the given level of ground shaking (ATC-40).

To account for the increased hysteretic damping as the building shifts from elastic into inelastic response, the spectral reduction factors in terms of effective damping are introduced. The effective damping (essentially the equivalent damping, β_{eq}) can be calculated as a function of the capacity curve, the estimated displacement demand and the resulting hysteresis loop. Figure 72 shows the building capacity spectrum with the idealized hysteresis loop for a ductile building with equivalent viscous damping less than 30% and subjected to relatively short duration of ground shaking. For more realistic approximation of the hysteretic energy dissipated by the structure, the effective viscous damping (β_{eff}) concept is utilized with the consideration of a damping modification factor (κ). By the incorporation of Figure 72, the effective damping is defined as:

$$\beta_{eff} = \kappa\beta_0 + 5 = \frac{63.7\kappa(a_y d_{pi} - d_y a_{pi})}{a_{pi} d_{pi}} + 5 \qquad [20]$$

where β_0 is the hysteretic damping and "5" stands for the 5% viscous damping inherent in the structure (assumed to be constant).

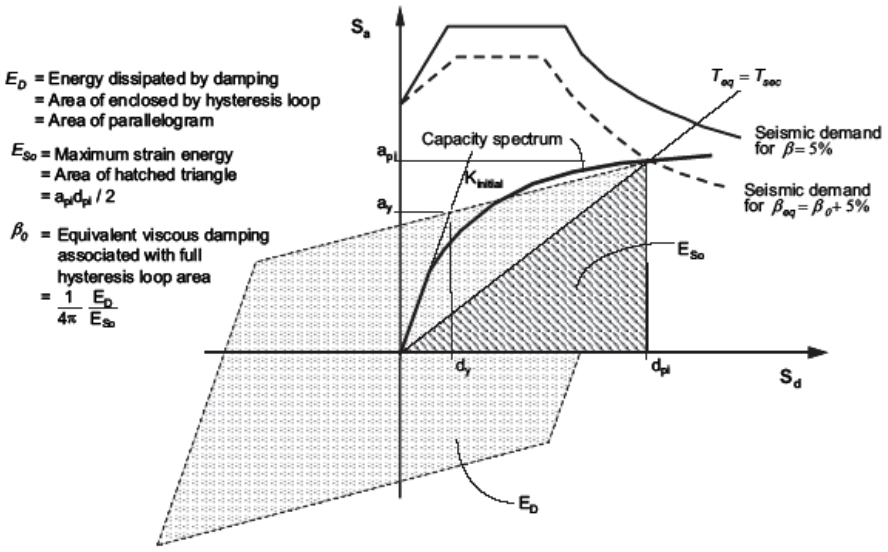

Figure 72. Graphical representation of the idealized hysteretic damping and the reduction of the 5%-damped elastic demand spectrum (modified after ATC-40)

The κ-factor is related to the structural behavior and the earthquake duration. ATC-40 provides three categories of structural behavior: Type A– stable, reasonably full hysteresis loops, Type B– moderately reduced hysteretic behavior and Type C– poor hysteretic behavior. Based on the evaluation of the building's seismic resisting system and the earthquake duration, the structural behavior types are given in Table 41 and the variation of κ values is presented in Table 42.

Table 41. Structural behavior types

Duration of Earthquake	Essentially New Building	Average Existing Building	Poor Existing Building
Short	Type A	Type B	Type C
Long	Type B	Type C	Type C

Table 42. The variation of κ values

Structural Behavior Type	β_0	κ
Type A	≤ 0.1625	1.0
	> 0.1625	$1.13 - 0.51(\pi/2)\,\beta_0$
Type B	≤ 0.25	0.67
	> 0.25	$0.845 - 0.446(\pi/2)\,\beta_0$
Type C	Any value	0.33

To obtain the reduced demand spectrum ATC-40 applies the following spectral reduction factors:

$$SR_A = \frac{3.21 - 0.68\ln(\beta_{eff})}{2.12} \quad [21]$$

$$SR_V = \frac{2.31 - 0.41\ln(\beta_{eff})}{1.65} \quad [22]$$

SR_A and SR_V are, respectively, applied to the constant acceleration and the constant velocity regions of the 5%-damped elastic demand spectrum. SR_A and SR_V are limited by the values given in Table 43.

Table 43. Minimum allowable values for the spectral reduction factors

Structural Behavior Type	SR_A	SR_v
Type A	0.33	0.50
Type B	0.44	0.56
Type C	0.56	0.67

For the determination of the performance point two criteria needs to be satisfied: 1) the point must lie on the capacity spectrum to represent the structure at a given displacement and 2) the point must lie on a reduced demand spectrum that represents the nonlinear demand at the same structural displacement. In order to achieve this, three iterative procedures based on trial

and error search are suggested in ATC-40. The so-called Procedure A is utilized in the implementation of the CSM herein. In Procedure A, a trial performance point (a_{pi}, d_{pi}), is selected then, the bilinear capacity spectrum and the reduced demand spectrum are drawn on the same plot. It is determined whether the demand spectrum intersects the capacity spectrum at the point (a_{pi}, d_{pi}) or if the displacement at which the demand spectrum intersects the capacity spectrum, d_i, is within acceptable tolerance of d_{pi}. Figure 73 illustrates the determination of the performance point by Procedure A.

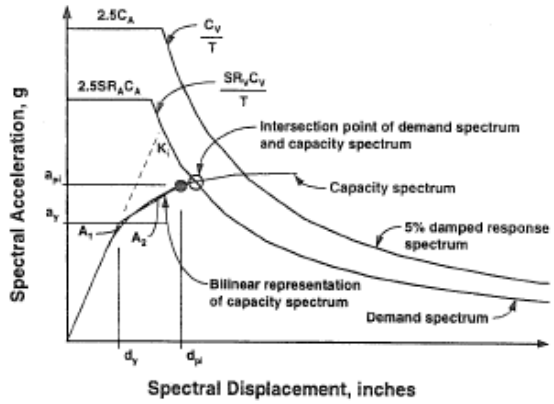

Figure 73. Capacity and demand spectra, and the performance point at the last step of Procedure A (taken from ATC-40)

Modified Acceleration- Displacement Response Spectrum (MADRS) Method

The CSM rests on the idea of reducing the elastic acceleration spectrum with an equivalent viscous damping of a linear single-degree-of-freedom (SDOF) system represented by its secant stiffness at maximum displacement. There has been a debate since the inception of the method on whether the empirically defined spectrum reduction factors are representative of the inelastic behavior of the equivalent SDOF system and the method has been improved in FEMA-440 (2005) through the introduction of the so-called Modified Acceleration-Displacement Response Spectrum (MADRS) method. The MADRS method estimates the maximum displacement response of nonlinear system with an equivalent linear system using the effective period (T_{eff}) and effective damping (β_{eff}).the effective linear parameters are functions of the capacity spectrum, the corresponding initial period and damping, and the ductility demand (μ).

The use of effective period and damping generate a maximum displacement that coincides with the intersection of the radial effective period line and the ADRS demand. The intersection point is presented by the a_{max} and d_{max} (Figure 74).

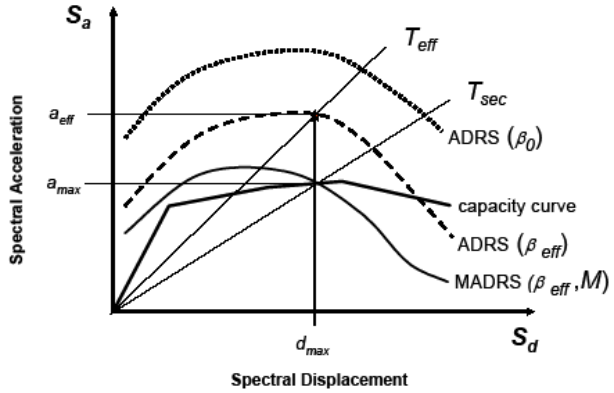

Figure 74. Modified acceleration-displacement response spectrum (MADRS) for use with secant period (taken from FEMA-440)

The modified ADRS demand curve (MADRS) is obtained by multiplying the ordinates of the ADRS demand corresponding to the effective damping, β_{eff}, by the modification factor M,

$$M = \frac{a_{\max}}{a_{eff}} = \left(\frac{T_{eff}}{T_{\sec}}\right)^2 = \left(\frac{T_{eff}}{T_0}\right)^2 \left(\frac{T_0}{T_{\sec}}\right)^2 \quad [23]$$

where

$$\left(\frac{T_0}{T_{\sec}}\right)^2 = \frac{1+\alpha(\mu-1)}{\mu} \quad [24]$$

α is the post-elastic stiffness and μ is the ductility demand and given by:

$$\alpha = \frac{\left(\frac{a_{pi}-a_y}{d_{pi}-d_y}\right)}{\frac{a_y}{d_y}} \quad [25]$$

$$\mu = \frac{d_{pi}}{d_y} \quad [26]$$

Similar to the CSM, spectral reduction factors are applied to obtain reduced demand spectra for the appropriate level of effective damping, β_{eff}. In the MADRS method, these factors are termed damping coefficients, $B(\beta_{eff})$, and used to adjust spectral acceleration ordinates given as follow:

$$(S_a)_\beta = \frac{(S_a)_0}{B(\beta_{eff})} \quad [27]$$

$$B = \frac{4}{5.6 - \ln \beta_{eff}(in\%)} \quad [28]$$

FEMA-440 considers three different types of inelastic behavior which are used as the equivalent counterparts to simulate the maximum response of an actual inelastic system: BLH –bilinear hysteretic, STDG –stiffness degrading and STRDG –strength degrading model (Figure 75). For the implementation of the equivalent linearization in the MADRS method, the equivalent linear parameters, the effective damping (β_{eff}) and effective period (T_{eff}), can be calculated for all types of hysteretic models by the following equations:

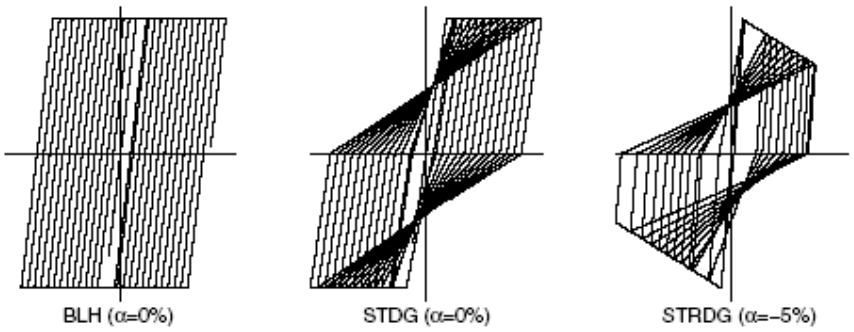

Figure 75. Types of inelastic behavior considered in MADRS method as provided by FEMA-440

for $1.0 < \mu < 4.0$:

$$\beta_{eff} = A(\mu - 1)^2 + B(\mu - 1)^3 + \beta_0 \quad [29]$$

$$T_{eff} = \left[G(\mu - 1)^2 + H(\mu - 1)^3 + 1\right]T_0 \quad [30]$$

for $4.0 \le \mu \le 6.5$:

$$\beta_{eff} = C + D(\mu - 1) + \beta_0 \quad [31]$$

$$T_{eff} = \left[I + J(\mu - 1) + 1\right]T_0 \quad [32]$$

for $\mu > 6.5$:

$$\beta_{eff} = E\left[\frac{F(\mu - 1) - 1}{[F(\mu - 1)]^2}\right]\left(\frac{T_{eff}}{T_0}\right)^2 + \beta_0 \quad [33]$$

$$T_{eff} = \left\{K\left[\sqrt{\frac{(\mu - 1)}{1 + L(\mu - 2)}} - 1\right] + 1\right\}T_0 \quad [34]$$

Values of the coefficients in the equations for effective damping and effective period of the model oscillators are tabulated in Table 44 and Table 45, respectively. It should be noted these are a function of the characteristics of the capacity curve for the oscillator in terms of basic hysteretic type and post-elastic stiffness, α.

Table 44. Coefficients to be used for the calculation of Effective Damping (β_{eff})

Model	α (%)	A	B	C	D	E	F
Bilinear hysteretic	0	3.2	-0.66	11	0.12	19	0.73
Bilinear hysteretic	2	3.3	-0.64	9.4	1.1	19	0.42
Bilinear hysteretic	5	4.2	-0.83	10	1.6	22	0.40
Bilinear hysteretic	10	5.1	-1.1	12	1.6	24	0.36
Bilinear hysteretic	20	4.6	-0.99	12	1.1	25	0.37
Stiffness degrading	0	5.1	-1.1	12	1.4	20	0.62
Stiffness degrading	2	5.3	-1.2	11	1.6	20	0.51
Stiffness degrading	5	5.6	-1.3	10	1.8	20	0.38
Stiffness degrading	10	5.3	-1.2	9.2	1.9	21	0.37
Stiffness degrading	20	4.6	-1.0	9.6	1.3	23	0.34
Strength degrading	-3	5.3	-1.2	14	0.69	24	0.90
Strength degrading	-5	5.6	-1.3	14	0.61	22	0.90

Table 45. Coefficients to be used for the calculation of Effective Period (T_{eff})

Model	α (%)	G	H	I	J	K	L
Bilinear hysteretic	0	0.11	-0.017	0.27	0.09	0.57	0
Bilinear hysteretic	2	0.10	-0.014	0.17	0.12	0.67	0.02
Bilinear hysteretic	5	0.11	-0.018	0.09	0.14	0.77	0.05
Bilinear hysteretic	10	0.13	-0.022	0.27	0.10	0.87	0.10
Bilinear hysteretic	20	0.10	-0.015	0.17	0.094	0.98	0.20
Stiffness degrading	0	0.17	-0.032	0.10	0.19	0.85	0
Stiffness degrading	2	0.18	-0.034	0.22	0.16	0.88	0.02
Stiffness degrading	5	0.18	-0.037	0.15	0.16	0.92	0.05
Stiffness degrading	10	0.17	-0.034	0.26	0.12	0.97	0.10
Stiffness degrading	20	0.13	-0.027	0.11	0.11	1.0	0.20
Strength degrading	-3	0.18	-0.033	0.17	0.18	0.76	-0.03
Strength degrading	-5	0.20	-0.038	0.25	0.17	0.71	-0.05

On the other hand, the effective damping and the effective period could be determined through the following approximate equations independent of hysteretic model type or alpha value:

for $1.0 < \mu < 4.0$:

$$\beta_{eff} = 4.9(\mu - 1)^2 - 1.1(\mu - 1)^3 + \beta_0 \quad [35]$$

$$T_{eff} = \left\{0.20(\mu - 1)^2 - 0.038(\mu - 1)^3 + 1\right\} T_0 \quad [36]$$

for $4.0 \leq \mu \leq 6.5$:

$$\beta_{\text{eff}} = 14.0 + 0.32(\mu - 1) + \beta_0 \quad [37]$$

$$T_{\text{eff}} = \left[0.28 + 0.13(\mu - 1) + 1\right] T_0 \quad [38]$$

for $\mu > 6.5$:

$$\beta_{\text{eff}} = 19 \left[\frac{0.64(\mu - 1) - 1}{\left[0.64(\mu - 1)\right]^2}\right]\left(\frac{T_{\text{eff}}}{T_0}\right)^2 + \beta_0 \quad [39]$$

$$T_{\text{eff}} = \left\{0.89\left[\sqrt{\frac{(\mu - 1)}{1 + 0.05(\mu - 2)}} - 1\right] + 1\right\} T_0 \quad [40]$$

The user has the ability to choose one of the hysteretic models or the approximate equations for the buildings under consideration in the implementation of the MADRS method. However, FEMA-440 indicates that the results are an estimate of median response and imply no factor of safety for structures that may exhibit poor performance and/or large uncertainty in behavior. The effective parameters for equivalent linearization are functions of ductility. Since ductility (the ratio of maximum displacement to yield displacement) is the object of the analysis, the solution must be found using iterative or graphical techniques. FEMA-440 suggests three procedures for the determination of the performance point although it should be noted that these procedures may not be reliable for extremely high ductilities (e.g., greater than 10 to 12). The so-called Procedure C is utilized in the implementation of the MADRS method herein. The Procedure C uses the modified acceleration-response spectrum for multiple assumed solutions (a_{pi}, d_{pi}) and the corresponding ductilities to generate a locus of possible performance points. The actual performance point is located at the intersection of this locus and the capacity spectrum (Figure 76).

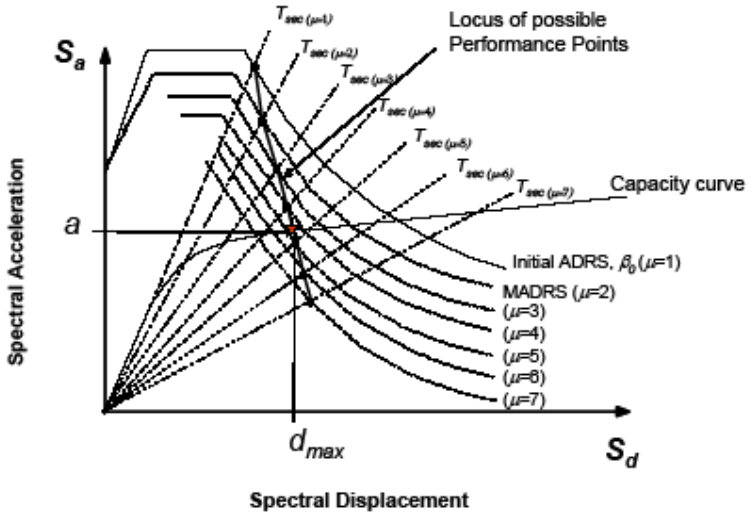

Figure 76. Locus of possible performance points using MADRS. (Procedure C)

Reduction Factor Method (RFM)

The Reduction Factor Method (RFM) utilizes the constant-ductility inelastic response spectra obtained through application of a reduction factor R_μ to the elastic response spectra in order to account the inelastic behavior (Vidic et. al, 1994 and Fajfar, 2000).

For an inelastic single degree of freedom system with a bi-linear force-deformation relationship, the inelastic spectral acceleration (S_{ai}) and the inelastic spectral displacement (S_{di}) can be determined as:

$$S_{ai} = S_{ae} / R_\mu \quad [41]$$

$$S_{di} = \frac{\mu}{R_\mu} S_{de} = \frac{\mu}{R_\mu} \frac{T^2}{4\pi^2} S_{ae} = \mu \frac{T^2}{4\pi^2} S_{ai} \quad [42]$$

where μ is the ductility factor defined as the ratio between maximum displacement and yield displacement and R_μ is the reduction factor (Figure 77) given by:

$$R_\mu = (\mu - 1)\frac{T_e}{T_C} + 1 \quad \text{and} \quad S_{di} = \frac{\mu}{R_\mu} S_{de} \qquad \text{for } T_e < T_C \quad [43]$$

$$R_\mu = \mu \quad \text{and} \quad S_{di} = S_{de} \qquad \text{for } T_e \geq T_C \quad [44]$$

where T_e is the elastic period of the SDOF system and T_C is the characteristic period of the ground motion.

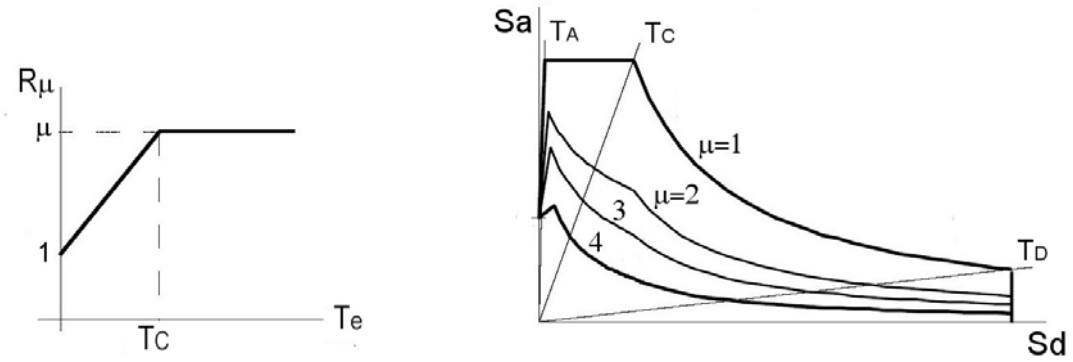

Figure 77. Reduction Factor and the Demand Spectrum (Modified after Fajfar, 2000)

The performance point S_{dp} (in terms of the spectral displacement) can be defined as functions of the structural capacity curve (T_e, S_{ay} and μ) and seismic demand curve (S_{ae}, T_C, T_D, μ).

For cases where the elastic period T_e is less than T_C and $S_{ae} > S_{ay}$ (Figure 78), through the use of equations 39 and 40 the performance point can be given as:

$$S_{dp} = \mu S_{dy} = \frac{S_{de}(T_e)}{R_\mu}\left(1 + (R_\mu - 1)\frac{T_C}{T_e}\right) \quad [45]$$

where $R_\mu = (\mu - 1)\frac{T_e}{T_C} + 1$ and $\mu = (R_\mu - 1)\frac{T_C}{T_e} + 1$ [46]

Using Equation 41 and from Figure 79, it can be assessed that for cases where T_e is between T_C and T_D and $S_{ae}>S_{ay}$ the performance point is equal to the elastic spectral demand.

$$S_{dp} = S_{de}(T_e) \quad [47]$$

$$R_\mu = \frac{S_{ae}(T_e)}{S_{ay}} = \mu \quad [48]$$

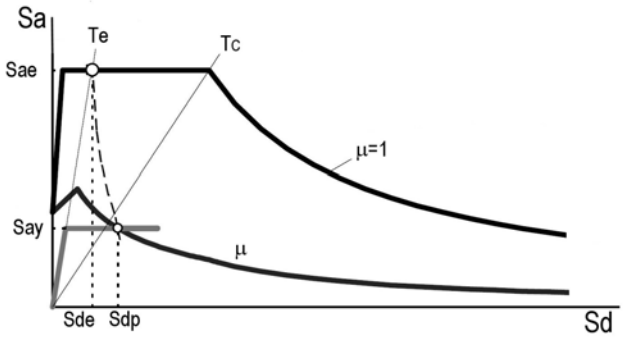

Figure 78. Performance point for $T_e < T_C$ (Modified after Fajfar, 2000)

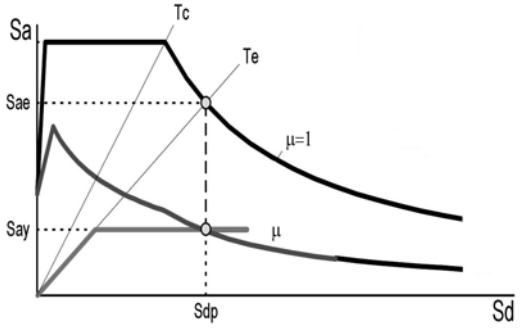

Figure 79. Performance point for $Te \geq T_C$ (Modified after Fajfar, 2000)

For cases where T_e is greater that T_D and $S_{ae}>S_{ay}$ the performance point will be equal to the constant elastic spectral displacement level and can be given as:

$$S_{dp} = S_{de}(T_D) = \frac{S_{ae}(T_D)T_D^2}{4\pi^2} \quad [49]$$

where T_D is the period that defines the beginning of the constant spectral displacement range.

For $S_{ay}>S_{ae}$ and for all positions of T_e (with respect to T_C and T_D) the performance point can be given as:

$$S_{dp} = S_{de}(T_e) \quad [50]$$

The Reduction Factor Method has been utilized by Lagomarsino and Giovinazzi (2006) in the derivation of the fragility and capacity curves for the RISK-UE building typologies. Those fragility and capacity curve parameters are proposed for the European building taxonomy in the ELER database.

Coefficient Method (CM)

The Coefficient Method (CM), presented as a nonlinear static analysis procedure in FEMA-356 (2000) and FEMA-273 (1977) essentially modifies the linear elastic response of the equivalent SDOF system by multiplying it by a series coefficients to generate an estimate of the target displacement (performance point). The coefficient method has been critically evaluated in FEMA-440 (2005) and the results reflected in ASCE/SEI 41-06 (2007).

Using this method the inelastic spectral displacement demand (the performance point, S_{dp}) is obtained through multiplying the elastic spectral displacement (S_{de}) by the C_0, C_1 and C_2 coefficients.

$$S_{dp} = C_0 C_1 C_2 S_{de} \quad [51]$$

The elastic spectral displacement is computed at the fundamental period (T_e) of the equivalent SDOF system.

C_0 is the modification factor that relates the spectral displacement of the equivalent SDOF system to the roof displacement of the building's MDOF structural system. C_0 is equal to the first mode participation factor at the roof level ($C_0=\Gamma$ of Equation 51 if the amplitude of the mode at the roof level is set to unity). Table 3.2 of ASCE/SEI 41-06 (2007) provides tabulated values of C_0 for general building types. C_0 increases with number of floors and varies between 1 and 1.5 (Table 46).

Table 46. C_0 coefficient

Number of Stories	C_0
1	1
2	1.2
3	1.3
5	1.4
10+	1.5

from Table 3.2 of ASCE41-06 for any load pattern

The C_1 coefficient, defined as the modification factor to relate expected maximum inelastic displacements to displacements calculated for linear elastic response, is given by (ASCE/SEI 41-06, 2007):

$$C_1 = 1 + (R_y - 1)/(aT_{eff}^2) \quad [52]$$

$$C_1 \leq C_1(T_{eff}=0.2s) \qquad \text{for } T_{eff} \leq 0.2s \quad [53]$$

$C_1 = 1.0$ for $T_{eff} \geq 1s$ [54]

where T_{eff} is the effective fundamental period of the building computed by modifying the fundamental mode vibration period (T_e, obtained from linearly elastic dynamic analysis) by:

$$T_{eff} = T_e \sqrt{\frac{K_i}{K_{eff}}} \quad [55]$$

where K_i is the elastic stiffness of the building and K_{eff} is the effective stiffness of the building obtained by idealizing the pushover curve as a bilinear relationship. In the application of Coefficient Method herein, it is assumed that T_{eff} is equal to T_e.

R_y represents the ratio of elastic strength demand to yield strength:

$$R_y = \frac{S_{ae}(T_{eff})}{S_{ay}} \quad [56]$$

where $S_{ae}(T_{eff})$ represents the elastic spectral acceleration at the effective fundamental period of the structure and S_{ay} refers to the yield spectral acceleration.

The factor "a" in Equation 52 is called the site class factor and is assigned the following values:

a=130 for NEHRP site class A and B
a=90 for NEHRP site class C
a=60 for NEHRP site class D, E and F

The C_2 coefficient represents the modification factor for the effect of pinched hysteresis shape, cyclic stiffness degradation and strength deterioration (ASCE/SEI 41-06, 2007):

$$C_2 = 1 + \frac{1}{800}\left(\frac{R_y - 1}{T_{eff}}\right)^2 \quad [57]$$

$C_2 = 1.0$ for $T_{eff} \geq 0.7s$ [58]

When comparing the Coefficient Method with the other three methods of Level 2 analysis, the user might expect differences to some degree in damage estimations. Whereas the first three methods rely on more complicated procedures, e.g. equivalent linearization, reduction of the demand spectra and the iterative procedures for estimating the performance point, the Coefficient Method modifies the elastic spectral displacement by multiplying some coefficients to obtain the performance point.

Building Damage Probability

The conditional probability of damage being in or exceeding a particular damage state k (or D_k) for a given spectral displacement level (performance point, S_{dp}) is given by the following relationship:

$$P\left[Damage \geq D_k \mid S_{dp} \right] = \Phi\left[(1/\beta_k) \ln(S_{dp} / \overline{S}_{d,k}) \right] \quad [59]$$

where Φ is the standard normal (Gaussian) complementary cumulative function, S_{dp} is the inelastic spectral displacement demand (performance point), $\overline{S}_{d,k}$ is the median spectral displacement at which the structure reaches the threshold of the damage state (*k)* and β_k is the standard deviation of the natural logarithm of the $S_{d,k}$.

The spectral displacement $S_{d,k}$ that defines the threshold of a particular damage state (k) is assumed to be given by:

$$S_{d,k} = \overline{S}_{d,k} \varepsilon_k \quad [60]$$

where $\overline{S}_{d,k}$ is the median value and ε_k is the log-normal variable with a unit median value and a normalized composite log-normal standard deviation β_k, that incorporates aspects of uncertainty and randomness for both capacity and demand.

The application of the spectral capacity-based vulnerability assessment requires the provision of $\overline{S}_{d,k}$ and β_k values for different model building types and the damage states are needed for the assessment of damage predictions to buildings, casualties and socio-economic losses due to structural damage. Slight, Moderate, Extensive and Complete damage states for each building model types of HAZUS99 as well as for the European building taxonomy are adopted in Level 2 analysis.

Building Damage State Probability

HAZUS99 (FEMA, 1999) and Kircher et al. (1997) provide the median values of the threshold spectral displacements ($\overline{S}_{d,k}$) at the damage state k as:

$$\overline{S}_{d,k} = \delta_k \alpha_2 H \quad [61]$$

where, δ_k is the drift ratio at the threshold of the damage state k, α_2 is the fraction of the building (roof) height at the location of the pushover mode displacement and H is the typical roof level height of the building type considered. HAZUS-MH (FEMA, 2003) provides α_2 and H values for different building types. The δ_k and values are provided as a function of the seismic design level and damage state for different building types.

For the European building taxonomy, Lagomarsino and Giovinazzi (2006) identify the following damage limit states (damage state thresholds) on the capacity curve:

$$\overline{S}_{d,1} = 0.7 S_{dy} \quad [62]$$

$$\overline{S}_{d,2} = 1.5 S_{dy} \quad [63]$$

$$\overline{S}_{d,3} = 0.5(S_{dy} + S_{du}) \quad [64]$$

$$\overline{S}_{d,4} = S_{du} \quad [65]$$

where $\overline{S}_{d,k}$ (k=1, 2, 3, 4) identify the median value of the damage state threshold spectral displacements. Four damage levels (D_k, k=1, 2, 3, 4) are associated with these damage limit states: Slight-D_1 (Slight in EMS'98), Moderate-D_2 (Moderate in EMS'98), Extensive-D_3 (Heavy in EMS'98) and Complete-D_4 (Very heavy + Destruction in EMS'98).

The lognormal standard deviation β_k, which describes the total variability of the fragility curve damage states, has been modeled (Kircher et al, 1997) by the variability of the capacity curve (β_C), demand spectrum (β_D) and of the damage state threshold ($\beta_{T,k}$). Each of these variabilities are represented by the log-normal standard deviation parameter.

$$\beta_k = \sqrt{(CONV[\beta_C, \beta_D])^2 + (\beta_{T,k})^2} \quad [66]$$

where "CONV" represents the convolution of respective probability distributions. Following general values are provided in HAZUS99 (FEMA, 1999).

β_C=0.25 (for code buildings and β_C=0.30 for pre-code buildings)
β_D=0.45 (at short periods and β_D=0.50 at long periods)
$\beta_{T,k}$=0.4 (for all building types and damage states)
HAZUS-MH (FEMA, 2003) provides tables of β_k for low-, mid- and high-rise with different κ, $\beta_{T,k}$ and β_C ranges.

For the European building taxonomy, Lagomarsino and Giovinazzi (2006) express the total variability, β_k, as:

$$\beta_k = \sqrt{\beta_C^2 + \beta_D^2 + \beta_{T,k}^2} \quad [67]$$

Lagomarsino and Giovinazzi (2006) and Giovinazzi (2005) have evaluated β_k :

by using binomial and lognormal distributions with a 50% probability of occurrence for each damage state as:

β_k=0.40 lnμ [68]

and by forcing the lognormal fragility curves on beta fragility curves stated as:

β_k=0.62 lnμ [69]

where μ is the ductility factor.

The lognormal standard variation given by Equation 66 is adopted for the fragility functions of European building taxonomy.

Fragility Curves

To estimate the performance of a group of buildings of a particular class under given ground shaking, the spectral response of the building at the performance point for the standard building of that class, as defined above, is used in conjunction with a set of fragility curves for that class, which estimate the probability of any particular building exceeding each of the damage states after shaking at any given spectral response level.

The fragility curves represent the probability-based relation between the expected response and the performance limits in terms of the cumulative density function of the probability of exceeding of specific damage limit states for a given peak value of a seismic demand. If structural capacity and seismic demand are random variables that roughly conform to either a normal or log-normal distribution then, following the central limit theorem, it can be shown that the composite performance outcome will be log-normally distributed. Therefore, the probabilistic distribution is expressed in the form of a so-called fragility curve given by a log-normal cumulative probability density function.

The analytical expression of each fragility curve is based on the assumption that earthquake damage distribution can be represented by the cumulative standard lognormal distribution function, Φ, (HAZUS99, Kircher et al. 1997). The horizontal axis represents the spectral displacement demand and vertical axis refers to the cumulative probability of structural damage reaching or exceeding the threshold of a given damage state (Figure 80).

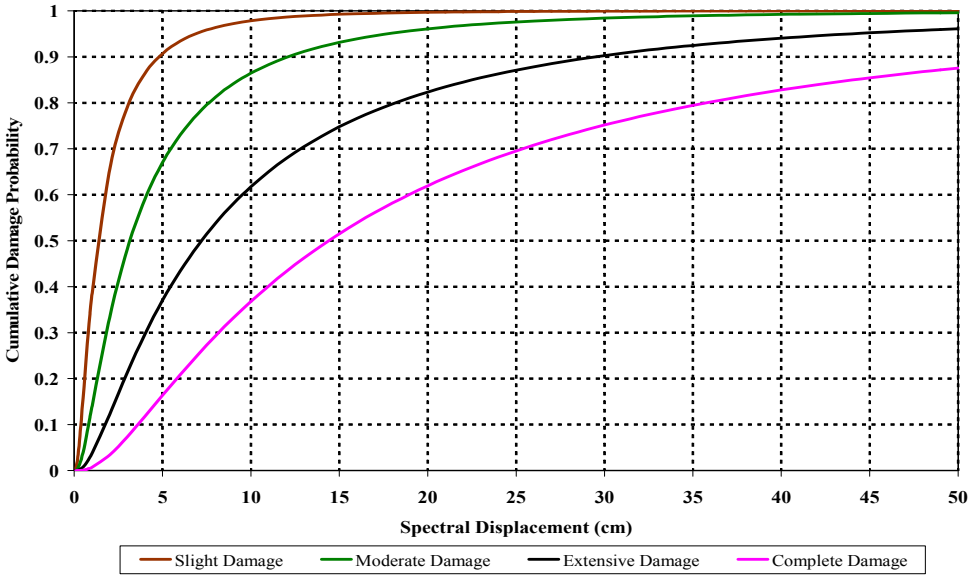

Figure 80. Example fragility curves for four damage levels

For the building taxonomies, i.e. model building types of HAZUS99 and RISK-UE building typologies, the fragility curve parameters as described above are provided in the ELER database and can be found in Appendix B.

Casualty Estimation

The casualty estimation in Level 2 analysis is based on HAZUS99 (FEMA, 1999) and HAZUS-MH (FEMA, 2003) methodologies. The output from the module consists of a casualty breakdown by injury severity level, defined by a four level injury severity scale (Durkin and Thiel, 1993; Coburn and Spence, 1992; Cheu, 1994). Table 47 defines the injury classification scale used in the methodology.

Table 47**.** Description of injury severity levels

INJURY SEVERITY	INJURY DESCRIPTION
Level 1	Injuries requiring basic medical aid without requiring hospitalization
Level 2	Injuries requiring medical care and hospitalization, but not expected to progress into a life threatening status
Level 3	Injuries that pose an immediate life threatening condition if not treated adequately and expeditiously. The majority of these injuries result because of structural collapse and subsequent collapse or impairment of the occupants.
Level 4	Instantaneously killed or mortally injured

The HAZUS99 (FEMA, 1999) casualty rates were obtained by revising those suggested in ATC-13 (1985) using limited post-earthquake fatality data. The casualty model itself in fact is based on the models suggested by Coburn and Spence (1992), Murakami (1992) and Shiono et al. (1991). However, unlike other approaches, the methodology is in event-tree format (Figure 81) and thus is capable of taking into account non-collapse related casualties. To estimate the casualties from structural damage, the model combines a variety of inputs from other HAZUS99 modules including the probability of being in the damage state and the relationship between the general occupancy classes and the model building type with specific casualty inputs provided for each damage state (D1-slight, D2 moderate, D3 Extensive, D4 Complete, D5 complete with collapse structural damage) in combination with occupancy data and time event.

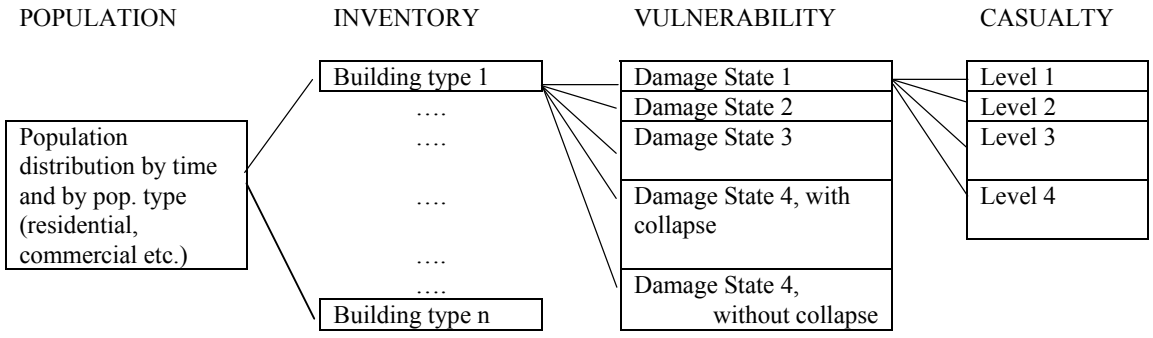

Figure 81**.** Event tree being used for the estimation of casualties (Source: HAZUS-MH – FEMA, 2003).

The probability of suffering i- severity (i=1:4) level is calculated by:

$$p_{Si} = \sum_{k=1}^{5} w_{Si,k} p_k \quad [70]$$

where p_{si} is the probability for people involved in an earthquake to suffer a *i*- severity (i=1:4) p_k, is the probability of a damage D_k,(k=1:5) occurrence and $w_{si,k}$ is the casualty rate considered for p_k probability.

The expected number of occupants in severity level *i* (EN_i) is the product of the number of occupants of the building at the time of earthquake (*Noccupants*) and the probability of an occupant suffering severity level *i* (P_{si}).

$$EN_i = Noccupants * P_{si} \quad [71]$$

Casualty rates for R/C and masonry structures as given in HAZUS99 are tabulated in Table 48 and Table 49, respectively.

The methodology used in Level 2 for the estimation of number of casualties is the same methodology suggested by HAZUS99. If, in addition to the grid based building inventory, a grid based population distribution is defined by the user, the software computes the number of dwelling units (using user defined estimated number of dwellings per building type) and an average population per dwelling unit for each cell. Then, casualties for any given building type, building damage level and injury severity level can be calculated by the following equation:

K_{ij} = *Population per Building * Number of Damaged Building in damage state j* Casualty Rate for severity level i and damage state j* [72]

At present three casualty models are included in ELER. These are HAZUS99 (FEMA, 1999), HAZUS-MH (FEMA, 2003) and the KOERI casualty model for Turkey developed by Erdik and Aydınoglu (2002) using the casualty data from 1992 Erzincan and 1999 Kocaeli earthquakes. Mainly two building types are considered in all three models: RC and masonry. The casualty rates given in the three models for the two building types are presented in Table 48 through Table 52. As in Level 1, if a user defined grid based population is not available, the program calculates an average population per dwelling unit for the whole study area using the default Landscan population and calculates casualties accordingly.

By changing the population distribution, different casualty estimates may be obtained for different times of the day, such as for a night-time scenario or a day-time scenario.

Table 48. Casualty rates for Reinforced Concrete Moment Frame Structures (HAZUS99)

Injury Severity	Casualty Rates for R/C structures (%)			
	Slight Damage	Moderate Damage	Extensive Damage	Complete Damage
Severity 1	0.05	0.2	1	5* - 50**
Severity 2	0.005	0.02	0.1	1* - 10**
Severity 3	0	0	0.001	0.01* – 2**
Severity 4	0	0	0.001	0.01* – 2**

*the smaller values are related with partial collapse of the buildings

**the larger values are given for total collapse (the pancake type of collapse)

Table 49. Casualty rates for Unreinforced Masonry Structures (HAZUS99)

Injury Severity	Casualty Rates for R/C structures (%)			
	Slight Damage	Moderate Damage	Extensive Damage	Complete Damage
Severity 1	0.05	0.4	2	10* - 50**
Severity 2	0.005	0.04	0.2	2* - 10**
Severity 3	0	0	0.002	0.02* – 2**
Severity 4	0	0	0.002	0.02* – 2**

*the smaller values are related with partial collapse of the buildings
**the larger values are given for total collapse (the pancake type of collapse)

HAZUS-MH introduced some variations in the casualty rates especially for the damage states of moderate and complete damage with collapse. Casualty rates for R/C and masonry structures as given in HAZUS-MH are tabulated in Table 50 and Table 51, respectively.

Table 50. Casualty rates for Reinforced Concrete Moment Frame Structures (HAZUS-MH)

Injury Severity	Casualty Rates for R/C structures (%)			
	Slight Damage	Moderate Damage	Extensive Damage	Complete Damage
Severity 1	0.05	0.25	1	5* - 40**
Severity 2	-	0.03	0.1	1* - 20**
Severity 3	-	-	0.001	0.01* – 5**
Severity 4	-	-	0.001	0.01* – 10**

*the smaller values are related with partial collapse of the buildings
**the larger values are given for total collapse (the pancake type of collapse)

Table 51. Casualty rates for Unreinforced Masonry Structures (HAZUS-MH)

Injury Severity	Casualty Rates for R/C structures (%)			
	Slight Damage	Moderate Damage	Extensive Damage	Complete Damage
Severity 1	0.05	0.35	2	10* - 40**
Severity 2	-	0.04	0.2	2* - 20**
Severity 3	-	-	0.002	0.02* – 5**
Severity 4	-	-	0.002	0.02* – 10**

*the smaller values are related with partial collapse of the buildings
**the larger values are given for total collapse (the pancake type of collapse)

Estimation of Direct Economic Loss

The economic losses resulting from building damages calculated in Level 2 are estimated with the same approach used in Level 1 (given in Section C.4.2). The only difference is that the loss ratios in Level 2 have to be defined for 4 damage states (slight, moderate, extensive, complete) in contrast to the 5 damage states used in Level 1.

HAZUS-MH (FEMA, 2003) default values of direct economic loss for structural and nonstructural systems are based on the following assumptions of the loss ratio corresponding to each state of damage:

- Slight damage would be a loss of 2% of building's replacement cost
- Moderate damage would be a loss 10% of the building's replacement cost
- Extensive damage would be a loss of 50% of the building's replacement cost
- Complete damage would be a loss of 100% of the building's replacement cost.

C.4.4. PIPELINE DAMAGE

The pipeline damage module in ELER v3.0 can be used to estimate damages to urban pipeline systems such as potable water, wastewater and natural gas. Observations acquired from past urban earthquakes supplemented by the worldwide experience are used as a guide to assess the physical vulnerabilities of pipelines. ATC 25 (1991) provides an extensive compilation of lifeline vulnerability functions and estimates of required time to restore the facilities. A number of empirical correlations relating expected pipeline damage to PGV are available in the literature. O'Rourke and Ayala (1993), Eidinger and Avila (1999) and O'Rourke and Deyoeto (2004) can be cited among them. These correlations may be used to estimate repair rate and number of repairs in the pipeline system due to wave propagation. ELER uses the HAZUS-MH (FEMA, 2003) methodology, which is based on O'Rourke and Ayala (1993), to estimate pipeline damages. The O'Rourke and Ayala (1993) model correlates the repair rate with PGV and material type as given in the equation below.

$$\text{Repair Rate} \cong 0.0001*[\text{PGV}]^{(2.25)} \quad \text{(for brittle type material)} \qquad [73]$$

$$\text{Repair Rate} \cong 0.00003*[\text{PGV}]^{(2.25)} \quad \text{(for ductile type material)} \qquad [74]$$

where repair rate is the number of repairs per a km of pipeline and PGV is in cm/sec. In this methodology, damages due to seismic waves are expected to consist of 80% leaks and 20% breaks.

For the preparation of input files for pipeline damage analysis, please refer to Section B.6 in the Users Guide. Numbers of expected repairs at each cell are calculated as the product of repair rate and total pipeline length

C.5. VERIFICATION & VALIDATION (V&V) STUDIES

C.5.1. Earthquake Hazard

To compare ELER with USGS ShakeMap, the September 29, 2004 Central California earthquake of M5.0 and depth 11.0km is analyzed. Boatwright et al., (2003) ground motion prediction equation has been utilized for the assessment of ground motion. The PGA distributions of USGS ShakeMap and ELER on bedrock level are shown in Figure 82.

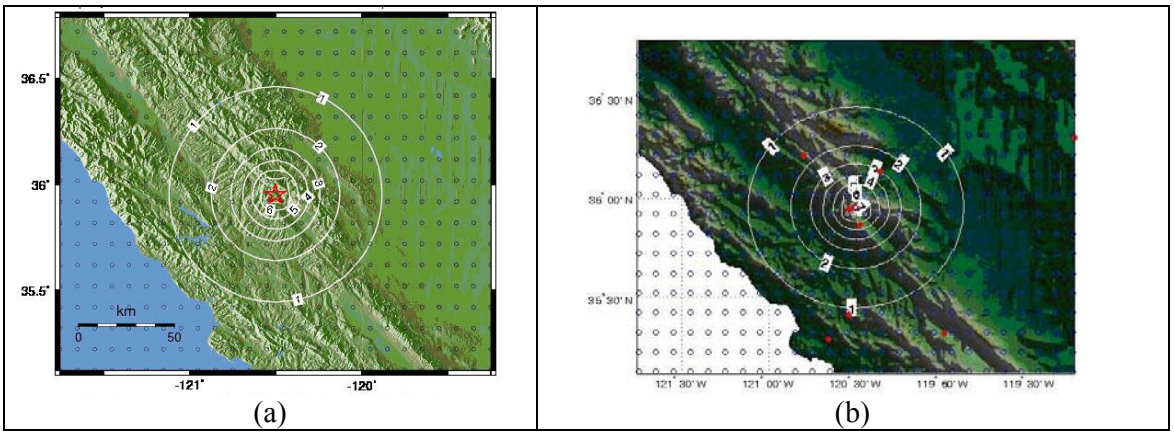

(a) (b)

Figure 82. Comparison of PGA distribution of USGS ShakeMap and ELER for a point source earthquake (M5.0 Central California, Wednesday, September 29, 2004 at 17:10:04 UTC, 35.9533N 120.502W, ID: nc51148805), (a) PGA(%g) distribution from USGS ShakeMap, (b) PGA(%g) distribution from ELER.

PGA distribution obtained with bias correction of available actual station information on bedrock level is shown for USGS ShakeMap and ELER in Figure 83.

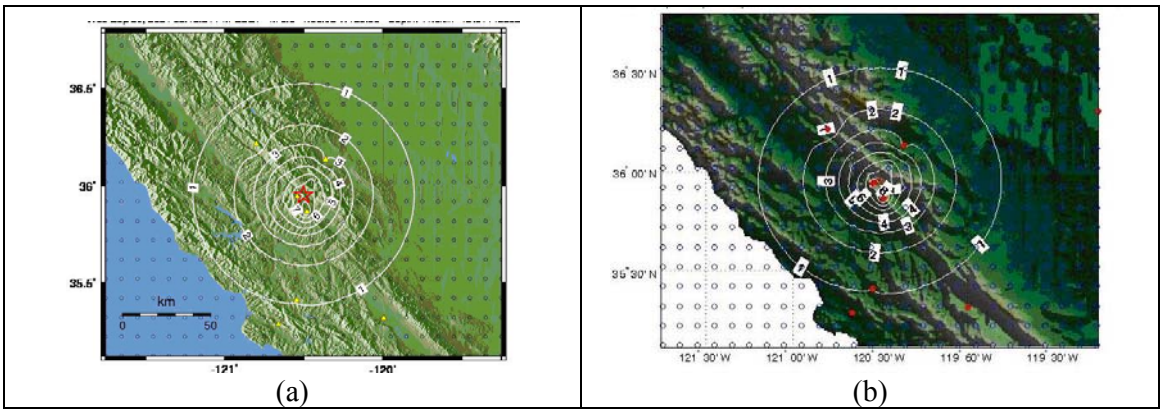

(a) (b)

Figure 83. Comparison of bias corrected PGA distributions for the same event (a) Bias corrected PGA(%g) distribution from USGS ShakeMap, (b) Bias corrected PGA(%g) distribution from ELER.

Both bias and site corrected PGA distributions obtained from USGS ShakeMap and ELER are shown in Figure 84.

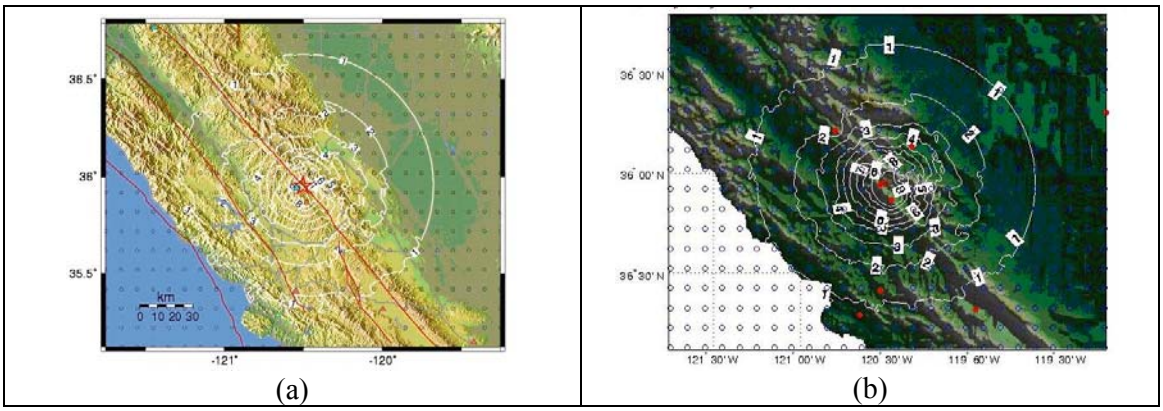

(a) (b)

Figure 84. Comparison of bias and site corrected USGS ShakeMap and ELER for M5.0 Central California, Wednesday, September 29, 2004 at 17:10:04 UTC, 35.9533N 120.502W, ID: nc51148805, (a) site corrected PGA(%g) distribution from USGS ShakeMap, (b) site corrected PGA(%g) distribution from ELER.

C.5.2. Earthquake Loss

Level 0

Samardjieva and Badal (2002) Empirical Approach

We tested this method for Turkish earthquakes and found satisfactory results. Table 52 summarizes the results obtained from this method for Turkish earthquakes. It can be observed from Table 52 that we have used somewhat higher population density values to obtain estimated casualties close to the actual ones. This would imply higher casualties from moderate size Turkish earthquakes than those calculated from the model. The main reason for that could be the low quality construction practice common especially in Eastern Anatolia. The method has also been tested by other researchers (R. Bossu, personal communication) and proved to work well for European earthquakes.

Table 52. Human losses for Turkish earthquakes obtained from Equation 6

Event	M	Estimated Population Density (people/km^2)	logNk	Estimated Casualties (Nk)	Actual Casualties (as given in the paper)
1939 Erzincan	7.8	> 200	4.618	41,495	32,700
1942 Erbaa	7.1	100-200	3.297	1,982	3,000
1943 Ladik	7.3	100-200	3.451	2,825	4,000
1944 Gerede	7.6	100-200	3.682	4,808	5,000
1953 Yenice-Gonen	7.2	50-100	2.918	828	1,103

1966 Varto	6.8	100-200	3.036	1,086	2,520
1970 Gediz	7.1	50-100	2.834	682	1,100
1971 Bingol	6.8	100-200	3.036	1,086	995
1975 Lice	6.6	>200	3.252	1,786	2,370
1983 Erzurum	6.7	100-200	2.944	879	1,342
1999 Kocaeli	7.6	>200	4.222	16,672	17,118

1999 Athens Earthquake:

The 7 September 1999 M6 Athens earthquake constitues an example of the distructiveness of moderate magnitude earthquakes occurring in densely populated areas. In total 143 people were killed, 1600 people were injured and at least 53,000 buildings were reported to be damaged by this earthquake. The observed intensity distributions are presented in Figure 85 and Figure 86. The estimated intensity distribution is presented in Figure 87.

Figure 85. Dashed circles denote regions were Modified Mercalli (MM) intensity was from VIII to IX degrees

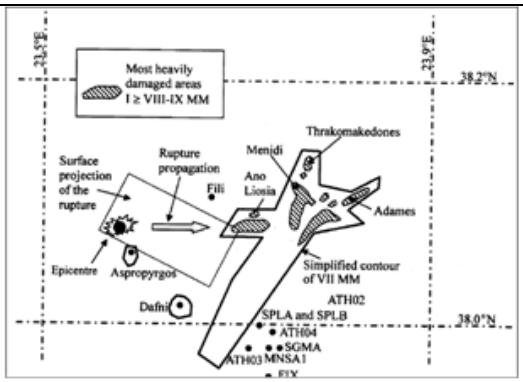

Figure 86. Regional overview of the epicentre, meizoseismal area, isoseismal lines, and distribution of the accelerographs (Elesan, 2003)

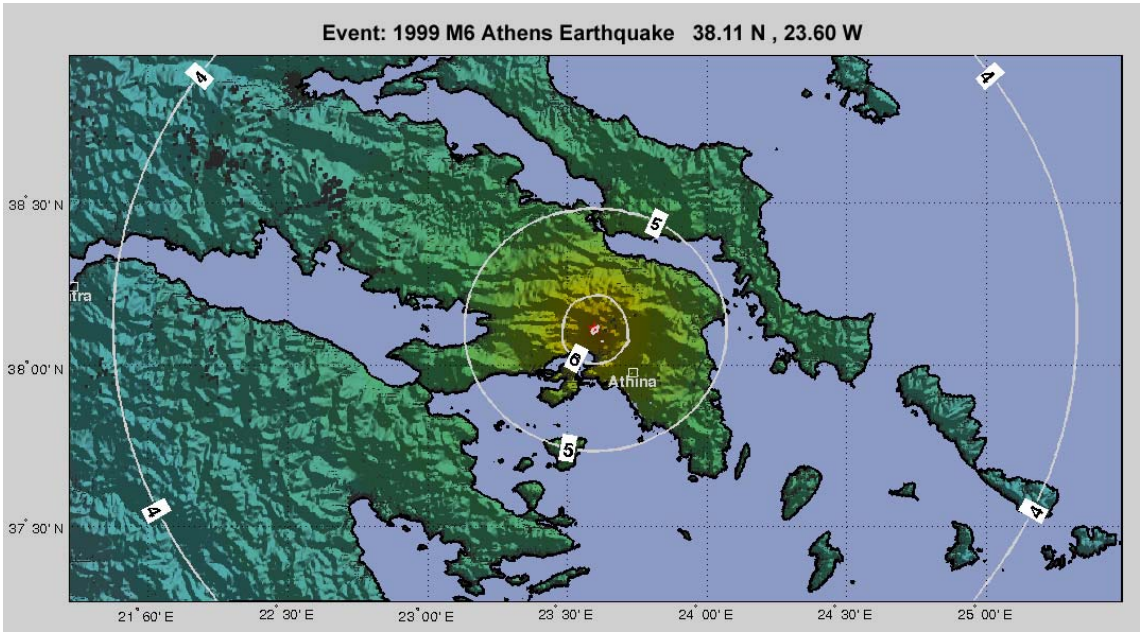

Figure 87. Estimated Intensity Distribution

The estimated distribution of fatalities for the 1999 Athens Earthquake is presented in Figure 88. The total number of fatalities is obtained as 467 for a population density >200 (Samardjieva & Badal, 2002) in Level 0 loss assessment.

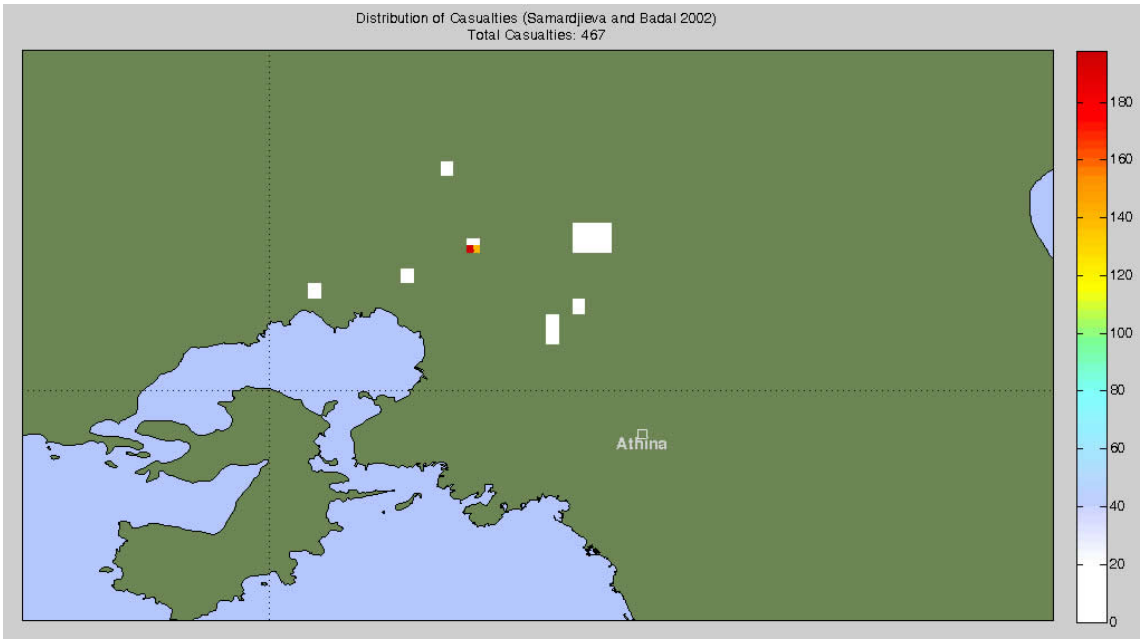

Figure 88. Fatality estimation for Level 0

1999 Kocaeli Earthquake:

The 17 August 1999 M7.4 Kocaeli earthquake was a very destructive event occurring in a densely populated and highly industrialized area. In total 17,000 people were killed, 40,000 people were injured. The intensity distribution associated with the 1999 M7.6 Kocaeli Earthquake was obtained using a regional intensity prediction equation (Sesetyan et al., 2005) as shown in Figure 89. The observed intensity distribution of the event is provided in Figure 90.

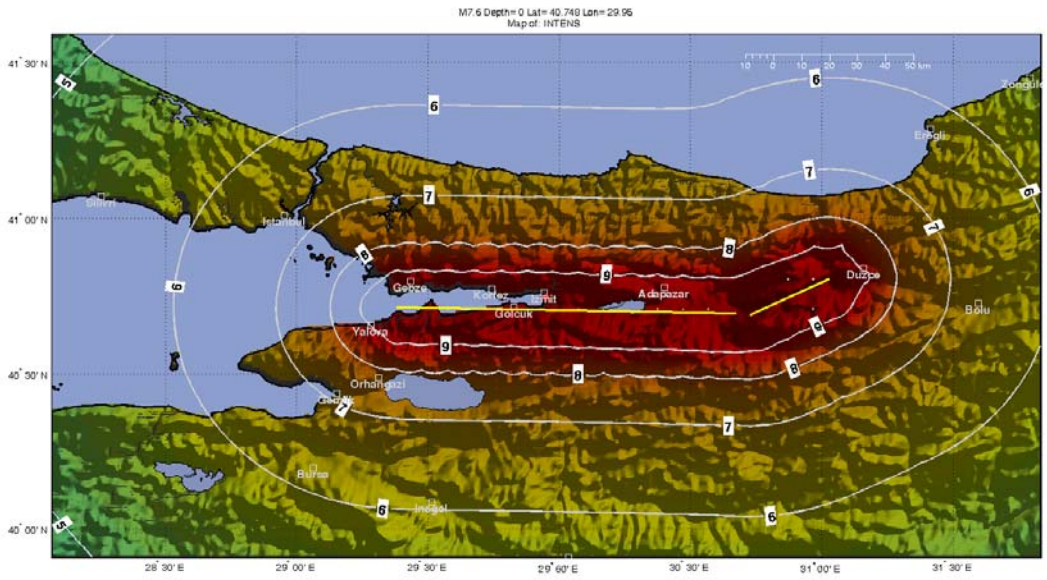

Figure 89. Estimated Intensity distribution by regional intensity prediction equation for the 1999 M7.6 Kocaeli Earthquake (Sesetyan et al., 2005)

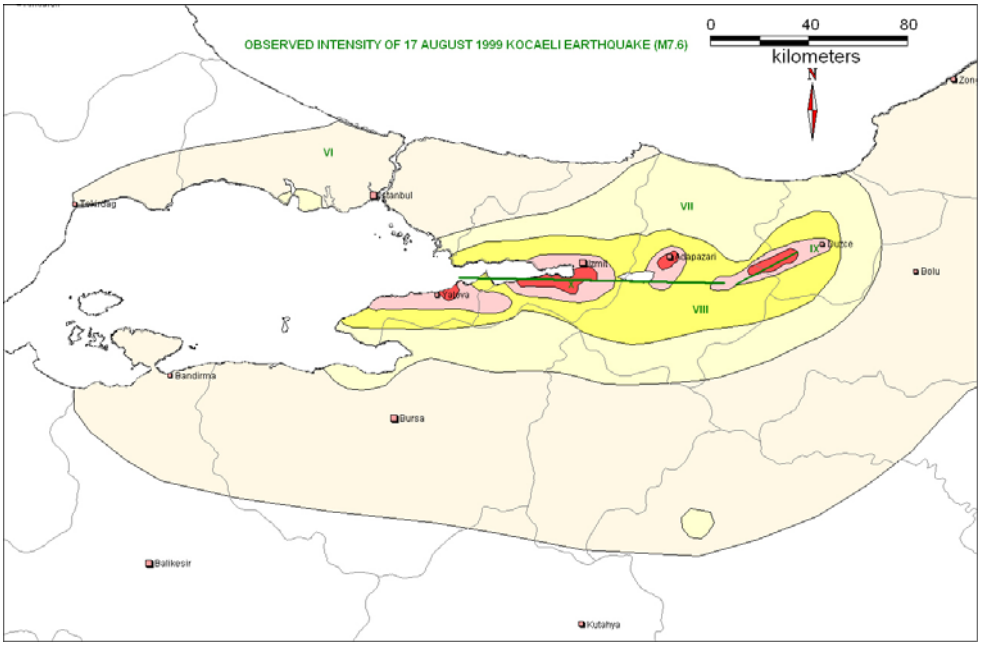

Figure 90. Observed Intensity Distribution for 1999 Kocaeli Earthquake (Ozmen, 2000).

Level 0 fatality estimations for the 1999 Kocaeli earthquake and the estimated geographical distribution of the fatalities are provided in Table 53 and Figure 91 respectively.

Table 53. Level 0 Fatality estimation for the 1999 Kocaeli earthquake

Intensity	Population	Density	Model 1	Model 2	Model 3
VI	1,0471,677	408	366	110	-
VII	2,063,938	408	1,205	294	-
VIII	754,819	408	3,666	871	-
IX	1,894,400	408	11436	30,980	-
TOTAL	15,184,834	408	16672	32,255	5359

Model 1: Samardjieva and Badal, 2002
Model 2: RGELFE, 1992
Model 3: Vacareanu et al., 2004

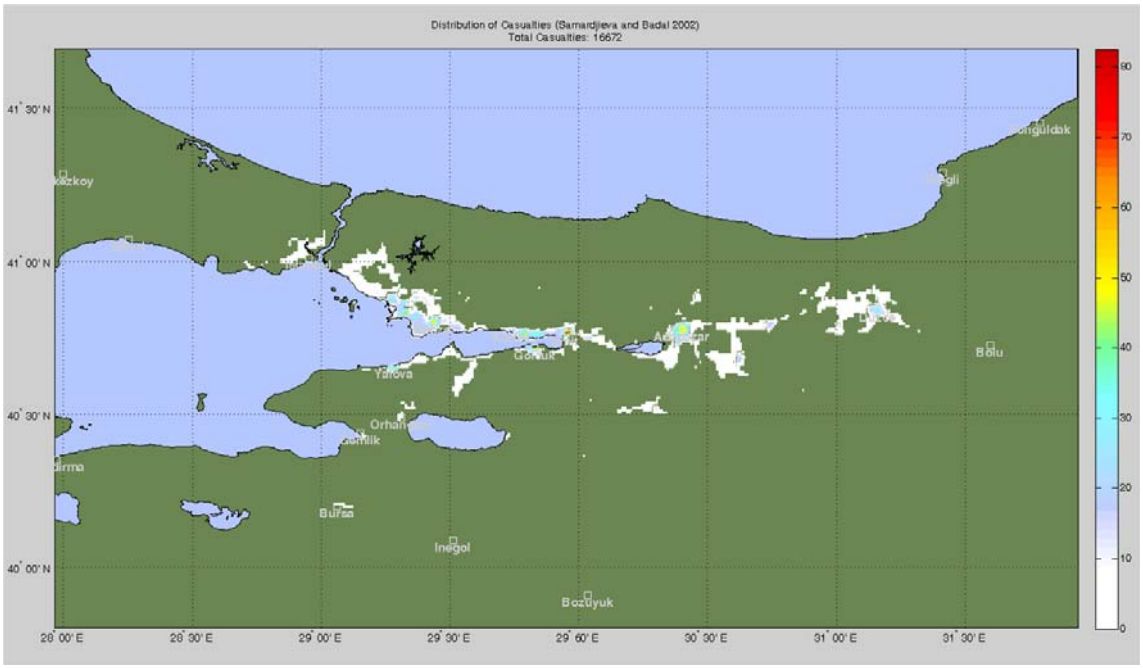

Figure 91. Casualty estimation for Level 0

Comparison of Samardjieva and Badal (2002) and Vacareanu et al. (2004) Approaches

A comparison of the two magnitude dependent empirical fatality prediction models is given in Table 54 and Figure 92.

Table 54. Number of fatalities obtained from Samardjieva and Badal (2002) and Vacareanu et al. (2004) Approaches

	Vacareanu et al. (2004)			Samardjieva and Badal (2002)			
M	Upper Bound	Median	Lower Bound	D>200	D:100-200	D: 50-100	D: 25-50
6	3,241	486	16	468	200	81	15
6.5	6,862	1,029	34	1,429	575	214	36
7	14,526	2,179	73	4,365	1,660	562	85
7.5	30,752	4,613	154	13,335	4,786	1,479	202
8	65,102	9,765	326	40,738	13,804	3,890	479

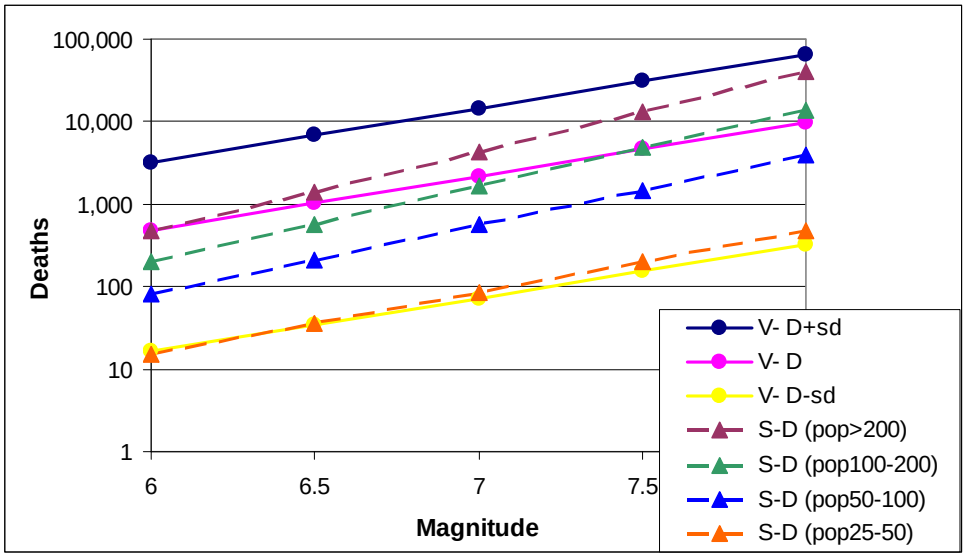

Figure 92. Number of fatalities obtained from Samardjieva and Badal (2002) and Vacareanu et al. (2004) Approaches

Figure 92 reveals that the upper bound and lower bound curves given by the Vacareanu et al. (2004) model also form upper and lower bounds for the Samardjieva and Badal (2002) model which estimates the number of fatalities as a function of earthquake magnitude and the population density in the affected area. The lower bound curve of the first model is strongly comparable to the low population density estimations of the second. The median curve estimates fatalities comparable to medium to high population density results, the number of fatalities increasing with the magnitude, but with a shallower slope. The upper bound curve, however, estimates higher fatalities even for the highest population density range. Nevertheless, the results should be applicable to regions that are either overpopulated (D much larger than 200 people/km^2, such as the affected region of the 1999 Kocaeli earthquake) or more vulnerable (such as the region affected by 1988 Spitak earthquakes). As such, taking into account the population density and vulnerability of the affected region both empirical

models can be used to estimate fatalities and the associated geographic distribution directly from the earthquake magnitude.

Level 1

1999 Athens Earthquake

Figure 93 presents the estimated building distribution for Greece obtained from the approximation approach based on the Corine Land Cover data. The estimated total number of damaged buildings at damage states D3, D4 and D5 (a total of 3080 buildings) and the estimated number of fatalities obtained from Level 1 analysis are presented in Figure 94 and Figure 95 respectively.

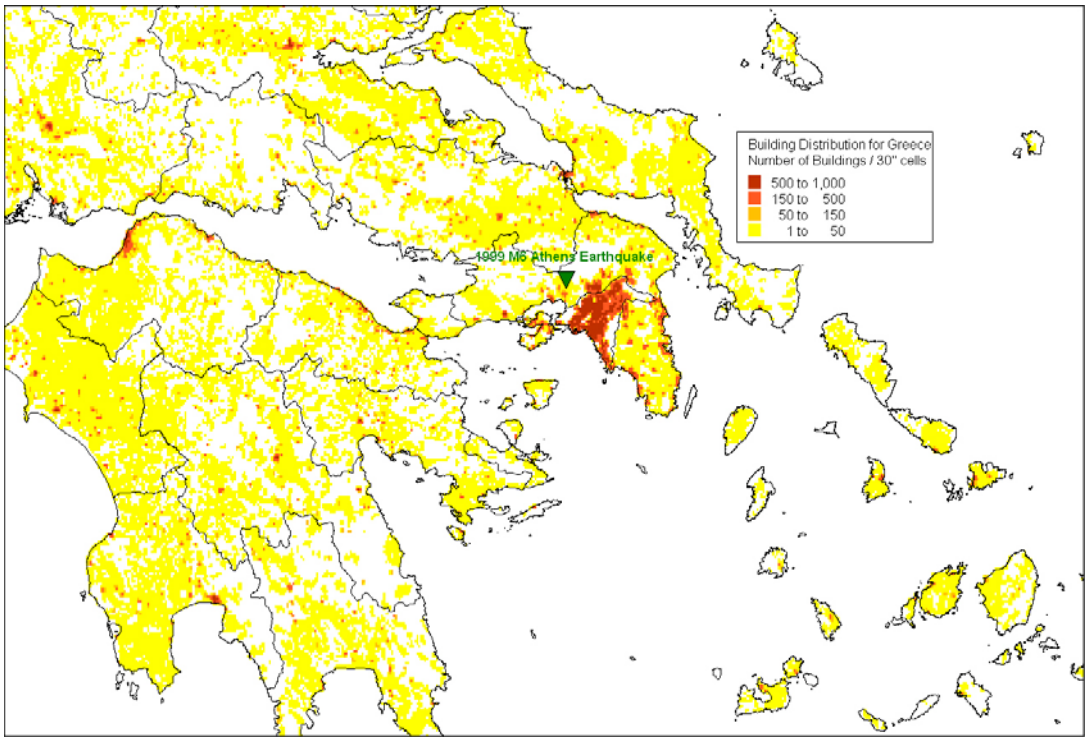

Figure 93. Estimated building distribution for Greece

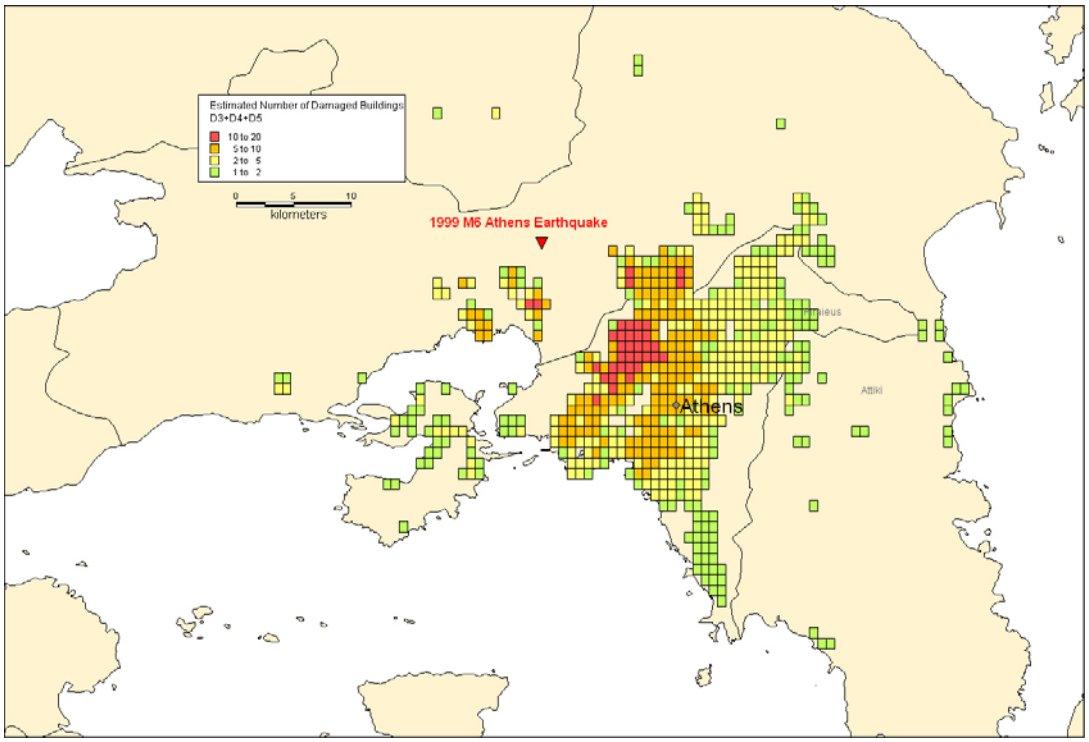

Figure 94. Building damage estimation for Level 1.

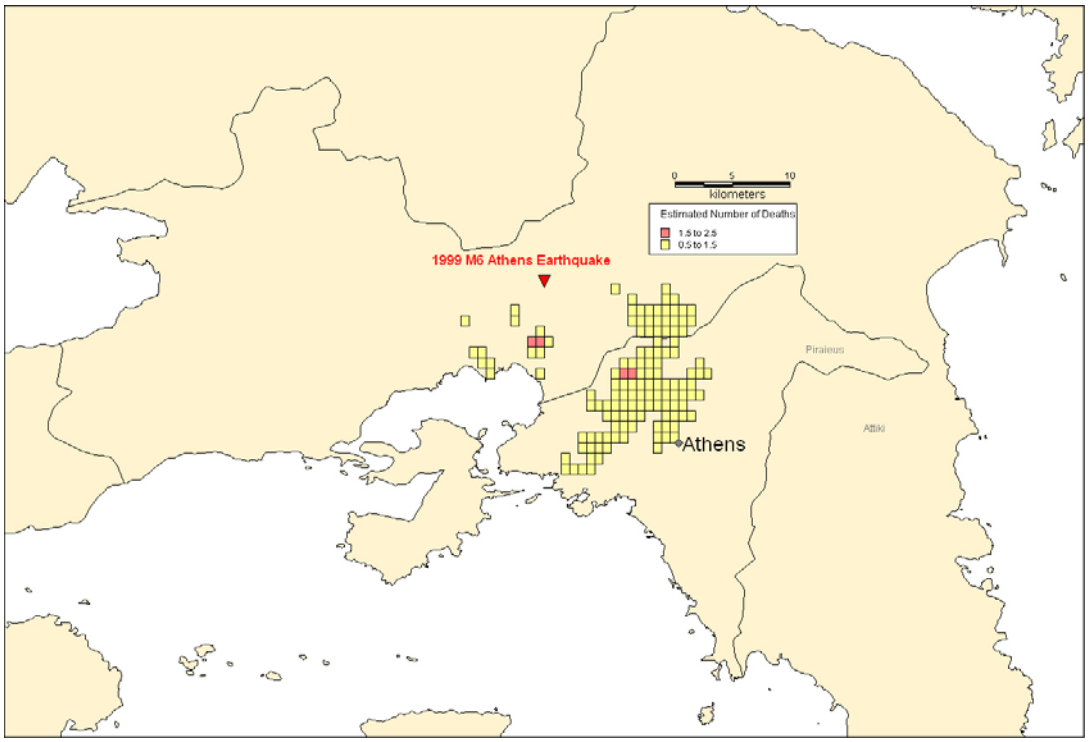

Figure 95. Casualty estimation for Level 1.

1999 Kocaeli Earthquake

Sesetyan et al. (2005) intensity prediction equation was used to estimate intensity distribution and the building damage was calculated by Giovinazzi and Lagomarsino (2005) approach. The building damage distributions for various damage states are presented in Figure 96 through Figure 102.

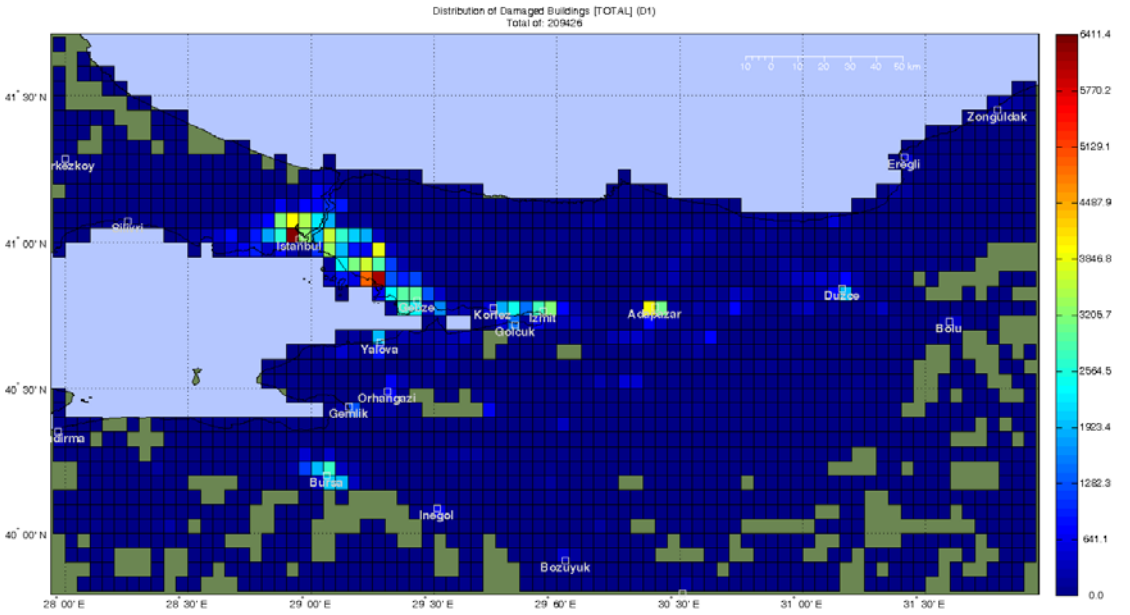

Figure 96. Building damage distribution for damage state D1

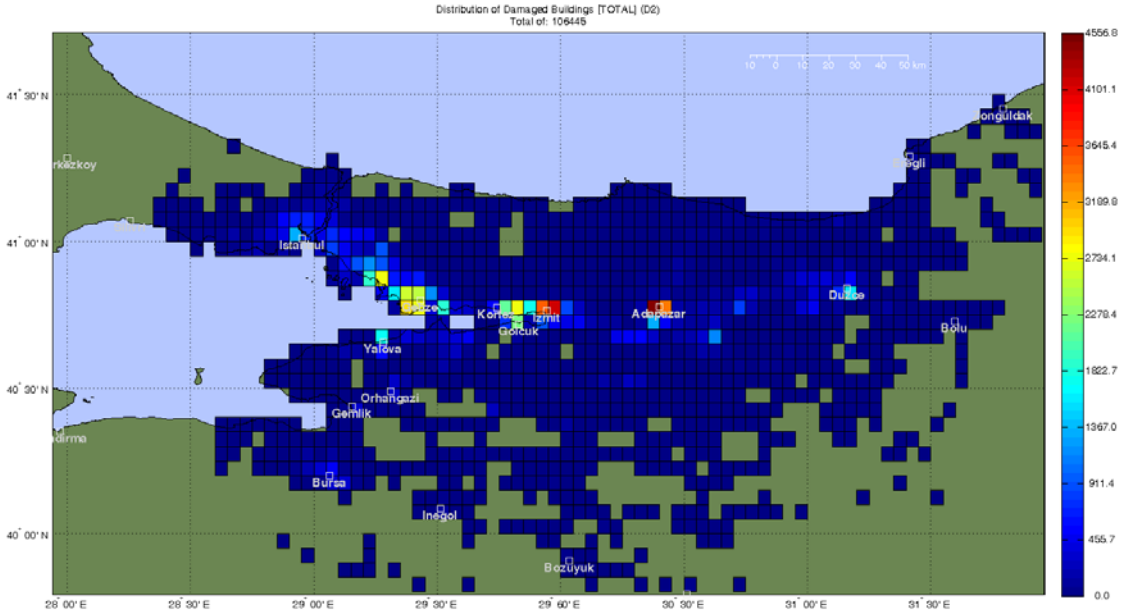

Figure 97. Building damage distribution for damage state D2

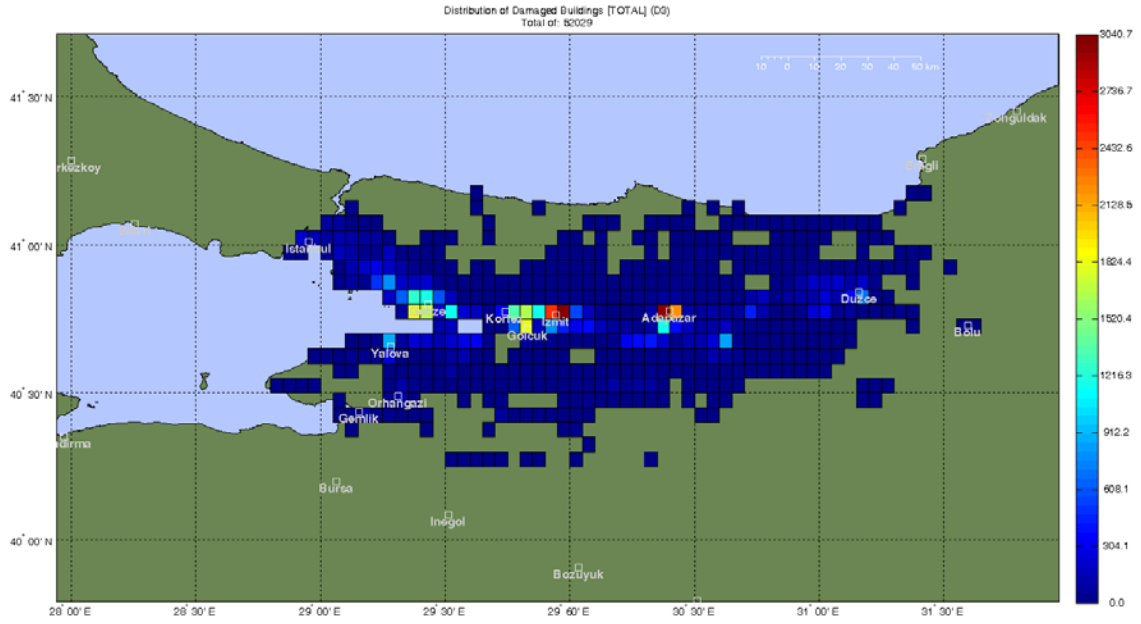

Figure 98. Building damage distribution for damage state D3

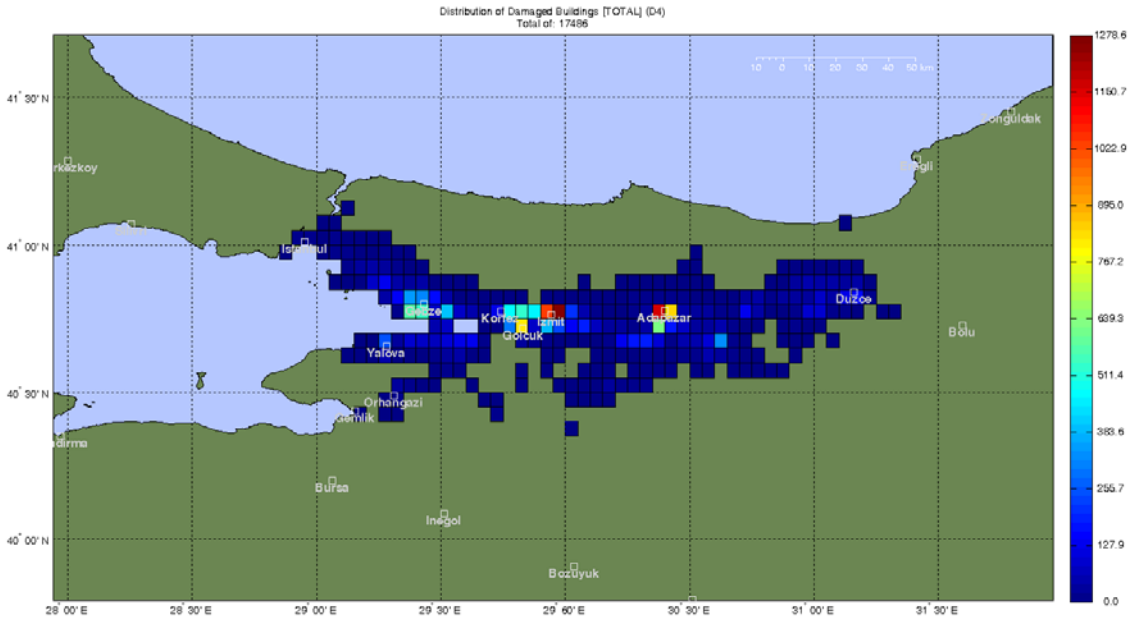

Figure 99. Building damage distribution for damage state D4

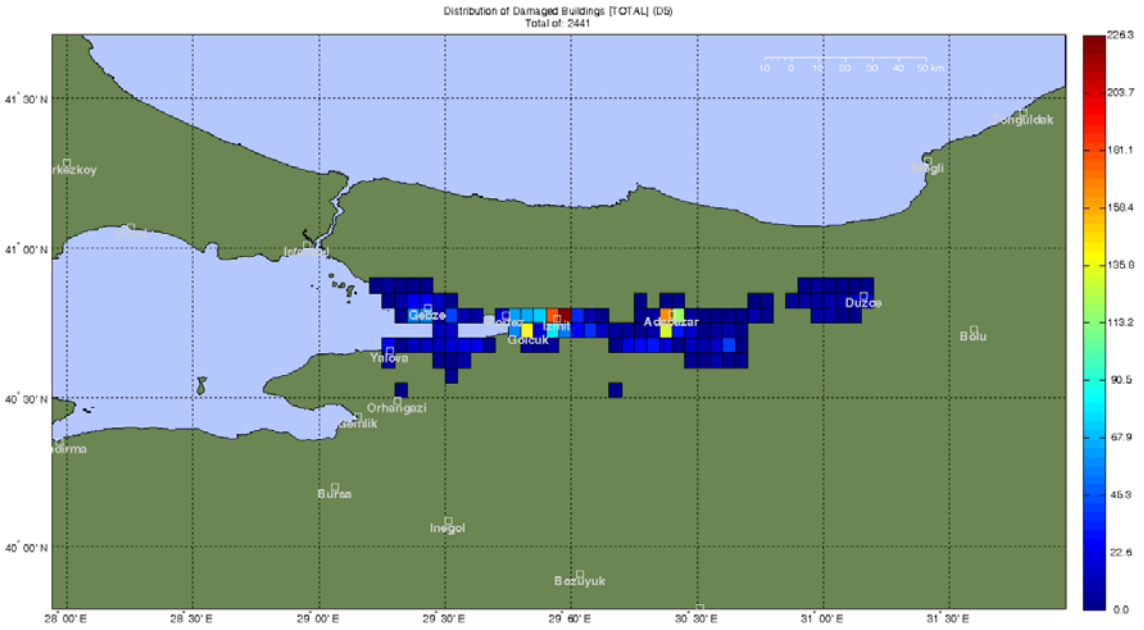

Figure 100. Building damage distribution for damage state D5

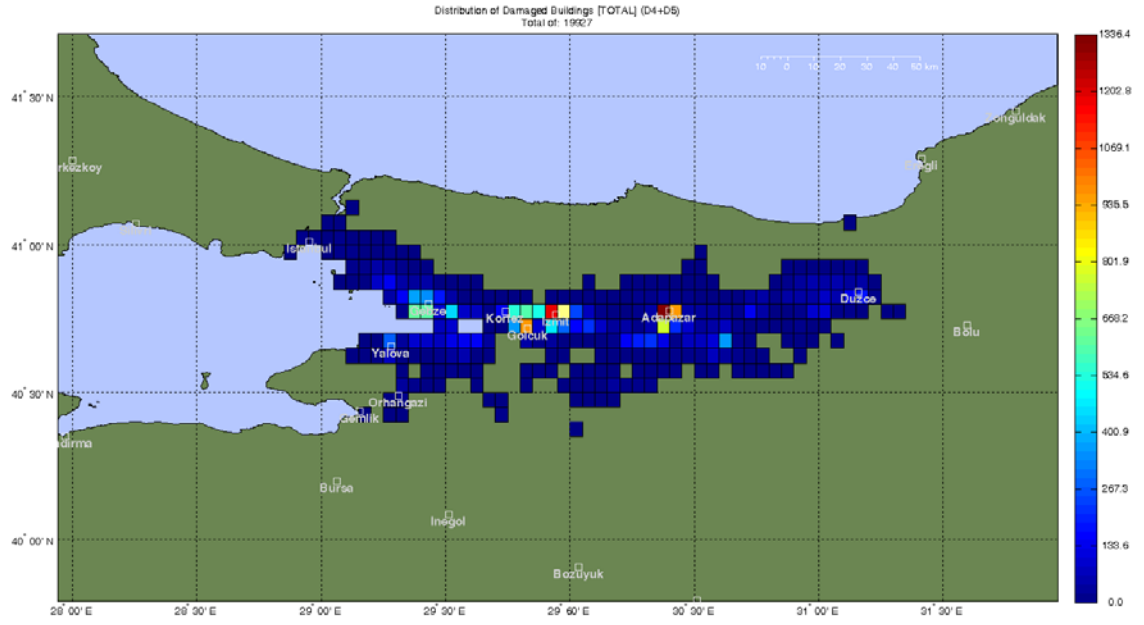

Figure 101. Building damage distribution for damage state D4+D5

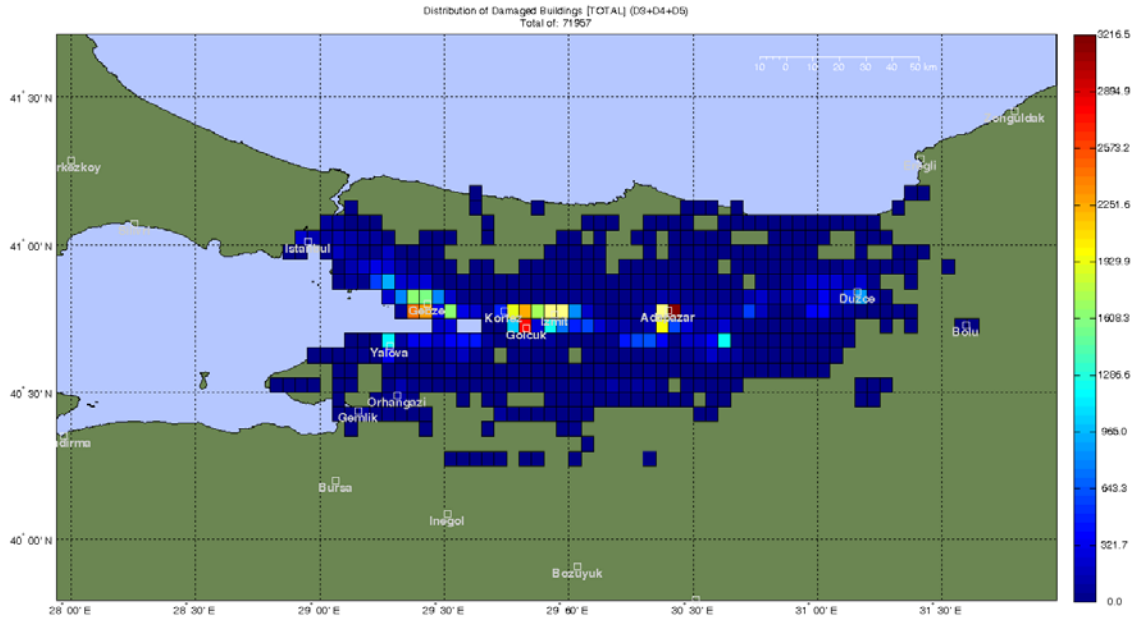

Figure 102. Building damage distribution for damage state D3+D4+D5

Table 55. Building Damage Estimation for Kocaeli earthquake Level 1

Damage States	Number of Building Damage
D1	209,426
D2	106,445
D3	52,029
D4	17,486
D5	2441
D4+D5	19,927
D3+D4+D5	71,956

For the casualty estimation, there are three models used in Level 1 module. The casualty distributions are presented in Figure 103 through Figure 105 for each model. In Table 56 the results for each model are shown.

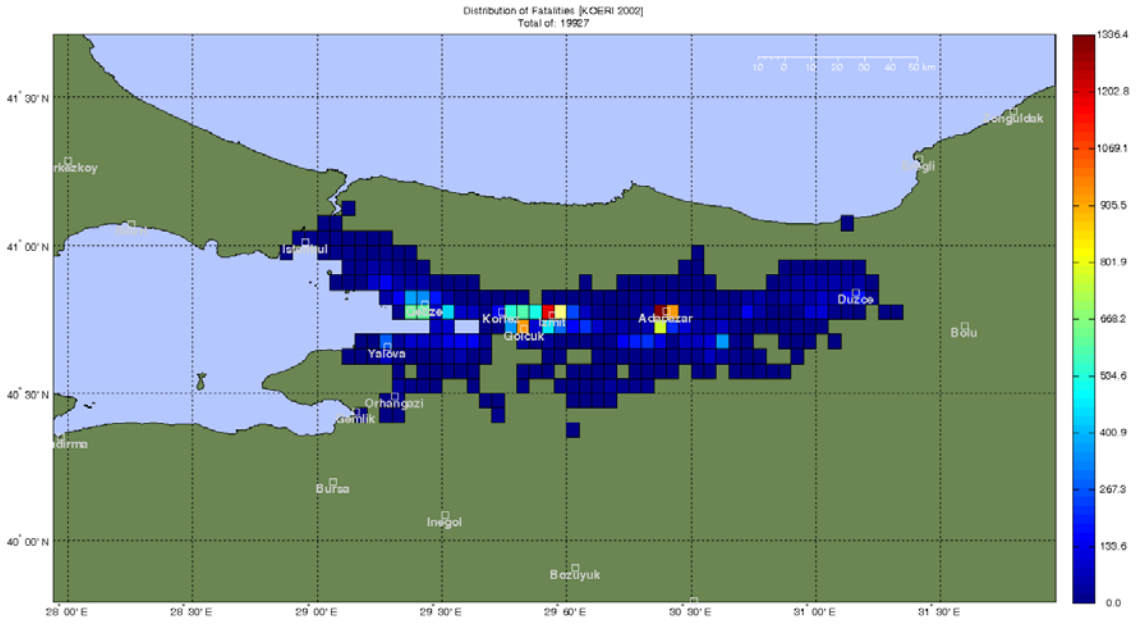

Figure 103. Casualty estimation for KOERI, 2002

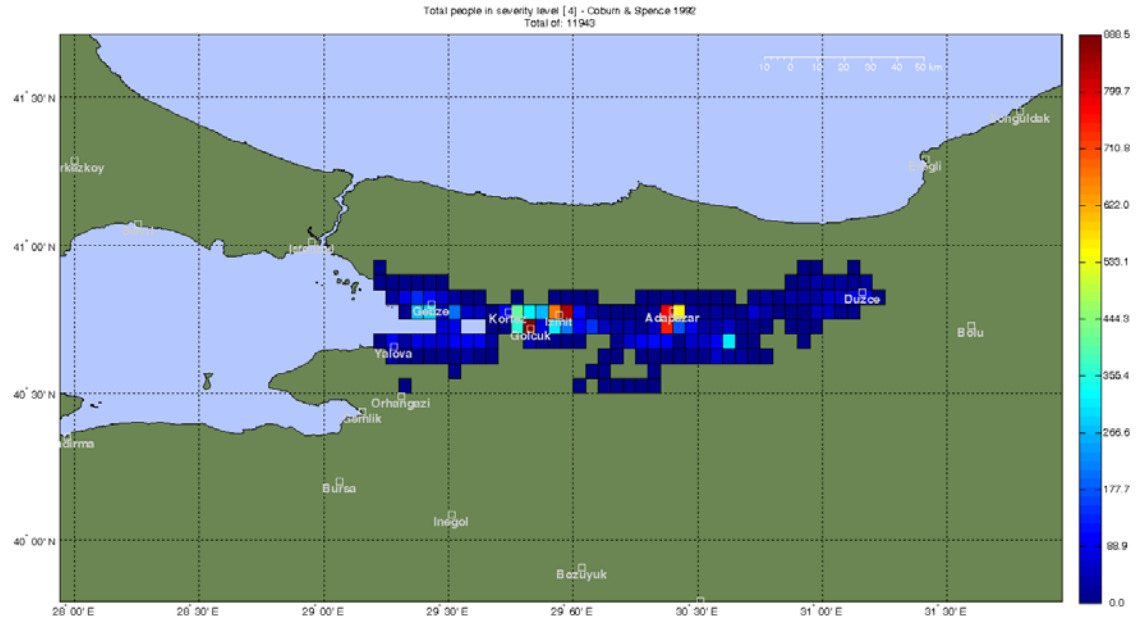

Figure 104. Casualty estimation with Coburn & Spence 1992 model

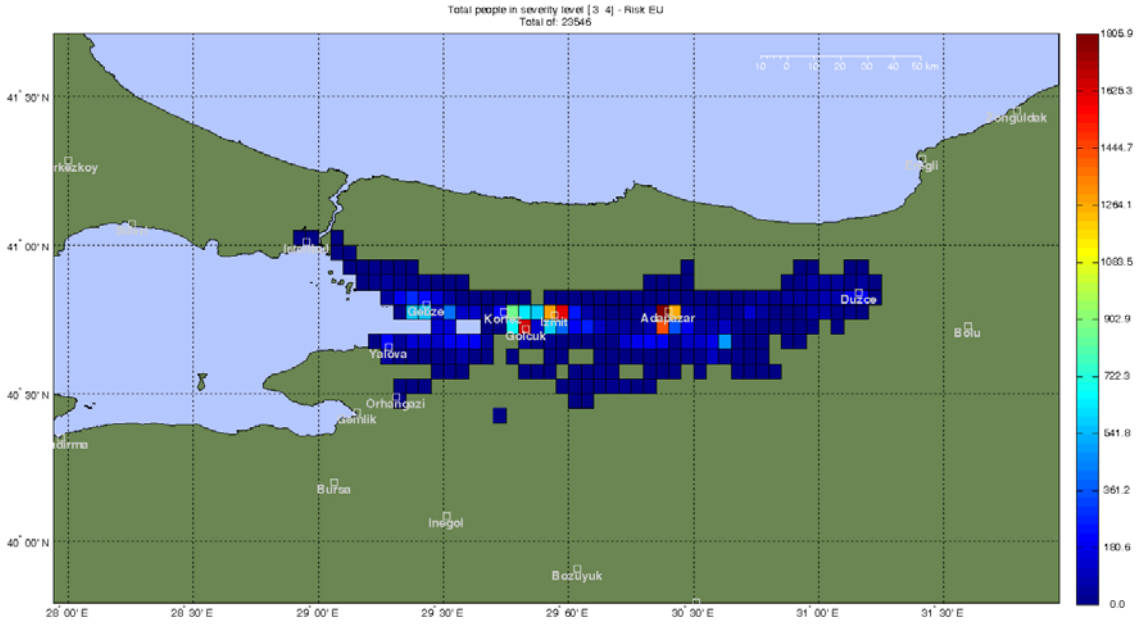

Figure 105. Casualty estimation for RISK-UE.

Table 56. Casualty estimation for Level 1

	KOERI, 2002	Coburn & Spence, 1992	RISK-UE
Total Buildings	-	1,455,500	1,455,500
Total Dwellings	-	5,962,924	5,962,924
Severity Level [4]	-	11,943	23,546
Fatalities	19,927	-	-
Seriously Injured (ATC-13)	79,709	-	-

Level 2

The analysis methods of *Level 2 Loss Assessment* have been applied to the selected building types of European and HAZUS99 (FEMA, 1999) building taxonomies. The methods adopted for Level 2 analysis have been also compared with the other studies, e.g. SELENA v4.0 (Molina et al, 2008), ATC-55 (Yang 2005). The results are presented in the following sections.

Applications with European Building Taxonomy

Damage to the selected buildings, namely *RC1 -RC frame*, *RC3 -RC frame with infill walls* and *M6 -unreinforced masonry*, are calculated by each method of Level 2 analysis. It is assumed that all three types of buildings are mid-rise structures with low ductility. The analyses are performed for two different scenario earthquakes which are given in Table 57 and the seismic demand is represented by EC8 Type 1 and Type 2 response spectra. The resulting damage probabilities from CSM, MADRS, RFM and CM for four damage levels are presented in Figure 106, Figure 107, Figure 108, Figure 109, Figure 110 and Figure 111.

The Capacity Spectrum Method (CSM), the Modified Acceleration-Displacement Response Spectrum (MADRS) Method and the Reduction Factor Method (RFM) produce similar results whereas the Coefficient Method (CM) yields different damage probabilities for all three types of buildings especially for the Scenario I earthquake which might be considered as a relatively stronger ground shaking. The CM estimates the performance point of the buildings by modifying the elastic spectral displacement while the CSM, MADRS and RFM compute the performance point by intersecting the demand and capacity spectra and the performance point (inelastic seismic demand) is limited by the ultimate point of the capacity spectrum.

Table 57. Example scenario earthquake parameters

Scenario I	**Scenario II**
PGA=0.4g	PGA=0.2g
Magnitude = 7.0	Magnitude = 5.0
Ground Type: B	Ground Type: B

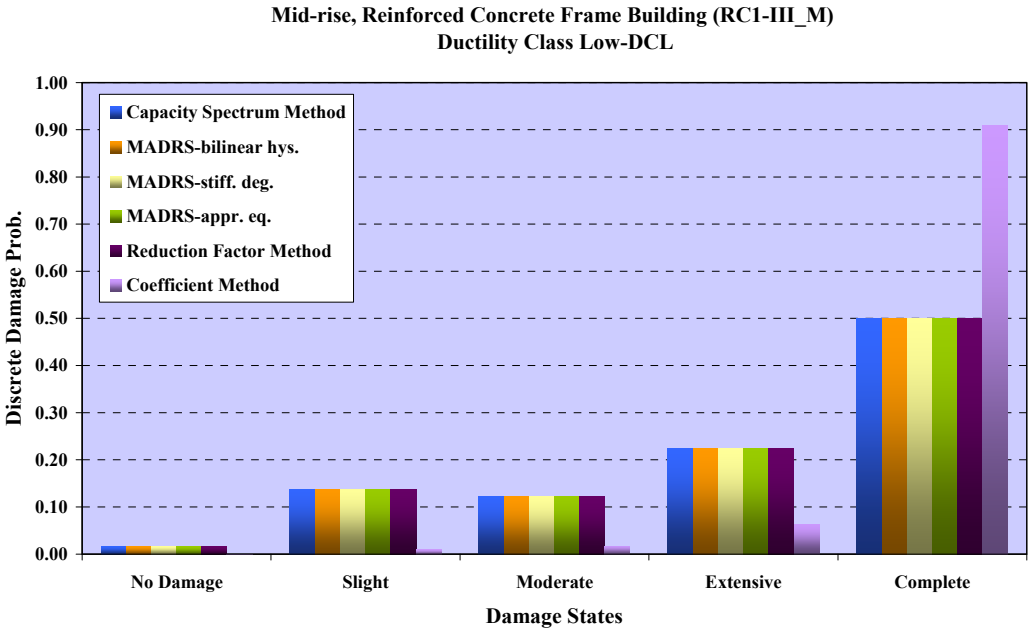

Figure 106. Discrete damage probabilities for building RC1_III_M_DCL under Scenario I earthquake

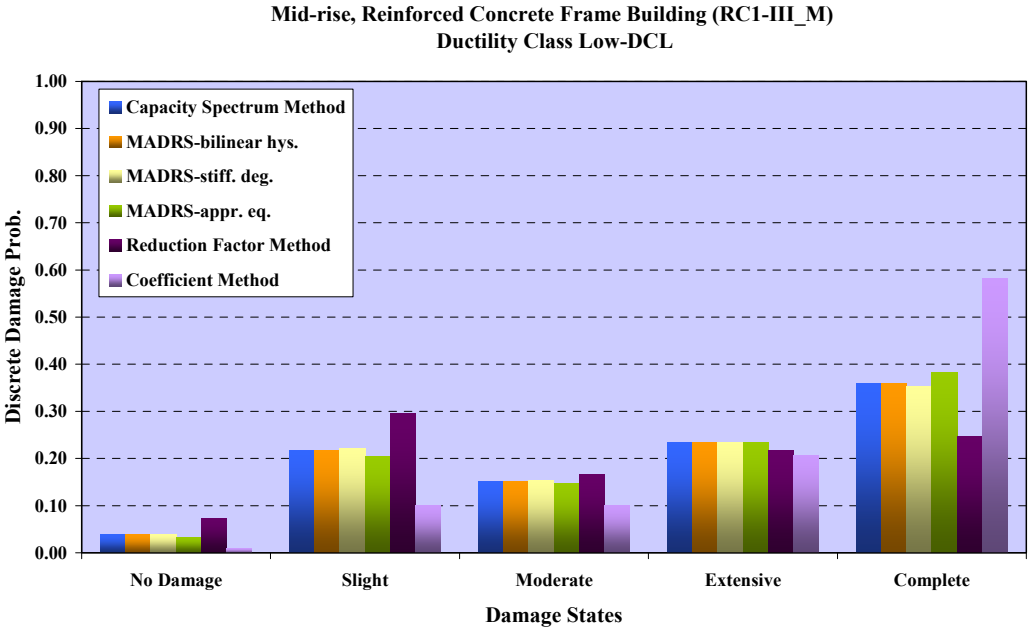

Figure 107. Discrete damage probabilities for building RC1_III_M_DCL under Scenario II earthquake

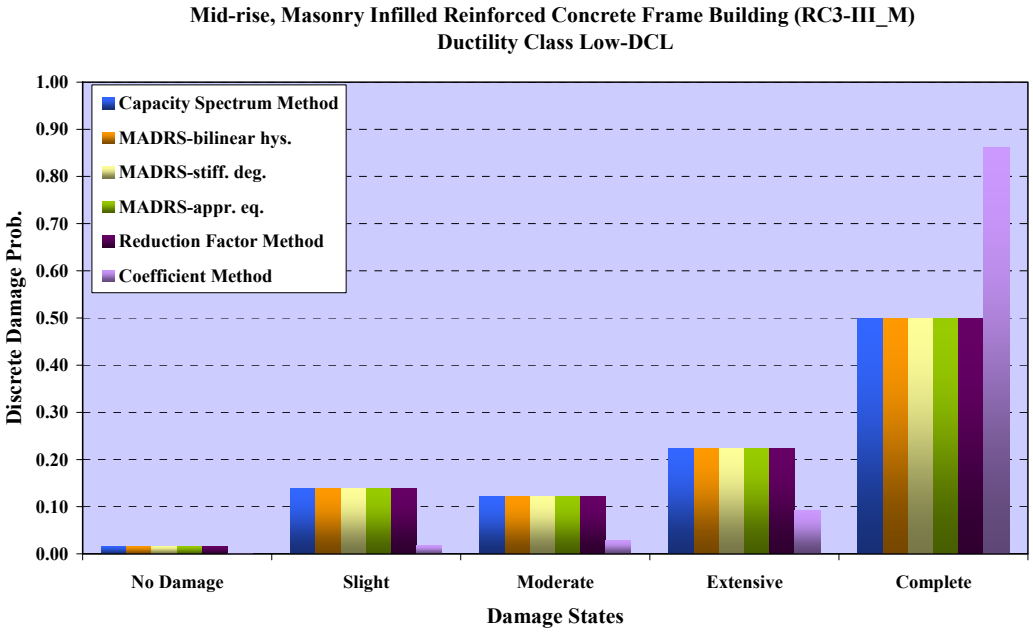

Figure 108. Discrete damage probabilities for building RC3_III_M_DCL under Scenario I earthquake

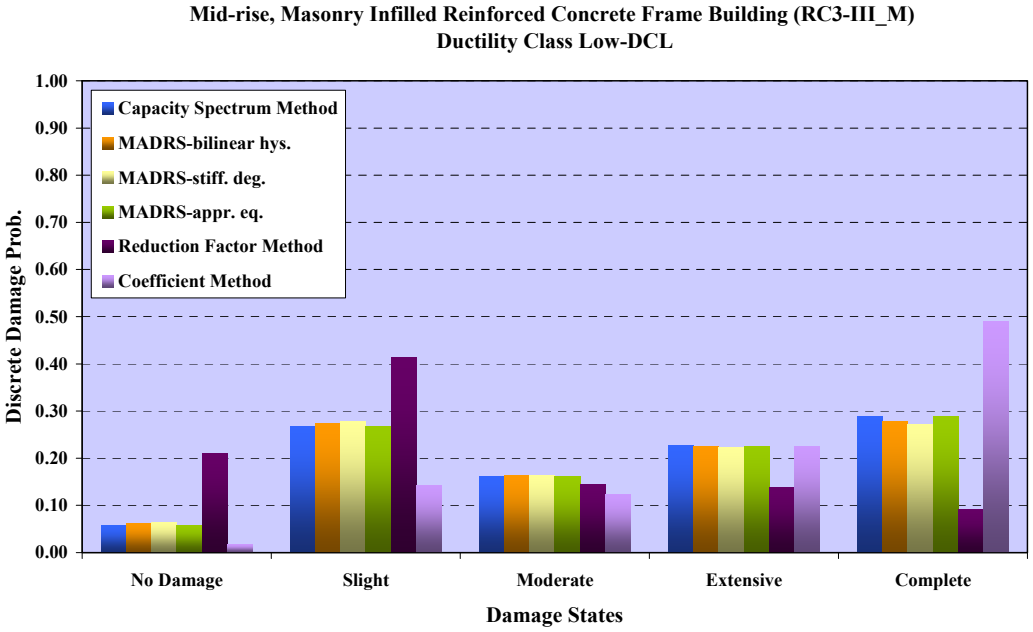

Figure 109. Discrete damage probabilities for building RC3_III_M_DCL under Scenario II earthquake

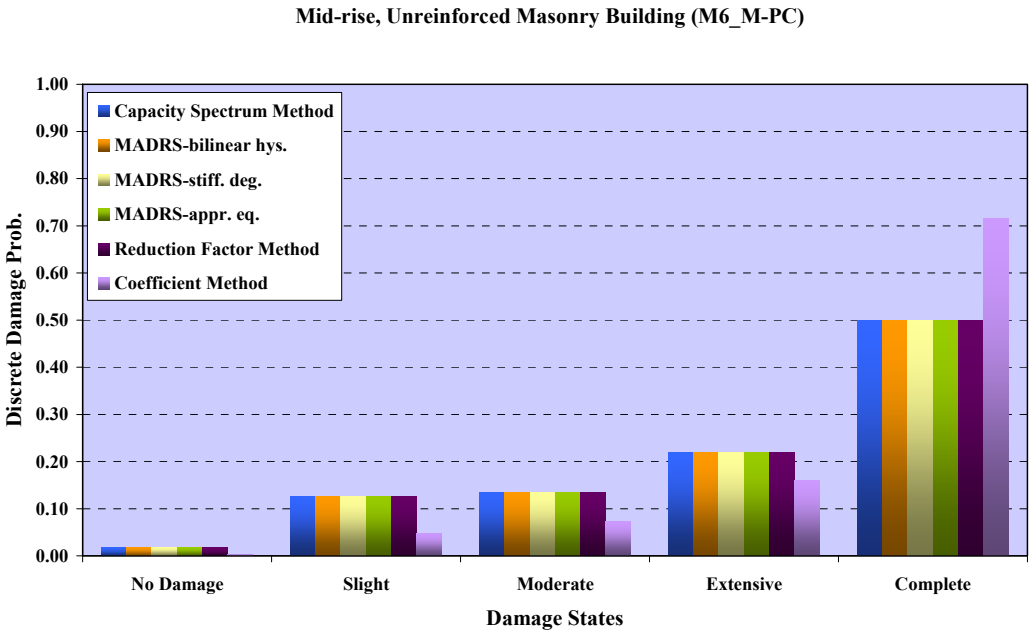

Figure 110. Discrete damage probabilities for building M6_M_PC under Scenario I earthquake

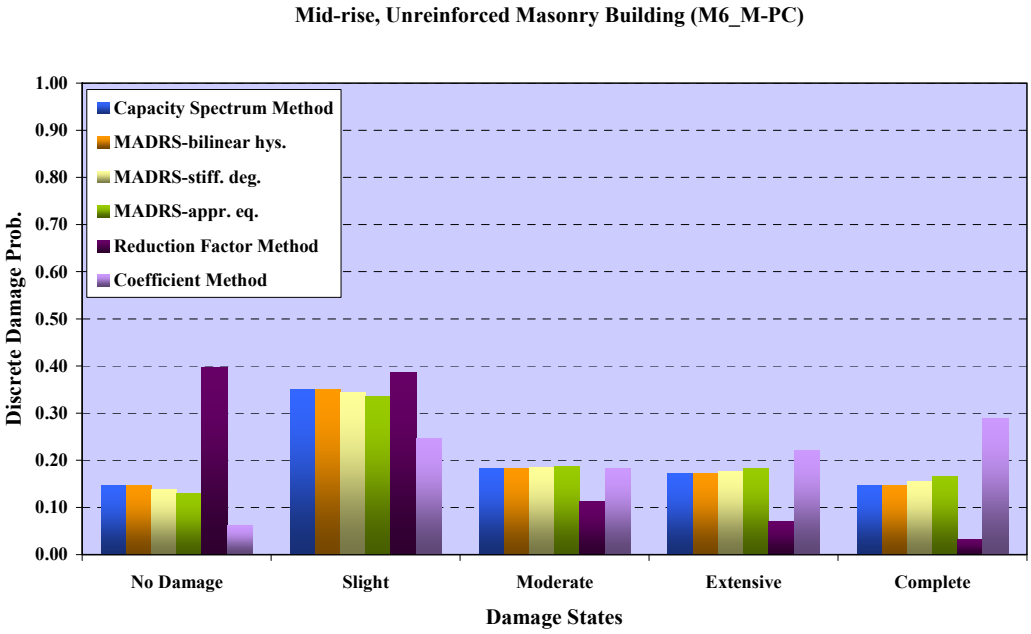

Figure 111. Discrete damage probabilities for building M6_M_PC under Scenario II earthquake

Applications with HAZUS99 Building Taxonomy

Damage to the selected buildings, namely *C1 -RC frame*, *C3 -RC frame with infill walls* and *URM -unreinforced masonry*, are calculated by each method of Level 2 analysis. It is assumed that all three types of buildings are mid-rise structures and comply with low-code seismic design level. The analyses are performed for two different scenario earthquakes which are given in Table 58 and the seismic demand is represented by IBC 2006 standard response spectrum. The resulting damage probabilities from CSM, MADRS, RFM and CM for four damage levels are presented in Figure 112, Figure 113, Figure 114, Figure 115, Figure 116 and Figure 117.

Similarly to the application with the European buildings, the Capacity Spectrum Method (CSM), the Modified Acceleration-Displacement Response Spectrum (MADRS) Method and the Reduction Factor Method (RFM) produce highly comparable results whereas the Coefficient Method (CM) yields different damage probabilities for all three types of buildings especially for the Scenario I earthquake which might be considered as a relatively stronger ground shaking. The CM estimates the performance point of the buildings by modifying the elastic spectral displacement while the CSM, MADRS and RFM compute the performance point by intersecting the demand and capacity spectra and the performance point (inelastic seismic demand) is limited by the ultimate point of the capacity spectrum.

Table 58. Example scenario earthquake parameters

Scenario I	**Scenario II**
S_s= 1.0g	S_s = 0.5g
S_1 = 0.5g	S_1 = 0.25g
Magnitude = 7.0	Magnitude = 7.0
Site Class: B	Site Class: B

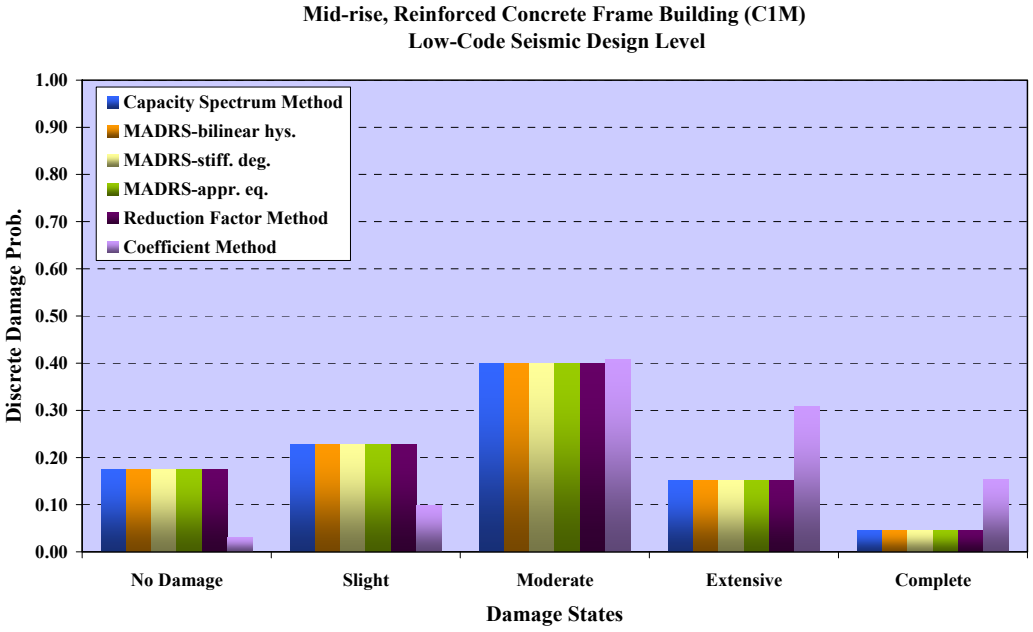

Figure 112. Discrete damage probabilities for building C1M under Scenario I earthquake

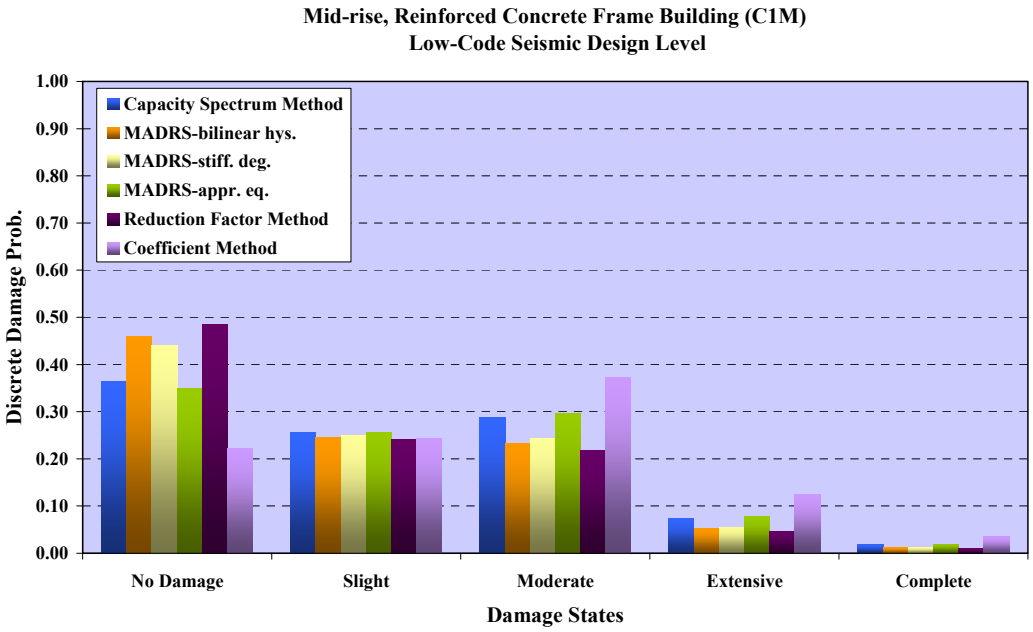

Figure 113. Discrete damage probabilities for building C1M under Scenario II earthquake

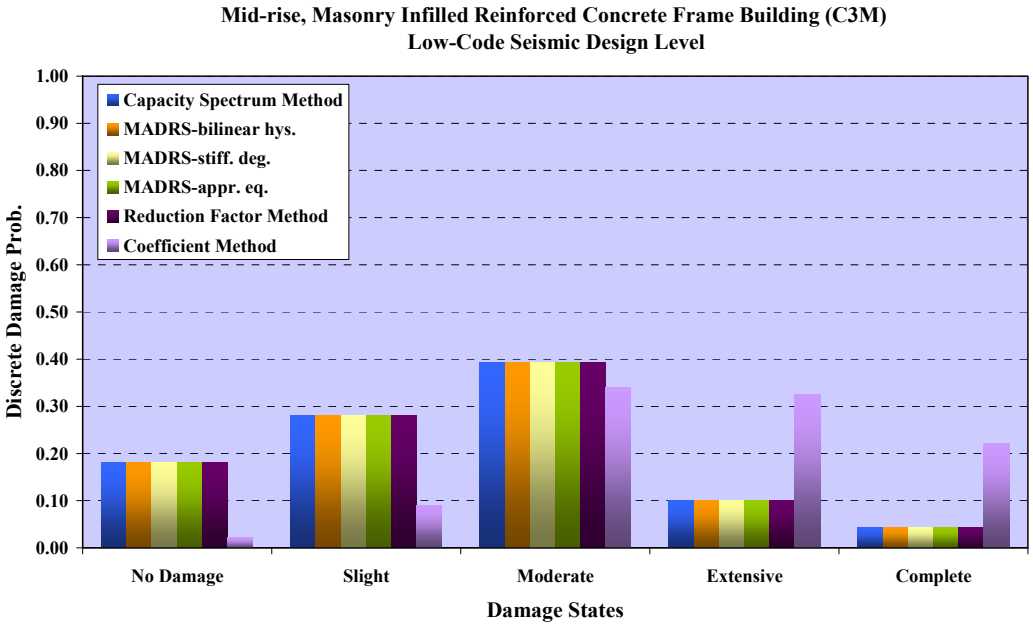

Figure 114. Discrete damage probabilities for building C3M under Scenario I earthquake

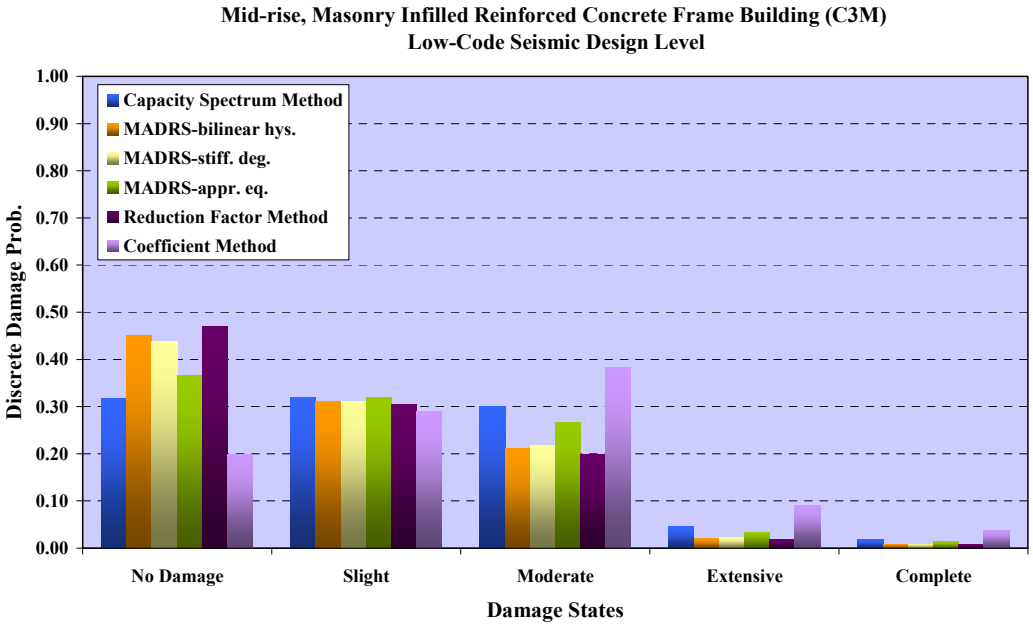

Figure 115. Discrete damage probabilities for building C3M under Scenario II earthquake

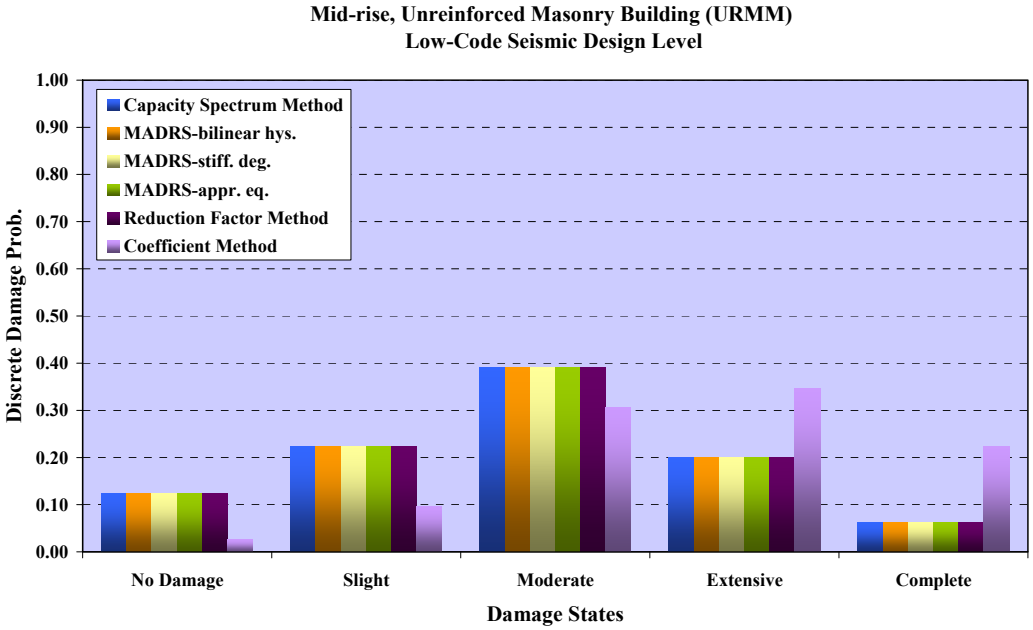

Figure 116. Discrete damage probabilities for building URMM under Scenario I earthquake

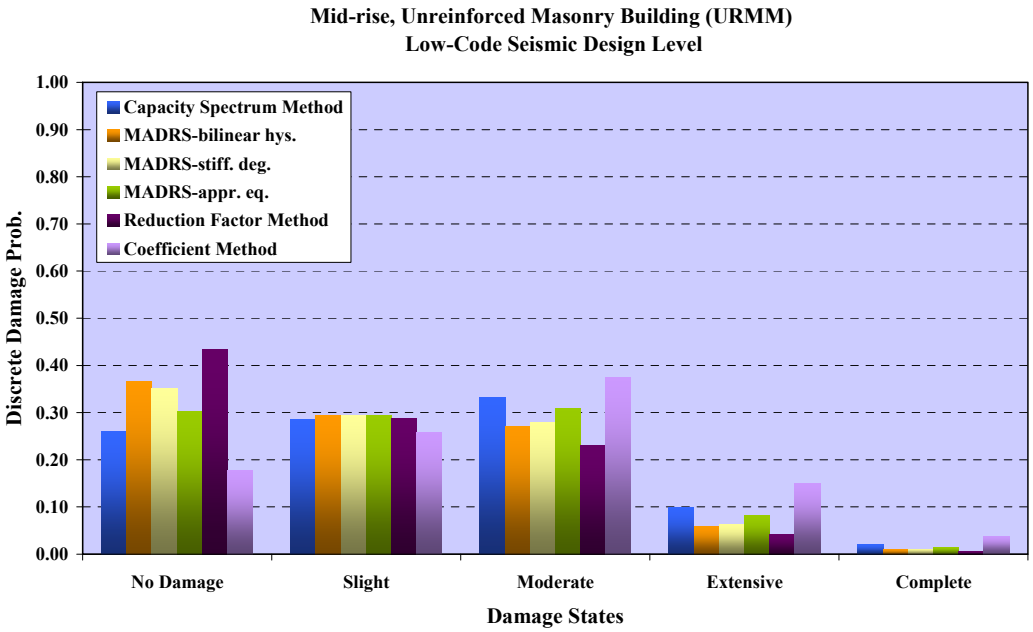

Figure 117. Discrete damage probabilities for building URMM under Scenario II earthquake

Comparison with the Other Studies

The methods of Level 2 analysis have been compared with the other software and studies available in the literature. SELENA v4.0- Seismic Loss Estimation Using a Logic Tree Approach (Molina et al, 2008) provides loss estimations for HAZUS99 model buildings by CSM and MADRS-stiffness degrading hysteretic model. The study of Yang, (2005) computes the performance point for the model building types of HAZUS99 by CSM and MADRS-approximate equations.

Figure 118, Figure 119 and Figure 120 compare the discrete damage probabilities resulting from ELER, SELENA and T. Yang for HAZUS99 model buildings, namely *C1 -RC frame*, *C2 -RC shear wall and C3 -RC frame with infill walls*. It is assumed that all three types of buildings are mid-rise structures and correspond to pre-code seismic design level. The analyses are performed for the Scenario II earthquake which is given in Table 58 and the seismic demand is represented by IBC 2006 standard response spectrum.

As it can be observed from Figure 118, Figure 119 and Figure 120, all three applications produce similar results.

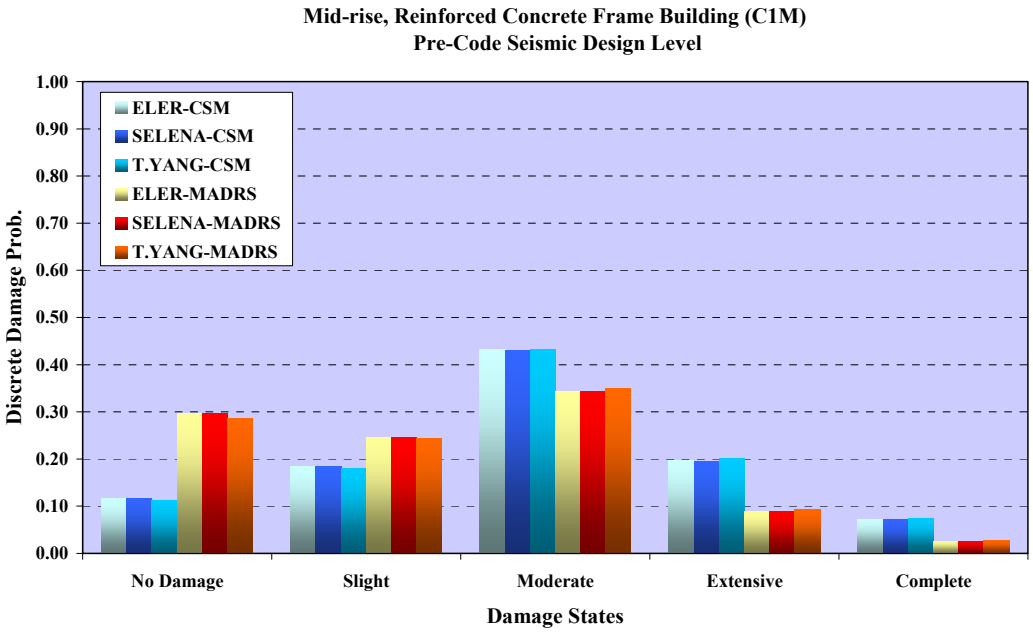

Figure 118. Discrete damage probabilities for building C1M under Scenario II earthquake

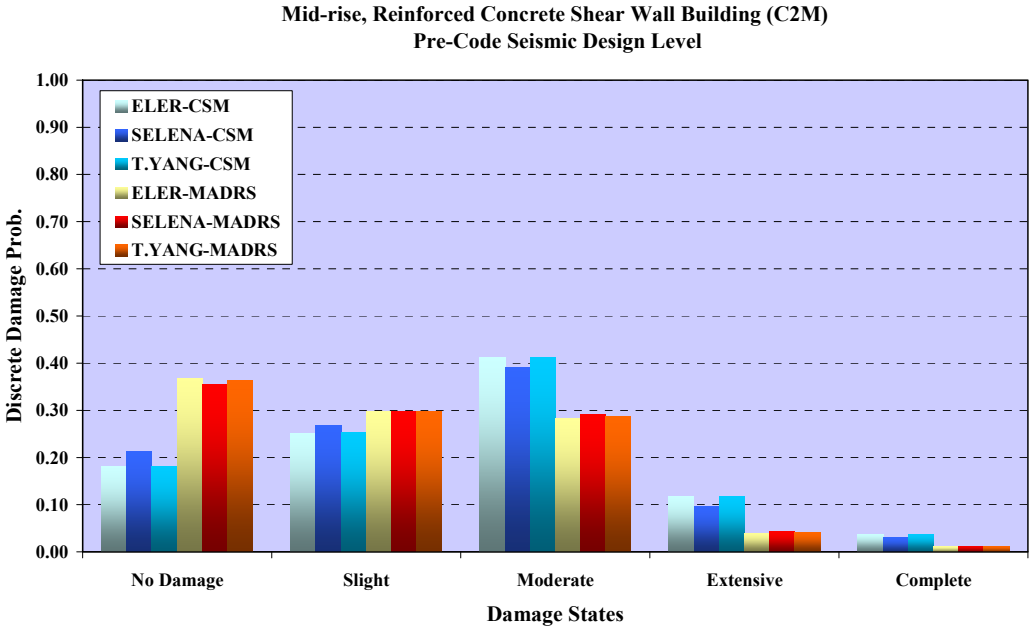

Figure 119. Discrete damage probabilities for building C2M under Scenario II earthquake

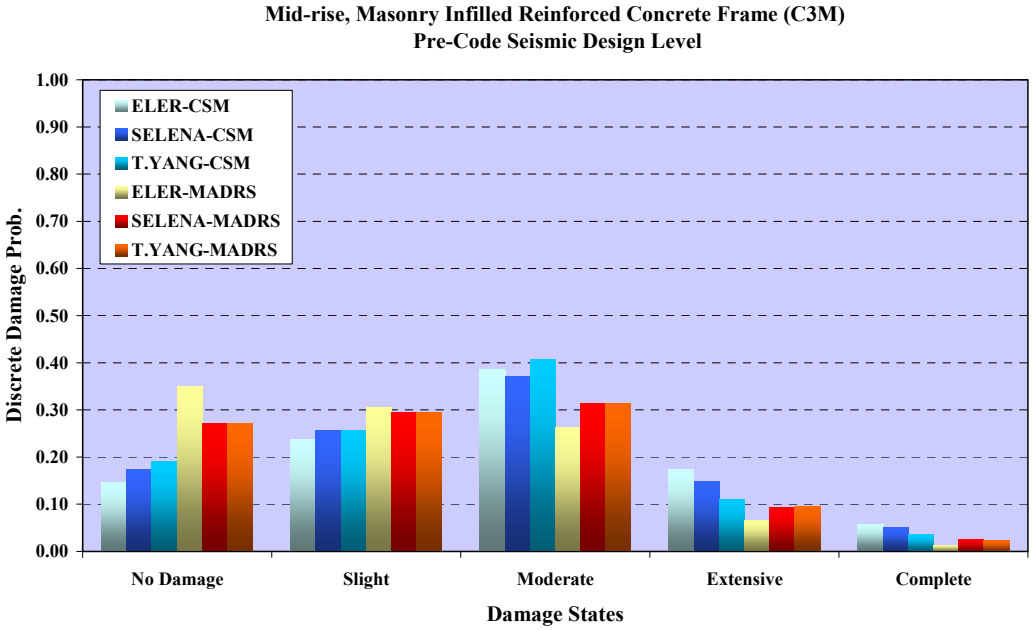

Figure 120. Discrete damage probabilities for building C3M under Scenario II earthquake

A comparative damage estimation exercise under the credible worst case scenario earthquake (see Section C.5.3 for details) has also been conducted for the Istanbul building inventory. Number of damaged buildings has been estimated by three different software packages: ELER, KOERILoss (KOERI, 2002) and DBELA (Crowley et al, 2004). KOERILoss follows the FEMA 356 (2000) procedure for the calculation of the performance point and the resulting damage estimates. DBELA uses mechanically derived formulae to describe the displacement capacity of classes of buildings (grouped by structural type and failure mechanism) at three limit states.

The input ground motions resulting from the credible worst case scenario earthquake are based on the Boore et al, 1997 and Sadigh et al, 1997 ground motion prediction equations. The number of damaged buildings is presented in Figure 121. All three software packages produce similar results.

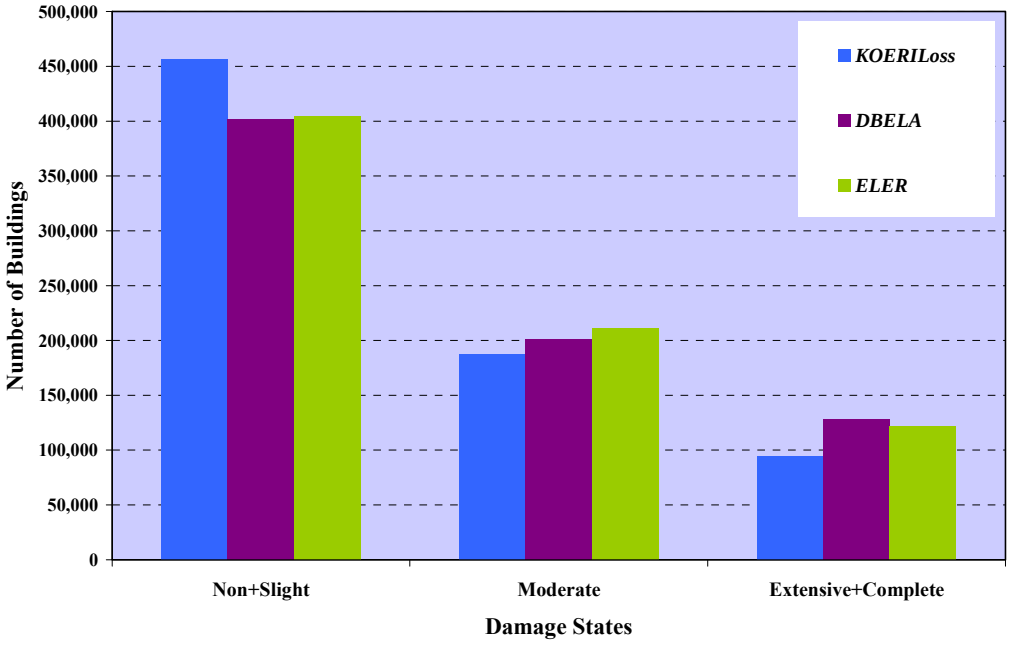

Figure 121. Comparison of the results for Istanbul building inventory (DBELA results taken from Strasser et al., 2007)

C.5.3. Case Studies: Earthquake Loss Assessment for the Zeytinburnu District of Istanbul

1999 Kocaeli Earthquake Scenario

Zeytinburnu is located at the western side of the city of Istanbul, at a distance of approximately 50.km from the westernmost end of the 1999 Kocaeli rupture. The intensity distribution of the 1999 Kocaeli earthquake obtained from the regional intensity prediction equation and the location of Zeytinburnu district are presented in Figure 122.

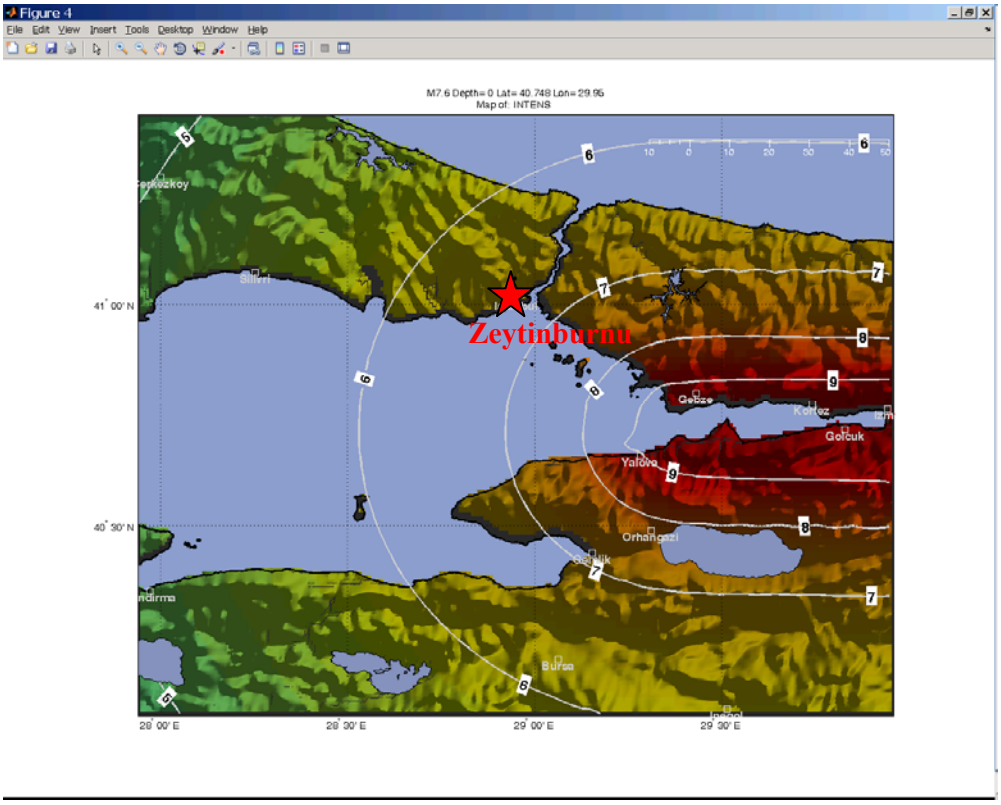

Figure 122. The intensity distribution of the 1999 Kocaeli earthquake and the location of the Zeytinburnu district.

Level 0 Loss Assessment

Level 0 loss assessment is essentially aimed for studies in larger regions. A closer view to the Zeytinburnu district reveals about 12 fatalities using the Samerdjieva and Badal (2002) approach.

Level 1 Loss Assessment

An analysis is conducted for the Zeytinburnu district using the building inventory of Istanbul based on 0.005°*0.005° geocells as elaborated in 0 The distribution of the damaged buildings in various damage states obtained from Level 1 analysis is presented in Figure 123. Casualty assessment in the district reveals about 1 fatality using the Coburn and Spence (1992) approach and about 5 fatalities using the Risk-UE model. The KOERI model yields 14 casualties and 56 severe injuries.

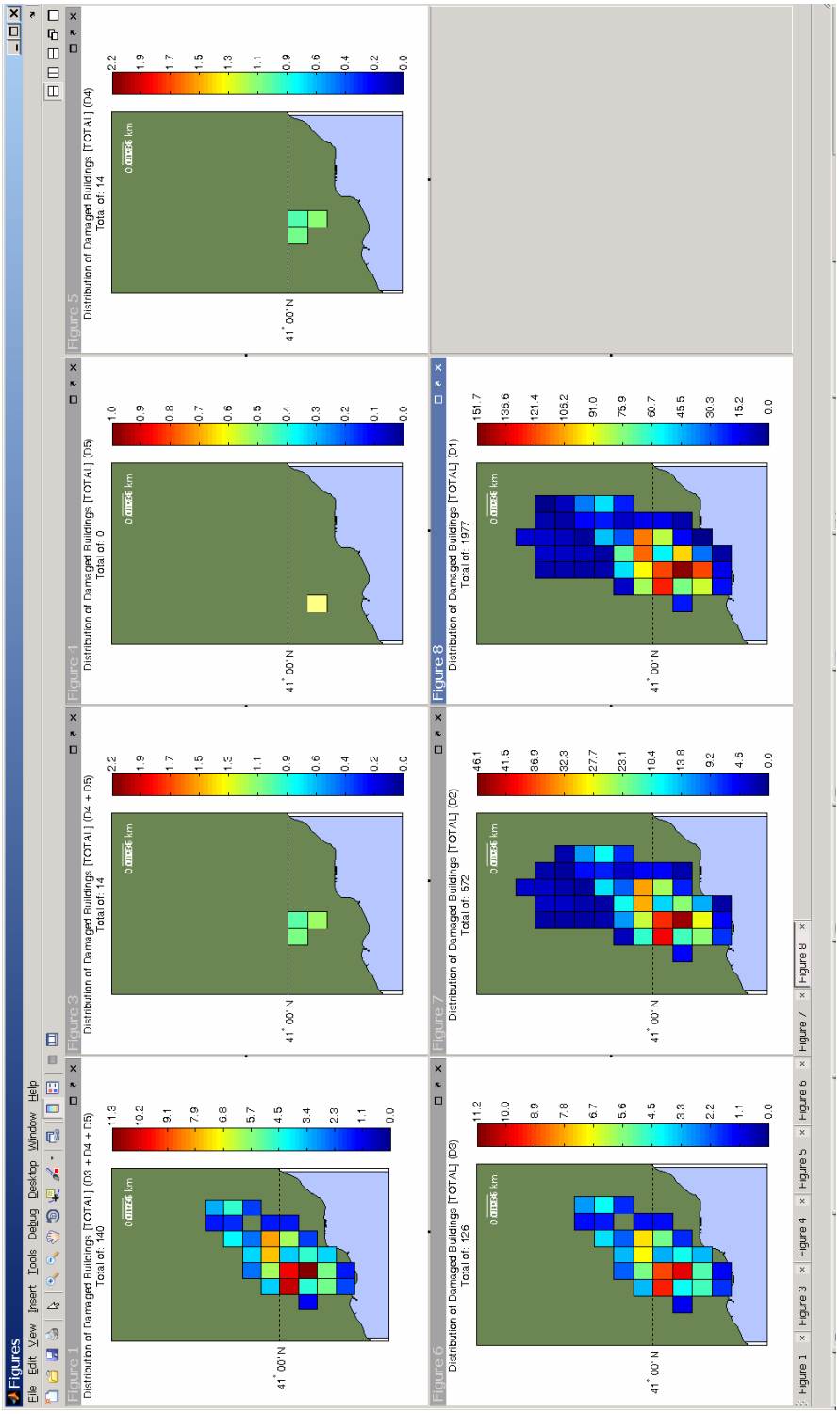

Figure 123. The distribution of damaged buildings in Zeytinburnu district resulting from the 1999 Kocaeli earthquake scenario – Level 1 Analysis.

Level 2 Loss Assessment

Spectral accelerations at T=0.2 sec and T=1.0 sec obtained from the Campbell and Bozorgnia (2008) ground motion prediction equation are presented in Figure 124.

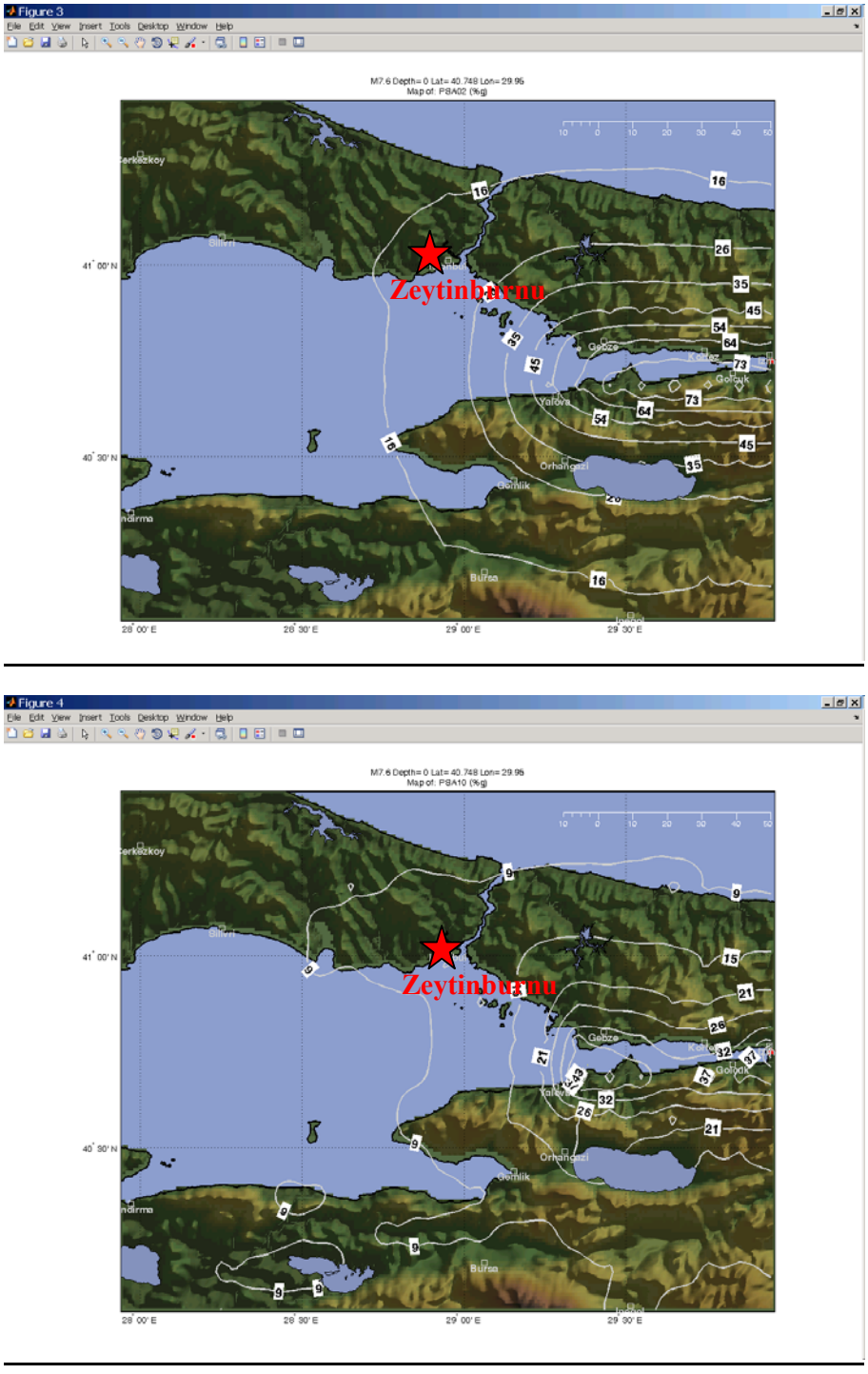

Figure 124. Spectral accelerations (%g) at T=0.2 sec (upper panel) and T=1.0 sec (lower panel) obtained from the Campbell and Bozorgnia (2008) ground motion prediction equation

The building damage distributions at each damage state obtained using the Coefficient Method are presented in Figure 125.

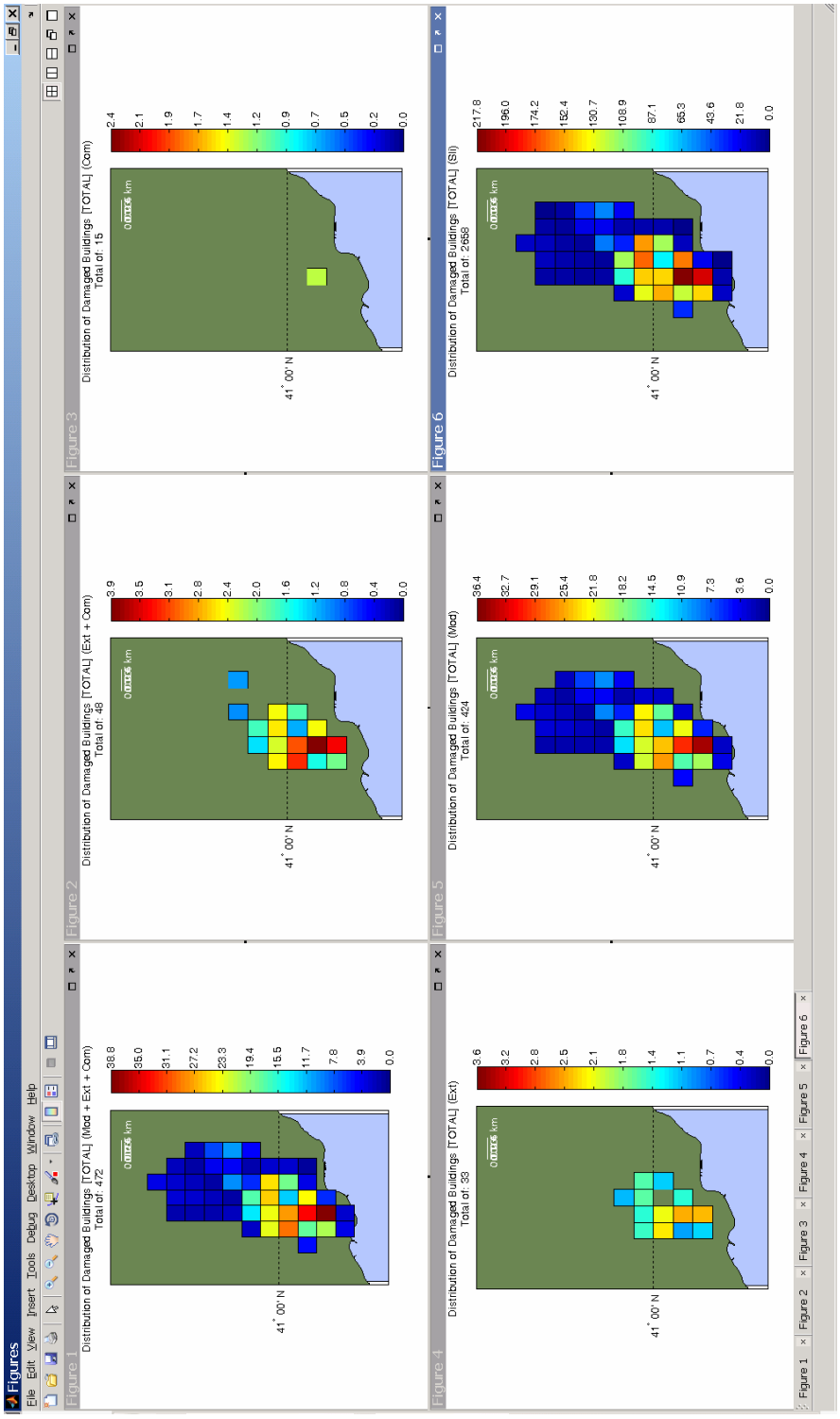

Figure 125. The distribution of damaged buildings in Zeytinburnu district resulting from the 1999 Kocaeli earthquake scenario – Level 2 Analysis.

The distribution of casualties obtained using the HAZUS-MH model are presented in Figure 126.

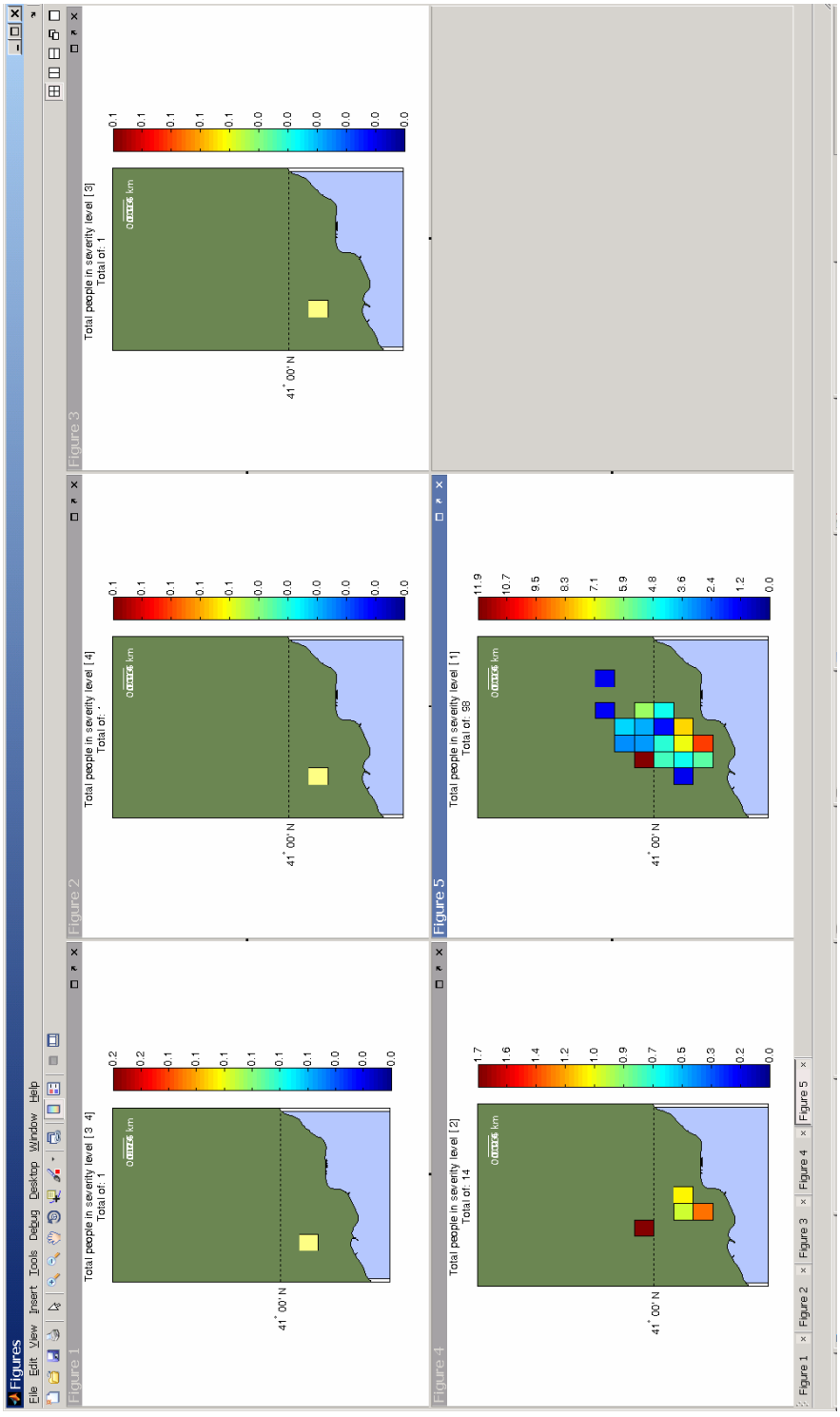

Figure 126. The distribution of casualties in Zeytinburnu district resulting from the 1999 Kocaeli earthquake scenario – Level 2 Analysis.

Credible Worst Case Scenario Earthquake for Istanbul:

An Mw=7.5 (similar to 1999 Kocaeli earthquake in magnitude and in total rupture length) on the Main Marmara Fault is selected as the "Credible Worst Case" Scenario event, for the city of Istanbul. The ruptured segments, the resulting intensity distribution obtained from the regional intensity prediction equation and the location of Zeytinburnu district are presented in Figure 127.

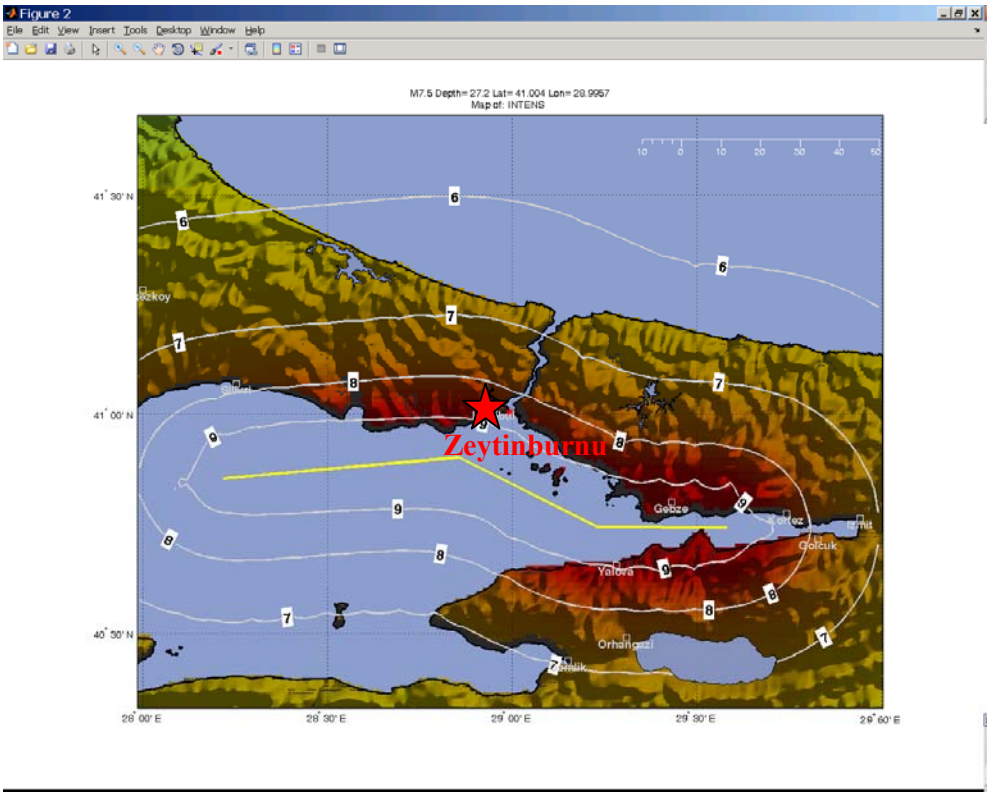

Figure 127. The intensity distribution of the worst case scenario earthquake and the location of the Zeytinburnu district.

Level 0 Loss Assessment

Level 0 loss assessment is essentially aimed for studies in larger regions. A closer view to the Zeytinburnu district reveals about 90 fatalities using the Samerdjieva and Badal (2002) approach. The geographic distribution of the casualties is presented in Figure 128.

Level 1 Loss Assessment

An analysis is conducted for the Zeytinburnu district using the building inventory of Istanbul based on 0.005°*0.005° geocells as elaborated in 0 The distribution of the damaged buildings in various damage states obtained from Level 1 analysis is presented in Figure 129. The

geographic distribution of the casualties is presented in Figure 130 (Coburn and Spence, 1992 model).

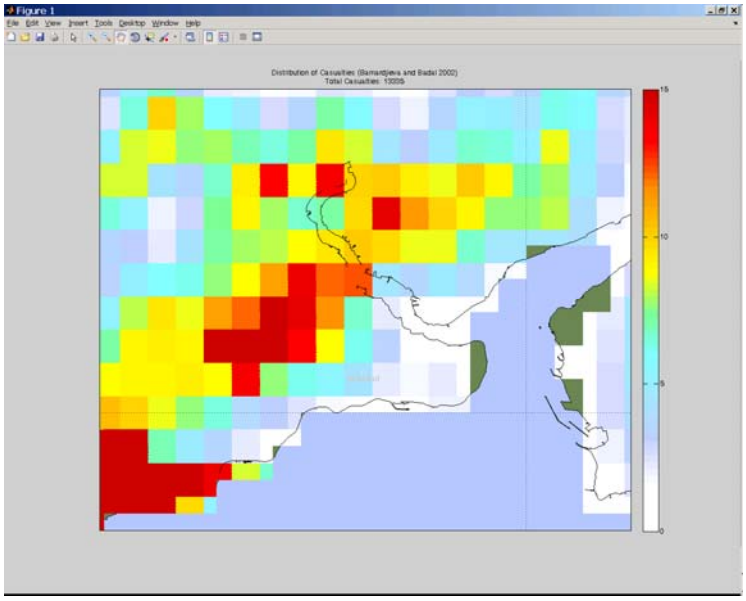

Figure 128. The distrbution of casualties in the vicinity of Zeytinburnu obtained from Level 0 analysis.

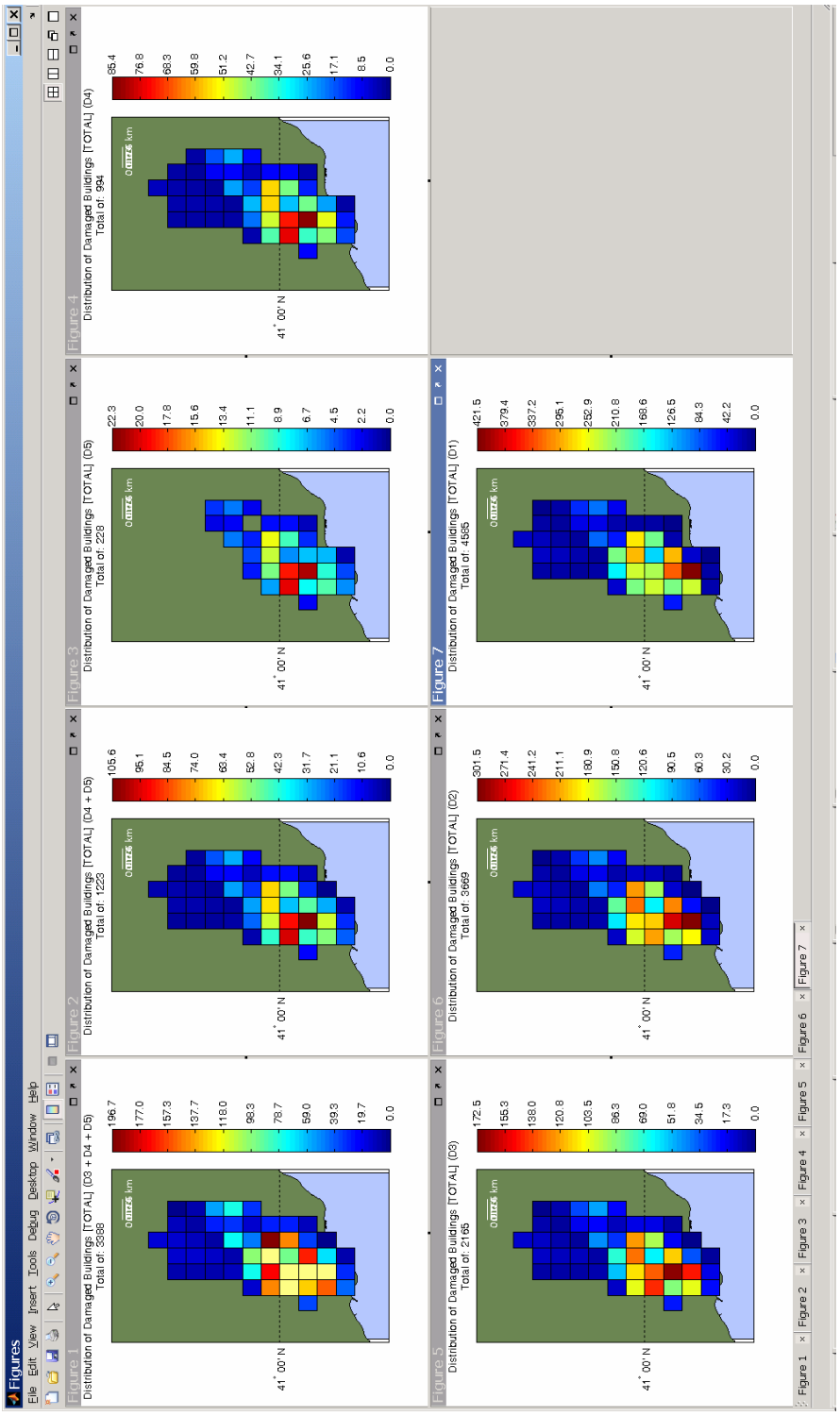

Figure 129. The distribution of damaged buildings in Zeytinburnu district resulting from the worst case scenario earthquake – Level 1 Analysis.

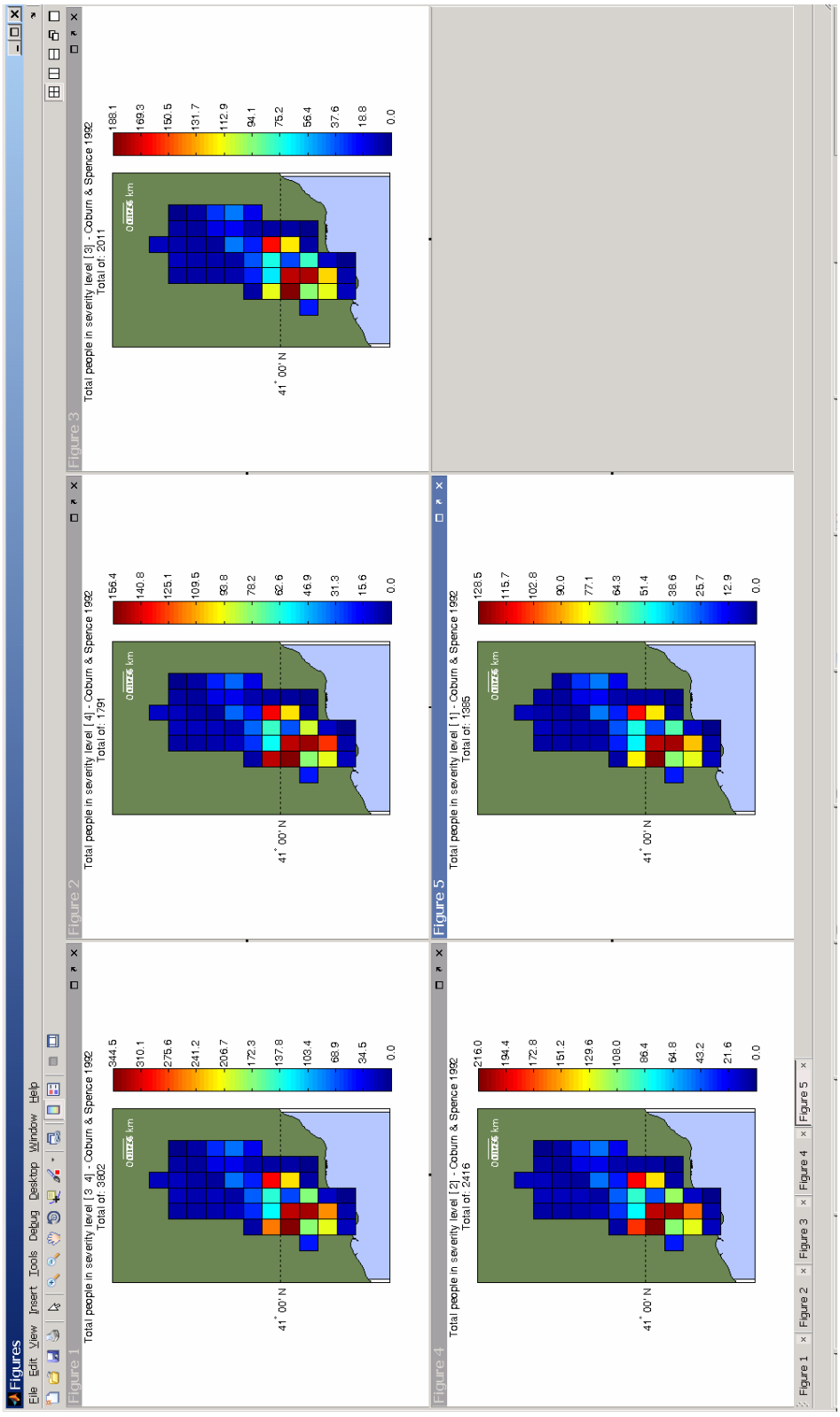

Figure 130. The distribution of casualties in Zeytinburnu district resulting from the worst case scenario earthquake – Level 1 Analysis (Coburn and Spence, 1992 model).

Level 2 Loss Assessment

Spectral accelerations at T=0.2 sec and T=1.0 sec obtained from the Campbell and Bozorgnia (2008) ground motion prediction equation are presented in Figure 131.

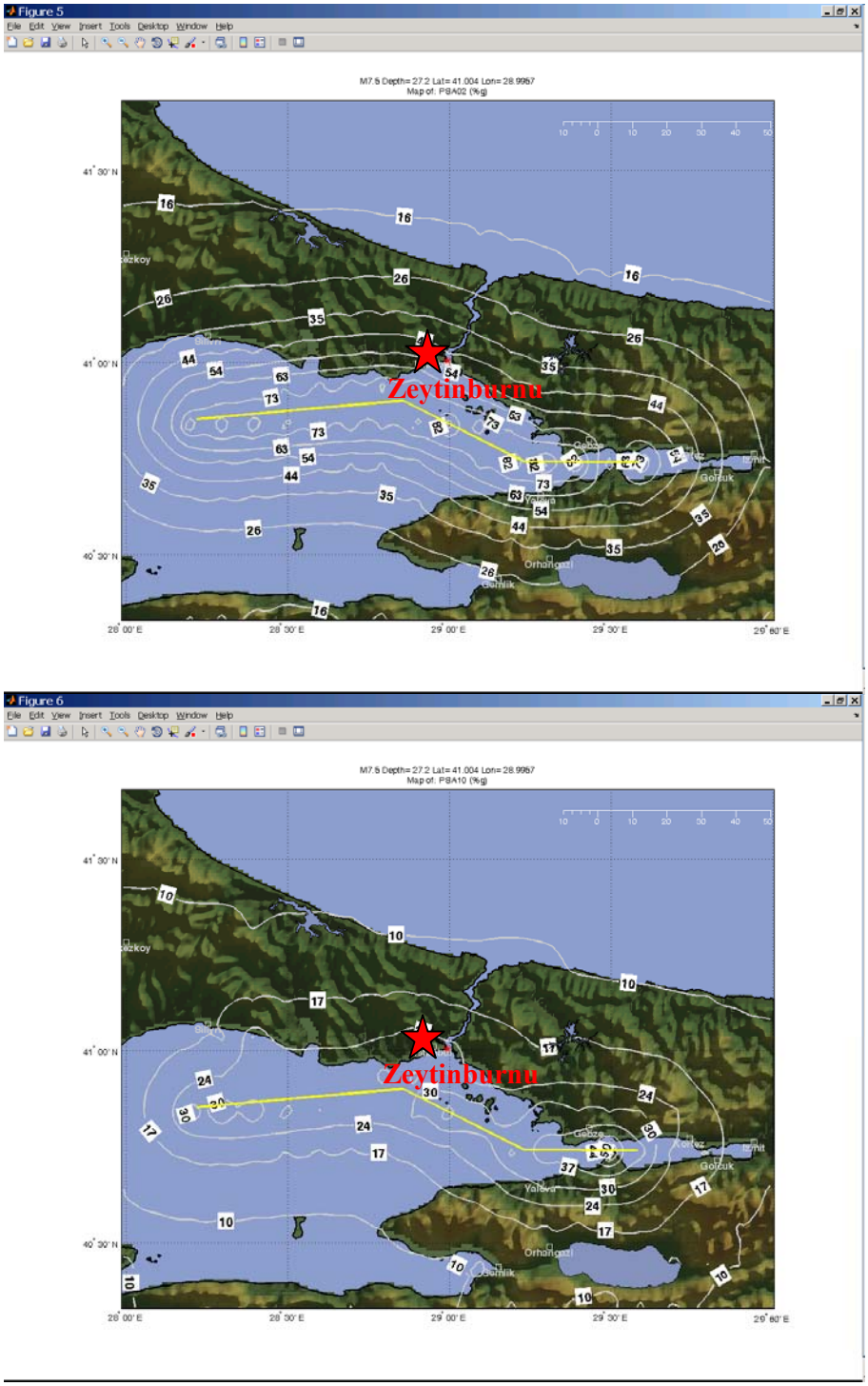

Figure 131. Spectral accelerations (%g) at T=0.2 sec (upper panel) and T=1.0 sec (lower panel) obtained from the Campbell and Bozorgnia (2008) ground motion prediction equation

The building damage distributions at each damage state obtained using the Coefficient Method are presented in Figure 132.

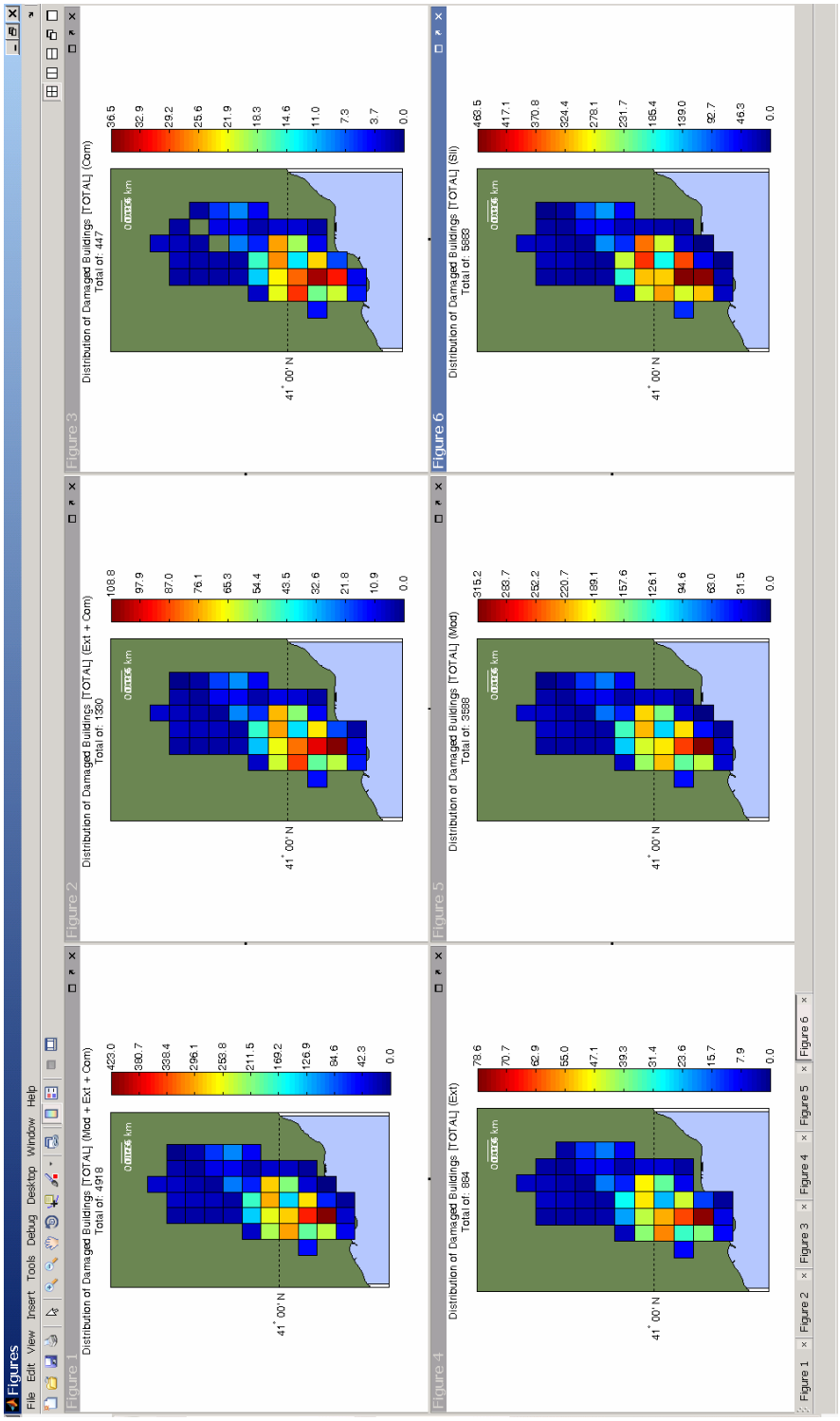

Figure 132. The distribution of damaged buildings in Zeytinburnu district resulting from the from the worst case scenario earthquake – Level 2 Analysis.

The distribution of casualties obtained using the HAZUS-MH model are presented in Figure 133.

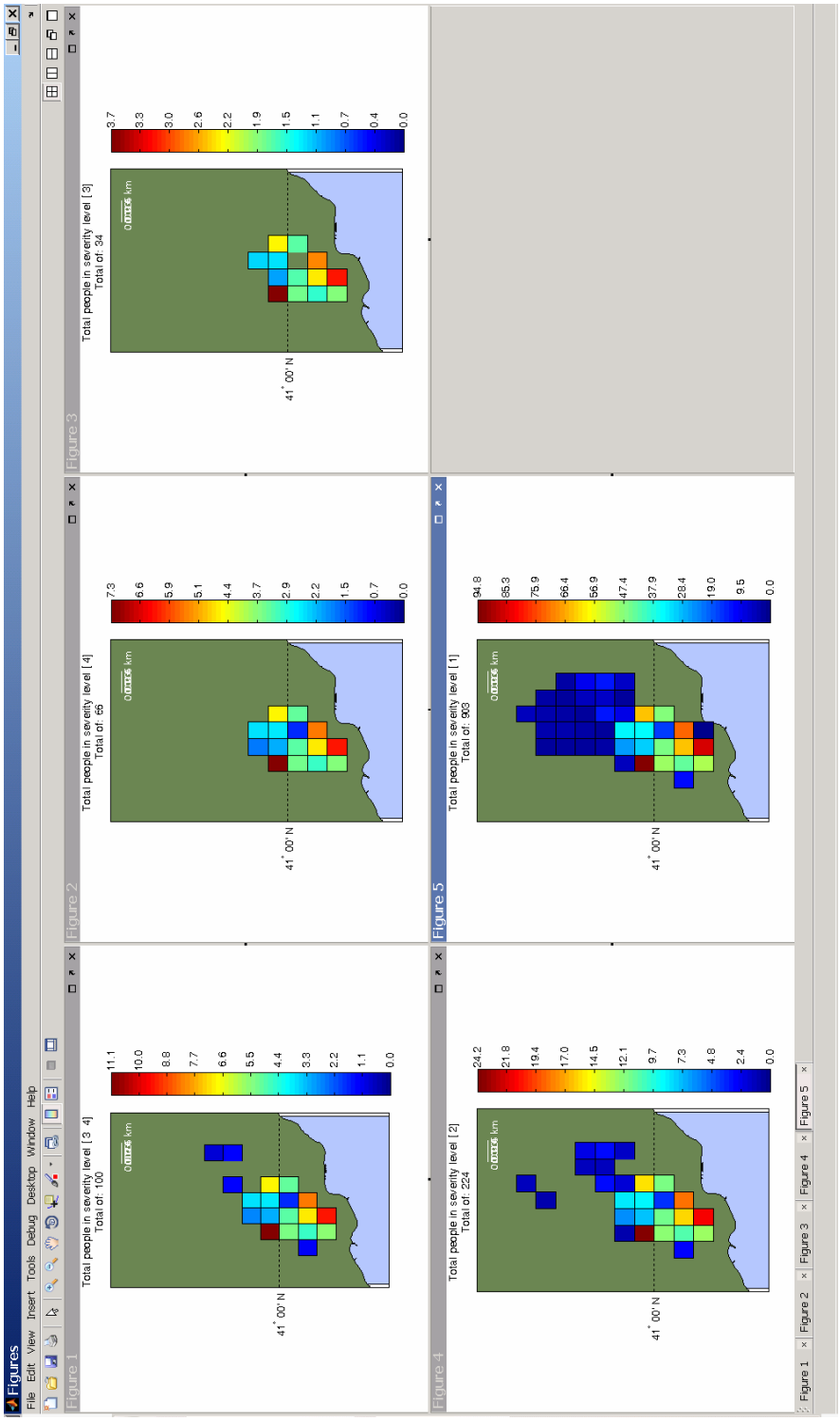

Figure 133. The distribution of casualties in Zeytinburnu district resulting from the from the worst case scenario earthquake – Level 2 Analysis.

REFERENCES

Allen, T. I., and Wald, D. J. (2007). Topographic Slope as a Proxy for Seismic Site Conditions (Vs30) and Amplification around the Globe, U.S. Geological Survey, Open File Report 2007-1357.

ASCE/SEI 41-06 (2007), "Seismic Rehabilitation of Existing Buildings", American Association of Civil Engineers, ASCE Standard No. ASCE/SEI 41-06.

ATC 13 (1987). Earthquake damage evaluation data for California. Applied Technology Council, Redwood City, California.

ATC 25 (1991), Seismic Vulnerability and Impact of Disruption of Lifelines in the Conterminous United States . Redwood City, California, Applied Technology Council Report; 440 pp

ATC 40 (1996). Seismic evaluation and retrofit of concrete buildings. Applied Technology Council, Redwood City, California.

Boatwright, J., H. Bundock, J. Luetgert, L. Seekins, L. Gee and P. Lombard (2003). The dependence of PGA and PGV on distance and magnitude inferred from Northern California ShakeMap data. Bull. Seism. Soc. Am., 93, no. 5, 2043-2055.

Boore, D. M., W. B. Joyner, and T.E. Fumal (1997). Equations for Estimating Horizontal Response Spectra and Peak Accelerations from Western North American Earthquakes: A Summary of Recent Work, Seism. Res. Lett., 68, 128-153.

Boore, D. M., and Atkinson, G. M., 2008. Ground-motion prediction equations for the average horizontal component of PGA, PGV, and 5%-damped PSA at spectral periods between 0.01 s and 10.0 s, Earthquake Spectra 24, 99–138.

Borcherdt, R. D. (1994). Estimates of site-dependent response spectra for design (methodology and justification), Earthquake Spectra, 10, 617-654.

Bramerini F., Di Pasquale G., Orsini A., Pugliese A., Romeo R., Sabetta F., (1995). Rischio sismico del territorio italiano. Proposta per una metodologia e risultati preliminari. Rapporto tecnico del Servizio Sismico Nazionale SSN/RT/95/01, Roma (In Italian).

Campbell, K. W., and Bozorgnia, Y., 2008. Campbell-Bozorgnia NGA horizontal ground motion model for PGA, PGV, PGD and 5% damped linear elastic response spectra, Earthquake Spectra 24, 139–171.
Campbell, K.W. and Bozorgnia, Y. (2003). Updated near-source ground motion (attenuation) relations for the horizontal and vertical components of peak ground acceleration and acceleration response spectra. Bulletin of the Seismological Society of America 93, 314–331.

Campbell, K.W. and Bozorgnia, Y. (1994), "Emprical analysis of strong motion from the 1992 Landers, California earthquake", Bulletin of the Seismological Society of America 8483), 573-588.

Campbell, K.W. (1997). Empirical near-source attenuation relationships for horizontal and vertical components of peak ground acceleration, peak ground velocity, and pseudo-absolute acceleration response spectra. Seismological Research Letters 68, 154–179.

Cheu, D.H. (1995). Northridge Earthquake – January 17, 1994: The Hospital Response. Universal City,CA: FEMA. 17 January 1995:1-15. Northridge Earthquake: One Year Later.

Chiou, B., and Youngs, R. R., 2008. An NGA model for the average horizontal component of peak ground motion and response spectra, Earthquake Spectra 24, 173–215.

Christoskov, L., and E. Samardjieva (1984). An approach for estimation of the possible number of casualties during strong earthquakes, Bulg. Geophys. J. 4, 94–106.

Christoskov, L., Samardjieva, E., and Solakov, D., 1990, "Improvement of the approach in determining the possible human losses during strong earthquakes", Bulg. Geophys. J. XVI 4, 85–92.

Coburn A. and Spence R. (1992). Earthquake Protection. John Wiley & Sons Ltd., Chichester, England.

Coburn, A. and Spence R. (2002). Earthquake Protection (Second Edition), John Wiley and Sons Ltd., Chichester, England.

Crowley, H., Bommer, J.J., Pinho, R., Bird, J., (2004). "A probabilistic displacement-based vulnerability assessment procedure for earthquake loss estimation." *Bulletin of Earthquake Engineering,* vol. 2, pp.173-219.

Durkin M. E., and Thiel C. C. (1993). Towards a Comprehensive Regional Earthquake Casualty Modeling Process. Proc. of National Earthquake Conference. Vol I, Central U.S. Earthquake Consortium, pp. 557-566

Eidinger J, Avila E. (1999) "Guidelines for the seismic upgrade of water transmission facilities" Monograph no. 15, TCLEE/ASCE.

Erdik M. (1993). Seismicity and Strong Ground Motion, in Damage Report on 1992 Erzincan Earthquake, Turkey, pp.2-1,7, Architectural Institute of Japan, Japan Society of Civil Engineers and Boğaziçi University, Tokyo, Japan.

Erdik, M. and Aydınoglu, N., (2002). "Earthquake performance and vulnerability of buildings in Turkey." The World Bank Group Disaster Management Facility Report.

Erdik M., E. Durukal, B. Siyahi, Y. Fahjan, K. Şeşetyan, M. B. Demircioğlu, H. Akman (2003). "Earthquake Risk Mitigation in Istanbul", Chapter 7, in Earthquake Science and Seismic Risk Reduction, Ed. by F. Mulargia and R.J. Geller, Kluwer.

Eurocode 8 (2003), Design of Structures for Earthquake Resistance, Draft No. 6, European Committee for Standardization, Brussels.

Fajfar P. (2000). A non linear analysis method for performance-based seismic design, Earthquake Spectra, 16, 3, pp. 573-591.

FEMA 222A (1994). NEHRP recommended provisions for the development of seismic regulations for new buildings, 1994 edition, Part 1 – provisions, Federal Emergency Management Agency, 290.

FEMA, (1999). "HAZUS99 user and technical manuals". Federal Emergency Management Agency Report: HAZUS 1999, Washington D.C.,USA.

FEMA (2003). "HAZUS-MH Technical Manual", Federal Emergency Management Agency, Washington, DC, U.S.A

FEMA 440, (2005). "Improvement of nonlinear static seismic analysis procedures". Federal Emergency Management Agency (FEMA) Report no.440, Applied Technology Council, Washington D.C., USA.

FEMA 356 (2000), NEHRP Guidelines for the seismic rehabilitation of buildings. Federal Emergency Management Agency. Washington DC.

Giovinazzi S. and Lagomarsino S. (2004). A Macroseismic Model for the vulnerability assessment of buildings. 13th World Conference on Earthquake Engineering. Vancouver, Canada.

Giovinazzi S., (2005). "Vulnerability assessment and the damage scenario in seismic risk analysis". PhD Thesis, Department of Civil Engineering of the Technical University Carolo-Wilhelmina at Braunschweig and Department of Civil Engineering, University of Florence, Italy.

Giovinazzi S. and Lagomarsino S. 2005. Fuzzy-Random Approach for a Seismic Vulnerability Model. Proc. of ICOSSAR 2005, Rome, Italy.

Grünthal, G. (editor) (1998). European macroseismic scale 1998. Cahiers du Centre Européen de Géodynamique et de Séismologie. Conseil de l'Europe. Luxembourg, 1998.

Harmandar, E. (2009). Spatial Variation of Strong Ground Motion, P.h. D. Dissertation, Bogazici University, Istanbul.

IBC (2006), "International Building Code", International Code Council, USA.

Isaaks, E. H. and R. M. Srivastava. 1989. An Introduction to Applied Geostatistics. Oxford Univ. Press, New York, Oxford.

KOERI (Department of Earthquake Engineering), 2002, "Earthquake Risk Assessment for Istanbul Metropolitan Area", Report prepared for American Red Cross and Turkish Red Crescent, Bogazici Univeristy, Istanbul, Turkey.

Kircher CA, Nassar AA, Kustu O, Holmes WT (1997) Development of building damage functions for earthquake loss estimation. Earthquake Spectra, 13(4):663–682.

Krige, D. G., 1966, Two-Dimensional Weighted Moving Average Trend Surfaces for Ore Valuation, Journal of the South African Institute of Mining and Metallurgy, Vol. 66, pp. 13-38.

Lagomarsino, S., and Giovinazzi, S., (2006). " Macroseismic and mechanical models for the vulnerability and damage assessment of current buildings." Bulletin of Earthquake Engineering, Vol.4, pp.415-443.

MATLAB® (R2008b), the MathWorks, Inc.

Molina, S. and Lindholm, C.D. (2006). A Capacity Spectrum Method based Tool developed to properly include the uncertainties in the seismic risk assessment, under a logic tree scheme, ECI. Geohazards – Technical, Economical and Social Risk Evaluation. 18–21 June 2006, Lillehammer, Norway.

Molina, S. , lang D. H.and Lindholm, C.D. (2008), ""SELENA v4.0 User and Technical Manual v4.0",NORSAR, Kjeller, Norway, October.

Murakami H. O., (1992). "A simulation model to estimate human loss for occupants of collapsed buildings in an earthquake," Proceedings of the 10. WCEE, Madrid, Spain, pp.5969 -5974.

Oliveira C.S. and Mendes Victor L.A. (1984), "Prediction of seismic impact in a metropolitan area based on hazard analysis and microzonation: Methodology for the town of Lisbon", Proc. Of the 18th World Conference on earthquake Engineering, El Cerito, California, Vol. VII, pp. 639- 646.

O'Rourke M, Ayala G. (1993) "Pipeline damage due to wave propagation", Journal of Geotechnical Engineering, Vol: 119(9):1490–8.

O'Rourke M, Deyoe E. (2004) "Seismic damage to segmented buried pipe" Earthquake Spectra, Vol: 20:1167–83.

Özmen, B., 2000, 17 Ağustos 1999 İzmit Körfezi Depremi'nin Hasar Durumu (Rakamsal Verilerle), Türkiye Deprem Vakfı (TDV), 132 pages, in Turkish.

RGELFE (Research Group for Estimating Losses from Fututre Earthquakes), 19952, "Estimating Losses form Earthquakes in China in the Forthcoming 50 years," State Seismological Bureau, Seismological Press, Beijing.

RISK-UE 2004 The European Risk-Ue Project: An Advanced Approach to Earthquake Risk Scenarios.(2001-2004) www.risk-ue.net

Sadigh, K., C.-Y. Chang, J.A. Egan, F. Makdisi, and R.R. Youngs 1997. "Attenuation Relationships for Shallow Crustal Earthquakes Based on California Strong Motion Data", Seismological Research Letters, Vol. 68, No. 1, pp. 180-189.

Samardjieva, E. and J. Badal, 2002. Estimation of the expected number of casualties caused by strong earthquakes. Bulletin of the Seismological Society of America, 92 (6), pp. 2310-2322, Aug 2002.

Sesetyan K., Durukal E., Demircioglu, M.B. and Erdik M., 2005, “A Revised Intensity Attenuation Relationships for Turkey”, EGU

Shiono, K., Krimgold, F. and Ohta, Y., (1991). "A Method for the Estimation of Earthquake Fatalities and its Applicability to the Global Macro-Zonation of Human Casualty Risk," Proc. Fourth International Conference on Seismic Zonation, Stanford, CA, Vol. III, pp. 277 - 284.

Strasser F.O., Bommer, J.J., Sesetyan, K., Erdik, M., Cagnan Z., Irizarry J., Goula X., Lucantoni A., Sabetta F., Bal I.E., Crowly H., Lindholm C., 2007, “A Comparative Study of European Earthquake Loss Estimation Tools for A Scenario in Istanbul”, Journal of Earthquake Enginnering.

TUIK (Turkiye Istatistik Kurumu, Turkish Statistical Institute), http://www.tuik.gov.tr/Start.do

Vacareanu R., Lungu D., Arion C., Aldea A. (2004). WP7 Report: Seismic Risk Scenarios. Risk-UE Project. An advanced approach to earthquake risk scenarios with applications http://www.risk-ue.net.

Vidic T., Fjfar P., Fischinger M., 1994, “Consistent inelastic design spectra: strength and displacement”, earthquake Engineering and Structural Dynamics, 23
pp.507-521.

Wald, D. J., V. Quitoriano, T. H. Heaton, H. Kanamori, C. W. Scrivner, and C. B. Worden, TriNet ShakeMaps: Rapid Generation of Instrumental Ground Motion and Intensity Maps for Earthquakes in Southern California, Earthquake Spectra, 15, 537-556, 1999a.

Wald, D. J., V. Quitoriano, T. H. Heaton, H. Kanamori (1999b). Relationship between Peak Ground Acceleration, Peak Ground Velocity, and Modified Mercalli Intensity for Earthquakes in California, Earthquake Spectra, Vol. 15, No. 3, 557-564

Wald, D, L. Wald, B. Worden, and J. Goltz (2003). ShakeMap — A Tool for Earthquake Response, U.S. Geological Survey Fact Sheet 087-03.

Wald, David J.; Worden, Bruce C.; Quitoriano, Vincent; Pankow, Kris L., 2005 ShakeMap manual: technical manual, user's guide, and software guide

Wald, D. J., V. Quitoriano, and J. W. Dewey (2006b). USGS "Did you feel it?" community internet intensity maps: macroseismic data collection via the internet, First European Conference on Earthquake Engineering and Seismology. Geneva, Switzerland.

Wald, D. J., and T. I. Allen (2007), “Topographic slope as a proxy for seismic site conditions and amplification”, Bull. Seism. Soc. Am.*97,* 1379-1395.

Wells, D. L., and K. J. Coppersmith, New empirical relationships among magnitude, rupture length, rutpure width, rupture area, and surface displacement, Bull. Seismol. Soc. Am., 84 , 974, 1994.

Yang, T., 2005, ATC-55 Project, http://peer.berkeley.edu/~yang/ATC55_website/

APPENDIX A: THE APPROXIMATED BUILDING DISTRIBUTION FOR EUROPE BASED ON CORINE LAND COVER DATA

The Corine Land Cover (CLC) is a geo-dataset showing the distribution of land use within European Countries using 44 classes of the 3-level Corine nomenclature (Table 59)

Table 59. Corine Land Cover Classes

Grid Code	Type	Sub Type	Grid Code	Type	Sub Type
1	Artificial surfaces	Continuous urban fabric	23	Forest and semi natural areas	Broad-leaved forest
2	Artificial surfaces	Discontinuous urban fabric	24	Forest and semi natural areas	Coniferous forest
3	Artificial surfaces	Industrial or commercial units	25	Forest and semi natural areas	Mixed forest
4	Artificial surfaces	Road and rail networks and associated land	26	Forest and semi natural areas	Natural grasslands
5	Artificial surfaces	Port areas	27	Forest and semi natural areas	Moors and heathland
6	Artificial surfaces	Airports	28	Forest and semi natural areas	Sclerophyllous vegetation
7	Artificial surfaces	Mineral extraction sites	29	Forest and semi natural areas	Transitional woodland-shrub
8	Artificial surfaces	Dump sites	30	Forest and semi natural areas	Beaches, dunes, sands
9	Artificial surfaces	Construction sites	31	Forest and semi natural areas	Bare rocks
10	Artificial surfaces	Green urban areas	32	Forest and semi natural areas	Sparsely vegetated areas
11	Artificial surfaces	Sport and leisure facilities	33	Forest and semi natural areas	Burnt areas
12	Agricultural areas	Non-irrigated arable land	34	Forest and semi natural areas	Glaciers and perpetual snow
13	Agricultural areas	Permanently irrigated land	35	Wetlands	Inland marshes
14	Agricultural areas	Rice fields	36	Wetlands	Peat bogs
15	Agricultural areas	Vineyards	37	Wetlands	Salt marshes
16	Agricultural areas	Fruit trees and berry plantations	38	Wetlands	Salines
17	Agricultural areas	Olive groves	39	Wetlands	Intertidal flats
18	Agricultural areas	Pastures	40	Water bodies	Water courses
19	Agricultural areas	Annual crops associated with permanent crops	41	Water bodies	Water bodies
20	Agricultural areas	Complex cultivation patterns	42	Water bodies	Coastal lagoons
21	Agricultural areas	Land principally occupied by agriculture, with significant areas of natural vegetation	43	Water bodies	Estuaries
22	Agricultural areas	Agro-forestry areas	44	Water bodies	Sea and ocean

The distribution of CLC classes by country and the percentage of total country population residing in each CLC class are presented in Figure 134.

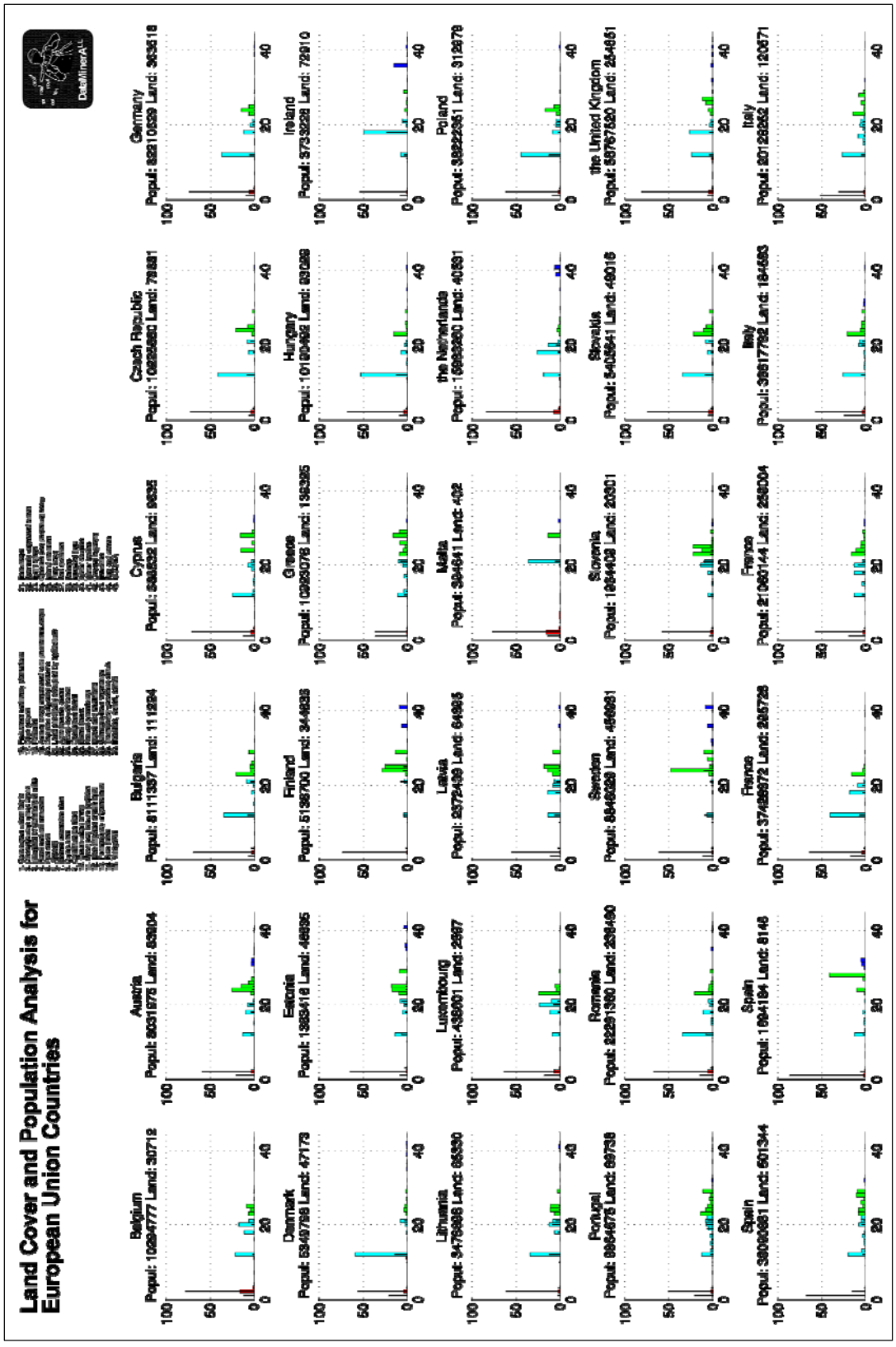

Figure 134. The Relationship between Corine Land Cover and Corine Population by Countries

As it can be observed from Figure 134, the distribution of population in different classes is not the same for all the countries. Although a large percentage of the population reside in and/or Discontinuous Urban Fabric Areas (Classes 1 or 2) in almost all countries, the concentration of population in all classes may vary. As such, the following principles have been adopted for data processing in each country:

1. Corine Land Cover Classes with population percentages larger than 2% should be considered in the analysis.
2. The population percentage of thus omitted CLC classes should be less then 10 % in total.
3. If the total population percentage of the omitted CLC classes was larger than 10% additional classes were also considered, such that at least 90% of the country population were included in the analysis.

Table 60 shows the CLC classes in Italy selected by the above procedure.

Table 60. CLC classes selected for analysis for Italy

CLC Grid Code	Cover Type	Population Percentage Living
1	Continuous urban fabric	34%
2	Discontinuous urban fabric	48%
12	Non-irrigated arable land	5%
20	Complex cultivation patterns	4%

Following the determination governing land cover classes for each country, the number of buildings per unit area in each class has been obtained by:

1. Selecting suitable sample areas from Google Earth for each CLC class in all countries
2. Counting the actual number of buldings in each sample area
3. Obtaining the total number of buildings in each country by spreading the sample area building counts to the country
4. Verifying and adjusting the number of buildings thus obtained by computing the population per building for each CLC class, and also checking with the actual number of buildings in a country if such an information has been obtained from the corresponding country's statistical office.

Table 61 shows the sample areas selected for the four land cover classes in Belgium. The total number of buildings obatined for all Corine countries are presented in Table 62 through Table 64.

Table 61. Sample areas for Belgium

Country Name	Grid Code	Sampling Areas
Belgium	1	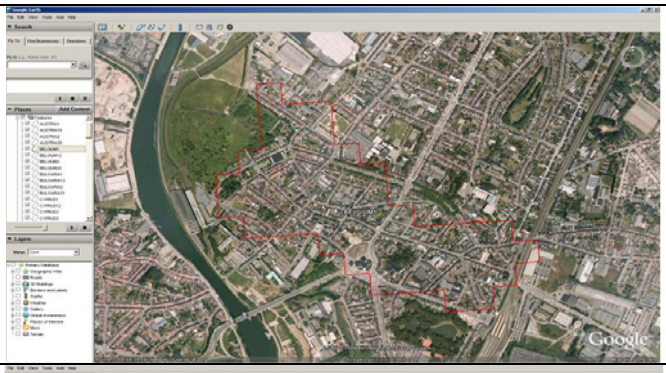
Belgium	2	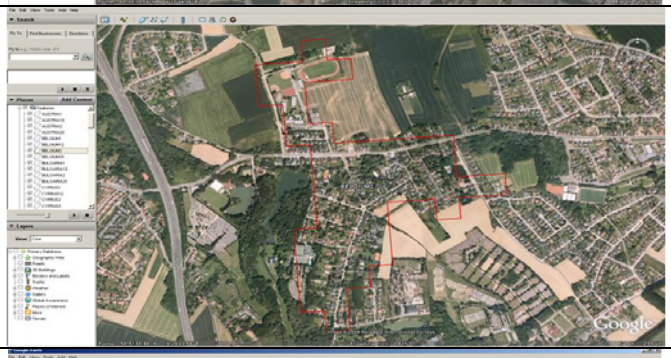
Belgium	12	
Belgium	20	

Table 62. Building database approximation results for Corine countries

COUNTRY	CLC CLASS	Sample Area(m^2)	Sum Sample Area(m^2)	Number of Buildings in Sample Area	Total Number of Buildings	Population	Population/ Number of Buildings	Information received from statistical offices		Country Population	Country Pop/Number of Buildings (Computed)	Country Pop/Number of Buildings (Sent by Office)
Austria	1	1.350.000	7,2070,000	750	40,039	1,657,732	41.40					
Austria	2	520.000	3,091,510,000	300	1,783,563	4,787,277	2.68					
Austria	18	280.000	8,242,630,000	5	147,190	324,402	2.20					
Austria	20	780.000	6,311,230,000	13	105,187	459,121	4.36	Residential building(2001)	**1,764,455**			
					2,075,979			Total (2001)	**2,046,712**	**8,031,975**	3.869	4.552
Belgium	1	570.000	48,440,000	980	83,283	1,257,878	15.10					
Belgium	2	480.000	5,110,620,000	275	2,927,959	8,063,976	2.75					
Belgium	12	1.060.000	6,724,230,000	12	76,123	210,981	2.77					
Belgium	20	1.390.000	5,408,990,000	20	77,827	324,010	4.16					
					3,011,242				**3,175,773**	**10,294,777**	3.419	3.242
Bulgaria	1	340.000	9,960,000	425	12,450	578,877	46.50					
Bulgaria	2	1.140.000	4,095,310,000	500	1,796,189	5,675,914	3.16					
Bulgaria	12	3.170.000	39,080,460,000	20	246,564	616,310	2.50					
Bulgaria	21	1.590.000	9,922,340,000	8	49,924	407,690	8.17					
					2,105,127			Residential building(2007)	**2,131,232**	**8,111,337**	3.853	3.806
Cyprus	1	579.446	5,670,000	800	7,828	91,094	11.64					
Cyprus	2	270.000	431,190,000	60	95,820	493,032	5.15					
Cyprus	3	730.000	114,730,000	50	7,858	21,414	2.73					
Cyprus	12	720.000	2,428,670,000	4	13,493	26,961	2.00					
					124,999					**688,832**	5.511	
Czech Republic	1	390.000	14,710,000	364	13,729	647,975	47.20					
Czech Republic	2	280.000	3,623,500,000	175	2,264,688	7,517,032	3.32					
Czech Republic	12	1.610.000	32,622,770,000	15	303,939	890,291	2.93					
Czech Republic	21	260.000	6,743,530,000	3	77,810	478,488	6.15					
					2,660,166			Total (2008)	**2,517,742**	**10,225,660**	3.844	4.061
Denmark	1	1.030.000	61,790,000	520	31,195	1,121,279	35.94					
Denmark	2	190.000	191,3140,000	105	1,057,262	3,011,847	2.85					
Denmark	12	640.000	27,929,440,000	8	349,118	770,999	2.21					
					1,437,575					**5,349,798**	3.721	
Estonia	1	440.000	4,130,000	400	3,755	115,019	30.63					
Estonia	2	1.220.000	507,240,000	650	270,251	886,564	3.28					
Estonia	12	1.700.000	6,636,090,000	8	31,229	85,272	2.73					
Estonia	18	1.720.000	2,576,180,000	5	7,489	32,379	4.32					
Estonia	20	480.000	1,792,430,000	5	18,671	42,557	2.28					
Estonia	21	500.000	3.740.800.000	5	37,408	83,122	2.22					
					368,802					**1,363,416**	3.697	
Finland	2	1,155,000	3,530,220,000	400	1,222,587	3,825,881	3.13					
Finland	12	2,090,000	15,975,320,000	10	76,437	259,257	3.39					
Finland	21	1,100,000	13,072,220,000	8	95,071	394,275	4.15					
Finland	24	900,000	99,340,930,000	1	110,379	266,115	2.41					
					1,504,473			Total (2007)	**1,406,000**	**5,138,700**	3.416	3.655
France	1	800,000	468,110,000	750	438,853	10,563,753	24.07					
France	2	700,000	19,795,940,000	400	11,311,966	36,215,964	3.20					
France	12	4,530,000	153,466,810,000	20	677,558	3,452,291	5.10					
France	20	720,000	58,831,900,000	10	817,110	3,000,747	3.67					
					13,245,486			Total (1999)	**14,622,254**	**58,489,017**	4.416	4.000

Table 63. Building database approximation results for Corine countries (cont.)

COUNTRY	CLC CLASS	Sample Area(m^2)	Sum Sample Area(m^2)	Number of Buildings in Sample Area	Total Number of Buildings	Population	Population/ Number of Buildings	Information received from statistical offices		Country Population	Country Pop/Number of Buildings (Computed)	Country Pop/Number of Buildings (Sent by Office)
Greece	1	1,770,000	166,660,000	2510	236,337	4,023,905	17.03					
Greece	2	550,000	1,634,750,000	416	1,236,465	4,033,105	3.26					
Greece	12	880,000	15,349,420,000	11	191,868	437,297	2.28					
Greece	20	2,360,000	7,690,830,000	90	293,294	597,919	2.04					
Greece	21	2,110,000	14,244,830,000	27	182,280	881,342	4.84					
					2,140,244			Total (2001)	**2,942,305**	**10,923,076**	5.104	3.712
Hungary	1	570,000	31,780,000	350	19,514	949,442	48.65					
Hungary	2	1,010,000	4,140,280,000	500	2,049,644	6,977,778	3.40					
Hungary	12	830,000	49,484,610,000	8	476,960	1,298,411	2.72					
					2,546,118					**10,190,492**	4.002	
Ireland	1	1,570,000	50,060,000	980	31,248	310,549	9.94					
Ireland	2	720,000	862,200,000	350	419,125	2,023,298	4.83					
Ireland	12	330,000	5430,050,000	4	65,819	149,459	2.27					
Ireland	18	2,860,000	36,257,240,000	30	380,321	887,357	2.33					
					896,512					**3,733,226**	4.164	
Italy	1	1,110,000	1,462,690,000	980	1,291,384	19,450,156	15.06					
Italy	2	880,000	9,326,830,000	600	6,359,202	27,075,201	4.26					
Italy	12	1,050,000	79,888,700,000	15	1,141,267	2,735,906	2.40					
Italy	20	650,000	21,892,740,000	22	740,985	2,247,562	3.03					
					9,532,838			Total (2001)	**12,774,131**	**56,746,034**	5.953	4.442
Latvia	1	1,030,000	7,610,000	725	5,357	272,512	50.87					
Latvia	2	850,000	517,040,000	248	150,854	1,317,896	8.74					
Latvia	12	2,440,000	9,159,290,000	9	33,784	153,737	4.55					
Latvia	18	5,970,000	92,862,60,000	30	46,665	132,178	2.83					
Latvia	20	1000,000	5,523,070,000	8	44,185	185,538	4.20					
Latvia	21	500,000	4,373,970,000	5	43,740	113,009	2.58					
					324,584			Total (2007)	**347,919**	**2,372,439**	7.309	6.819
Lithuania	1	460,000	2,490,000	450	2,436	105,414	43.28					
Lithuania	2	310,000	1,477,730,000	75	357,515	2,145,164	6.00					
Lithuania	12	1,560,000	22,217,000,000	10	142,417	433,143	3.04					
Lithuania	20	340,000	8,190,000,000	5	120,441	297,947	2.47					
Lithuania	21	410,000	5,252,800,000	6	76,870	179,028	2.33					
					699,679					**3,478,898**	4.972	
Luxembourg	1	270,000	7,300,000	250	6,759	80,373	11.89					
Luxembourg	2	660,000	175,040,000	400	106,085	281,425	2.65					
Luxembourg	18	1,030,000	303,550,000	6	1,768	9,594	5.43					
Luxembourg	20	1,210,000	614,240,000	18	9,137	32,403	3.55					
					123,750			Total (2001)	**119,961**	**438,601**	3.544	3.656
Malta	1	300,000	3,510,000	610	7,137	57,773	8.09					
Malta	2	340,000	65,470,000	420	80,875	304,294	3.76					
					88,012					**394,641**	4.484	
Netherlands	2	1,290,000	2,980,350,000	995	2,298,797	13,501,062	5.87					
Netherlands	3	1,070,000	617,970,000	125	72,193	347,878	4.82					
Netherlands	18	6,540,000	10,714,770,000	80	131,068	428,324	3.27					
Netherlands	20	570,000	5,539,260,000	35	340,130	768,336	2.26					
					2,842,187					**15,983,260**	5.624	

Table 64. Building database approximation results for Corine countries (cont.)

COUNTRY	CLC CLASS	Sample Area(m^2)	Sum Sample Area(m^2)	Number of Buildings in Sample Area	Total Number of Buildings	Population	Population/ Number of Buildings	Information received from statistical offices		Country Population	Country Pop/Number of Buildings (Computed)	Country Pop/Number of Buildings (Sent by Office)
Poland	1	740,000	82,630,000	500	55,831	3,574,149	64.02					
Poland	2	520,000	7,794,210,000	180	2,697,996	23,803,050	8.82					
Poland	12	1,390,000	139,666,090,000	10	1,004,792	4,960,702	4.94					
Poland	20	680,000	17,405,240,000	20	511,919	1,716,659	3.35					
Poland	21	310,000	15,289,170,000	7	345,239	1,345,136	3.90					
					4,615,777			Total (2002)	**4,772,728**	**38,222,350**	8.281	8.008
Portugal	1	770,000	139,510,000	700	126,827	2,014,649	15.88					
Portugal	2	320,000	1,612,050,000	350	1,763,180	5,000,844	2.84					
Portugal	19	520,000	4,203,520,000	20	161,674	657,660	4.07					
Portugal	20	860,000	6,227,880,000	20	144,834	674,967	4.66					
Portugal	21	910,000	6,816,200,000	15	112,355	584,054	5.20					
					2,308,870			Non-Official	**2,982,313**	**9,864,675**	4.273	3.308
Romania	1	510,000	107,780,000	400	84,533	3,292,165	38.95					
Romania	2	550,000	12,876,730,000	210	4,916,570	14,925,739	3.04					
Romania	12	2,210,000	81,518,550,000	5	184,431	1,637,846	8.88					
					5,185,534			Non-Official	**4,834,063**	**22,291,360**	4.299	4.611
Slovakia	1	480,000	10,130,000	350	7,386	282,788	38.28					
Slovakia	2	1,030,000	2,256,940,000	450	986,042	4,022,801	4.08					
Slovakia	12	670,000	16,672,630,000	5	124,423	452,279	3.64					
Slovakia	21	1,050,000	3,927,010,000	13	48,620	242,887	5.00					
					1,166,471					**5,405,641**	4.634	
Slovenia	1	540,000	1,860,000	448	1,543	73,279	47.49					
Slovenia	2	390,000	416,910,000	313	334,597	1,134,904	3.39					
Slovenia	12	690,000	1,124,960,000	5	8,152	42,134	5.17					
Slovenia	18	240,000	1,162,970,000	2	9,691	45,700	4.72					
Slovenia	20	410,000	2,783,770,000	10	67,897	296,211	4.36					
Slovenia	21	270,000	1,824,070,000	6	40,535	196,767	4.85					
					462,415					**1,964,409**	4.248	
Spain	1	910,000	2,686,910,000	1550	4,576,605	27,951,166	6.11					
Spain	2	890,000	2,818,380,000	700	2,216,703	6,171,909	2.78					
Spain	12	7,140,000	100,024,340,000	50	700,451	1,229,472	1.76					
Spain	20	3,050,000	38,642,740,000	55	696,836	1,746,681	2.51					
					8,190,595			Total (2001)	**9,284,513**	**40,785,066**	4.979	4.393
Sweden	1	1,950,000	44,700,000	700	16,046	994,468	61.98					
Sweden	2	280,000	4,023,680,000	120	1,724,434	5,429,653	3.15					
Sweden	12	660,000	30,042,930,000	3	136,559	816,676	5.98					
Sweden	24	6,090,000	216,537,710,000	4	142,225	855,323	6.01					
					2,019,264					**8,846,029**	4.381	
Germany	1	1,500,000	231,320,000	1250	192,767	8,108,556	42.06					
Germany	2	2,000,000	22,212,330,000	1650	18,325,172	61,505,580	3.36					
Germany	12	3,020,000	136,770,110,000	20	905,762	4,771,425	5.27					
					19,423,701			Non-Official	**19,628,645**	**82,210,634**	4.232	4.188
United King.	1	3,290,000	286,640,000	1450	126,331	3,623,333	28.68					
United King.	2	750,000	12,200,910,000	750	12,200,910	47,407,330	3.89					
United King.	12	1,160,000	60,820,970,000	10	524,319	2,189,727	4.18					
					12,851,559					**58,767,522**	4.573	

The grid based distribution of the number of buidings and population thus obtained is aggregated to 30 and 150 sec arc grids to form the default data for Level 1 analysis. The PAGER project provides the percentages of different construction types in all countries of the world for both urban and rural settlements and residential and non-residential occupancy types, making use of a HAZUS99 type classification. Corresponding European Building Taxonomy classes have been identfied for the structral types of the PAGER classification system. Then these percentages have been used to convert the approximated grid based number of buildings to an inventory of different structural types in each county. The assocation of the building types between Pager, European (RISK-UE) and EMS98 classifications and the corresponding mean vulnerability (V) and ductility (Q) indices are given in Table 65. As an example of the database thus obtained, the distributions of brick masonry and RC type structures in Italy are presented in Figure 135 and Figure 136 respectively.

Table 65. European (RISK-UE), EMS98 and PAGER building taxonomy matrices

European (RISK-UE)		**EMS98**	**PAGER**	**V**	**Q**
Type	Description	Type	Type		
M1	RUBBLE STONE	M1			
M1_M	Mid-Rise		(M or M1+M2) + RE + RS	0.87	2.3
M1_w_M	Mid-Rise, wood slabs		RS1+RS2+RS3	0.85	2.3
M1_v_M	Mid-Rise, masonry vaults		RS4	0.95	2.3
M2	ADOBE (EARTH BRICKS)	M2	A or A1+A2+A3+A4+A5	0.84	2.3
M3	SIMPLE STONE	M3	DS	0.74	2.3
M3_w_M	Mid-Rise, wood slabs		DS1+DS2+DS3+DS4	0.72	2.3
M4	MASSIVE STONE	M4			
M4_M	Mid-Rise		MS	0.62	2.3
M5	UNREINFORCED MASONRY (OLD BRICKS)	M5			
M5_M	Mid-Rise		(UFB or UFB1+UFB2) +UCB	0.72	2.3
M5_w_M	Mid-Rise, wood slabs		UFB3	0.70	2.3
M6	UNREINFORCED MASONRY (R.C. FLOORS)	M6			
M6_M_PC	Mid-Rise, Pre-Code		UFB4	0.65	2.3
M7	REINFORCED OR CONFINED MASONRY	M7	RM or RM1+RM2	0.45	2.6
M7_L	Low-Rise		RM1L+RM2L	0.37	2.6
M7_M	Mid-Rise		RM1M+RM2M	0.45	2.6
M7_H	High-Rise		RM2H	0.53	2.6
RC1	CONCRETE MOMENT FRAME	RC1			

RC1_L	Low-Rise		C4L	0.62	2.3
RC1_M	Mid-Rise		C or C4 or C4M	0.64	2.3
RC1_H	High-Rise		C4H	0.68	2.3
RC1_DCM_II_L	Low-Rise, Medium Ductility, Zone II		C1L	0.36	2.5
RC1_DCM_II_M	Mid-Rise, Medium Ductility, Zone II		C1 or C1M	0.38	2.8
RC1_DCM_II_H	High-Rise, Medium Ductility, Zone II		C1H	0.40	2.8
RC2	CONCRETE SHEAR WALLS	RC2			
RC2_DCL_II_L	Low-Rise, Low Ductility, Zone II		C2L	0.40	2.3
RC2_DCL_II_M	Mid-Rise, Low Ductility, Zone II		C2 or C2M	0.38	2.3
RC2_DCL_II_H	High-Rise, Low Ductility, Zone II		C2H	0.38	2.3
RC3	DUAL SYSTEM				
RC3_L	Low-Rise		C3L	0.57	2.3
RC3_M	Mid-Rise		C3 or C3M	0.59	2.3
RC3_H	High-Rise		C3H	0.63	2.3
RC3_DCL_II_L	Low-Rise, Low Ductility, Zone II		C5L	0.45	2.3
RC3_DCL_II_M	Mid-Rise, Low Ductility, Zone II		(C5 or C5M) +PC1+(PC2 or PC2L+PC2M+PC2H) +TU	0.43	2.3
RC3_DCL_II_H	High-Rise, Low Ductility, Zone II		C5H	0.43	2.3
S	Steel Moment Frames		All steel structures	0.324	2.3
W	Wood Structures		All wood structures	0.447	2.3

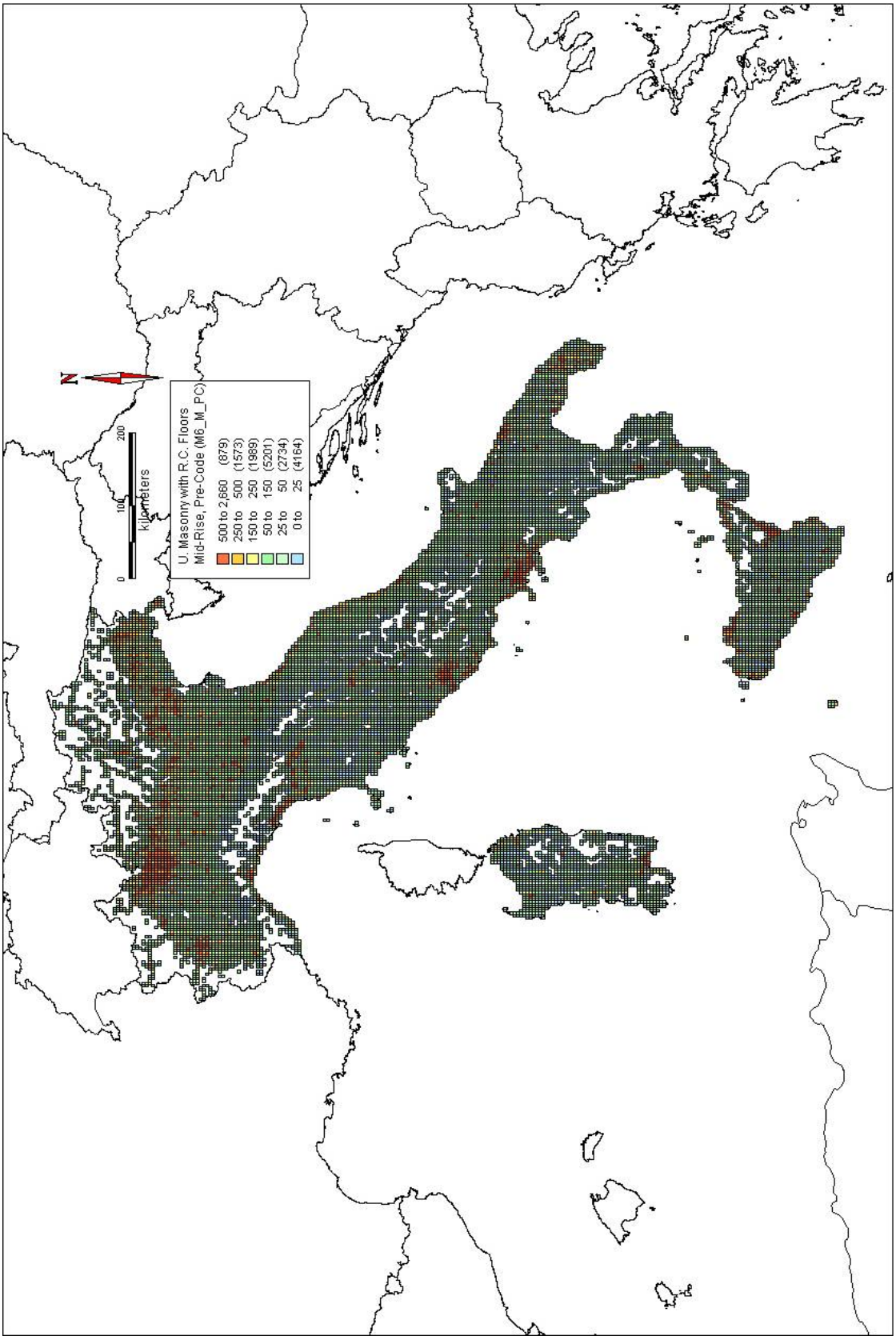

Figure 135. Distribution of masonry (M6) type structures in Italy

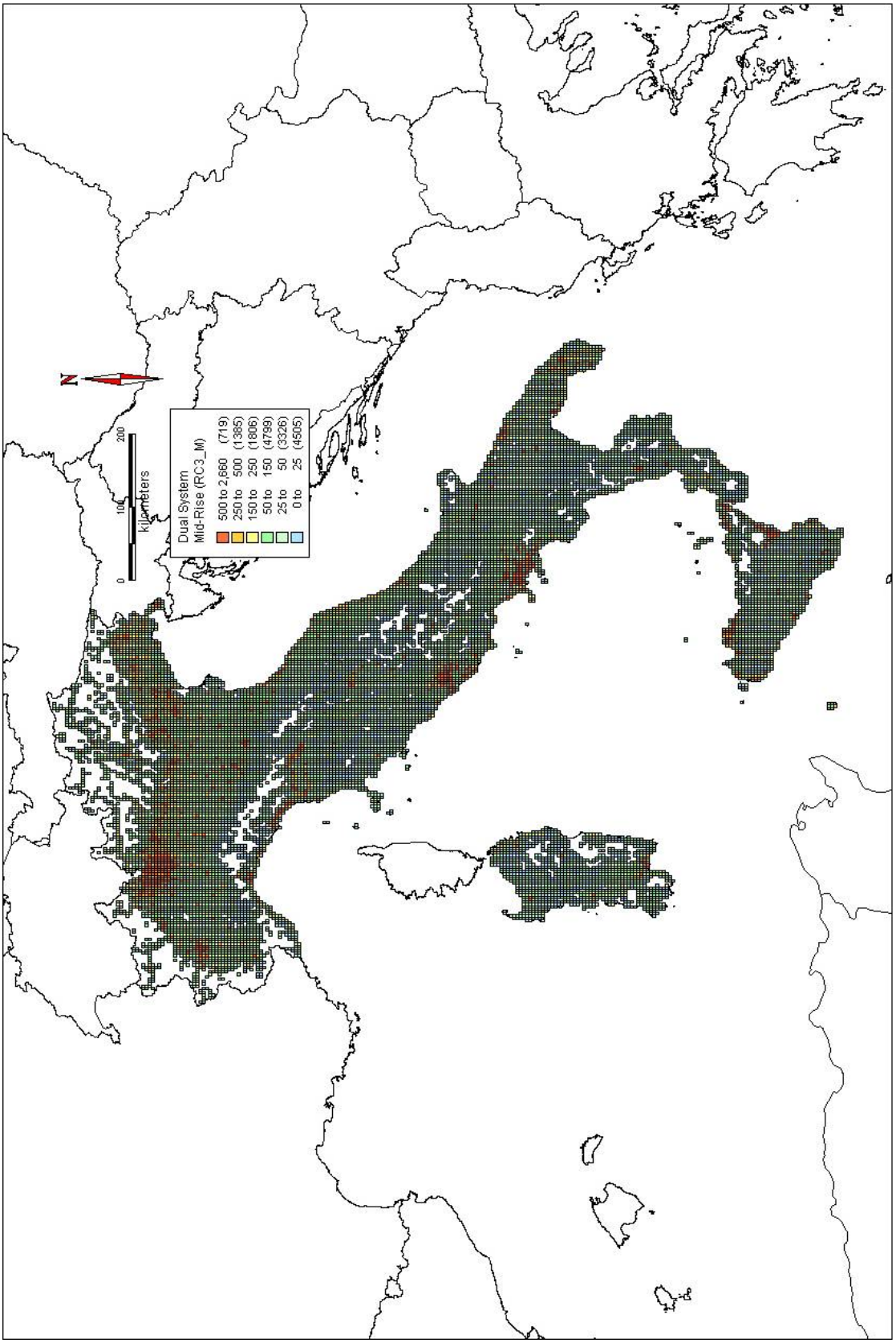

Figure 136. Distribution of RC structures (RC3) structures in Italy

APPENDIX B: CAPACITY AND FRAGILITY CURVE PARAMETERS FOR LEVEL 2 ANALYSIS

All values given in the following tables are in MKS units.

Table 66. Capacity Curve Parameters for Non-designed RC Buildings of European Building Taxonomy

Building Taxonomy		Capacity Curve Parameters				
Description	**Label**	**T**	**μ**	**a_y**	**d_y**	**d_u**
Concrete Moment Frame	**RC1_L**	0.54	3.0	0.2070	0.0150	0.0451
	RC1_M	0.85	3.0	0.1240	0.0224	0.0674
	RC1_H	1.30	3.0	0.0720	0.0304	0.0915
Concrete Shear Walls	**RC2_L**	0.54	3.0	0.2780	0.0201	0.0606
	RC2_M	0.85	3.0	0.1660	0.0300	0.0904
	RC2_H	1.30	3.0	0.0970	0.0407	0.1227
Concrete Frame with URM Infill Walls	**RC3_L**	0.54	3.0	0.2400	0.0174	0.0523
	RC3_M	0.85	3.0	0.1430	0.0259	0.0781
	RC3_H	1.30	3.0	0.0830	0.0352	0.1060

L: low-rise (1-3 stories)
M: mid-rise (4-7 stories)
H: high-rise (≥8 stories)

Table 67. Fragility Curve Parameters for Non-designed RC Buildings of European Building Taxonomy

Building Taxonomy		Fragility Curve Parameters for Four Damage Levels							
		Slight		Moderate		Extensive		Complete	
Description	**Label**	**$S_{d,s}$**	**β_s**	**$S_{d,m}$**	**β_m**	**$S_{d,e}$**	**β_e**	**$S_{d,c}$**	**β_c**
Concrete Moment Frame	**RC1_L**	0.011	0.68	0.023	0.68	0.030	0.68	0.045	0.68
	RC1_M	0.016	0.68	0.034	0.68	0.045	0.68	0.067	0.68
	RC1_H	0.021	0.68	0.046	0.68	0.061	0.68	0.092	0.68
Concrete Shear Walls	**RC2_L**	0.014	0.68	0.030	0.68	0.040	0.68	0.061	0.68
	RC2_M	0.021	0.68	0.045	0.68	0.060	0.68	0.090	0.68
	RC2_H	0.028	0.68	0.061	0.68	0.082	0.68	0.123	0.68
Concrete Frame with URM Infill Walls	**RC3_L**	0.012	0.68	0.026	0.68	0.035	0.68	0.052	0.68
	RC3_M	0.018	0.68	0.039	0.68	0.052	0.68	0.078	0.68
	RC3_H	0.025	0.68	0.053	0.68	0.071	0.68	0.106	0.68

L: low-rise (1-3 stories)
M: mid-rise (4-7 stories)
H: high-rise (≥8 stories)

Table 68. Capacity Curve Parameters for Code-Designed RC Buildings with Low Ductility (DCL) of European Building Taxonomy

Building Taxonomy		Capacity Curve Parameters				
Description	**Label**	**T**	**μ**	**a_y**	**d_y**	**d_u**
Concrete Moment Frame	**RC1-III_L**	0.44	3.0	0.2270	0.0108	0.0324
	RC1-II_L		3.0	0.3630	0.0173	0.0518
	RC1-I_L		3.0	0.5020	0.0239	0.0716
	RC1-III_M	0.64	3.0	0.1640	0.0168	0.0504
	RC1-II_M		3.0	0.2630	0.0269	0.0806
	RC1-I_M		3.0	0.3630	0.0371	0.1114
	RC1-III_H	0.91	3.0	0.1150	0.0239	0.0717
	RC1-II_H		3.0	0.1850	0.0382	0.1147
	RC1-I_H		3.0	0.2550	0.0528	0.1584
Concrete Shear Walls	**RC2-III_L**	0.44	3.0	0.3050	0.0145	0.0434
	RC2-II_L		3.0	0.4870	0.0232	0.0695
	RC2-I_L		3.0	0.6730	0.0320	0.0960
	RC2-III_M	0.64	3.0	0.2200	0.0225	0.0676
	RC2-II_M		3.0	0.3520	0.0361	0.1081
	RC2-I_M		3.0	0.4870	0.0498	0.1494
	RC2-III_H	0.91	3.0	0.1550	0.0321	0.0962
	RC2-II_H		3.0	0.2480	0.0513	0.1538
	RC2-I_H		3.0	0.3420	0.0709	0.2125
Concrete Frame with URM Infill Walls	**RC3-III_L**	0.44	3.0	0.2630	0.0125	0.0375
	RC3-II_L		3.0	0.4210	0.0200	0.0600
	RC3-I_L		3.0	0.5810	0.0276	0.0829
	RC3-III_M	0.64	3.0	0.1900	0.0195	0.0584
	RC3-II_M		3.0	0.3040	0.0311	0.0934
	RC3-I_M		3.0	0.4200	0.0430	0.1290
	RC3-III_H	0.91	3.0	0.1340	0.0277	0.0830
	RC3-II_H		3.0	0.2140	0.0443	0.1328
	RC3-I_H		3.0	0.2950	0.0612	0.1835

I: seismic zone 1 *L: low-rise (1-3 stories)*
II: seismic zone 2 *M: mid-rise (4-7 stories)*
III: seismic zone 3 *H: high-rise (≥8 stories)*

Table 69. Fragility Curve Parameters for Code-Designed RC Buildings with Low Ductility (DCL) of European Building Taxonomy

Building Taxonomy		Fragility Curve Parameters for Four Damage Levels							
		Slight		Moderate		Extensive		Complete	
Description	Label	$S_{d,s}$	β_s	$S_{d,m}$	β_m	$S_{d,e}$	β_e	$S_{d,c}$	β_c
Concrete Moment Frame	RC1-III_L	0.008	0.68	0.016	0.68	0.022	0.68	0.032	0.68
	RC1-II_L	0.012	0.68	0.026	0.68	0.035	0.68	0.052	0.68
	RC1-I_L	0.017	0.68	0.036	0.68	0.048	0.68	0.072	0.68
	RC1-III_M	0.012	0.68	0.025	0.68	0.034	0.68	0.050	0.68
	RC1-II_M	0.019	0.68	0.040	0.68	0.054	0.68	0.081	0.68
	RC1-I_M	0.026	0.68	0.056	0.68	0.074	0.68	0.111	0.68
	RC1-III_H	0.017	0.68	0.036	0.68	0.048	0.68	0.072	0.68
	RC1-II_H	0.027	0.68	0.057	0.68	0.076	0.68	0.115	0.68
	RC1-I_H	0.037	0.68	0.079	0.68	0.106	0.68	0.158	0.68
Concrete Shear Walls	RC2-III_L	0.010	0.68	0.022	0.68	0.029	0.68	0.043	0.68
	RC2-II_L	0.016	0.68	0.035	0.68	0.046	0.68	0.070	0.68
	RC2-I_L	0.022	0.68	0.048	0.68	0.064	0.68	0.096	0.68
	RC2-III_M	0.016	0.68	0.034	0.68	0.045	0.68	0.068	0.68
	RC2-II_M	0.025	0.68	0.054	0.68	0.072	0.68	0.108	0.68
	RC2-I_M	0.035	0.68	0.075	0.68	0.100	0.68	0.149	0.68
	RC2-III_H	0.022	0.68	0.048	0.68	0.064	0.68	0.096	0.68
	RC2-II_H	0.036	0.68	0.077	0.68	0.103	0.68	0.154	0.68
	RC2-I_H	0.050	0.68	0.106	0.68	0.142	0.68	0.213	0.68
Concrete Frame with URM Infill Walls	RC3-III_L	0.009	0.68	0.019	0.68	0.025	0.68	0.038	0.68
	RC3-II_L	0.014	0.68	0.030	0.68	0.040	0.68	0.060	0.68
	RC3-I_L	0.019	0.68	0.041	0.68	0.055	0.68	0.083	0.68
	RC3-III_M	0.014	0.68	0.029	0.68	0.039	0.68	0.058	0.68
	RC3-II_M	0.022	0.68	0.047	0.68	0.062	0.68	0.093	0.68
	RC3-I_M	0.030	0.68	0.065	0.68	0.086	0.68	0.129	0.68
	RC3-III_H	0.019	0.68	0.042	0.68	0.055	0.68	0.083	0.68
	RC3-II_H	0.031	0.68	0.066	0.68	0.089	0.68	0.133	0.68
	RC3-I_H	0.043	0.68	0.092	0.68	0.122	0.68	0.184	0.68

I: seismic zone 1 *L: low-rise (1-3 stories)*
II: seismic zone 2 *M: mid-rise (4-7 stories)*
III: seismic zone 3 *H: high-rise (≥8 stories)*

Table 70. Capacity Curve Parameters for Code-Designed RC Buildings with Moderate Ductility (DCM) of European Building Taxonomy

Building Taxonomy		Capacity Curve Parameters				
Description	**Label**	**T**	**μ**	**a_y**	**d_y**	**d_u**
Concrete Moment Frame	**RC1-III_L**	0.44	3.63	0.2660	0.0127	0.0459
	RC1-II_L		3.63	0.4260	0.0203	0.0735
	RC1-I_L		3.63	0.5890	0.0280	0.1015
	RC1-III_M	0.64	4.11	0.1760	0.0180	0.0742
	RC1-II_M		4.11	0.2820	0.0288	0.1187
	RC1-I_M		4.11	0.3890	0.0398	0.1639
	RC1-III_H	0.91	4.11	0.1170	0.0242	0.0995
	RC1-II_H		4.11	0.1870	0.0387	0.1592
	RC1-I_H		4.11	0.2580	0.0534	0.2199
Concrete Shear Walls	**RC2-III_L**	0.44	3.19	0.3910	0.0186	0.0594
	RC2-II_L		3.19	0.6250	0.0297	0.0950
	RC2-I_L		3.19	0.8640	0.0411	0.1312
	RC2-III_M	0.64	3.63	0.2580	0.0264	0.0959
	RC2-II_M		3.63	0.4130	0.0423	0.1534
	RC2-I_M		3.63	0.5710	0.0584	0.2119
	RC2-III_H	0.91	3.63	0.1710	0.0355	0.1286
	RC2-II_H		3.63	0.2740	0.0568	0.2058
	RC2-I_H		3.63	0.3790	0.0784	0.2842
Concrete Frame with URM Infill Walls	**RC3-III_L**	0.44	3.19	0.3370	0.0160	0.0513
	RC3-II_L		3.19	0.5400	0.0257	0.0820
	RC3-I_L		3.19	0.7460	0.0355	0.1133
	RC3-III_M	0.64	3.63	0.2230	0.0228	0.0828
	RC3-II_M		3.63	0.3570	0.0365	0.1324
	RC3-I_M		3.63	0.4930	0.0505	0.1829
	RC3-III_H	0.91	3.63	0.1480	0.0306	0.1110
	RC3-II_H		3.63	0.2370	0.0490	0.1776
	RC3-I_H		3.63	0.3270	0.0677	0.2454

I: seismic zone 1 *L: low-rise (1-3 stories)*
II: seismic zone 2 *M: mid-rise (4-7 stories)*
III: seismic zone 3 *H: high-rise (≥8 stories)*

Table 71. Fragility Curve Parameters for Code-Designed RC Buildings with Moderate Ductility (DCM) of European Building Taxonomy

Building Taxonomy		Fragility Curve Parameters for Four Damage Levels							
		Slight		Moderate		Extensive		Complete	
Description	Label	$S_{d,s}$	β_s	$S_{d,m}$	β_m	$S_{d,e}$	β_e	$S_{d,c}$	β_c
Concrete Moment Frame	RC1-III_L	0.009	0.80	0.019	0.80	0.029	0.80	0.046	0.80
	RC1-II_L	0.014	0.80	0.030	0.80	0.047	0.80	0.074	0.80
	RC1-I_L	0.020	0.80	0.042	0.80	0.065	0.80	0.102	0.80
	RC1-III_M	0.013	0.88	0.027	0.88	0.046	0.88	0.074	0.88
	RC1-II_M	0.020	0.88	0.043	0.88	0.074	0.88	0.119	0.88
	RC1-I_M	0.028	0.88	0.060	0.88	0.102	0.88	0.164	0.88
	RC1-III_H	0.017	0.88	0.036	0.88	0.062	0.88	0.100	0.88
	RC1-II_H	0.027	0.88	0.058	0.88	0.099	0.88	0.159	0.88
	RC1-I_H	0.037	0.88	0.080	0.88	0.137	0.88	0.220	0.88
Concrete Shear Walls	RC2-III_L	0.013	0.72	0.028	0.72	0.039	0.72	0.059	0.72
	RC2-II_L	0.021	0.72	0.045	0.72	0.062	0.72	0.095	0.72
	RC2-I_L	0.029	0.72	0.062	0.72	0.086	0.72	0.131	0.72
	RC2-III_M	0.018	0.80	0.040	0.80	0.061	0.80	0.096	0.80
	RC2-II_M	0.030	0.80	0.063	0.80	0.098	0.80	0.153	0.80
	RC2-I_M	0.041	0.80	0.088	0.80	0.135	0.80	0.212	0.80
	RC2-III_H	0.025	0.80	0.053	0.80	0.082	0.80	0.129	0.80
	RC2-II_H	0.040	0.80	0.085	0.80	0.131	0.80	0.206	0.80
	RC2-I_H	0.055	0.80	0.118	0.80	0.181	0.80	0.284	0.80
Concrete Frame with URM Infill Walls	RC3-III_L	0.011	0.72	0.024	0.72	0.034	0.72	0.051	0.72
	RC3-II_L	0.018	0.72	0.039	0.72	0.054	0.72	0.082	0.72
	RC3-I_L	0.025	0.72	0.053	0.72	0.074	0.72	0.113	0.72
	RC3-III_M	0.016	0.80	0.034	0.80	0.053	0.80	0.083	0.80
	RC3-II_M	0.026	0.80	0.055	0.80	0.084	0.80	0.132	0.80
	RC3-I_M	0.035	0.80	0.076	0.80	0.117	0.80	0.183	0.80
	RC3-III_H	0.021	0.80	0.046	0.80	0.071	0.80	0.111	0.80
	RC3-II_H	0.034	0.80	0.074	0.80	0.113	0.80	0.178	0.80
	RC3-I_H	0.047	0.80	0.102	0.80	0.157	0.80	0.245	0.80

I: seismic zone 1 *L: low-rise (1-3 stories)*
II: seismic zone 2 *M: mid-rise (4-7 stories)*
III: seismic zone 3 *H: high-rise (≥8 stories)*

Table 72. Capacity Curve Parameters for Code-Designed RC Buildings with High Ductility (DCH) of European Building Taxonomy

Building Taxonomy		Capacity Curve Parameters				
Description	**Label**	**T**	**μ**	**a_y**	**d_y**	**d_u**
Concrete Moment Frame	**RC1-III_L**	0.44	4.67	0.2510	0.0119	0.0557
	RC1-II_L		4.67	0.4010	0.0191	0.0890
	RC1-I_L		4.67	0.5540	0.0263	0.1230
	RC1-III_M	0.64	5.65	0.1410	0.0144	0.0814
	RC1-II_M		5.65	0.2250	0.0231	0.1302
	RC1-I_M		5.65	0.3110	0.0319	0.1799
	RC1-III_H	0.91	5.65	0.0930	0.0193	0.1092
	RC1-II_H		5.65	0.1490	0.0309	0.1747
	RC1-I_H		5.65	0.2060	0.0427	0.2413
Concrete Shear Walls	**RC2-III_L**	0.43	4.11	0.3680	0.0175	0.0719
	RC2-II_L		4.11	0.5880	0.0280	0.1151
	RC2-I_L		4.11	0.8130	0.0386	0.1590
	RC2-III_M	0.64	4.97	0.2070	0.0211	0.1052
	RC2-II_M		4.97	0.3310	0.0338	0.1683
	RC2-I_M		4.97	0.4570	0.0467	0.2325
	RC2-III_H	0.91	4.97	0.1370	0.0284	0.1411
	RC2-II_H		4.97	0.2190	0.0454	0.2258
	RC2-I_H		4.97	0.3030	0.0627	0.3119
Concrete Frame with URM Infill Walls	**RC3-III_L**	0.44	4.11	0.3170	0.0151	0.0621
	RC3-II_L		4.11	0.5080	0.0242	0.0994
	RC3-I_L		4.11	0.7020	0.0334	0.1373
	RC3-III_M	0.64	4.97	0.1780	0.0183	0.0908
	RC3-II_M		4.97	0.2860	0.0292	0.1453
	RC3-I_M		4.97	0.3940	0.0404	0.2008
	RC3-III_H	0.91	4.97	0.1180	0.0245	0.1218
	RC3-II_H		4.97	0.1890	0.0392	0.1949
	RC3-I_H		4.97	0.2610	0.0541	0.2693

I: seismic zone 1 *L: low-rise (1-3 stories)*
II: seismic zone 2 *M: mid-rise (4-7 stories)*
III: seismic zone 3 *H: high-rise (≥8 stories)*

Table 73. Fragility Curve Parameters for Code-Designed RC Buildings with High Ductility (DCH) of European Building Taxonomy

Building Taxonomy		Fragility Curve Parameters for Four Damage Levels							
		Slight		Moderate		Extensive		Complete	
Description	Label	$S_{d,s}$	β_s	$S_{d,m}$	β_m	$S_{d,e}$	β_e	$S_{d,c}$	β_c
Concrete Moment Frame	RC1-III_L	0.008	0.96	0.018	0.96	0.034	0.96	0.056	0.96
	RC1-II_L	0.013	0.96	0.029	0.96	0.054	0.96	0.089	0.96
	RC1-I_L	0.018	0.96	0.039	0.96	0.075	0.96	0.123	0.96
	RC1-III_M	0.010	1.07	0.022	1.07	0.048	1.07	0.081	1.07
	RC1-II_M	0.016	1.07	0.035	1.07	0.077	1.07	0.130	1.07
	RC1-I_M	0.022	1.07	0.048	1.07	0.106	1.07	0.180	1.07
	RC1-III_H	0.014	1.07	0.029	1.07	0.064	1.07	0.109	1.07
	RC1-II_H	0.022	1.07	0.046	1.07	0.103	1.07	0.175	1.07
	RC1-I_H	0.030	1.07	0.064	1.07	0.142	1.07	0.241	1.07
Concrete Shear Walls	RC2-III_L	0.012	0.88	0.026	0.88	0.045	0.88	0.072	0.88
	RC2-II_L	0.020	0.88	0.042	0.88	0.072	0.88	0.115	0.88
	RC2-I_L	0.027	0.88	0.058	0.88	0.099	0.88	0.159	0.88
	RC2-III_M	0.015	0.99	0.032	0.99	0.063	0.99	0.105	0.99
	RC2-II_M	0.024	0.99	0.051	0.99	0.101	0.99	0.168	0.99
	RC2-I_M	0.033	0.99	0.070	0.99	0.140	0.99	0.233	0.99
	RC2-III_H	0.020	0.99	0.043	0.99	0.085	0.99	0.141	0.99
	RC2-II_H	0.032	0.99	0.068	0.99	0.136	0.99	0.226	0.99
	RC2-I_H	0.044	0.99	0.094	0.99	0.187	0.99	0.312	0.99
Concrete Frame with URM Infill Walls	RC3-III_L	0.011	0.88	0.023	0.88	0.039	0.88	0.062	0.88
	RC3-II_L	0.017	0.88	0.036	0.88	0.062	0.88	0.099	0.88
	RC3-I_L	0.023	0.88	0.050	0.88	0.085	0.88	0.137	0.88
	RC3-III_M	0.013	0.99	0.027	0.99	0.055	0.99	0.091	0.99
	RC3-II_M	0.020	0.99	0.044	0.99	0.087	0.99	0.145	0.99
	RC3-I_M	0.028	0.99	0.061	0.99	0.121	0.99	0.201	0.99
	RC3-III_H	0.017	0.99	0.037	0.99	0.073	0.99	0.122	0.99
	RC3-II_H	0.027	0.99	0.059	0.99	0.117	0.99	0.195	0.99
	RC3-I_H	0.038	0.99	0.081	0.99	0.162	0.99	0.269	0.99

I: seismic zone 1 *L: low-rise (1-3 stories)*
II: seismic zone 2 *M: mid-rise (4-7 stories)*
III: seismic zone 3 *H: high-rise (≥8 stories)*

Table 74. Capacity Curve Parameters for Masonry Buildings of European Building Taxonomy

Building Taxonomy		Capacity Curve Parameters				
Description	RISK-UE	T	μ	a_y	d_y	d_u
Rubble Stone	M1_L	0.21100	4.79	0.1680	0.0019	0.0089
	M1.w_L			0.1780	0.0020	0.0094
	M1.v_L			0.1320	0.0015	0.0070
	M1_M	0.35500	3.25	0.1330	0.0042	0.0135
	M1.w_M			0.1410	0.0044	0.0143
	M1.v_M			0.1050	0.0033	0.0107
Adobe	M2_L	0.268	3.98	0.1460	0.0026	0.0104
	M2.w_L			0.1550	0.0028	0.0111
	M2.v_L			0.1160	0.0021	0.0082
Simple Stone	M3_L	0.192	5.17	0.2480	0.0023	0.0117
	M3.w_L			0.2630	0.0024	0.0124
	M3.v L			0.1960	0.0018	0.0093
	M3.sm_L			0.2960	0.0027	0.0140
	M3 M	0.322	3.48	0.1960	0.0051	0.0176
	M3.w_M			0.2080	0.0054	0.0187
	M3.v M			0.1550	0.0040	0.0140
	M3.sm_M			0.2340	0.0060	0.0210
	M3_H	0.437	3.00	0.1420	0.0067	0.0202
	M3.w_H			0.1510	0.0071	0.0214
	M3.v_H			0.1120	0.0053	0.0160
	M3.sm_H			0.1700	0.0080	0.0241
Massive Stone	M4 L	0.173	5.63	0.3580	0.0026	0.0149
	M4.w_L			0.3790	0.0028	0.0158
	M4.v_L			0.2830	0.0021	0.0118
	M4 M	0.290	3.76	0.2830	0.0059	0.0222
	M4.w_M			0.3000	0.0063	0.0235
	M4.v_M			0.2230	0.0047	0.0176
	M4_H	0.393	3.03	0.2230	0.0086	0.0260
	M4.w H			0.2370	0.0091	0.0276
	M4.v_H			0.1770	0.0068	0.0206
Unreinforced Masonry (old bricks)	M5_L	0.173	5.63	0.2630	0.0019	0.0110
	M5.w L	0.201	4.97	0.2790	0.0028	0.0140
	M5.v_L	0.192	5.17	0.2080	0.0019	0.0098
	M5.sm_L			0.3140	0.0029	0.0148
	M5_M	0.290	3.76	0.2080	0.0044	0.0164
	M5.w_M	0.338	3.36	0.2210	0.0063	0.0211
	M5.v M	0.322	3.48	0.1650	0.0043	0.0148
	M5.sm_M			0.2480	0.0064	0.0223
	M5 H	0.393	3.03	0.1650	0.0063	0.0192
	M5.w_H	0.459	3.00	0.1520	0.0080	0.0239
	M5.v H	0.437	3.00	0.1190	0.0057	0.0170
	M5.sm_H			0.1800	0.0085	0.0256
Unreinforced Masonry (RC Floors)	M6_L-PC	0.211	4.79	0.3240	0.0036	0.0171
	M6_L-MC		5.98	0.3580	0.0040	0.0236
	M6 M-PC	0.355	3.25	0.2560	0.0080	0.0260
	M6_M-MC		3.96	0.2830	0.0088	0.0350
	M6 H-PC	0.481	3.00	0.1680	0.0097	0.0290
	M6_H-MC		3.63	0.1860	0.0107	0.0387
Reinforced/ Confined Masonry	M7_L	0.153	7.85	0.5080	0.0030	0.0233
	M7 M	0.258	5.07	0.4010	0.0066	0.0336
	M7 H	0.350	4.00	0.3170	0.0096	0.0386

w: wood slabs
v: masonry vaults
sm: composite steel and masonry slabs

L: low-rise (1-2 stories)
M: mid-rise (3-5 stories)
H: high-rise (≥6 stories)

Table 75. Fragility Curve Parameters for Masonry Buildings of European Building Taxonomy

Building Taxonomy		Fragility Curve Parameters for Four Damage Levels							
		Slight		Moderate		Extensive		Complete	
Description	RISK-UE	$S_{d,s}$	β_s	$S_{d,m}$	β_m	$S_{d,e}$	β_e	$S_{d,c}$	β_c
Rubble Stone	M1_L	0.0013	0.97	0.0029	0.97	0.005	0.97	0.009	0.97
	M1.w_L	0.0014		0.0030		0.006		0.009	
	M1.v_L	0.0011		0.0023		0.004		0.007	
	M1_M	0.0029	0.73	0.0063	0.73	0.009	0.73	0.014	0.73
	M1.w_M	0.0031		0.0066		0.009		0.014	
	M1.v_M	0.0023		0.0050		0.007		0.011	
Adobe	M2_L	0.0018	0.86	0.0039	0.86	0.007	0.86	0.010	0.86
	M2.w_L	0.0020		0.0042		0.007		0.011	
	M2.v_L	0.0015		0.0032		0.005		0.008	
Simple Stone	M3_L	0.0016	1.02	0.0035	1.02	0.007	1.02	0.012	1.02
	M3.w_L	0.0017		0.0036		0.007		0.012	
	M3.v L	0.0013		0.0027		0.006		0.009	
	M3.sm_L	0.0019		0.0041		0.008		0.014	
	M3 M	0.0036	0.77	0.0077	0.77	0.011	0.77	0.018	0.77
	M3.w_M	0.0038		0.0081		0.012		0.019	
	M3.v M	0.0028		0.0060		0.009		0.014	
	M3.sm_M	0.0042		0.0090		0.014		0.021	
	M3_H	0.0047	0.68	0.0101	0.68	0.013	0.68	0.020	0.68
	M3.w_H	0.0050		0.0107		0.014		0.021	
	M3.v_H	0.0037		0.0080		0.011		0.016	
	M3.sm_H	0.0056		0.0120		0.016		0.024	
Massive Stone	M4 L	0.0018	1.07	0.0039	1.07	0.009	1.07	0.015	1.07
	M4.w_L	0.0020		0.0042		0.009		0.016	
	M4.v_L	0.0015		0.0032		0.007		0.012	
	M4 M	0.0041	0.82	0.0089	0.82	0.014	0.82	0.022	0.82
	M4.w_M	0.0044		0.0095		0.015		0.024	
	M4.v_M	0.0033		0.0071		0.011		0.018	
	M4_H	0.0060	0.69	0.0129	0.69	0.017	0.69	0.026	0.69
	M4.w H	0.0064		0.0137		0.018		0.028	
	M4.v_H	0.0048		0.0102		0.014		0.021	
Unreinforced Masonry (old bricks)	M5_L	0.0013	1.07	0.0029	1.07	0.006	1.07	0.011	1.07
	M5.w L	0.0020	0.99	0.0042	0.99	0.008	0.99	0.014	0.99
	M5.v_L	0.0013	1.02	0.0029	1.02	0.006	1.02	0.010	1.02
	M5.sm_L	0.0020		0.0044		0.009		0.015	
	M5_M	0.0031	0.82	0.0066	0.82	0.010	0.82	0.016	0.82
	M5.w_M	0.0044	0.75	0.0095	0.75	0.014	0.75	0.021	0.75
	M5.v M	0.0030	0.77	0.0065	0.77	0.010	0.77	0.015	0.77
	M5.sm_M	0.0045		0.0096		0.014		0.022	
	M5 H	0.0044	0.69	0.0095	0.69	0.013	0.69	0.019	0.69
	M5.w_H	0.0056	0.68	0.0120	0.68	0.016	0.68	0.024	0.68
	M5.v H	0.0040	0.68	0.0086	0.68	0.011	0.68	0.017	0.68
	M5.sm_H	0.0060		0.0128		0.017		0.026	
Unreinforced Masonry (RC Floors)	M6_L-PC	0.0025	0.97	0.0054	0.97	0.010	0.97	0.017	0.97
	M6_L-MC	0.0028	1.11	0.0060	1.11	0.014	1.11	0.024	1.11
	M6 M-PC	0.0056	0.73	0.0120	0.73	0.017	0.73	0.026	0.73
	M6_M-MC	0.0062	0.85	0.0132	0.85	0.022	0.85	0.035	0.85
	M6 H-PC	0.0068	0.68	0.0146	0.68	0.019	0.68	0.029	0.68
	M6_H-MC	0.0075	0.80	0.0161	0.80	0.025	0.80	0.039	0.80
Reinforced/ Confined Masonry	M7_L	0.0021	1.28	0.0045	1.28	0.013	1.28	0.023	1.28
	M7 M	0.0046	1.01	0.0099	1.01	0.020	1.01	0.034	1.01
	M7 H	0.0067	0.86	0.0144	0.86	0.024	0.86	0.039	0.86

w: wood slabs
v: masonry vaults
sm: composite steel and masonry slabs
L: low-rise (1-2 stories)
M: mid-rise (3-5 stories)
H: high-rise (≥6 stories)

Table 76. Capacity Curve Parameters for Pre-Code Buildings of HAZUS99 Building Taxonomy

Building Taxonomy			Capacity Curve Parameters				
No.	Description	Label	d_y	a_y	d_u	a_u	d_e
1	**Wood, Light Frame**	W1	0.0061	1.962	0.1097	5.886	0.0043
2	**Wood, Commercial or Industrial**	W2	0.0041	0.981	0.0597	2.4525	0.0028
3	**Steel Moment Frame**	S1L	0.0038	0.6082	0.0699	1.8345	0.0027
4		S1M	0.0112	0.3826	0.1354	1.1478	0.0078
5		S1H	0.0295	0.2354	0.2662	0.7161	0.0206
6	**Steel Braced Frame**	S2L	0.0041	0.981	0.0478	1.962	0.0028
7		S2M	0.0155	0.8142	0.1232	1.6383	0.0108
8		S2H	0.0493	0.618	0.2951	1.2459	0.2 05
9	**Steel Light Frame**	S3	0.0041	0.981	0.0478	1.962	0.0028
10	**Steel Frame with Cast-in-Place Concrete Shear Walls**	S4L	0.0025	0.7848	0.033	1.7658	0.0018
11		S4M	0.0069	0.6573	0.0625	1.4715	0.0048
12		S4H	0.0221	0.5003	0.1494	1.1183	0.0155
13	**Steel Frame with URM Infill Walls**	S5L	0.003	0.981	0.0305	1.962	0.0021
14		S5M	0.0086	0.8142	0.0577	1.6383	0.0086 0
15		S5H	0.0277	0.618	0.1384	1.2459	0.0194
16	**Concrete Moment Frame**	C1L	0.0025	0.6082	0.0447	1.8345	0.0018
17		C1M	0.0074	0.5101	0.0879	1.5304	0.0052
18		C1H	0.0127	0.2354	0.1148	0.7161	0.0089
19	**Concrete Shear Walls**	C2L	0.003	0.981	0.0457	2.4525	0.0021
20		C2M	0.0066	0.8142	0.0066 0	2.0405	0.0046
21		C2H	0.0188	0.618	0.14	1.5598	0.0132
22	**Concrete Frame with URM Infill Walls**	C3L	0.003	0.981	0.0343	2.2073	0.0021
23		C3M	0.0066	0.8142	0.0495	1.8443	0.0046
24		C3H	0.0188	0.618	0.1049	1.4028	0.0132
25	**Pre-cast Concrete Tilt-**	PC1	0.0046	1.4715	0.0549	2.943	0.0032
26	**Pre-cast Concrete Frames with Concrete Shear Walls**	PC2L	0.003	0.981	0.0366	1.962	0.0021
27		PC2M	0.0066	0.8142	0.0528	1.6383	0.0046
28		PC2H	0.0188	0.618	0.112	1.2459	0.0132
29	**Reinforced Masonry Bearing Walls**	RM1L	0.0041	1.3047	0.0488	2.6193	0.0028
30		RM1M	0.0089	1.0889	0.0704	2.1778	0.0062
31	**Reinforced Masonry Bearing Walls**	RM2L	0.0041	1.3047	0.0488	2.6193	0.0028
32		RM2M	0.0089	1.0889	0.0704	2.1778	0.0062
33		RM2H	0.0249	0.8339	0.1494	1.6579	0.0174
34	**Unreinforced Masonry Bearing Walls**	URML	0.0061	1.962	1.962	3.924	0.0043
35		URMM	0.0069	1.0889	0.046	2.1778	0.0048
36	**Mobile Homes**	MH	0.0046	1.4715	0.0549	2.943	0.0032

Table 77. Fragility Curve Parameters for Pre-Code Buildings of HAZUS99 Building Taxonomy

Building Taxonomy			Fragility Curve Parameters for Four Damage Levels							
			Slight		Moderate		Extensive		Complete	
No.	Description	Label	$S_{d,s}$	β_s	$S_{d,m}$	β_m	$S_{d,e}$	β_e	$S_{d,c}$	β_c
1	Wood, Light Frame	W1	0.0102	1.01	0.0254	1.05	0.0785	1.07	0.1920	1.06
2	Wood, Commercial or Industrial	W2	0.0175	1.04	0.0434	0.97	0.1344	0.9	0.3292	0.99
3	Steel Moment Frame	S1L	0.0264	0.85	0.0419	0.82	0.0889	0.8	0.2195	0.95
4		S1M	0.0439	0.7	0.0701	0.75	0.1483	0.81	0.3658	0.98
5		S1H	0.0686	0.69	0.1092	0.71	0.2314	0.85	0.5705	0.93
6	Steel Braced Frame	S2L	0.0218	1.01	0.0351	0.96	0.0879	0.88	0.2195	0.98
7		S2M	0.0366	0.73	0.0584	0.75	0.1463	0.8	0.3658	0.98
8		S2H	0.0572	0.7	0.0912	0.7	0.2283	0.84	0.5705	0.91
9	Steel Light Frame	S3	0.0109	1.06	0.0175	1.03	0.0439	1.07	0.1201	0.89
10	Steel Frame with Cast-in-Place Concrete Shear Walls	S4L	0.0175	1.11	0.0282	1.03	0.0704	0.99	0.1920	0.98
11		S4M	0.0292	0.81	0.0470	0.8	0.1173	0.94	0.3200	1
12		S4H	0.0457	0.73	0.0732	0.75	0.1831	0.9	0.4994	0.97
13	Steel Frame with URM Infill Walls	S5L	0.0132	1.2	0.0264	1.11	0.0658	1.08	0.1537	0.95
14		S5M	0.0218	0.85	0.0439	0.83	0.1097	0.94	0.2560	0.99
15		S5H	0.0343	0.72	0.0686	0.75	0.1712	0.92	0.3993	0.96
16	Concrete Moment Frame	C1L	0.0183	0.98	0.0292	0.94	0.0732	0.9	0.1829	0.97
17		C1M	0.0305	0.73	0.0488	0.77	0.1219	0.83	0.3048	0.98
18		C1H	0.0439	0.71	0.0701	0.8	0.1755	0.94	0.4389	1.01
19	Concrete Shear Walls	C2L	0.0147	1.11	0.0279	1.09	0.0721	1.07	0.1829	0.93
20		C2M	0.0244	0.86	0.0465	0.83	0.1204	0.8	0.3048	0.98
21		C2H	0.0351	0.73	0.0671	0.75	0.1732	0.92	0.4389	0.97
22	Concrete Frame with URM Infill Walls	C3L	0.0109	1.19	0.0218	1.15	0.0549	1.15	0.1280	0.92
23		C3M	0.0183	0.9	0.0366	0.86	0.0914	0.9	0.2134	0.96
24		C3H	0.0264	0.73	0.0526	0.75	0.1316	0.9	0.3073	0.95
25	Pre-cast Concrete Tilt-Up Walls	PC1	0.0109	1.14	0.0175	1.14	0.0439	1.17	0.1201	0.98
26	Pre-cast Concrete Frames with Concrete Shear Walls	PC2L	0.0147	1.14	0.0234	1.1	0.0587	1.1	0.1600	0.93
27		PC2M	0.0244	0.87	0.0391	0.83	0.0978	0.91	0.2667	1
28		PC2H	0.0351	0.74	0.0561	0.75	0.1410	0.91	0.3840	0.96
29	Reinforced Masonry Bearing Walls	RM1L	0.0147	1.2	0.0234	1.17	0.0587	1.17	0.1600	0.94
30		RM1M	0.0244	0.91	0.0391	0.89	0.0978	0.89	0.2667	0.96
31	Reinforced Masonry Bearing Walls	RM2L	0.0147	1.14	0.0234	1.1	0.0587	1.15	0.1600	0.92
32		RM2M	0.0244	0.89	0.0391	0.87	0.0978	0.87	0.2667	0.96
33		RM2H	0.0351	0.75	0.0561	0.75	0.1410	0.84	0.3840	0.94
34	Unreinforced Masonry Bearing Walls	URML	0.0081	1.15	0.0165	1.19	0.0411	1.2	0.0960	1.18
35		URMM	0.0127	0.99	0.0257	0.97	0.0640	0.9	0.1494	0.88
36	Mobile Homes	MH	0.0097	1.11	0.0196	1.1	0.0584	0.95	0.1707	0.97

Table 78. Capacity Curve Parameters for Low-Code Buildings of HAZUS99 Building Taxonomy

Building Taxonomy			Capacity Curve Parameters				
No.	Description	Label	d_y	a_y	d_u	a_u	d_e
1	**Wood, Light Frame**	W1	0.0061	1.962	0.1097	5.886	0.0043
2	**Wood, Commercial or Industrial**	W2	0.0041	0.981	0.0597	2.4525	0.0028
3	**Steel Moment Frame**	S1L	0.0038	0.5886	0.0582	1.8639	0.0027
4		S1M	0.0112	0.3924	0.1128	1.1772	0.0078
5		S1H	0.0295	0.1962	0.2217	0.6867	0.0206
6	**Steel Braced Frame**	S2L	0.0041	0.981	0.0399	1.962	0.0028
7		S2M	0.0155	0.7848	0.1026	1.6677	0.0108
8		S2H	0.0493	0.5886	0.2459	1.2753	0.0345
9	**Steel Light Frame**	S3	0.0041	0.981	0.0399	1.962	0.0028
10	**Steel Frame with Cast-in-Place Concrete Shear Walls**	S4L	0.0025	0.7848	0.0274	1.7658	0.0018
11		S4M	0.0069	0.6867	0.0521	1.4715	0.0048
12		S4H	0.0221	0.4905	0.1245	1.0791	0.0155
13	**Steel Frame with URM Infill Walls**	S5L	0.003	0.981	0.0305	1.962	0.0021
14		S5M	0.0086	0.7848	0.0577	1.6677	0.006
15		S5H	0.0277	0.5886	0.1384	1.2753	0.0194
16	**Concrete Moment Frame**	C1L	0.0025	0.5886	0.0373	1.8639	0.0018
17		C1M	0.0074	0.4905	0.0732	1.5696	0.0052
18		C1H	0.0127	0.1962	0.0958	0.6867	0.0089
19	**Concrete Shear Walls**	C2L	0.003	0.981	0.981	2.4525	0.0021
20		C2M	0.0066	0.7848	0.0549	2.0601	0.0046
21		C2H	0.0185	0.1166	0.1166	1.5696	0.013
22	**Concrete Frame with URM Infill Walls**	C3L	0.003	0.981	0.0343	2.2563	0.0021
23		C3M	0.0066	0.7848	0.0495	1.8639	0.0046
24		C3H	0.0185	0.5886	0.1049	1.3734	0.013
25	**Pre-cast Concrete Tilt-**	PC1	0.0046	1.4715	0.0457	2.943	0.0032
26	**Pre-cast Concrete Frames with Concrete Shear Walls**	PC2L	0.003	0.981	0.0305	1.962	0.0021
27		PC2M	0.0066	0.7848	0.0439	1.6677	0.0046
28		PC2H	0.0185	0.5886	0.0932	1.2753	0.013
29	**Reinforced Masonry Bearing Walls**	RM1L	0.0041	1.2753	0.0406	2.6487	0.0028
30		RM1M	0.0089	1.0791	0.0587	2.1582	0.0062
31	**Reinforced Masonry Bearing Walls**	RM2L	0.0041	1.2753	0.0406	2.6487	0.0028
32		RM2M	0.0089	1.0791	0.0587	20.0062	0.0062
33		RM2H	0.0249	0.8829	0.1245	1.6677	0.0174
34	**Unreinforced Masonry Bearing Walls**	URML	0.0061	1.962	1.962	3.924	0.0043
35		URMM	0.0069	1.0791	0.046	2.1582	0.0048
36	**Mobile Homes**	MH	0.0046	1.4715	0.0549	2.943	0.0032

Table 79. Fragility Curve Parameters for Low-Code Buildings of HAZUS99 Building Taxonomy

Building Taxonomy			Fragility Curve Parameters for Four Damage Levels							
			Slight		Moderate		Extensive		Complete	
No.	Description	Label	$S_{d,s}$	β_s	$S_{d,m}$	β_m	$S_{d,e}$	β_e	$S_{d,c}$	β_c
1	Wood, Light Frame	W1	0.0127	0.93	0.03175	0.98	0.09804	1.02	0.24003	0.99
2	Wood, Commercial or	W2	0.02184	0.97	0.05436	0.9	0.16815	0.89	0.41148	0.99
3	Steel Moment Frame	S1L	0.03302	0.77	0.05258	0.78	0.11125	0.78	0.27432	0.96
4		S1M	0.05486	0.68	0.08738	0.78	0.18542	0.85	0.4572	0.98
5		S1H	0.0856	0.66	0.1364	0.7	0.28905	0.76	0.71323	0.92
6	Steel Braced Frame	S2L	0.02743	0.96	0.04394	0.89	0.10973	0.86	0.27432	0.98
7		S2M	0.04572	0.7	0.07315	0.73	0.18288	0.85	0.4572	0.98
8		S2H	0.07137	0.66	0.11405	0.67	0.28524	0.74	0.71323	0.92
9	Steel Light Frame	S3	0.01372	0.98	0.0221	0.99	0.05512	1.01	0.15011	0.9
10	Steel Frame with Cast-in-Place Concrete Shear Walls	S4L	0.02184	1.05	0.03505	0.98	0.08814	0.89	0.24003	0.98
11		S4M	0.03658	0.76	0.05867	0.78	0.14681	0.9	0.40005	0.99
12		S4H	0.05715	0.7	0.09144	0.75	0.22885	0.9	0.62408	0.98
13	Steel Frame with URM Infill Walls	S5L	0.01651	1.11	0.03302	1.04	0.0823	0.99	0.19202	0.95
14		S5M	0.02743	0.77	0.05486	0.79	0.13716	0.87	0.32004	0.98
15		S5H	0.04267	0.7	0.0856	0.73	0.21387	0.89	0.49936	0.97
16	Concrete Moment Frame	C1L	0.02286	0.95	0.03658	0.91	0.09144	0.85	0.2286	0.97
17		C1M	0.0381	0.7	0.06096	0.74	0.1524	0.86	0.381	0.98
18		C1H	0.05486	0.7	0.08788	0.81	0.21946	0.89	0.54864	0.98
19	Concrete Shear Walls	C2L	0.01829	1.04	0.0348	1.02	0.09017	0.99	0.2286	0.95
20		C2M	0.03048	0.82	0.05817	0.81	0.15037	0.81	0.381	0.99
21		C2H	0.04394	0.68	0.08382	0.73	0.21666	0.84	0.54864	0.95
22	Concrete Frame with URM Infill Walls	C3L	0.01372	1.09	0.02743	1.07	0.06858	1.08	0.16002	0.91
23		C3M	0.02286	0.85	0.04572	0.83	0.1143	0.79	0.2667	0.98
24		C3H	0.03302	0.71	0.06579	0.74	0.16459	0.9	0.38405	0.97
25	Pre-cast Concrete Tilt-Up Walls	PC1	0.01372	1	0.0221	1.05	0.05512	1.12	0.15011	0.89
26	Pre-cast Concrete Frames with Concrete Shear Walls	PC2L	0.01829	1.08	0.02921	1.03	0.07341	0.98	0.20015	0.96
27		PC2M	0.03048	0.81	0.04877	0.79	0.12217	0.84	0.33325	0.99
28		PC2H	0.04394	0.71	0.07036	0.75	0.17602	0.89	0.48006	0.98
29	Reinforced Masonry Bearing Walls	RM1L	0.01829	1.11	0.02921	1.1	0.07341	1.1	0.20015	0.92
30		RM1M	0.03048	0.87	0.04877	0.84	0.12217	0.79	0.33325	0.96
31	Reinforced Masonry Bearing Walls	RM2L	0.01829	1.05	0.02921	1.07	0.07341	1.09	0.20015	0.91
32		RM2M	0.03048	0.84	0.04877	0.81	0.12217	0.77	0.33325	0.96
33		RM2H	0.04394	0.69	0.07036	0.72	0.17602	0.87	0.48006	0.96
34	Unreinforced Masonry Bearing Walls	URML	0.01041	0.99	0.02057	1.05	0.05156	1.1	0.12014	1.08
35		URMM	0.016	0.91	0.032	0.92	0.08001	0.87	0.18669	0.91
36	Mobile Homes	MH	0.01219	0.91	0.02438	1	0.07315	1.03	0.21336	0.92

Table 80. Capacity Curve Parameters for Moderate-Code Buildings of HAZUS99 Building Taxonomy

Building Taxonomy			Capacity Curve Parameters				
No.	Description	Label	d_y	a_y	d_u	a_u	d_e
1	**Wood, Light Frame**	W1	0.0091	2.943	0.1643	8.829	0.0064
2	**Wood, Commercial or Industrial**	W2	0.0079	1.962	0.1194	4.905	0.0055
3	**Steel Moment Frame**	S1L	0.0079	1.1772	0.1397	3.7278	0.0055
4		S1M	0.0226	0.7848	0.0158	2.2563	0.0158
5		S1H	0.0592	0.4905	0.5324	1.4715	0.0414
6	**Steel Braced Frame**	S2L	0.0079	1.962	0.0955	3.924	0.0055
7		S2M	0.0307	1.6677	0.2464	3.2373	0.0215
8		S2H	0.0983	1.2753	0.5903	2.4525	0.0688
9	**Steel Light Frame**	S3	0.0079	1.962	0.0955	3.924	0.0055
10	**Steel Frame with Cast-in-Place Concrete Shear Walls**	S4L	0.0048	1.5696	0.0658	3.5316	0.0034
11		S4M	0.014	1.2753	0.1247	2.943	0.0098
12		S4H	0.0442	0.981	0.2987	2.2563	0.0309
13	**Steel Frame with URM Infill Walls**	S5L	-	-	-	-	-
14		S5M	-	-	-	-	-
15		S5H	-	-	-	-	-
16	**Concrete Moment Frame**	C1L	0.0051	1.1772	0.0894	3.7278	0.0036
17		C1M	0.0147	0.981	0.1755	3.0411	0.0103
18		C1H	0.0254	0.4905	0.2299	1.4715	0.0178
19	**Concrete Shear Walls**	C2L	0.0061	1.962	0.0914	4.905	0.0043
20		C2M	0.0132	1.6677	0.1318	4.1202	0.0092
21		C2H	0.0373	1.2753	0.2799	3.1392	0.0261
22	**Concrete Frame with URM Infill Walls**	C3L	-	-	-	-	-
23		C3M	-	-	-	-	-
24		C3H	-	-	-	-	-
25	**Pre-cast Concrete Tilt-**	PC1	0.0091	2.943	0.1097	5.886	0.0064
26	**Pre-cast Concrete Frames with Concrete Shear Walls**	PC2L	0.0061	1.962	0.0732	3.924	0.0043
27		PC2M	0.0132	1.6677	0.1054	3.2373	0.0092
28		PC2H	0.0373	1.2753	0.224	2.4525	0.0261
29	**Reinforced Masonry Bearing Walls**	RM1L	0.0081	2.6487	0.0975	5.1993	0.0057
30		RM1M	0.0175	2.1582	0.1407	4.3164	0.0123
31	**Reinforced Masonry Bearing Walls**	RM2L	0.0081	2.6487	0.0975	5.1993	0.0057
32		RM2M	0.0175	2.1582	0.1407	4.3164	0.0123
33		RM2H	0.0498	1.6677	0.2987	3.3354	0.0348
34	**Unreinforced Masonry Bearing Walls**	URML	-	-	-	-	-
35		URMM	-	-	-	-	-
36	**Mobile Homes**	MH	0.0046	1.4715	0.0549	2.943	0.0032

Table 81. Fragility Curve Parameters for Moderate-Code Buildings of HAZUS99 Building Taxonomy

Building Taxonomy			Fragility Curve Parameters for Four Damage Levels							
			Slight		Moderate		Extensive		Complete	
No.	Description	Label	$S_{d,s}$	β_s	$S_{d,m}$	β_m	$S_{d,e}$	β_e	$S_{d,c}$	β_c
1	Wood, Light Frame	W1	0.0127	0.84	0.03175	0.86	0.09804	0.89	0.24003	1.04
2	Wood, Commercial or	W2	0.02184	0.89	0.05436	0.95	0.16815	0.95	0.41148	0.92
3	Steel Moment Frame	S1L	0.03302	0.8	0.0569	0.75	0.12903	0.74	0.32918	0.88
4		S1M	0.05486	0.65	0.095	0.68	0.21488	0.69	0.54864	0.87
5		S1H	0.0856	0.64	0.14808	0.64	0.33553	0.71	0.85598	0.83
6	Steel Braced Frame	S2L	0.02743	0.93	0.0475	0.92	0.12802	0.93	0.32918	0.93
7		S2M	0.04572	0.7	0.07925	0.69	0.21336	0.69	0.54864	0.89
8		S2H	0.07137	0.66	0.1237	0.64	0.33274	0.69	0.85598	0.8
9	Steel Light Frame	S3	0.01372	0.88	0.02388	0.92	0.06401	0.97	0.18009	0.89
10	Steel Frame with Cast-in-Place Concrete Shear Walls	S4L	0.02184	0.96	0.0381	1	0.10262	1.03	0.28804	0.92
11		S4M	0.03658	0.75	0.0635	0.72	0.17094	0.72	0.48006	0.94
12		S4H	0.05715	0.66	0.09906	0.67	0.2667	0.7	0.74879	0.9
13	Steel Frame with URM Infill Walls	S5L	-	-	-	-	-	-	-	-
14		S5M	-	-	-	-	-	-	-	-
15		S5H	-	-	-	-	-	-	-	-
16	Concrete Moment Frame	C1L	0.02286	0.89	0.03962	0.9	0.10668	0.9	0.27432	0.89
17		C1M	0.0381	0.7	0.06604	0.7	0.1778	0.7	0.4572	0.89
18		C1H	0.05486	0.66	0.095	0.66	0.25603	0.76	0.65837	0.91
19	Concrete Shear Walls	C2L	0.01829	0.91	0.03861	0.97	0.10592	1.03	0.27432	0.87
20		C2M	0.03048	0.81	0.06426	0.77	0.17653	0.73	0.4572	0.91
21		C2H	0.04394	0.66	0.09246	0.68	0.254	0.7	0.65837	0.87
22	Concrete Frame with URM Infill Walls	C3L	-	-	-	-	-	-	-	-
23		C3M	-	-	-	-	-	-	-	-
24		C3H	-	-	-	-	-	-	-	-
25	Pre-cast Concrete Tilt-	PC1	0.01372	0.89	0.02388	0.92	0.06401	0.97	0.18009	1.04
26	Pre-cast Concrete Frames with Concrete Shear Walls	PC2L	0.01829	0.96	0.03175	1	0.0856	1.03	0.24003	0.88
27		PC2M	0.03048	0.82	0.05283	0.79	0.14249	0.75	0.40005	0.93
28		PC2H	0.04394	0.68	0.0762	0.69	0.20523	0.77	0.57607	0.89
29	Reinforced Masonry Bearing Walls	RM1L	0.01829	0.96	0.03175	0.99	0.0856	1.05	0.24003	0.94
30		RM1M	0.03048	0.81	0.05283	0.82	0.14249	0.8	0.40005	0.89
31	Reinforced Masonry Bearing Walls	RM2L	0.01829	0.91	0.03175	0.96	0.0856	1.02	0.24003	0.93
32		RM2M	0.03048	0.81	0.05283	0.8	0.14249	0.75	0.40005	0.88
33		RM2H	0.04394	0.67	0.0762	0.69	0.20523	0.7	0.57607	0.86
34	Unreinforced Masonry Bearing Walls	URML	-	-	-	-	-	-	-	-
35		URMM	-	-	-	-	-	-	-	-
36	Mobile Homes	MH	0.01219	0.91	0.02438	1	0.07315	1.03	0.21336	0.92

Table 82. Capacity Curve Parameters for High-Code Buildings of HAZUS99 Building Taxonomy

Building Taxonomy			Capacity Curve Parameters				
No.	Description	Label	d_y	a_y	d_u	a_u	d_e
1	**Wood, Light Frame**	W1	0.0122	3.924	0.2924	11.772	0.0085
2	**Wood, Commercial or Industrial**	W2	0.016	3.924	0.3183	9.81	0.0112
3	**Steel Moment Frame**	S1L	0.0155	2.4525	0.3726	7.3575	0.0108
4		S1M	0.045	1.5696	0.7214	4.6107	0.0315
5		S1H	0.1184	0.981	1.4194	2.8449	0.0829
6	**Steel Braced Frame**	S2L	0.016	3.924	0.2545	7.848	0.0112
7		S2M	0.0617	3.2373	0.6574	6.5727	0.0432
8		S2H	0.1969	2.4525	1.574	5.0031	0.1378
9	**Steel Light Frame**	S3	0.016	3.924	0.2545	7.848	0.0112
10	**Steel Frame with Cast-in-Place Concrete Shear Walls**	S4L	0.0097	3.1392	0.1755	7.0632	0.0068
11		S4M	0.0277	2.6487	0.3327	5.886	0.0194
12		S4H	0.0886	1.962	0.7968	4.5126	0.0621
13	**Steel Frame with URM Infill Walls**	S5L	-	-	-	-	-
14		S5M	-	-	-	-	-
15		S5H	-	-	-	-	-
16	**Concrete Moment Frame**	C1L	0.0099	2.4525	0.2385	7.3575	0.0069
17		C1M	0.0292	2.0601	0.4684	6.0822	0.0204
18		C1H	0.0511	0.981	0.6129	2.8449	0.0357
19	**Concrete Shear Walls**	C2L	0.0122	3.924	0.2436	9.81	0.0085
20		C2M	0.0264	3.2373	0.3515	8.1423	0.0185
21		C2H	0.0747	2.4525	0.7465	6.2784	0.0523
22	**Concrete Frame with URM Infill Walls**	C3L	-	-	-	-	-
23		C3M	-	-	-	-	-
24		C3H	-	-	-	-	-
25	**Pre-cast Concrete Tilt-**	PC1	0.0183	5.886	0.2924	11.772	0.0128
26	**Pre-cast Concrete Frames with Concrete Shear Walls**	PC2L	0.0122	3.924	0.1948	7.848	0.0085
27		PC2M	0.0264	3.2373	0.2812	6.5727	0.0185
28		PC2H	0.0747	2.4525	0.5974	5.0031	0.0523
29	**Reinforced Masonry Bearing Walls**	RM1L	0.0163	5.1993	0.2598	10.4967	0.0114
30		RM1M	0.0351	4.3164	0.3749	8.7309	0.0245
31	**Reinforced Masonry Bearing Walls**	RM2L	0.0163	5.1993	0.2598	10.4967	0.0114
32		RM2M	0.0351	4.3164	0.3749	8.7309	0.0245
33		RM2H	0.0996	3.3354	0.7963	6.6708	0.0697
34	**Unreinforced Masonry Bearing Walls**	URML	-	-	-	-	-
35		URMM	-	-	-	-	-
36	**Mobile Homes**	MH	0.0046	1.4715	0.0549	2.943	0.0032

Table 83. Fragility Curve Parameters for High-Code Buildings of HAZUS99 Building Taxonomy

Building Taxonomy			Fragility Curve Parameters for Four Damage Levels							
			Slight		Moderate		Extensive		Complete	
No.	Description	Label	$S_{d,s}$	β_s	$S_{d,m}$	β_m	$S_{d,e}$	β_e	$S_{d,c}$	β_c
1	Wood, Light Frame	W1	0.0127	0.8	0.03835	0.81	0.12802	0.85	0.32004	0.97
2	Wood, Commercial or	W2	0.02184	0.81	0.06579	0.88	0.21946	0.9	0.54864	0.83
3	Steel Moment Frame	S1L	0.03302	0.8	0.06579	0.76	0.16459	0.69	0.43891	0.72
4		S1M	0.05486	0.65	0.10973	0.66	0.27432	0.67	0.73152	0.74
5		S1H	0.0856	0.64	0.1712	0.64	0.42799	0.65	1.14122	0.67
6	Steel Braced Frame	S2L	0.02743	0.81	0.05486	0.89	0.16459	0.94	0.43891	0.83
7		S2M	0.04572	0.67	0.09144	0.67	0.27432	0.68	0.73152	0.79
8		S2H	0.07137	0.63	0.14275	0.63	0.42799	0.64	1.14122	0.71
9	Steel Light Frame	S3	0.01372	0.81	0.02743	0.82	0.0823	0.91	0.24003	0.9
10	Steel Frame with Cast-in-Place Concrete Shear Walls	S4L	0.02184	0.89	0.04394	0.89	0.13157	0.98	0.38405	0.87
11		S4M	0.03658	0.77	0.07315	0.72	0.21946	0.7	0.64008	0.89
12		S4H	0.05715	0.64	0.11405	0.66	0.34239	0.69	0.99847	0.77
13	Steel Frame with URM Infill Walls	S5L	-	-	-	-	-	-	-	-
14		S5M	-	-	-	-	-	-	-	-
15		S5H	-	-	-	-	-	-	-	-
16	Concrete Moment Frame	C1L	0.02286	0.81	0.04572	0.84	0.13716	0.86	0.36576	0.81
17		C1M	0.0381	0.68	0.0762	0.67	0.2286	0.68	0.6096	0.81
18		C1H	0.05486	0.66	0.10973	0.64	0.32918	0.67	0.87782	0.78
19	Concrete Shear Walls	C2L	0.01829	0.81	0.04572	0.84	0.13716	0.93	0.36576	0.92
20		C2M	0.03048	0.74	0.0762	0.77	0.2286	0.68	0.6096	0.77
21		C2H	0.04394	0.68	0.10973	0.65	0.32918	0.66	0.87782	0.75
22	Concrete Frame with URM Infill Walls	C3L	-	-	-	-	-	-	-	-
23		C3M	-	-	-	-	-	-	-	-
24		C3H	-	-	-	-	-	-	-	-
25	Pre-cast Concrete Tilt-	PC1	0.01372	0.76	0.02743	0.86	0.0823	0.88	0.24003	0.99
26	Pre-cast Concrete Frames with Concrete Shear Walls	PC2L	0.01829	0.84	0.03658	0.88	0.10973	0.98	0.32004	0.94
27		PC2M	0.03048	0.77	0.06096	0.81	0.18288	0.7	0.5334	0.82
28		PC2H	0.04394	0.64	0.08788	0.66	0.2634	0.68	0.7681	0.81
29	Reinforced Masonry Bearing Walls	RM1L	0.01829	0.84	0.03658	0.86	0.10973	0.92	0.32004	1.01
30		RM1M	0.03048	0.71	0.06096	0.81	0.18288	0.76	0.5334	0.75
31	Reinforced Masonry Bearing Walls	RM2L	0.01829	0.8	0.03658	0.81	0.10973	0.91	0.32004	0.98
32		RM2M	0.03048	0.71	0.06096	0.79	0.18288	0.7	0.5334	0.73
33		RM2H	0.04394	0.66	0.08788	0.65	0.2634	0.66	0.7681	0.72
34	Unreinforced Masonry Bearing Walls	URML	-	-	-	-	-	-	-	-
35		URMM	-	-	-	-	-	-	-	-
36	Mobile Homes	MH	0.01219	0.91	0.02438	1	0.07315	1.03	0.21336	0.92